TURUN
YLIOPISTO
UNIVERSITY
OF TURKU

GENOMIC EDITING TO ELUCIDATE THE EFFECTS OF PIM KINASES ON CANCER CELL SIGNALLING

Kwan Long Mung

TURUN YLIOPISTON JULKAISUJA – ANNALES UNIVERSITATIS TURKUENSIS
SARJA – SER. D OSA – TOM. 1698 | MEDICA – ODONTOLOGICA | TURKU 2023

TURUN
YLIOPISTO
UNIVERSITY
OF TURKU

GENOMIC EDITING TO ELUCIDATE THE EFFECTS OF PIM KINASES ON CANCER CELL SIGNALLING

Kwan Long Mung

TURUN YLIOPISTON JULKAISUJA – ANNALES UNIVERSITATIS TURKUENSIS
SARJA – SER. D OSA – TOM. 1698 | MEDICA – ODONTOLOGICA | TURKU 2023

University of Turku

Faculty of Science
Department of Biology
Section of Physiology and Genetics
University of Turku Graduate School (UTUGS)
Drug Research Doctoral Programme (DRDP)

Supervised by

Adjunct Professor Päivi J. Koskinen, PhD
Department of Biology
University of Turku
Turku, Finland

Reviewed by

Professor Ville Hietakangas, PhD
Faculty of Biological and
Environmental Sciences
University of Helsinki
Helsinki, Finland

Associate Professor Guillaume Jacquemet, PhD
Faculty of Science and Engineering
Åbo Akademi University
Turku, Finland

Opponent

Clinical Senior Lecturer Kathy Gately, PhD
Trinity Translational Medicine Institute
Trinity College Dublin, University of Dublin
Dublin, Ireland

ISBN 978-951-29-9194-5 (PRINT)
ISBN 978-951-29-9195-2 (PDF)
ISSN 0355-9483 (Print)
ISSN 2343-3213 (Online)
Painosalama, Turku, Finland 2023

UNIVERSITY OF TURKU
Faculty of Science
Department of Biology
Section of Physiology and Genetics
KWAN LONG MUNG: Genomic Editing to Elucidate the Effects of PIM Kinases on Cancer Cell Signalling
Doctoral Dissertation, 182 pp.
Drug Research Doctoral Programme (DRDP)
February 2023

ABSTRACT

In humans, there are three PIM family genes, the two first of which were originally identified from mice as proviral integration sites for Moloney leukemia virus. They encode serine/threonine kinases that are aberrantly expressed in a variety of hematological malignancies and solid tumors. PIM kinases contribute to cell proliferation, cell survival and cell motility by phosphorylating multiple downstream substrates. PIM kinases have emerged as attractive anti-cancer drug targets, and their distinct structures enable the generation of selective inhibitors.

The aim of this PhD study was to functionally validate three novel PIM targets that affect cancer cell signalling, namely actin capping proteins (CPs) that restrict elongation of actin fibers, liver kinase B1 (LKB1) that suppresses cell growth, and lactate dehydrogenase A (LDHA) that regulates cell metabolism. For this purpose, CRISPR/Cas9-based genome editing and structurally unrelated pharmacological PIM-selective inhibitors were used. PIM-targeted sites were identified by mass spectrometry and mutagenesis, after which the functional impacts of phosphorylation were studied in cultured cells or using a chick embryo xenograft model. In line with the pro-migratory function of PIM kinases, phosphorylation of CPs was shown to reduce their ability to bind to the plus ends of actin filaments and thereby to promote cell adhesion and migration. Catalytic activity of LKB1 towards its substrates such as AMPK was shown to be inhibited by PIM-dependent phosphorylation. These studies also indicated that the oncogenic effects of PIMs and the tumor-suppressive effects of LKB1 are tightly controlled at the cellular level. In the case of LDHA, PIM-dependent phosphorylation was observed to prevent nuclear LDHA from being degraded via K48-mediated ubiquitination, highlighting the connection between PIM kinases and the regulation of glycolytic enzymes. Altogether, the results from these studies help to better understand the mechanisms, through which PIM kinases stimulate cancer cell signalling.

KEYWORDS: PIM kinases, phosphorylation, CRISPR, genomic editing, actin capping proteins, LKB1, LDHA, cancer cell signalling

TURUN YLIOPISTO
Matemaattis-luonnontieteellinen tiedekunta
Biologian laitos
Fysiologian ja genetiikan osasto
KWAN LONG MUNG: Genomin muokkaus PIM-kinaasien vaikutusten tutkimiseksi syöpäsoluissa
Väitöskirja, 182 s.
Lääkekehityksen tohtoriohjelma
Helmikuu 2023

TIIVISTELMÄ

Ihmisen *PIM*-geeniperheen kolmesta jäsenestä kaksi ensimmäistä löydettiin alun perin hiiristä Moloney-leukemiaviruksen integraatiokohtina. Niiden koodaamat seriini/treoniinikinaasit ilmentyvät poikkeavasti erilaisissa hematologisissa sekä kiinteissä kasvaimissa. PIM-kinaasit edistävät solujen lisääntymistä, eloonjäämistä sekä liikkuvuutta fosforyloimalla useita kohdeproteiinejaan. Kiinnostus PIM-kinaasien toimintaa estäviä syöpälääkkeitä kohtaan on viime aikoina lisääntynyt, ja niiden poikkeava rakenne mahdollistaa valikoivien estolääkkeiden kehittämisen.

Tämän väitöstutkimuksen tavoitteena oli toiminnallisesti tutkia kolmea uutta syöpäsolujen viestintään vaikuttavaa PIM-kohdeproteiinia: aktiinisäikeiden pitenemistä rajoittavia CP-proteiineja, solujen kasvua rajoittavaa LKB1-kinaasia ja aineenvaihduntaa säätelevää laktaattidehydrogenaasia A (LDHA). Tutkimuksissa käytettiin CRISPR/Cas9-pohjaista genominmuokkausta sekä rakenteellisesti erilaisia PIM-selektiivisiä estolääkkeitä. PIM-kinaasien fosforyloimat kohdat paikannettiin massaspektrometrian ja mutageneesin avulla, ja fosforylaation merkitystä tutkittiin soluviljelmissä tai kananmunan alkion siirrännäismallin avulla. CP-proteiinien fosforylaation osoitettiin vähentävän niiden kykyä sitoutua aktiinisäikeiden plus-päihin, ja siten edistävän solujen adheesiota ja migraatiota, selittäen PIM-kinaasien kykyä lisätä solujen liikkuvuutta. PIM-fosforylaatio heikensi LKB1:n katalyyttistä aktiivisuutta ja siten esti sitä fosforyloimasta omia kohdeproteiinejaan, kuten AMPK-kinaasia. Nämä tutkimukset myös osoittivat, että PIM-kinaasien onkogeenisia ja LKB1:n vastakkaisia vaikutuksia säädellään ristiin solutasolla. LDHA:n tapauksessa fosforylaation havaittiin estävän LDHA-proteiinin hajoamista tumassa K48-välitteisen ubikitinaation kautta, korostaen PIM-kinaasien ja glykolyyttisten entsyymien säätelyn välistä yhteyttä. Kaiken kaikkiaan näiden tutkimusten tulokset auttavat paremmin ymmärtämään niitä mekanismeja, joilla PIM-kinaasit stimuloivat syöpäsolujen viestintää.

AVAINSANAT: PIM-kinaasit, fosforylaatio, CRISPR, genominen muokkaus, aktiinia rajoittavat proteiinit, LKB1, LDHA, syöpäsolujen signalointi

Table of Contents

Abbreviations

α-HB	alpha hydroxybutyrate
α-KB	alpha ketobutyrate
αKG	alpha ketoglutarate
ACTB	actin beta
Ala	alanine
AMPK	adenosine monophosphate-activated protein kinase
AKT	v-akt murine thymoma viral oncogene homolog
AR	androgen receptor
BAD	BCL2-associated agonist of cell death
BCL2	B-cell lymphoma 2
CAM	chorioallantoic membrane
Cas	CRISPR-associated proteins
CP	capping protein
CRISPR	Clustered regularly interspaced short palindromic repeats
CXCR	chemokine (C-X-C motif) receptor
CXCL	chemokine (C-X-C motif) ligand
DHPCC-9	dihydropyrrolocarbazole compound 9
DMSO	dimethyl sulfoxide
EMT	epithelial-mesenchymal transition
HeLa	Henrietta Lacks
KO	knock-out
KRAS	Kirsten rat sarcoma 2 viral oncogene homolog
LDHA	lactate dehydrogenase A
LKB1	Liver kinase B1
Lys	lysine
mRNA	messenger RNA
MTOR	mechanistic target of rapamycin
NFATC	nuclear factor of activated T-cells
NF-κB	nuclear factor of kappa light polypeptide gene enhancer in B-cells
PCR	polymerase chain reaction
PI3K	phosphoinositide 3-kinase
PIM	proviral integration site for Moloney murine leukemia virus
PLA	proximity ligation assay
PRAS40	proline-rich Akt substrate, 40 kDa
PTEN	phosphatase and tensin homolog
Ser	serine
Thr	threonine
UTR	untranslated region

List of Original Publications

This dissertation is based on the following original publications, which are referred to in the text by their Roman numerals:

I Santio NM, Vainio V, Hoikkala T, **Mung KL**, Lång M, Vahakoski R, Zdrojewska J, Coffey ET, Kremneva E, Rainio EM, Koskinen PJ. PIM1 accelerates prostate cancer cell motility by phosphorylating actin capping proteins. *Cell Communication and Signaling* 2020 Aug 8;18(1):121.

II **Mung KL**, Eccleshall WB, Santio NM, Rivero-Müller A, Koskinen PJ. PIM kinases inhibit AMPK activation and promote tumorigenicity by phosphorylating LKB1. *Cell Communication and Signaling* 2021 Jun 30;19(1):68.

III **Mung KL**, Meinander A, Koskinen PJ. PIM kinases phosphorylate lactate dehydrogenase A at serine 161 and suppress its nuclear ubiquitination. *The FEBS Journal* 2022 Oct 14.

1 Introduction

Proviral Integration site for Moloney murine leukemia virus (PIM) kinases are serine/threonine kinases that were discovered in the 1980s in the murine leukemia virus-induced lymphoma model (Cuypers *et al.* 1984). PIM1, PIM2, and PIM3 are the three family members that have been discovered to date. They exhibit partial functional redundancy and share substantial amino acid sequence homology (Nawijn, Alendar and Berns 2011). By phosphorylating a variety of substrates, PIM kinases promote cell survival, proliferation, and motility (Nawijn, Alendar and Berns 2011; Warfel and Kraft 2015; Santio and Koskinen 2017). Their kinase activities are well correlated to protein expression levels, which are markedly increased in a variety of malignancies, such as myelomas, leukemias, prostate, breast, and pancreatic cancer. In an orthotopic mouse xenograft model for human prostate cancer, pharmacological inhibitors of PIM kinases have effectively slowed tumor growth and limited the ability of tumor cells to metastasize (Santio *et al.* 2010, 2015), suggesting that targeting PIM kinases may provide clinical benefits to cancer patients.

Collaboration of PIMs with other oncoproteins such as MYC results in pronounced tumor formation (J. Wang *et al.* 2010; Jang and Chung 2012; Saurabh *et al.* 2014), indicating that PIM kinases are tightly linked into pro-tumorigenic cellular signalling pathways. In this study, CRISPR/Cas9-based genomic editing technology as well as small molecule pan-PIM pharmacological inhibitors were employed to inhibit PIM expression or activities in cultured cancer cell lines. The experimental findings obtained by these two approaches were expected to enable validation of novel downstream targets of PIM kinases as well as their potential crosstalk with oncogenic or tumor suppressive signalling pathways, providing essential knowledge to support the development of PIM-targeted therapies.

2 Review of the Literature

2.1 General overview of mechanisms underlying tumorigenesis

2.1.1 Proto-oncogenes and tumor suppressors

Most cancers develop over time, after accumulation of a series of mutations that in combination to promote formation of malignant tumors. These mutations frequently occur in oncogenic or tumor-suppressive genes, and thereby affect crucial signalling pathways that regulate cell cycle progression, metabolic processes, motility, genomic and epigenetic stability, and immunological detection. Deregulation of these pathways provides cancer cells with a growing list of new properties, recognized as the hallmarks of cancer (Hanahan and Weinberg 2011; Hanahan 2022).

Proto-oncogenes refer to genes that are essential for the maintenance of normal cellular growth, yet they are hyperactivated in cancer cells, resulting in uncontrolled cellular proliferation. Retroviral mutagenesis has been proven to be a valuable tool in the identification of proto-oncogenes, as retroviruses induce oncogenic mutations via the insertion of proviral sequences into their host genomes. These insertions enhance the expression of genes by different means. They may cause disruption of destabilizing elements present in the 3' UTR (untranslated region) and thereby enhance the stability of mRNA, or they can serve as enhancers in the 5'UTR to facilitate gene transcription (Uren *et al*. 2005).

For example, *PIM1* (**P**roviral **i**ntegration site for **M**oloney murine leukemia virus) was identified as a proto-oncogene that was frequently activated in Molony murine leukemia virus-induced lymphomas (Cuypers *et al*. 1984) and whose protein product was found to possess serine/threonine kinase activity (D. Hoover *et al*. 1991), whereas the AKT1 (v-**akt** murine thymoma viral oncogene homolog 1) serine/threonine kinase was first identified as a protein encoded by the proto-oncogene *AKT8* in retrovirus-transformed mice (Staal, Hartley, and Rowe 1977). Also, other well-known proto-oncogenes such as *ABL1* (**Ab**elson murine **l**eukemia viral oncogene homolog **1**), *MYC* (Avian **my**elo**c**ytomatosis viral oncogene

homolog), and *KRAS* (**K**irsten **ra**t **s**arcoma 2 viral oncogene homolog) have all been identified via retroviral mutagenesis.

Point mutations, gene amplification and chromosomal rearrangements are common mechanisms for proto-oncogene activation. Point mutations in the protein-coding region of the KRAS gene have been observed frequently in pancreatic ductal adenocarcinoma (PDAC) (Prior, Lewis, and Mattos 2012). The KRAS protein binds guanine nucleotides and has intrinsic guanosine triphosphatase (GTPase) activity. Wild-type KRAS is inactivated after hydrolysis of GTP to GDP, but mutated KRAS remains persistently in a GTP-bound constitutively active form, turning on various effector pathways to drive tumor growth (Waters and Der 2018). MYC is a basic helix-loop-helix leucine zipper protein that modulates gene expression to promote cell proliferation and metabolism (Fernandez *et al*. 2003; Meyer and Penn 2008), and the *MYC* gene has been found to be amplified in 20-30% of breast and ovarian cancers (Brison 1993). In chronic myeloid leukemia (CML), it has been frequently observed that part of the chromosome 9 with the *ABL1* gene has merged with the *BCR* (**b**reakpoint **c**luster **r**egion protein) gene on chromosome 22, leading to the formation of a chimeric protein that accounts for the constitutive tyrosine kinase activity of ABL1 and that hence leads to uncontrolled growth of leukemic cells (Cilloni and Saglio 2012). To put it in a nutshell, proto-oncogenes can be aberrantly activated to become oncogenes via different mechanisms that in turn provide a growth advantage to cells to drive tumorigenesis.

Tumor suppressors refer to genes that normally inhibit cell proliferation and tumor development, but that are often inactivated in cancer cells and contribute to the abnormal growth of tumors. TP53 is probably the best known tumor suppressor, owing to its well-characterised role in triggering cell arrest or elimination of cells after DNA damage or exposure to proteotoxic stress (Mantovani, Collavin, and Del Sal 2019). PTEN (**P**hosphatase and **ten**sin homolog) is a lipid phosphatase that negatively regulates PI3K/AKT signalling via suppression of intracellular levels of phosphatidylinositol-3,4,5-trisphosphate (Stambolic *et al*. 1998). Germline loss-of-function mutations of *PTEN* are linked to an increased risk of breast and endometrial cancer (Hollander, Blumenthal, and Dennis 2011). LKB1, also known as STK11 (**S**erine-**t**hreonine **k**inase 11), phosphorylates a variety of downstream targets that regulate diverse cellular functions such as cellular bioenergetics (Shackelford and Shaw 2009). *LKB1* germline mutations cause Peutz-Jeghers syndrome, which predisposes to cancer development (Hemminki *et al.* 1998).

Sequencing of thousands of DNA samples from human patient tumors has revealed 71 tumour suppressor genes and 54 oncogenes that are frequently altered in cancer (Vogelstein *et al.* 2013). Of note, several studies have shown that either hyperactivation of the *MYC* proto-oncogene or homozygous inactivation of the *TP53* tumor suppressor gene is insufficient to cause prostate cancer, but that the

combination of *MYC* hyperactivation with inactivation of *TP53* promotes solid tumor formation or even drives metastasis (J. Kim *et al*. 2012). This has led to the hypothesis that the co-occurrence of proto-oncogene hyperactivation and tumor suppressor inactivation is a pre-requisite for tumorigenesis. However, there are numerous pieces of evidence to indicate that activation of multiple proto-oncogenes or inactivation of multiple tumor suppressors can also result in carcinogenesis. For example, one study showed that high expression of either PIM1 or MYC alone was not sufficient to induce high-grade prostate cancer in normal prostate epithelium, but co-overexpression of PIM1 and MYC proteins induced prostate carcinoma within 6 weeks in mice (J. Wang *et al*. 2010). In addition, bone marrow cells transduced with both *PIM2* and *MYC* genes formed myeloid sarcoma within 25 days in mice, whereas there were no signs of tumors in *MYC*-transduced cells even after 90 days (Jang and Chung 2012). It has been further demonstrated that all three PIM kinase family members can collaborate with MYC to induce tumorigenesis (Saurabh *et al*. 2014). Asides from proto-oncogenes, deletion of the tumor suppressor *LKB1* gene alone is inconsequential to prostate tumorigenesis, but loss of *LKB1* and *PTEN* together causes early tumor formation (Hermanova *et al*. 2020). Notably, one study even showed that subtle downregulation of *PTEN* expression is sufficient to initiate tumorigenesis in a murine model for breast cancer (Alimonti *et al*. 2010). All these findings not only demonstrate that dysregulation of proto-oncogenes or tumor suppressors is involved in tumorigenesis, but also show that delineation of their intertwined connections as well as their tissue-specific regulation is essential for the rationale development of cancer therapies.

2.1.2 Metabolic reprogramming

Metabolic reprogramming is one of the cancer hallmarks, caused by both deregulated signalling and the increased metabolic needs of rapidly proliferating cancer cells (Vander Heiden, Cantley, and Thompson 2009). The ability of cancer cells to metabolically adapt to changing microenvironmental conditions allows them to thrive and migrate to secondary locations (Faubert, Solmonson, and DeBerardinis 2020). Furthermore, the tumor microenvironment of solid tumors is frequently deprived of both oxygen and nutrients, leading to metabolic reprogramming as one of the survival strategies (Hanahan and Weinberg 2011; Boroughs and DeBerardinis 2015). To this end, it is impossible not to mention Otto Warburg, a Nobel laureate from 1931, who pioneered the idea that cancer cells exhibit high rates of glycolysis even in the presence of oxygen (Koppenol, Bounds, and Dang 2011). This phenomenon was eventually termed the Warburg effect or aerobic glycolysis. He proposed that the impairment of respiration is the primary cause of the increase in glycolysis in cancer cells. However, it has been found that the majority of cancers

still retain functional respiratory systems (Zu and Guppy 2004), and that activities of the TCA cycle and the electron transport chain are important for tumour cell growth and survival (Weinberg *et al*. 2010). Regardless, Warburg's discovery is an important contribution to the field, as it underpins the principle and development of fluorodeoxyglucose positron emission tomography (FDG-PET) (Miles and Williams 2008) for tumor imaging.

The Warburg effect is driven by both the hypoxic tumor microenvironment and the activities of oncogenes (Courtnay *et al*. 2015). Under hypoxia, the stabilised hypoxia-inducible transcription factor 1 alpha (HIF-1α) interacts with several proteins and binds to promoter regions of different target genes, resulting in increased expression of multiple glycolytic enzymes and thus enhanced glycolysis (Lum *et al*. 2007). Oncoproteins such as AKT increase the expression of glucose transporters as well as activate multiple glycolytic enzymes by phosphorylation (Robey and Hay 2009). Enhanced glycolysis allows the generation of ample glycolytic intermediates to be shunted into the pentose phosphate pathway for NADPH production as well as nucleotide synthesis, hexosamine pathway for glycosylation, glycerol synthesis for lipid synthesis, and serine-glycine-one-carbon metabolism for methylation reactions and glutathione synthesis, collectively providing essential precursors for cell growth (Vander Heiden, Cantley, and Thompson 2009; DeBerardinis and Chandel 2020). Notably, despite the increased glycolysis, oxidative phosphorylation accounts for the majority of ATP production in both normoxic and hypoxic cancer cells (Jing Fan *et al*. 2013). In addition to glucose, glutamine is another crucial source of carbon and reducing power to sustain anabolic development, and enhanced glutamine metabolism is often recognized as another typical example of metabolic reprogramming of cancer cells (DeBerardinis *et al*. 2007).

In addition to meeting the demands for growth and homeostasis, the origin of the tumor is another important factor determining the metabolic reconfiguration of cancer cells. In terms of metabolic gene expression, cancers from the same organ share more similarities with each other than cancers from different organs (Jie Hu *et al*. 2013). Of note, MYC induction triggers increased glutamine synthesis in mouse liver tumors but increased glutamine catabolism in mouse lung tumors (Yuneva *et al*. 2012), suggesting that the tissue of origin may impact the execution of metabolic programmes triggered by an oncogenic driver. The metabolic reconfiguration of cancer cells is also influenced by stromal cells in the tumor microenvironment (Sousa *et al*. 2016). Aside from metabolic heterogeneity among tumors, there can also be intra-tumor variability depending on abnormal vascular architecture that provides differential amounts of nutrients and oxygen to distinct parts of solid tumors (Pandkar, Dhamdhere, and Shukla 2021).

Mutations in the isocitrate dehydrogenase 1 and 2 (*IDH1* and *IDH2*) genes are another known example of how metabolic reprogramming promotes tumorigenesis. Mutations that affect key residues within the active sites of IDH1 or IDH2 have been found in a wide range of tumors including acute myeloid leukemia (AML), glioblastomas (GBMs) and intrahepatic cholangiocarcinoma (IHCC) (Dang, Yen, and Attar 2016). While wild-type IDH1/2 proteins convert isocitrate to α-ketoglutarate (αKG) with the expense of nicotinamide adenine dinucleotide phosphate ($NADP^+$), mutated IDH1 and IDH2 convert αKG to D-2-hydroxyglutarate (2-HG). Elevated 2-HG metabolite levels have been found in patients with *IDH1/2* mutations, in which 2-HG inhibits αKG-dependent histone and DNA demethylases, leading to changes in cellular epigenetic status and enhanced tumor progression (Chowdhury *et al*. 2011; W. Xu *et al*. 2011; C. Lu *et al*. 2012). Furthermore, in IHCC, it has been found that 2-HG production by mutant IDH causes silencing of the transcription factor HNF-4α (**h**epatocyte **n**uclear **f**actor 4 **alpha**), which contributes to increased cell proliferation and impairment of hepatocyte differentiation (S. K. Saha *et al*. 2014). To this end, drugs targeting the IDH1 mutation, such as Ivosidenib, have yielded favourable benefits for patients in clinical trials (Ax *et al*. 2021) and have been approved for marketing by the FDA in 2019. Although this successful approach demonstrates the potential of better understanding cancer metabolic reprogramming in the development of effective therapies, the heterogeneity among tumors necessitates specific tailoring of therapeutic strategies by matching each treatment to patient-specific tumor metabolism.

2.1.3 Cellular motility in invasion and metastasis

Cellular motility is important for cancer progression, and plays a crucial role in the development of metastases, as increased motility enables cancer cells to migrate and invade secondary sites. Coupled with the motor protein myosin, remodelling of the actin cytoskeleton empowers cells to change their shapes in response to external cues (Blanchoin *et al*. 2014; Svitkina 2018; Conway and Jacquemet 2019). For instance, lamellipodia are branched and crosslinked actin filament structures located in the cell front that are responsible for rapid cellular movements. Filopodia in turn are small protrusions that can extend beyond cell edges and coordinate precise directional responses. Depending on the need for fast locomotion or precise navigation, lamellipodia or filopodia are formed within the cell edges, respectively (Svitkina 2018). Cells can migrate either individually or as a cohesive group of cells. Single-cell migration can be further classified into mesenchymal or amoeboid motility (Parri and Chiarugi 2010; Te Boekhorst, Preziosi, and Friedl 2016). Both types of motility depend on the remodeling of the actin cytoskeleton. While mesenchymal motility is achieved by cells extending pseudopodia or finger-like

extensions to push against their surroundings, amoeboid motility is characterised by cells with rounded morphology that allows them to squeeze through narrow spaces by flowing (Parri and Chiarugi 2010; Te Boekhorst, Preziosi, and Friedl 2016).

Cellular movements in a tridimensional extracellular matrix (ECM) primarily consist of repeated cycles of protrusion and attachment in the front end, followed by retraction and detachment in the rear end. In the leading cell edge, the dynamic polymerisation and depolymerization of barbed and naked ends of actin filaments serve as the major driving force for actin-based motility (Pantaloni, Le Clainche, and Carlier 2001). The barbed end of the actin filament is the growing end that often points towards cell membranes or sarcomere Z-disks, while the naked end refers to the opposite end of the filament (Edwards *et al*. 2014). With the coordinated actions of profilin and actin- depolymerizing factors, actin monomers are added into the barbed end of the actin filament with the expense of ATP, while depolymerization occurs in the naked end of the filament, eventually providing free actin monomers available for future polymerisation at the barbed end. This workflow is also described as actin treadmilling. In addition to profilin and actin depolymerizing factors, the capping protein is another important regulator governing the dynamics of actin treadmilling (Pantaloni, Le Clainche, and Carlier 2001). It binds and blocks the barbed end of the actin filament and renders polymerisation of capped actin filament unfeasible. This not only prevents complete exhaustion of the cellular pool of unpolymerised actin, but also helps in the channelling of actin monomers to be incorporated into non-capped actin filaments, preventing indefinite elongation of a specific actin filament. Thus, the interplay between profilin, actin-depolymerizing factors and capping proteins enables maintenance of a steady number of growing barbed ends at the cell edges. In addition to the numbers of active growing ends, the direction of the growing actin filament can be further fine-tuned by subsets of proteins, including the Arp2/3 complex (Mullins, Heuser, and Pollard 1998; Pollard and Borisy 2003).

The propulsive force generated by actin dynamics permits diverse motility events such as metastasis. Tumor metastasis involves a series of steps including cell invasion within the primary tumor site, intravasation into blood vessels, extravasation from there and colonization into distant sites to form secondary tumors (Fares *et al*. 2020). Initiation of tumor metastasis has been linked to the process of epithelial-mesenchymal transition (EMT), in which immotile epithelial cells acquire mesenchymal properties and equip themselves with motility machinery to migrate through the extracellular matrix and to invade different sites (Hay 1995; Kalluri and Weinberg 2009). Reorganization of the cytoskeleton, loss of cell-cell adhesions and apical-basal polarity, decreased expression of E-cadherin and increased expression of vimentin are some of the typical features during EMT (Lamouille, Xu, and Derynck 2014). Notably, there is emerging evidence to show that metastasis could

already occur as an early event of cancer development (Hüsemann *et al*. 2008; Podsypanina *et al*. 2008; Rhim *et al*. 2012), rather than as a late or final event in tumor progression. It is also worth noting that EMT is not a strictly binary process, as cells can express both epithelial and mesenchymal markers at the same time or lose epithelial characteristics without acquiring mesenchymal characteristics (M. S. Brown *et al*. 2022; Rhim *et al*. 2012). In fact, a notion that has been gaining more appreciation is that the flexibility of interchanging epithelial and mesenchymal traits is one of the key factors in determining the success of metastasis. According to emerging theories, activation of EMT promotes effective cell emigration from the main tumor site while activation of MET (reversal of EMT) at the proper moment promotes colonization and proliferation of circulating tumor cells in the secondary site (Tsai *et al*. 2012; Ocaña *et al*. 2012). Along with the cellular plasticity of EMT/MET transitions, other factors such as vascular permeability, the microenvironmental niche of both primary and secondary tumor sites, and the cellular abilities to cope with oxidative stress all contribute to the progression of metastases(Nguyen, Bos and Massagué 2009; Ubellacker *et al.* 2020), underlining the complexities of cancer metastasis.

2.2 PIM kinases and cancer

2.2.1 Identification and regulation of PIM family members

PIM proteins are serine/threonine kinases that phosphorylate a myriad of downstream targets that regulate cell survival, cell proliferation, cell metabolism and cell motility (Nawijn, Alendar and Berns 2011; Warfel and Kraft 2015; Santio and Koskinen 2017). To date, three PIM family members have been identified (Nawijn, Alendar and Berns 2011). *PIM1* was identified as a proto-oncogene frequently activated in Moloney murine leukemia virus-induced lymphomas during the 1980s (Cuypers *et al.* 1984). Aberrant high mRNA expression levels of *PIM1* were correlated with the insertion of proviral sequences into either 3' or 5' UTR of the *PIM1* gene (Selten, Cuypers, and Berns 1985; Selten *et al*. 1986). *PIM2* was subsequently found in another provirus tagging experiment in mice (Breuer, Cuypers, and Berns 1989), and *PIM3*, also known as *KID-1* (**k**inase **i**nduced by **d**epolarization), was identified from PC12 pheochromocytoma cells (J. D. Feldman *et al*. 1998). *PIM1*, *PIM2* and *PIM3* are located on chromosome 6, chromosome X and chromosome 22, respectively. There are two isoforms of PIM1 proteins, namely PIM-1L (44 kDa) and PIM-1S (33 kDa), which are encoded by two alternative translation initiation sites of the same gene (Saris, Domen, and Berns 1991) (**Figure 1A**). Three PIM2 protein isoforms with molecular masses of 34, 37 and 40 kDa have been identified, and they are also encoded by different alternative initiation sites of

the same gene. By contrast, there is only one isoform for the PIM3 protein, with a molecular mass of 34 kDa (Narlik-Grassow, Blanco-Aparicio, and Carnero 2014). All three PIM family members (PIMs) are highly homologous to each other. At the amino acid level, PIM1 is 54% and 67% identical to PIM2 and PIM3, respectively, while PIM2 and PIM3 are 55% identical to each other (**Figure 1B**).

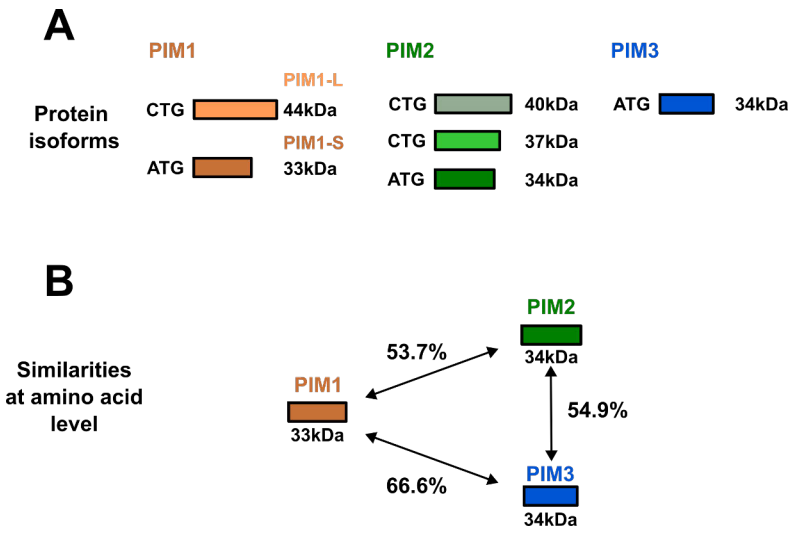

Figure 1. Protein isoforms of each PIM family member and their similarities. A) PIM protein isoforms with the indicated molecular masses are encoded from various initiation sites (ATG or CTG). B) At the amino acid level, members of the PIM family are highly homologous to each other.

PIM kinases are highly conserved in multicellular organisms, with orthologs found in the zebrafish *Danio rerio*, the African clawed frog *Xenopus laevis*, and the nematode *Caenorhabditis elegans* (Kalichamy *et al*. 2019). Surprisingly however, there are no obvious PIM orthologs in the fruit fly *Drosophila melanogaster*. Multiple attempts have been made to identify the consensus PIM target sequence for phosphorylation (Friedmann *et al*. 1992; Bullock *et al*. 2005), which has been revealed as follows, K/R–X–X–X–S/T–X (X is neither a basic group nor a large hydrophobic residue). This sequence is very similar to the AKT consensus sequence (R–X–R–X–X–S/T) (Obata *et al*. 2000), underlining the fact that PIM and AKT kinases share both overlapping and non-overlapping downstream substrates to regulate cell signalling (Warfel and Kraft 2015). Contrary to most other protein kinases, PIM kinases possess no regulatory domains and thus are constitutively active inside cells (Qian *et al*. 2005). This property is attributed to the unique structure of their ATP-binding pockets as well as their activation loops which are perpetually in an open conformation towards the external environment (Qian *et al*.

2005). Of note, the absence of regulatory domains implies that PIM activities are linked to their expression levels, which are tightly controlled by different mechanisms.

A wide array of cytokines and growth hormones, including interferons (IFNα, IFNγ), interleukins (IL-2, IL-3, IL-7, IL-12, IL-15), leukemia inhibitory factor, granulocyte-macrophage colony-stimulating factor, erythropoietin and prolactin have been shown to induce *PIM1* expression (Dautry *et al.* 1988; Sato *et al.* 1993; Miura *et al.* 1994; Buckley *et al.* 1995; Yip-Schneider, Horie and Broxmeyer, 1995; Matikainen *et al.* 1999; Malinen *et al.* 2013; Mary Photini *et al.* 2017; James *et al.* 2021), mainly via the Janus kinases/signal transducers and activators of transcription (JAK/STAT) pathway (Shirogane *et al.* 1999; Aksoy *et al.* 2007; Uddin *et al.* 2015; Szydłowski *et al.* 2017). Conversely, JAK inhibition results in a remarkable decrease in protein expression of all three PIM family members (Szydłowski *et al*. 2017). Other than JAK, TAK1 (**t**ransforming growth factor-β-**a**ctivated **k**inase **1**) has been reported to induce *PIM1* expression via STAT3 signalling independent of JAK activity (Q. Li *et al*. 2020). Moreover, internal tandem duplication mutations of the gene encoding the FMS-like tyrosine kinase 3 (FLT3/ITD) or expression of the chimeric BCR/ABL fusion protein have been shown to upregulate *PIM1* expression via augmentation of STAT5 signalling (K.-T. Kim *et al*. 2005; Nieborowska-Skorska *et al*. 2002). Notably, PIMs phosphorylate and activate SOCS1 and SOCS3 (**S**uppressors **o**f **c**ytokine **s**ignalling) (Chen *et al.* 2002; Peltola *et al.* 2004), which in turn inactivate STAT signalling and thus constitute a negative feedback loop to keep *PIM* expression under control.

While multiple pathways converge into STAT signalling to regulate *PIM* expression, other transcription factors have been reported to upregulate *PIM* expression in different cellular contexts including ERG (**E**TS-**r**elated **g**ene) (Magistroni *et al.* 2011; Eerola *et al.* 2021), NF-κB (**N**uclear **f**actor **kappa** light chain enhancer of activated **B** cells) (Wingett, Reeves and Magnuson 1991; Zhu *et al.* 2002), KLF5 (**K**rüppel-**l**ike **f**actor **5**) (Y. Zhao *et al*. 2008), HOXA9 (**ho**meobo**x** protein **A9**) (Y.-L. Hu *et al*. 2007), HBP1 (**H**MG **b**ox-containing **p**rotein **1**) (S. Wang *et al*. 2017) and ETS1 (**ETS** proto-oncogene **1**) (Y.-Y. Li *et al*. 2009). By contrast, CHES1 (**che**ckpoint **s**uppressor **1**) binds to the promoter region of *PIM2* and negatively regulates *PIM2* expression (Huot *et al*. 2014). In several cases of T-cell lymphoma, enhanced *PIM1* expression has been detected due to chromosomal translocation of T-cell receptor sequences into the genomic region of *PIM1* (La Starza *et al*. 2018; De Smedt *et al*. 2019). The presence of diverse pathways ensures that *PIM* expression is tightly controlled at the transcriptional level in response to a dynamic cellular external environment.

At translational level, mRNA transcripts of *PIM*s are short-lived due to the presence of several destabilising AU-rich elements in their 3'UTRs (Domen *et al*.

1987). Those elements have been shown to be target sites for ZFP36 (**z**inc **f**inger **p**rotein **36** homolog), which triggers decay of both *PIM1* and *PIM3* transcripts (Selmi *et al.* 2012). Furthermore, HuR (**Hu** antigen **R**) protein can bind to the AU-rich elements, but it on the contrary stabilises *PIM1* mRNA levels (Blanco *et al*. 2016). Tristetraprolin, another AU-rich element-binding protein, causes mRNA decay of *PIM1* transcripts but has no effect on *PIM2* or *PIM3* mRNAs (C. Ren *et al*. 2018), indicating differential translational regulation of different *PIM* family members. In addition to the AU-rich elements, the 3'UTRs of *PIM* mRNAs harbor binding sites for microRNAs that destabilise mRNA transcripts (**Table 1**). In the 5'UTR of *PIM1*, there are long GC-rich regions that can repress translation, but whose effects can be overcome by the cap-dependent translation modulator eIF-4E protein (D. S. Hoover *et al*. 1997; Z. Wang, Weaver, and Magnuson 2005). Thus, effective translation of *PIM1* mRNA transcripts relies heavily on cap-dependent translation.

Akin to the short-lived features of mRNA transcripts, PIM proteins have short half-lives, ranging from 10 to 100 minutes in a cell context-dependent manner (Amson *et al*. 1989; Shay *et al*. 2005; Adam *et al*. 2015). Because PIM proteins are degraded via the ubiquitin-proteasome pathway (Shay *et al*. 2005), their stabilities are primarily determined by the factors that influence their degradation pathways. HSP90 (**h**eat **s**hock **p**rotein **90**) and TCTP (**t**ranslationally **c**ontrolled **t**umor **p**rotein) have been shown to bind with PIM1 and PIM3 proteins, respectively, and subsequently prevent their ubiquitin-mediated degradation (Shay *et al*. 2005; X. F. Hu *et al*. 2009; Fei Zhang *et al*. 2013). Furthermore, the deubiquitinase USP28 (**u**biquitin-**s**pecific **p**eptidase **28**) has been shown to preferentially bind to PIM1 protein and suppress its degradation through deubiquitination under both normoxic and hypoxic conditions (Toth, Solomon, and Warfel 2022). Conversely, protein phosphatase 2A dephosphorylates PIM1 and promotes its ubiquitin-mediated degradation (J. Ma *et al*. 2007). SUMOylation of PIM1 has also been reported to promote PIM1 ubiquitination via recruitment of the ubiquitin ligase RNF4 (**r**i**n**g **f**inger protein **4**), yet SUMOylated PIM1 displays stronger kinase activity than non-SUMOylated PIM1 (Iyer *et al*. 2017). Besides, PIM1 has been identified as a frequently mutated gene in lymphoma cohorts (Takakuwa, Miyauchi, and Aozasa 2009; Bruno *et al*. 2014; Kuo *et al*. 2016; Qiong Zhu *et al*. 2022). While some of the patient-associated mutations in the *PIM1* coding region have been attributed to increased PIM1 half-life or kinase activity (Kumar *et al*. 2005; Kuo *et al*. 2016;), S188N and L284F mutations of PIM1 have unexpectedly increased its affinity towards ATP-competitive inhibitors, strengthening the anti-proliferative effects of PIM inhibitors (Ma *et al.* 2020).

Table 1. MicroRNAs that target the 3'UTRs of *PIM* family members, resulting in down-regulation of *PIM* mRNA transcripts

PIM family members	MicroRNAs targeting their 3'UTRs
PIM1	miR-15b (Roy *et al*. 2013), miR-16 (K.-T. Kim *et al*. 2012), miR-33a (Thomas *et al*. 2012), miR-124a (Bellon, Lu, and Nicot 2016), miR-195 (Z. Zhang *et al*. 2020), miR-214 (J. Zhou *et al*. 2021), miR-410-5p (Xia *et al*. 2020), miR-497-5p (Qiaojuan Zhu *et al*. 2019), miR-542-3p (Rang *et al*. 2016), miR-761 (W. Wang *et al*. 2022), miR-3135b (Y. Wang *et al*. 2021)
PIM2	miR-24-3p (F. Wang *et al*. 2021), miR-26b-5p (Han *et al*. 2019), miR-135-5p (H. Zhang 2017)
PIM3	miR-33a (Y. Wang, Liu, and Hu 2019), miR-203b (Dong *et al*. 2022), miR-370-5p (Feng *et al*. 2022), miR-574-3p (W. Song and Shi 2021)

2.2.2 PIM expression in healthy tissues and cancers

During normal fetal development, PIM1 protein expression is highly enriched in hematopoietic cells, the central nervous system and epithelia (Domen, van der Lugt, Laird, Saris, and Berns 1993; Eichmann *et al*. 2000). Notably, the PIM1 protein was found to be absent in adult liver and spleen but highly expressed in fetal liver and spleen (Amson *et al*. 1989), implying that PIM1 expression is developmentally regulated. According to the RNA-seq database from the NIH Genotype-Tissue Expression (GTEx) project (GTEx Consortium 2013), which contains data of 17,382 tissue samples obtained from 948 post-mortem adult individuals as well as two cell lines, *PIM1* is marginally regarded as a highly expressed gene in the esophagus and adipose tissue (**Figure 2**). This has been determined according to guidelines provided by EMBL's European Bioinformatics Institute, where TPMs (transcripts per million) higher than 1000 are regarded as highly expressed. For *PIM2* and *PIM3*, the top hits from healthy tissues are the spleen and the lungs, respectively, but their TPM values are well below 1000, indicating that they are not highly expressed even in these tissues.

In contrast to their modest expression in normal adult tissues, all three PIM family members have been found to be over-expressed in a multitude of cancers. Table 2 lists the cancer types where PIM proteins have been detected by immunohistochemistry or western blotting in clinical samples derived from patients. Elevated expression of PIMs grant cancer cells different types of benefits, which will be further discussed in Chapter 2.3, but the remarkable difference in PIM expression levels between tumor tissues and their normal counterparts provide therapeutic possibilities for targeting PIMs in cancer. Notably, mice deficient in all three PIM family members are viable and fertile, but with a smaller body size and subtle hematological changes (Mikkers *et al*. 2004; An, Kraft, and Kang 2013). Thus, it should be possible to develop PIM-selective inhibitors with favourable tolerability. On account of this, different pan-PIM inhibitors such as DHPCC9 (Akué-Gédu *et al*. 2009), AZD1208 (Keeton *et al*. 2014) and PIM447 (Burger *et al*. 2015) have been developed and some of them are being evaluated in clinical trials (Julson *et al*. 2022).

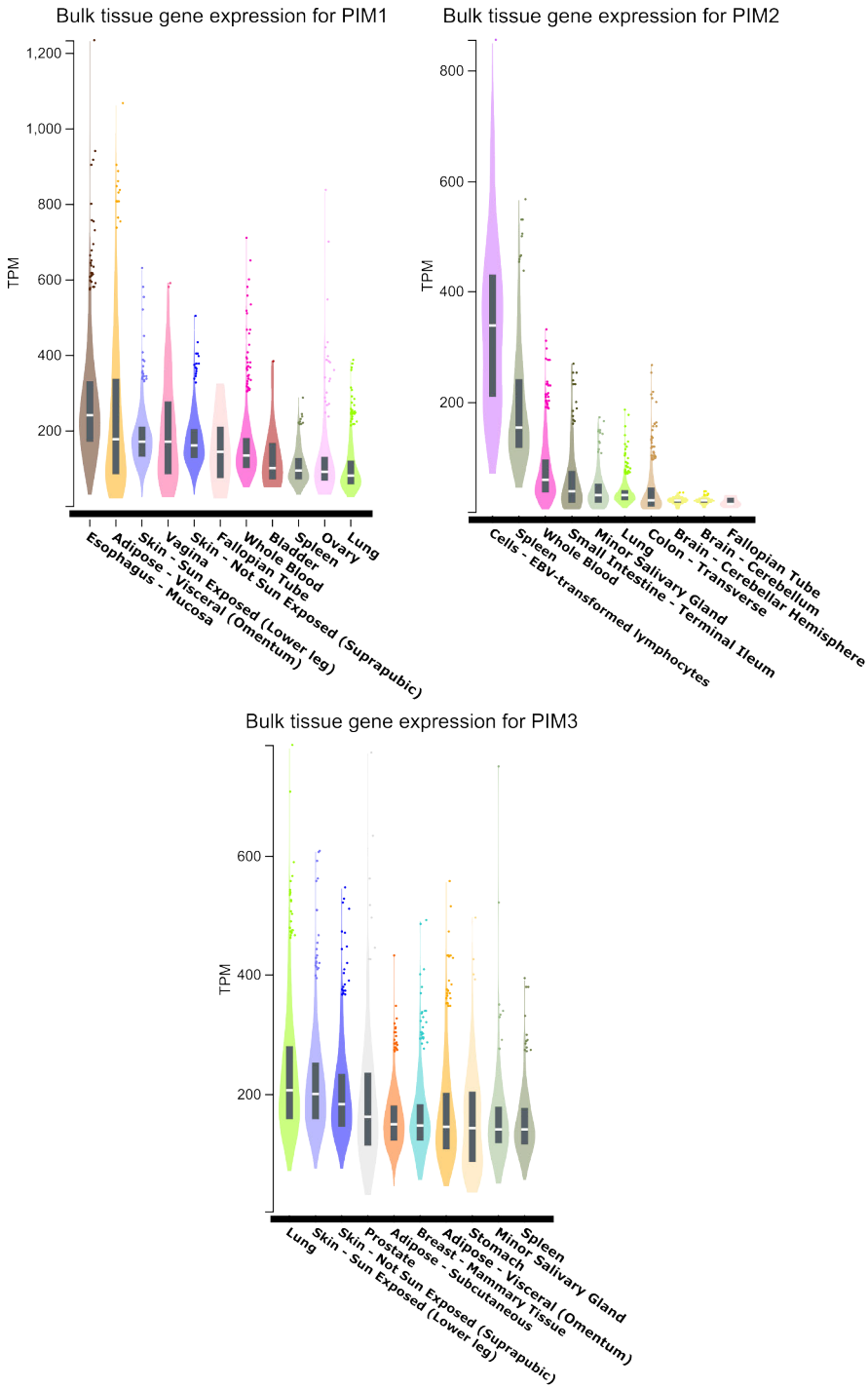

Figure 2. RNA-seq data of three *PIM* family members extracted from GTEx Analysis Release (V8). The top 10 tissue sites or cell lines have been arranged in descending order according to the expression levels of each *PIM* mRNA.

Table 2. Detection of PIM protein expression in patient samples of different cancer subtypes

PIM family members	Cancer subtypes	References
PIM1	Acute myeloid leukemia	(Meja *et al.* 2014)
	Astrocytoma	(Deng *et al*. 2016)
	Bladder cancer	(Guo *et al*. 2010)
	B-cell acute lymphocytic leukemia	(Kuang *et al*. 2019)
	Chronic lymphocytic leukemia	(Decker *et al*. 2014; Białopiotrowicz *et al*. 2018)
	Clear cell renal cell carcinoma	(Zhao *et al.* 2018)
	Colorectal cancer	(Zhang *et al.* 2018; Q. Li *et al.* 2020)
	Diffuse large B-cell lymphoma	(Brault *et al*. 2012)
	Endometrial carcinoma	(Takeuchi *et al*. 2022)
	Esophageal squamous cell carcinoma	(Wu *et al.* 2016)
	Gallbladder cancer	(Xue *et al*. 2018)
	Gastric cancer	(Yan *et al*. 2012)
	Head and neck squamous cell carcinomas	(Beier *et al*. 2007; K. Peltola *et al*. 2009)
	Hepatocellular carcinoma	(Leung *et al*. 2015)
	Hodgkin's lymphoma	(Szydłowski *et al*. 2017)
	Mantle cell lymphoma	(Yang *et al.* 2012)
	Melanoma	(Shannan *et al*. 2016)
	Multiple myeloma	(Ramachandran *et al*. 2016)
	Non-small-cell lung carcinoma	(Jin *et al.* 2012; Moore *et al.* 2021)
	Oral squamous cell carcinoma	(Chiang *et al*. 2006)
	Osteosarcoma	(Mou *et al.* 2016)
	Pancreatic cancer	(J. Xu *et al.* 2016)
	Pancreatic ductal adenocarcinoma	(D. Xu *et al.* 2011)
	Papillary thyroid carcinoma	(Wen *et al.* 2021)
	Primary mediastinal large B-cell lymphoma	(Szydłowski, Dębek, *et al*. 2021)
	Prostate cancer	(Dhanasekaran *et al.* 2001; Valdman *et al.* 2004; Eerola *et al.* 2021)
	Salivary gland adenoid cystic carcinoma	(Zhu *et al.* 2018)
	Small cell lung carcinoma	(Motylewska, Braun, and Stępień 2020)
	Triple-negative breast cancer	(Horiuchi *et al*. 2016)
	Tongue squamous cell carcinoma	(S. Tanaka *et al*. 2009)
	Urothelial carcinoma	(Foulks *et al.* 2014)
PIM2	Acute myeloid leukemia	(Meja *et al.* 2014)
	B-cell acute lymphocytic leukemia	(Kuang *et al.* 2019)
	Breast cancer	(Ren *et al.* 2018; Yang *et al.* 2019)
	Chronic lymphocytic leukemia	(Decker *et al*. 2014; Białopiotrowicz *et al*. 2018; Cervantes-Gomez *et al*. 2019; Kapelko-Słowik *et al.* 2019)

PIM family members	Cancer subtypes	References
	Diffuse large B-cell lymphoma	(Gómez-Abad *et al.* 2011; Brault *et al.* 2012; Marino *et al.* 2022)
	Gastric cancer	(H. Xin, Deng, and Cao 2018)
	Hepatocellular carcinoma	(Gong *et al.* 2009; Tang *et al.* 2020; J.-C. Wang *et al.* 2022)
	Hodgkin's lymphoma	(Szydłowski *et al.* 2017)
	Mantle cell lymphoma	(Q. Yang *et al.* 2012)
	Melanoma	(Shannan *et al.* 2016)
	Multiple myeloma	(Ramachandran *et al.* 2016)
	Osteosarcoma	(Mou *et al.* 2016)
	Primary mediastinal large B-cell lymphoma	(Szydłowski, Dębek, *et al.* 2021)
	Prostate cancer	(Ren *et al.* 2013; Eerola *et al.* 2021)
	Urothelial carcinoma	(Foulks *et al.* 2014)
PIM3	Bronchopulmonary neuroendocrine neoplasms	(Motylewska, Braun, and Stępień 2020)
	Chronic lymphocytic leukemia	(Decker *et al.* 2014; Białopiotrowicz *et al.* 2018)
	Colorectal cancer	(Popivanova *et al.* 2007; Zhang *et al.* 2017)
	Diffuse large B-cell lymphoma	(Forshell *et al.* 2011; Brault *et al.* 2012; Szydłowski, Garbicz, *et al.* 2021)
	Gastric cancer	(Zheng *et al.* 2008; Lou *et al.* 2014; Dong *et al.* 2022)
	Hepatoblastoma	(Stafman *et al.* 2019)
	Hepatocellular carcinoma	(Fujii *et al.* 2005)
	Hodgkin's lymphoma	(Szydłowski *et al.* 2017)
	Mantle cell lymphoma	(Forshell *et al.* 2011; Yang *et al.* 2012)
	Melanoma	(Shannan *et al.* 2016)
	Multiple myeloma	(Ramachandran *et al.* 2016)
	Nasopharyngeal carcinoma	(Ai *et al.* 2016)
	Osteosarcoma	(Mou *et al.* 2016)
	Pancreatic cancer	(Li *et al.* 2006)
	Pancreatic ductal adenocarcinoma	(Xu *et al.* 2013; Zhang *et al.* 2013)
	Primary mediastinal large B-cell lymphoma	(Szydłowski, Dębek, *et al.* 2021)
	Prostate cancer	(Eerola *et al.* 2021)
	Small cell lung carcinoma	(Motylewska, Braun, and Stępień 2020)
	Urothelial carcinoma	(Foulks *et al.* 2014)

2.2.3 PIM kinases in prostate and breast tumorigenesis

As androgens are essential for the growth of the normal prostate, androgen ablation therapy is often initially used in order to cure prostate cancer. However, as prostate tumors progress, they gradually lose their dependency on androgens, rendering anti-androgen therapies ineffective (B. J. Feldman and Feldman 2001). In parallel, the androgen receptor (AR) is expressed in normal prostate and throughout the prostate cancer progression, as well as in androgen-independent prostate cancer, in which the transcriptional activity of AR is frequently associated with the mitotic growth and survival of prostate (Heinlein and Chang 2004).

PIM1 protein is highly expressed in malignant prostate cancer samples but not in their benign counterparts (Dhanasekaran *et al*. 2001; Valdman *et al*. 2004; Hui-chan He *et al*. 2009). PIM1 has been shown to phosphorylate AR, resulting in decreased androgen-mediated activation of AR (Thompson *et al*. 2003; Ha *et al*. 2013). Yet it has also been shown that PIM1 promotes IL-6-mediated androgen-independent activation of AR (Chen, Wang and Farrar 2000; Kim *et al.* 2004). Notably, elevated IL6 serum levels have been observed in prostate cancer patients with androgen-independence as well as metastatic prostatic carcinoma (Hoosein *et al*. 1995; Adler *et al*. 1999). It is thus tempting to speculate that PIM1 is involved in the development of androgen-independent prostate cancer. Aside from androgen signalling, PIM1 protein promotes a number of oncogenic events, including prostate tumor growth (W. W. Chen *et al*. 2005) and metastasis (Santio *et al*. 2015). While positive or no correlations between PIM1 expression and prostate tumor stage have been reported (Dhanasekaran *et al*. 2001; Valdman *et al*. 2004; Cibull *et al*. 2006; M. P. Jiménez-García *et al*. 2016; Eerola *et al*. 2021), co-expression of PIM1 and MYC is linked to higher Gleason grades (J. Wang *et al*. 2010). This could be explained in part by the synergistic effects of PIM1 and MYC in tumor progression (J. Wang *et al*. 2012), as PIM1 has been reported to inhibit MYC degradation (Y Zhang *et al*. 2008) and modulate expression of MYC-regulated genes (Zippo *et al*. 2007). Additionally, PIM1 expression has been found to be upregulated in metastatic prostate carcinomas in TP53 and RB (the **r**etino**b**lastoma tumour suppressor) double knock-out mice (Z. Zhou *et al*. 2006), indicating that it plays an important role in prostate tumorigenesis.

Both PIM1 and PIM2 have been found to be highly expressed in breast tumors compared to normal counterparts (M.-P. Jiménez-García *et al*. 2017). PIM1 protein expression has also been found to be inducible by both estrogen (Malinen *et al*. 2013; Santio, Landor, *et al*. 2016) as well as progesterone (Gapter *et al*. 2006) in various cancer cell lines. Among breast cancer subtypes, triple-negative breast cancer (TNBC) has the worst clinical outcome. This cancer type is classified by the absence of estrogen receptors, progesterone receptors and human epidermal growth factor receptor 2 (HER2) and it accounts for 12-17% of all breast cancers (Foulkes, Smith

and Reis-Filho 2010; Newman *et al.* 2015). Both PIM1 and MYC expression levels have been found to be significantly higher in TNBC cells than in non-TNBC cells (Horiuchi *et al*. 2016). Notably, MYC expression was found to be a factor in TNBC cell sensitivity to PIM inhibition: the higher the MYC expression, the stronger the anti-proliferative effects of PIM inhibition (Horiuchi *et al*. 2016). This is of importance, because chemotherapy is still the standard treatment for TNBC (Isakoff 2010; Wahba and El-Hadaad 2015) and MYC amplification contributes to the chemotherapy resistance in residual TNBC cells (Balko *et al*. 2014). Targeting PIM in TNBC cases with high MYC expression levels may thus provide clinical benefits to patients. In addition to TNBC, PIM1 has been shown to maintain HER2 expression in HER2-positive cells (B.-W. Wang *et al*. 2021) and has been identified as a candidate to confer resistance to anti-HER2 treatment in HER2-positive breast cancer (Moody *et al*. 2015). Taken together, PIM kinases provide promising therapeutic targets for both prostate and breast cancer.

2.3 Signalling pathways regulated by PIM kinases

2.3.1 Regulation of cell survival

PIMs support cell survival in part via phosphorylation of effector proteins that regulate apoptotic processes (**Figure 3**). For instance, BAD (**B**cl-2 **a**gonist of cell **d**eath) is a proapoptotic member of the BCL-2 (**B**-**c**ell **l**ymphoma **2**) family and can form heterodimers with the anti-apoptotic proteins BCL-2 or BCL-Xl (Elmore 2007). Binding of BAD with BCL-2 or BCL-xL triggers aggregation of BAX (**B**cl-2-**a**ssociated **X** protein) or BAK (**B**cl-2 homologous **a**ntagonist **k**iller) proteins into the mitochondrial membrane. This causes mitochondrial outer membrane permeabilization (MOMP), followed by the release of cytochrome C and caspase activation (Martinou and Youle 2011). PIMs phosphorylate BAD at multiple sites and promote interactions between BAD and the 14-3-3 protein (Aho *et al*. 2004; Macdonald *et al*. 2006; Saurabh *et al*. 2014). This prevents the binding of BAD with BCL-2 or BCL-xL and thereby inhibits BAD-mediated apoptosis.

Apart from regulating BAD protein, PIMs also influence the protein expression levels of other members of the BCL-2 family. In particular, expression of the anti-apoptotic BCL-2 and BCL-xL proteins are induced by over-expression of PIM1 (Muraski *et al*. 2007), while expression of the apoptotic protein BIM (**B**cl-2 **I**nteracting **M**ediator of cell death) is decreased by over-expression of PIM2 (Y. Xu *et al*. 2016). Conversely, silencing PIM2 protein expression induces expression of the proapoptotic BAX protein (Hospital *et al.* 2018). Other members of the BCL-2 family, such as the anti-apoptotic MCL-1 (**m**yeloid **c**ell **l**eukemia sequence **1**), and the proapoptotic NOXA (phorbol-12-myristate-13-acetate-induced protein 1), have

been shown to be downregulated and upregulated, respectively, in cancer cell lines lacking PIM expressions or activities (Jin H. Song and Kraft 2012).

During apoptosis, the dynamin-related protein 1 (DRP1) promotes mitochondrial fission and mediates the subsequent release of cytochrome C into the cytosol (Wasiak, Zunino, and McBride 2007). PIM1 phosphorylates DRP1 at Ser367 and inhibits the translocation of DRP1 towards the mitochondrial membrane, thereby preventing leakage of cytochrome C from mitochondria (Din *et al*. 2013). In addition to DRP1, the association of hexokinase with the outer mitochondrial membrane has been documented to prevent release of cytochrome C from mitochondria (Majewski *et al*. 2004), and to be dependent on the phosphorylation of hexokinase at Thr473 by AKT kinase (Roberts *et al*. 2013). Notably, PIM2 shares the same phosphorylation site on hexokinase as AKT, but the corresponding consequences on apoptosis suppression have not been studied (T. Yang *et al*. 2018).

In addition to preventing apoptosis, PIMs also play important roles in maintaining cell survival under other types of stressful conditions. In response to chemotherapeutic drugs, PIM-1L has been reported to interact with and activate ETK, leading to suppression of TP53-mediated apoptosis (Y. Xie *et al*. 2006). In relation to this, DAPK3 (**d**eath-**a**ssociated **p**rotein **k**inase **3**) has been shown to attenuate TP53 activity (Craig *et al*. 2007). PIM2 phosphorylates DAPK3 at Ser306, facilitating the nuclear export of DAPK3 and thereby repressing TP53-mediated apoptosis (Lei Wang *et al*. 2021). Moreover, PIM1 protein is also involved in modulation of cellular drug resistance, in part via phosphorylation of different drug efflux exporters such as BCRP (**b**reast **c**ancer **r**esistance **p**rotein) (Yingqiu Xie *et al*. 2008) and P-gp (**P**-**g**lyco**p**rotein) (Yingqiu Xie *et al*. 2010), which enable cytotoxic drugs to be efficiently pumped out of the cells. Additionally, under H_2O_2-induced stress conditions, PIM1 maintains cell survival by inactivating the proapoptotic ASK1 (**a**poptosis **s**ignal-regulating **k**inase **1**) via phosphorylation at Ser83 (Gu *et al*. 2009).

Other than direct phosphorylation of proapoptotic or anti-apoptotic effectors, PIMs also regulate gene expression related to cell survival. PIMs promote the transcriptional activities of the NF-κB transcription factor through phosphorylation of the NF-κB subunit RelA/p65 (Nihira *et al.* 2010) as well as phosphorylation of the COT kinase (**c**ancer **o**saka **t**hyroid kinase) (Hammerman *et al*. 2004). PIM1 also phosphorylates and inactivates the forkhead transcription factors FOXO1A and FOXO3A, causing the expression of apoptosis-related genes to be reduced (Huang and Tindall 2007; Morishita *et al.* 2008). Very recently, it has even been shown that PIM1 overexpression suppresses ferroptosis, in part via decreased expression of ferroptotic genes as well as increased production of glutathione (Yuan *et al*. 2022).

The diverse effects of PIM kinases on cell survival, both in terms of regulation of gene expression or directly acting on effector proteins, provide therapeutic

opportunities for cancer treatment. In particular, immunotherapy has been emerging as a novel pillar for cancer treatment, yet non-responders to immune checkpoint inhibitors are prevalent. The resistance to immunotherapy is strongly correlated with the immunosuppressive effects of myeloid derived suppressor cells (MDSCs) located within tumors. It has recently been demonstrated that the immunosuppressive effect of PIM-1-deficient MDSCs is greatly diminished, as is their ability to inhibit T-cell proliferation (G. Xin *et al*. 2021). In line with this, there are several reports independently showing that PIM inhibition results in enhanced antitumor effects with PD-L1 blockade (G. Xin *et al*. 2021; J.-C. Wang *et al*. 2022), suggesting that use of PIM inhibitors may improve the functional outcomes of immunotherapy.

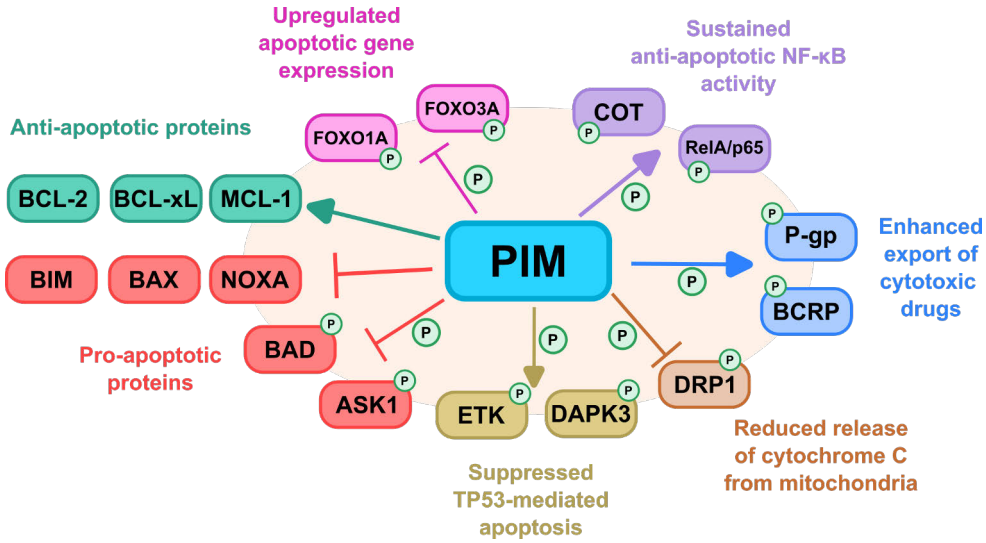

Figure 3. PIMs regulate cell survival by phosphorylating multiple downstream targets and modulating expression of proteins regulating apoptosis. PIMs phosphorylate and inactivate BAD, ASK1 and DRP1 proteins as well as FOXO1A and FOXO3A transcription factors to suppress apoptosis. PIMs phosphorylate both ETK and DAPK3 proteins as a means to suppress TP53-mediated apoptosis. PIMs also phosphorylate BCRP and P-gp to facilitate the export of cytotoxic drugs, while sustaining anti- apoptotic NF-κB activities via phosphorylation of the NF-κB subunit RelA/p65 and COT kinase. PIMs upregulate the expression of anti-apoptotic proteins such as BCL-2, BCL-xL and MCL-1, while they downregulate the expression of pro-apoptotic proteins such as BIM, BAX and NOXA.

2.3.2 Regulation of cell proliferation

Cell cycle progression is intimately connected to cell proliferation, as it determines the timing of DNA synthesis as well as mitosis, enabling the generation of two daughter cells from a single parent cell. PIMs have been shown to promote cell cycle

progression through various mechanisms (**Figure 4**). One of them is the regulation of cyclin-dependent kinase (CDK) activity. CDKs facilitate cell cycle progression via the phosphorylation of multiple downstream targets. They remain in an inactivated state when both Thr14 and Tyr15 residues are phosphorylated (Malumbres 2014). PIM1 phosphorylates and activates the phosphatase activity of Cdc25A (M-phase inducer phosphatase 1), which dephosphorylates CDKs at both Thr14 and Tyr15 residues, leading to cell cycle progression (Mochizuki *et al*. 1999) (**Figure 4A**). Cyclin E-CDK2 complexes, which are in charge of G1/S progression, are inhibited upon binding of p27 protein (G1 checkpoint cyclin-dependent kinase inhibitor 1B) (Morishita *et al*. 2008). All three PIM members have been shown to phosphorylate p27 and promote interactions between 14-3-3 proteins and p27 protein, resulting in proteasome-dependent degradation of p27 (Morishita *et al.* 2008). Moreover, PIM1 phosphorylates and stabilises SKP2 (**S**-Phase **k**inase associated **p**rotein **2**), which is an E3 ligase that facilitates ubiquitination of p27 and thus promotes degradation of the p27 protein (Cen *et al*. 2010). Lastly, PIM1 phosphorylates and inactivates the forkhead transcription factors FOXO1A and FOXO3A that otherwise promote the expression of p27 mRNA transcripts (Morishita *et al.* 2008). PIMs also target another cyclin-dependent kinase inhibitor p21 (G1 checkpoint cyclin-dependent kinase inhibitor 1A). PIMs phosphorylate p21 and support its cytosolic accumulation, so that p21 is no longer able to interact with and inhibit nuclear cyclin E-CDK2 complexes, favoring progression in the G1/S phase (Yandong Zhang, Wang, and Magnuson 2007; Z. Wang *et al*. 2010).

In addition to G1-S phase progression, PIM1 also facilitates cell cycle progression at the G2/M phase (**Figure 4B**). PIM1 phosphorylates and activates the phosphatase activity of Cdc25C (M-phase inducer phosphatase 3), which in turn dephosphorylates and activates the corresponding cyclin-dependent kinases for G2/M phase progression (Bachmann *et al*. 2006). C-TAK1 (Cdc25C-associated kinase 1) has been shown to inhibit the phosphatase activity of Cdc25C (Bachmann *et al*. 2004). Via phosphorylation, PIM1 relieves the inhibitory effects of C-TAK1 towards Cdc25C, allowing Cdc25C to function effectively to promote G2/M phase progression (Bachmann *et al*. 2004), and the subsequent phase involving mitosis and cytokinesis. During mitosis, PIM1 has been shown to interact with the nuclear mitotic apparatus (NuMA) and the heterochromatin-associated protein 1 beta (HP1beta), while ablation of these interactions has been shown to result in apoptosis (Bhattacharya *et al*. 2002).

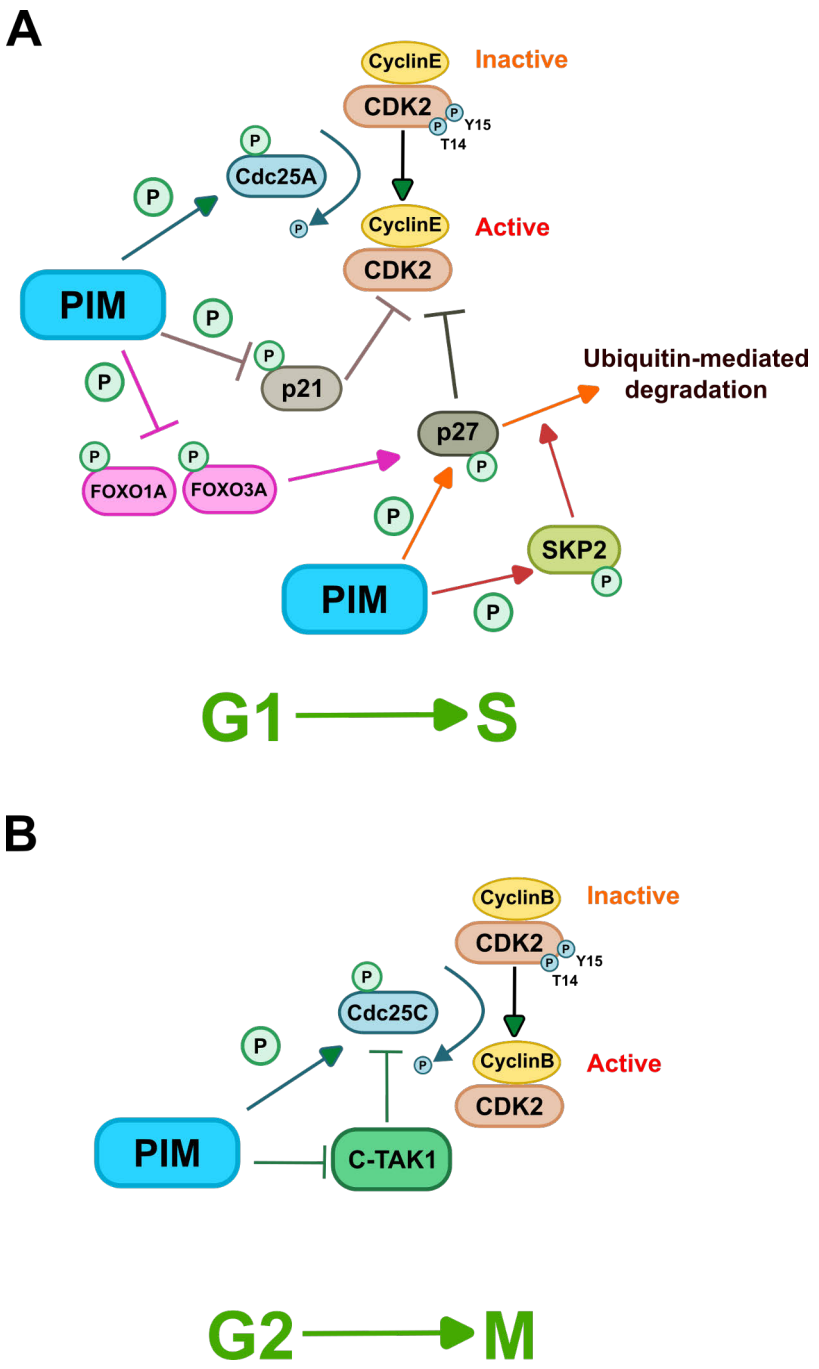

Figure 4. PIMs regulate cell cycle progression at the G1/S and G2/M phases. PIMs phosphorylate different regulatory proteins, which in turn activate cyclinE-CDK2 and cyclinB-CDK1 complexes to favor cell cycle progression.

On the other hand, mTORC1 (**m**echanistic **t**arget **o**f **r**apamycin **c**omplex **1**) is another serine/threonine kinase that promotes cellular growth through activation of anabolic reactions (Hietakangas and Cohen 2009; Ben-Sahra and Manning 2017). PIMs have been shown to increase the activity of mTORC1 via different mechanisms (**Figure 5**). PIM1 and PIM2 phosphorylate PRAS40 (**p**roline-**r**ich **A**KT **s**ubstrate **40** kDa) at Thr426 (Fengxue Zhang *et al*. 2009) and TSC2 (**t**uberous **s**clerosis **c**omplex **2**) at Ser1798 (J. Lu *et al*. 2013), which relieves their suppressive effects on mTORC1 and thus lead to increased mTORC1 activities. During amino acid starvation, mTORC1 activity is suppressed by regulatory protein complexes involving GATOR1 (**G**TPase-**a**ctivating protein **to**ward **R**ags **1**) (Wolfson *et al*. 2017). PIMs phosphorylate one of the components of the GATOR1 complex, DEPDC5 (**DEP** **d**omain-**c**ontaining **5**), resulting in alleviation of mTORC1 suppression (Padi *et al*. 2019). In addition to targeting the upstream effectors of mTORC1, PIMs also act on several downstream targets of mTORC1 signalling. For example, PIM1 and PIM2 phosphorylate eIF4B (**e**ukaryotic translation **i**nitiation **f**actor **4B**) at Ser406 and Ser422, facilitating the binding of eIF4B to eIF3 (**e**ukaryotic **i**nitiation **f**actor **3**), which is required for effective protein synthesis (J. Yang *et al*. 2013). Moreover, enhanced PIM1 or PIM2 protein expression increases phosphorylation levels of 4E-BP1 (**e**ukaryotic translation **i**nitiation **f**actor **4E**-**b**inding **p**rotein **1**) (Fox *et al.* 2003; Chen *et al.* 2005), leading to decreased affinity of 4EBP1 towards eIF4E (**e**ukaryotic translation **i**nitiation **f**actor **4E**) complex, and thus facilitating cap-dependent translation. In concert with this, reduced cap-dependent translation activity has been observed in MEFs (**M**ouse **E**mbryonic **F**ibroblasts) deficient of all three PIM kinase members (Beharry *et al*. 2011). mTORC1 is a major regulator that ensures homeostatic cell growth and division in normal cells, but it is abnormally activated in cancer cells and contributes to uncontrolled tumor growth. In this regard, the activation of several proteins both upstream and downstream of mTORC1 pathways by PIM kinases represents a clear link to the pro-proliferative role of PIM kinases.

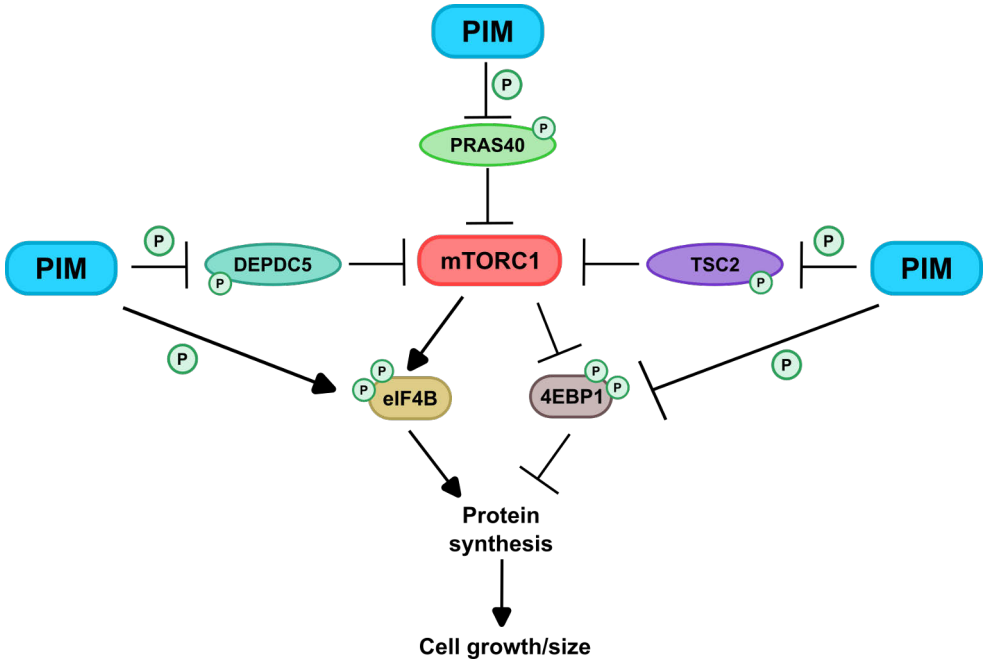

Figure 5. PIMs regulate different components of the mTORC1 signalling pathway. PIMs phosphorylate and inactivate PRAS40, TSC2 and DEPDC5 proteins, relieving their suppressive effects on the mTORC1 kinase, and enabling the phosphorylation of eIF4B and 4EBP1 by mTORC1 to facilitate protein synthesis. Notably, PIMs also promote protein synthesis via phosphorylation of eIF4B and 4EBP1.

2.3.3 Regulation of cell metabolism

Cell metabolism is intricately linked to tumor progression, as effective biosynthesis of macromolecules underpins the needs of rapidly proliferating cancer cells. Experimental results from several studies indicate that PIMs are involved in the regulation of cell metabolism. For instance, inactivation of PIM kinases has resulted in alteration of mitochondrial morphology (Din *et al*. 2014), impaired glycolytic phenotypes (Leung *et al*. 2015; J H Song *et al*. 2015; Chatterjee *et al*. 2019) as well as decreased expression levels of HIF-1α (**h**ypoxia-**i**nducible **f**actor **1**-**alpha**) (Casillas *et al*. 2021).

Mechanistic studies have revealed that PIMs are positive regulators of glycolysis in part via phosphorylation of multiple glycolytic enzymes (**Figure 6**). PIM2 phosphorylates HK2 (**h**exo**k**inase-**II**) at Thr473 (T. Yang *et al*. 2018), PKM2 (**p**yruvate **k**inase **m**uscle isoform **2**) at Thr454 (Z. Yu *et al*. 2013) and PFKFB3 (6-**p**hospho**f**ructose-2-**k**inase/**f**ructose-2,6-**b**isphosphatase **3**) at Ser478 (C. Lu *et al*. 2021), preventing all of them from undergoing degradation and thus enabling sustained cellular glycolysis. Other than direct phosphorylation of glycolytic enzymes, PIMs also interact with transcription factors that regulate glucose

metabolism. PIM1 phosphorylates HIF-1α at Thr455 and prevents HIF1α from undergoing ubiquitination, resulting in increased expression of HK2 mRNA transcripts even under normoxic conditions (Casillas *et al*. 2021). NRF2 (**n**uclear factor erythroid 2–**r**elated **f**actor **2**) is a transcription factor that binds to the promoter regions of genes involved in the pentose phosphate pathway (PPP). The absence of NRF2 protein expression is linked to defects in PPP activity (Mitsuishi *et al*. 2012). PIM1 has been shown to increase NRF2 transcriptional activity by inhibiting its ubiquitin-mediated degradation, hence contributing to an increase in PPP activity (Jin H. Song *et al*. 2018). All three PIM family members phosphorylate IRS1 (**i**nsulin **r**eceptor **s**ubstrate **1**) at Ser1101 and mildly increase its half-life (Jin H Song *et al*. 2016), but the impact of PIM-mediated phosphorylation has remained unknown. *PIM3* knock-out mice, on the other hand, show an increase in insulin sensitivity as well as glucose tolerance, implying that PIMs play an unexplored role in the regulation of insulin signalling (Vlacich *et al*. 2010).

In addition to direct phosphorylation-dependent regulation of enzymes or transcription factors involved in glucose metabolism, it has been shown that inhibition of PIM expression or activity leads to activation of AMPK (5'**AMP**-activated protein **k**inase) (Beharry *et al.* 2011), a well-known master regulator of metabolism (Long and Zierath 2006). AMPK phosphorylates and inhibits the activity of ACC (**a**cetyl-**C**oA **c**arboxylase), which catalyses the conversion of acetyl CoA to malonyl CoA in the cytoplasm. Malonyl CoA is an essential regulator of fatty acid metabolism owing to its two special properties. First, it provides the carbon atoms essential for fatty acid synthesis. Secondly, it is an inhibitor of the mitochondrial fatty acid transporter carnitine palmitoyl transferase 1 (CPT1) (A. K. Saha and Ruderman 2003). Thus, when AMPK phosphorylates and inactivates ACC activity, less malonyl CoA is generated. This triggers a decline in fatty acid synthesis as well as alleviates the inhibition of CPT1, so that fatty acids can be readily transported to mitochondria via CPT1, contributing to increased fatty acid oxidation. In line with this, an acute treatment with the pan-PIM inhibitor AZD1208 triggered AMPK phosphorylation with consequential inactivation of ACC, leading to increased fatty acid oxidation, which caused a decrease in both lipid droplets and triglyceride contents in 3T3-L1 cells (Yadav *et al*. 2019). Of note, it has been shown that during prolonged AMPK activation, fatty acid metabolism is decoupled from ACC activity, but instead regulated by other factors such as peroxisome proliferator-activated receptor (PPARα) and PGC-1α (**p**eroxisome proliferator-activated receptor **g**amma **c**oactivator **1**-alpha) (W. J. Lee *et al*. 2006; Wojtaszewski *et al*. 2002). To this end, cardiac lysates as well as fibroblasts derived from mice deficient of all three PIM family members displayed decreased expression of PGC-1α, leading to alteration of gene expression related to fatty acid oxidation, which could be reversed by PGC-1α overexpression (Beharry *et al*. 2011; Din *et al*. 2014). The data presented

above suggest that PIM kinases regulate both glucose and fatty acid metabolism. However, there is surprisingly little research into the effects of PIM kinases on amino acid metabolism, such as glutamine, serine, or glycine. In particular, as MYC is a well-known transcriptional factor that accounts for glutamine addiction in cancer cells (Wise *et al*. 2008), and as PIM1 has been shown to prevent MYC degradation (Y Zhang *et al*. 2008) and facilitate the expression of a subset of MYC-regulated genes (Zippo *et al*. 2007), it is reasonable to expect PIM kinases to play a regulatory role also in glutamine metabolism of cancer cells.

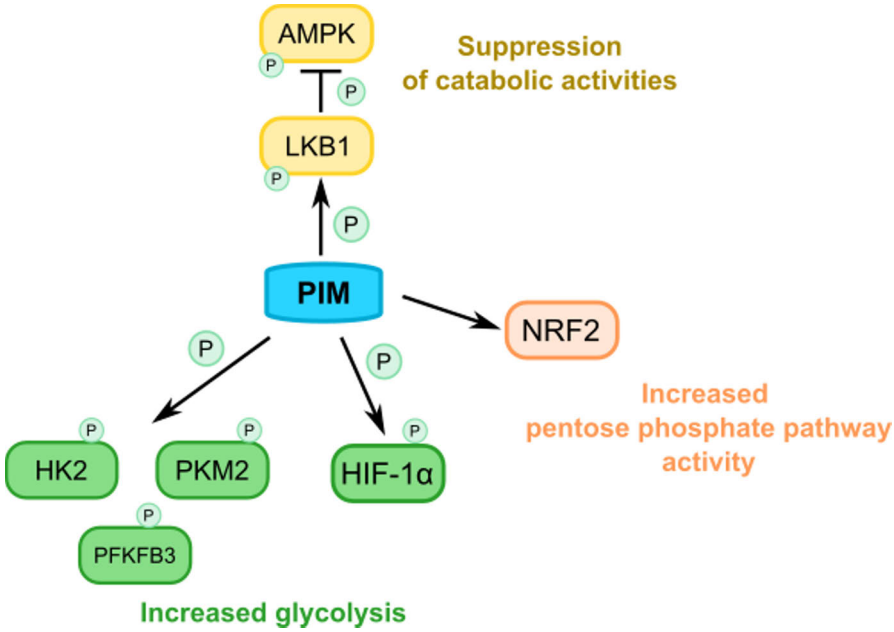

Figure 6. PIMs regulate cell metabolism predominantly by phosphorylating downstream targets. PIMs promote glycolysis via the phosphorylation of multiple glycolytic enzymes such as HK2, PKM2 and PFKFB3 as well as the transcription factor HIF-1α. PIMs interact with NRF2 and prevent its degradation, in turn leading to increased pentose phosphate pathway activity. PIMs also suppress catabolic activities such as fatty acid oxidation in part via inhibition of AMPK activation.

2.3.4 Regulation of cell motility

Over-expression of any of the PIM family members has been shown to promote migration of prostate cancer cells (Santio *et al*. 2010). Conversely, inactivation of PIMs has diminished cancer cell metastasis in xenograft mouse models (Santio *et al.* 2010; Tang *et al.* 2020). These data suggest that PIMs are involved in the regulation of cell motility. During EMT, tumor cells acquire mesenchymal features to enable cellular movements and migration. PIM1 upregulates expression of EMT-associated

transcription factors in part via phosphorylation of SMAD2 (mothers against decapentaplegic homolog 2), SMAD3 (mothers against decapentaplegic homolog 3) (B. Zhao *et al*. 2018) and MYC protein (B. Zhao *et al*. 2018; Gao *et al*. 2019). In accordance with this, knockdown of PIM1 or PIM2 in cancer cell lines has resulted in increased expression of E-cadherin and decreased expression of N-cadherin as well as EMT-associated transcription factors (Uddin *et al*. 2015; B. Zhao *et al*. 2018; H. Xin, Deng, and Cao 2018; J.-C. Wang *et al*. 2022), whereas over-expression of PIM1 has exhibited opposite trends (Gao *et al.* 2019; Liu *et al.* 2020; X. Zhang *et al.* 2020). Degradation of the extracellular matrix by matrix metalloproteinases (MMPs) provides room for cellular migration and has been shown to contribute to cell invasion and metastasis. PIM inhibition has been shown to decrease MMP2 and MMP9 protein expression in cultured cancer cell lines (B. Zhao *et al*. 2018; Eerola *et al*. 2019). Also, mouse embryonic fibroblasts deficient in all three family members displayed remarkably decreased MMP9 protein expression and were less aggressive towards bone invasion in a mouse model where tumor formation was induced by methylcholanthrene (Narlik-Grassow *et al*. 2012). In this regard, NFATC1 (**n**uclear **f**actor of **a**ctivated **T**-cells, **c**ytoplasmic **1**) is a transcription factor that positively regulates both MMP2 and MMP9 mRNA expression (Wang *et al.* 2015), and its transcriptional activity is increased upon phosphorylation by PIM1 (Rainio, Sandholm, and Koskinen 2002; Glazova *et al*. 2005; Eerola *et al*. 2019). Accordingly, over-expression of the NFATC1 protein promoted the migration of prostate cancer cells, while its pro-migratory effects were abolished upon treatment with the pan-PIM inhibitor DHPPC9 (Santio *et al*. 2010). These data indicate that PIMs regulate cell motility in part via regulation of the transcriptional activity of NFATC1.

In addition to tumor cell detachment from the primary site, colonization of the secondary site also determines the outcome of metastasis. Metastatic niche signals aid in the homing of circulating tumor cells into secondary sites, which is in part governed by the specific interactions between chemokines in the target organs and chemokine receptors on the surface of cancer cells. CXCR4 (**C**-**X**-C **c**hemokine **r**eceptor type **4**) is found to be highly expressed in the cell surfaces of breast cancer cell lines as well as primary tumors, while its cognate ligand CXCL12 (**C**-**X**-C motif **c**hemokine **l**igand **12**) is abundant in the common metastatic sites of breast cancers, such as bone marrow and lung (Müller *et al*. 2001). The importance of the CXCR4/CXCL12 signalling axis in metastasis is illustrated by the experimental data showing that silencing of CXCR4 protein expression in breast cancer cells reduced lung metastasis (Müller *et al*. 2001; Liang *et al*. 2005). Of note, PIM1 is frequently found to be over-expressed in the circulating tumor cells from prostate cancer patients (Markou *et al*. 2020). To this end, PIM1 and PIM3 but not PIM2 phosphorylate CXCR4 protein at Ser339, which enhances expression of the CXCR4

protein on the cell surface, and thus assists the migration of cancer cells towards the CXCL12 chemokine gradient (Grundler *et al.* 2009; Decker *et al.* 2014; Santio *et al.* 2015). In addition to CXCR4, phosphorylation of several downstream targets of PIMs such as GSK3B (**g**lycogen **s**ynthase **k**inase **3** **beta**), FOXP3 (**fo**rkhead bo**x** **P3**), NOTCH1 (neurogenic locus notch homolog protein 1) and NDRG1 (**N**-myc **d**ownstream-**r**egulated **g**ene **1**) have also been indicated to promote cancer cell migration and invasion (Santio *et al.* 2010, 2020; Santio, Landor, *et al.* 2016; Santio, Salmela, *et al.* 2016; Ledet *et al.* 2021), supporting the pro-migratory role of PIM kinases.

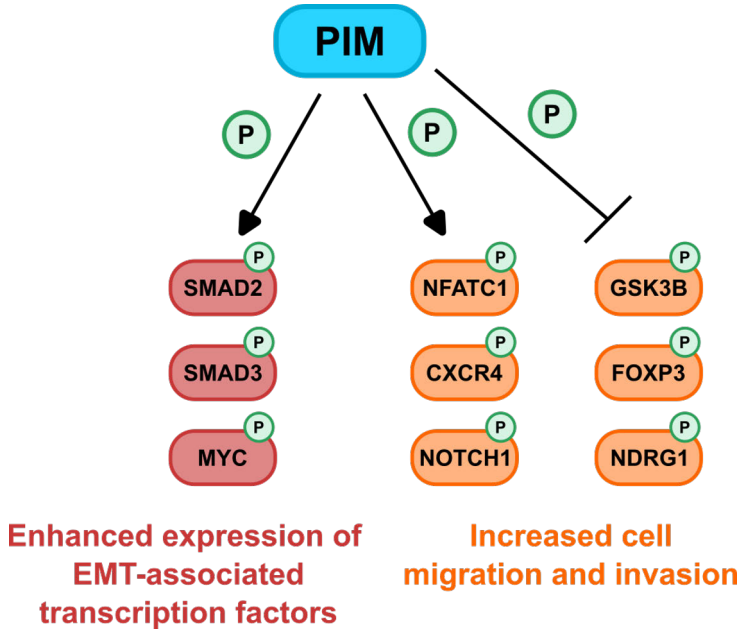

Figure 7. PIMs regulate cell motility by phosphorylating downstream targets. PIMs upregulate EMT-associated transcription factors in part via phosphorylation of SMAD2, SMAD3 and MYC proteins. Via phosphorylation of multiple targets, including NFATC1, CXCR4, GSK3B, FOXP3, NOTCH1, CAPZ and NDRG1, PIMs promote the migration and invasion of cancer cells.

2.4 PIM kinase substrates identified in this study

2.4.1 Actin capping proteins

The capping protein (CP), also known as β-actinin or CapZ, is found in almost all cells in eukaryotic organisms including humans, fungi and plants (John A. Cooper and Sept 2008). It was first purified from muscle in the 1960s and found to inhibit actin polymerisation *in vitro* (Maruyama 1966). It was subsequently isolated from

Acanthamoeba castellanii in the 1980s and shown to bind to the barbed ends of actin filaments (Isenberg, Aebi, and Pollard 1980). CP is a heterodimer composed of α and β subunits with a combined molecular mass of around 64kDa. CP subunits are unstable when they are monomeric but become stable when they are heterodimerised (John A. Cooper and Sept 2008).

Elongation of actin filaments is accomplished via polymerisation of actin monomers at the barbed ends. CP heterodimers bind to the barbed ends of actin filaments with 1:1 stoichiometry, and thus terminate elongation of these filaments, enabling cells to maintain a fine control on both the spatial and temporal distribution of actin filaments (Wear *et al.* 2003; Edwards *et al.* 2014). In muscle cells, CP binds to the barbed ends of actin thin filaments in Z-discs, effectively inhibiting actin polymerisation or depolymerization (Caldwell *et al*. 1989). In non-muscle cells, CP binds to the barbed ends of the multiple filaments at the cell edges and prevents extended elongation of specific actin filaments, enabling the formation of short and stiff actin filaments that aid leading-edge motility via effective actin treadmilling (Pollard and Borisy 2003; Le Clainche and Carlier 2008). This explains why CP has been detected in the leading edges of mammalian migrating cells and why its inactivation has impaired cell migration (Sinnar *et al*. 2014). Additionally, CP is involved in the regulation of membrane protrusions, as CP depletion increases the formation of filopodia in cultured cells (Mejillano *et al*. 2004; Aragona *et al*. 2013).

For human CP, there are three isoforms of α subunits encoded by three different genes, *CAPZA1*, *CAPZA2* and *CAPZA3*, which encode α1, α2 and α3 subunits of CP, respectively. For β subunits, three isoforms of β subunits are encoded by alternative splicing of one single gene *CAPZB* (Schafer *et al.* 1994; Hart, Korshunova and Cooper 1997; von Bülow *et al.* 1997; Miyagawa *et al.* 2002). CAPZA1 and CAPZA2 proteins are located in both muscle and non-muscle cells (Casella *et al*. 1989; J. A. Cooper *et al*. 1991), while CAPZB1 and CAPZB2 proteins are predominantly expressed in muscle and non-muscle cells, respectively (Casella *et al.* 1987; Schafer *et al.* 1994). Meanwhile, both CAPZA3 and CAPZB3 proteins are exclusively expressed in male germ cells (Tanaka *et al.* 1994; von Bülow *et al.* 1997). CAPZA2 knock-out mice are not fully viable and have defects in nervous system (Perez-Garcia *et al.* 2018), implying that CAPZA1 alone is not sufficient to rescue the CAPZA2-deficient phenotypes. Likewise, CAZPB1 and CAPZB2 proteins cannot substitute each other in terms of functionalities, suggesting that they have their own distinct roles in their designated sites (Hart and Cooper 1999).

Actin binding activities of CP are negatively regulated by PIP2 (phosphatidylinositol 4, 5-bisphosphate) (Schafer, Jennings and Cooper 1996; Huang *et al.* 2019) as well as several proteins such as CARMIL (capping protein Arp2/3 complex myosin-I linker) (Uruno, Remmert and Hammer 2006) or V-1/myotrophin (Bhattacharya *et al.* 2006). The interactions between CP and actin, in

particular, change rapidly in response to mechanical stress (Y.-H. Lin *et al*. 2013), implying that post-translational modifications may be involved in the regulation of CP activities. In line with this, CAPZA1 and CAPZB1 were found to be phosphorylated by casein kinase II at Ser9 (Canton *et al*. 2005) and protein kinase C epsilon at Ser204 (Y. H. Lin *et al*. 2016), respectively, leading to decreased actin binding activities of CP.

2.4.2 Liver kinase B1 (LKB1)

Liver kinase B1 (LKB1), also known as SKT11, is a tumor suppressor with serine/threonine kinase activity that has been linked to the heritable cancer disorder Peutz-Jeghers Syndrome (PJS) (Hemminki *et al*. 1998). Patients with PJS carry germline mutations of LKB1 and are characterised by the frequent formation of hamartomatous polyps in the gastrointestinal tract and mucocutaneous melanin pigmentation (Giardiello and Trimbath 2006). While the LKB1 mutation is frequently observed in lung and cervical cancers (Sanchez-Cespedes, MontserratParrella *et al.* 2002; Wingo *et al.* 2009), cases of PJS patients having lung cancer are surprisingly rare, but they are highly predisposed to gastrointestinal cancers (Giardiello and Trimbath 2006). In the screening of lung adenocarcinomas, *LKB1* has been ranked as the third most frequently mutated gene, following *TP53* and *KRAS* (Ding *et al*. 2008). The co-occurrence of KRAS or TP53 mutations with LKB1 mutation is common in lung cancer patients, suggesting that the loss of LKB1 may be required to cooperate with other signalling pathways to drive tumorigenesis (Caiola *et al*. 2018; Barta and McMahon 2019). This idea is supported by the experimental results showing that deletion of LKB1 alone is inconsequential for prostate tumorigenesis, while metastatic prostate cancer is observed with a combined loss of LKB1 and PTEN (Hermanova *et al*. 2020).

LKB1 is widely expressed in all tissues (Hemminki *et al*. 1998). It has been identified as a tumor suppressor owing to its ability to induce cell cycle arrest when over-expressed (Tiainen, Ylikorkala and Mäkelä 1999; Tiainen *et al.* 2002). It is found to be expressed in both the cytoplasm and the nucleus. The complex formation of LKB1 with STRAD (**ST**E20-**r**elated **ad**aptor pseudokinase) and the scaffolding protein MO25 (**mo**use protein **25**) facilitates translocation of nuclear LKB1 into the cytoplasm and allows LKB1 to attain its optimal kinase activity (Baas *et al*. 2003; Boudeau *et al*. 2003). AMPK, a key sensor of cellular energy and nutrient status in eukaryotic cells, is a well-documented downstream target of LKB1 (Hawley *et al*. 2003; Woods *et al*. 2003). It consists of an α catalytic subunit as well as regulatory β and γ subunits. LKB1 phosphorylates the α catalytic subunit of human AMPK at Thr183 (Thr172 in rats), resulting in a 100-fold increase in AMPK catalytic activities in vitro (M *et al*. 2006). The naming of AMPK is attributed to the stimulating effect

of AMP on its kinase activity, whereas AMP binds to the γ subunits of AMPK, causing conformational changes that in turn trigger three of the following: 1) AMPK allosteric activation, 2) LKB1-mediated AMPK phosphorylation enhancement, and 3) inhibition of AMPK dephosphorylation by protein phosphatases (Gowans *et al.* 2013). Coupled with the action of adenylate kinases (2ADP⇋ATP +AMP), a drop in ATP and the corresponding rise in ADP during energetic stress favor the equilibrium position shifting to the right hand side of the equation, causing a rapid increase in AMP and thus in AMPK activity, ultimately empowering AMPK supreme sensitivity on cellular energy status (Hardie and Hawley 2001). As a result, activation of AMPK results in downregulation of ATP-consuming anabolic pathways and upregulation of ATP-producing catabolic pathways, linking its upstream kinase LKB1 as a regulator of energy sensor (Russell and Hardie 2020). In addition to AMPK, LKB1 phosphorylates and activates 12 other AMPK-related kinases that are involved in the regulation of cell polarity and cell metabolism (Shackelford and Shaw 2009). For example, suppression of the EMT transcription factor SNAIL1 is mediated by LKB1-mediated activation of the AMPK-related kinases MARK1 (**m**icrotubule **a**ffinity **r**egulating **k**inase **1**) and MARK4 (**m**icrotubule **a**ffinity **r**egulating **k**inase **4**), in a manner independent of the AMPK activity (Goodwin *et al*. 2014).

Post-translational modifications of LKB1 are widely reported. PKC ζ (**P**rotein **k**inase **C** **zeta**) phosphorylates LKB1 at Ser428 and promotes cytosolic translocation of LKB1 in endothelial cells (Z. Xie *et al*. 2008). Conversely, phosphorylation of LKB1 at Ser334 by AKT (Liu *et al.* 2012) as well as at Tyr261 and Tyr365 by FYN kinase (Yamada *et al*. 2010) results in nuclear sequestration of LKB1. In addition to phosphorylation, SUMOylation of LKB1 at Lys178 has been demonstrated to be required for its interaction with AMPK during cellular energetic stress (Ritho, Arold, and Yeh 2015). Meanwhile, polyubiquitination via K63 linkage in the N-terminal part of LKB1 by SKP2 maintains the interaction between LKB1 and the STRAD/MO25 complex and facilitates AMPK phosphorylation during energy stress (S.-W. Lee *et al*. 2015).

2.4.3 Lactate dehydrogenase A (LDHA)

The tetrameric enzyme lactate dehydrogenase (LDH) catalyses the inter-conversion of pyruvate to lactate or α-ketobutyrate (α-KB) to α-hydroxybutyrate (α-HB) with the expense of NADH to NAD^+ (Valvona *et al*. 2016; Intlekofer *et al*. 2017). LDH exists as a homotetramer or heterotetramer composed of different LDH subunits at varying ratios. To date, four LDH protein subunits with an identical molecular mass of 35kDa have been identified, which are encoded by separate genes, *LDHA*, *LDHB*, *LDHC* and *LDHD*. LDHA and LDHB proteins are predominantly expressed in the

heart and muscle, respectively (Stambaugh and Post 1966). LDHC protein is specifically expressed in testis (Goldberg *et al*. 2010) and LDHD protein targets D-lactate instead of L-lactate (Flick and Konieczny 2002), whose concentration in human blood is 100 times higher than that of D-lactate (Talasniemi *et al*. 2008).

When compared to normal breast tissue, malignant breast tumors have higher LDHA activities (Balinsky, Platz, and Lewis 1984). In line with activity data, LDHA has been found to be over-expressed in various cancers, including prostate and breast cancer (Zhao *et al.* 2009; Kayser *et al.* 2010; Rong *et al.* 2013; Koukourakis *et al.* 2014), which correlates with a poor prognosis for patients (M. I. Koukourakis *et al*. 2003). Multiple studies have indicated that LDHA inhibition increases production of reactive oxygen species as well as decreases tumor growth (A. Le *et al*. 2010; Y. Liu *et al*. 2018; E.-Y. Kim *et al*. 2019), suggesting that LDHA expression helps cancer cells survive. Likewise, LDHB overexpression has been observed in aggressive basal-like and triple-negative breast cancers (McCleland *et al*. 2012; Dennison *et al*. 2013). However, silencing of LDHB expression by promoter methylation has been observed in several instances, including MCF7 breast cancer cells (Maekawa *et al.* 2003; Leiblich *et al.* 2006; Brown *et al.* 2013). Activation of FGF signalling has been shown to facilitate methylation of the promoter region of LDHB, via suppression of the TET1 (**T**en-**e**leven **t**ranslocation methylcytosine dioxygenase **1**) enzyme that catalyses DNA demethylation (J. Liu *et al*. 2018). A recent phosphoproteomic screen identified the LDHB Thr302 residue as a potential PIM1 phosphorylation site (Ledet *et al*. 2021), but the finding has yet to be validated *in vitro* and *in vivo*. Despite differential expression of LDHA and LDHB in cancers of different origins, combined inactivation of both LDHA and LDHB is required to achieve complete suppression of lactate production in cultured cancer cell lines (Ždralević *et al*. 2018). Notably, homozygous knock-out of LDHA is embryonic lethal in mice and conditional knock-out of LDHA for up to 6 weeks resulted in severe hemolytic anemia in mice (H. Xie *et al*. 2014). This is believed to be related to the necessity of LDHA to maintain sustained glycolysis in red blood cells, as LDHB expression was not upregulated upon LDHA inactivation (Y.-H. Wang *et al*. 2014).

LDHA is expressed in both the cytoplasm and the nucleus of cancer cells (M. I. Koukourakis *et al*. 2003; Michael I. Koukourakis, Giatromanolaki, and Sivridis 2003; Y.-J. Chen *et al*. 2016). Multiple initiation sites have been identified in the promoter region of the *LDHA* gene including cAMP response element, E-box motif and hypoxia response elements. Binding of the transcription factors CREB (**c**AMP-**r**esponse **e**lement **b**inding protein), MYC, and HIF1α to their respective sites increased LDHA expression (Short *et al.* 1994; Semenza *et al.* 1996; Shim *et al.* 1997). Additionally, transcription factors FOXM1 and KLF4 have been shown to bind to the promoter region of LDHA with distinct effects. While FOXM1 leads to enhanced LDHA expression, KLF4 suppresses it (Cui *et al*. 2014; Shi *et al*. 2014).

LDHA activities are subjected to post-translational modifications in addition to transcriptional control. FGFR1 (**fi**broblast **g**rowth **f**actor **r**eceptor **1**) phosphorylates LDHA at Tyr10 and Tyr83, enhancing the formation of LDHA tetramers as well as its binding affinity towards NADH (J. Fan *et al*. 2011). Both HER2 and SRC have also been reported to phosphorylate LDHA at Tyr10 (L. Jin *et al*. 2017). Other than phosphorylation, acetylation of LDHA at Lys5 and succinylation of LDHA at Lys22 promote and prevent the lysosomal degradation of LDHA, respectively (D. Zhao *et al*. 2013; X. Li *et al*. 2020).

3 Aims

PIM kinases are modestly expressed in healthy human adult tissues but frequently overexpressed in both solid tumors and haematological malignancies. We as well as others have demonstrated that PIMs are versatile kinases that regulate cell proliferation, survival, metabolism and motility via phosphorylation of multiple substrates, including the transcriptional regulators NFATC1 and NOTCH1, the BAD pro-apoptotic protein, the CXCR4 chemokine receptor, and the p21/CDKN1A and p27/CDKN1B cell cycle inhibitors (Nawijn, Alendar, and Berns 2011; Warfel and Kraft 2015; Santio and Koskinen 2017). While many of the known PIM downstream targets are not listed here, it is anticipated that the number of new PIM-interacting substrates will increase as mass spectrometry becomes more widely used to explore the human kinase interaction network (Buljan *et al*. 2020). To facilitate the validation of novel PIM downstream targets as well as the investigation of PIM-dependent cellular functions, CRISPR genomic editing technology was employed in this study to generate prostate (PC3) or breast (MCF7) cancer cell clones deficient of individual or all PIM family members. The CRISPR system enables gene inactivation at the genomic level, allowing complete blockage of protein expression. Thus, in the CRISPR-based knock-out cells there are no co-founding effects caused by residual protein expression that is observed in knock-down cells produced by the RNA interference technology.

While cancer cell signalling covers a wide range of topics, this thesis focused on the phosphorylation-dependent regulation of cell motility, cell proliferation, and cell metabolism by PIM kinases. To this end, the following aims were chosen based on the listed rationales:

- **Aim 1**: Investigation of the regulation of actin capping proteins by PIM kinases

  Rationale: The pro-migratory effects of PIM kinases have been linked to the phosphorylation-dependent activation of several substrates, such as NFATC1 or CXCR4 or inactivation of FOXP3 or GSK3B (**Figure 3**). These previously identified PIM substrates, however, do not regulate cellular movements by interacting directly with the actin cytoskeleton. Phosphoproteomics screen of rat brain extracts from our lab identified actin

capping protein Capza2 as a potential PIM downstream target, but the functional relationship between capping proteins and PIM kinases remained unknown. As actin-based motility enables cancer cells to migrate and invade secondary sites, understanding the effects of PIM kinases on actin capping proteins was expected to provide further insight into the role of PIM kinases in regulation of cell motility.

- **Aim 2**: Dissection of the mechanism of the regulation of AMPK by PIM kinases

  Rationale: Inhibiting PIM expression or activity had previously been shown to increase AMPK phosphorylation (Beharry *et al*. 2011), but the exact mechanism underlying this phenomenon had remained unknown. The well-known tumor suppressor LKB1 is one of the upstream kinases of AMPK (Hawley *et al*. 2003; Woods *et al*. 2003), which regulates cell growth in an opposite manner to the oncogenic PIM kinases. Investigation on how LKB1 and PIM kinases interact to influence AMPK activation was thus expected to improve our understanding of the regulation of tumor growth, and possible even to provide insights into targeting PIM kinases for the treatment of LKB1-deficient tumors.

- **Aim 3**: Investigation of the effects of phosphorylation of LDHA by PIM kinases

  Rationale: Previous studies with either *in vitro* kinase assays or a yeast two-hybrid screen had identified LDHA as a potential substrate for PIM kinases (D. Hoover *et al*. 1991; Leverson *et al*. 1998), but the precise PIM target site(s) in LDHA and the functional consequences of PIM-dependent phosphorylation had remained unknown. PIM kinases have been shown to phosphorylate multiple glycolytic enzymes such as HK2, PKM2 and PFKFB3 (**Figure 6**) and thereby promote glycolysis. Understanding the functional consequences of PIM-dependent phosphorylation of LDHA was thus expected to provide additional evidence on how PIM kinases promote glycolysis.

4 Materials and Methods

Materials and methods used in this study have been listed in **Tables 3-14**, whereas more detailed information on them can be found from the original articles (I, II, III).

This study employed gene editing with the CRISPR/Cas9 system (Jinek *et al*. 2012; Adli 2018; Katti *et al*. 2022). This system consists of two main components: the guide RNA (gRNA) and the Cas9 nuclease. The gRNA in turn consists of two components: the trans-activating CRISPR RNA (tracr RNA) that acts as a binding scaffold for the Cas9 nuclease and the CRISPR RNA (crRNA), which is a 17–20 nucleotide sequence complementary to the desired region to be edited. Upon the formation of a ribonucleoprotein complex between gRNA and Cas9, the catalytic domains (HNH and RuvC) of Cas9 work together to create a DNA double stranded break (DSB) in the specific region containing a protospacer adjacent motif that is complementary to the crRNA sequence in gRNA (Nishimasu *et al*. 2014). The resulting DSB is repaired by different DNA repair mechanisms such as homology-directed repair (HDR), non-homologous end joining (NHEJ) or microhomology-mediated end joining (MMEJ) (Van Vu *et al*. 2021). HDR copies the sequence from a template with flanking sequence homology, while MMEJ relies on areas flanking a DSB with 5–25 bp of microhomology. In the absence of repair templates, ends of DSB are joined via NHEJ in a error-prone manner resulting in nucleotide insertions and deletions that can cause frameshift mutations.

In this study, the CRISPR/Cas9 system was used to generate knock-out clones by introducing site-specific DSBs in two genomic regions corresponding to exon sequences of genes of interest. Ligation of two ends by NHEJ resulted in the removal of a large portion of the coding sequences, preventing gene expression via the nonsense-mediated decay system. The crRNA sequences were designed using the online CRISPOR (http://crispor.tefor.net) program. Two crRNAs were chosen to target genomic DNA inside exons 2 and 6 of PIM1, exons 2 and 6 of PIM2, exon 5 and 6 of PIM3, or exon 3 and 7 of LKB1 in order to knock out desired genes (**Table 5**).

These crRNA sequences combined with respective U6 promoters and tracr RNA sequences were obtained as gBlocks® gene fragments (**Table 6**) and ligated into the BbsI-digested pSpCas9(BB)-2A-Puro (PX459) or pSpCas9(BB)-2A-GFP (PX458)

vector to express two gRNAs and the Cas9 nuclease simultaneously. FuGENE® HD Transfection Reagent (Promega, Madison, WI, USA) was used for plasmid transfection according to the manufacturer's protocol. Transfected cells were either selected for 3–7 days with puromycin or sorted into 96-well plates using the FACSAria cell sorter (Becton Dickinson, Franklin Lakes, NJ, USA). Knock-out cell screening was done by PCR amplification of the genomic DNA regions surrounding the CRISPR/Cas9 target sites. Genomic DNA extraction and PCR amplification were performed by using the Mouse Direct PCR Kit (B40013; Bio-Connect, TE Huissen, The Netherlands) according to the manufacturer´s protocol, with the PCR annealing temperature set to 60 °C and the extension time to 1 min. The validity of knock-out cells was confirmed by both DNA gel electrophoresis and western blotting.

Table 3. Pan-PIM inhibitors

Short Name	Formal name	Article
DHPCC-9	1,10-dihydropyrrolo[2,3-a]carbazole-3-carbaldehyde	I,II
AZD-1208	(5Z)-[[2-[(3R)-3-amino-1-piperidinyl][1,1'-biphenyl]-3-yl]methylene]-2,4-thiazolidinedione	I,II
SGI-1776	N-[(1-methylpiperidin-4-yl)methyl]-3-[3-(trifluoromethoxy)phenyl]imidazo[1,2-b]pyridazin-6-amine	I

Table 4. Plasmid vectors

Tag	Backbone	Insert	Purpose	Article
Flag	pFlag-CMV-2	*LKB1*	Mammalian expression plasmid	II
	pFlag-CMV-2	*LDHA*	Mammalian expression plasmid	III
	pFlag-CMV-2	*Capzb2* (mouse)	Mammalian expression plasmid	I
HA	pCDNA3	*HA-14-3-3 epsilon*	Mammalian expression plasmid	III
	pCDNA3	*HA-Ubiquitin*	Mammalian expression plasmid	III
His	pSF-CMV-CMV-SbfI-Ub-Puro	*Capza1* (mouse) or *CAPZA2* with *Capzb2* (mouse)	Mammalian dual expression plasmids	I
	pcDNA™3.1/V5-His-C	*PIM1*	Mammalian expression plasmid	I,II,III
	pRFSDuet-1	*LKB1*	Bacterial expression plasmid	II
GFP	pEGFP-C1	*Capzb2* (mouse)	Mammalian expression plasmid	I
	pEGFP-C2	*LDHA*	Mammalian expression plasmid	III
	pcDNA™6.2/N-EmGFP-DEST	*LKB1*	Mammalian expression plasmid	II
	pSpCas9(BB)-2A-GFP (PX458)	sgRNA sequences for *PIM1*, *PIM2*, *PIM3* and *LKB1*	Mammalian expression plasmid for CRISPR editing	*LKB1* in II; *PIM1*, *PIM2* and *PIM3* in II and III
RFP	pTag-RFP-N	*PIM1*	Mammalian expression plasmid	I,II
GST	pGEX-6P-1	*PIM1*, *PIM2*, *PIM3*	Bacterial expression plasmid	*PIM1* in I, all three members in II and III
	pGEX-6P-1	*LDHA*	Bacterial expression plasmid	III
	pGEX-6P-1	*LKB1*	Bacterial expression plasmid	II
	pGEX-4T3	murine *Notch1* intracellular domain	Bacterial expression plasmid	I
--	pSpCas9(BB)-2A-Puro (PX459)	sgRNA sequences for *PIM1*, *PIM2*, *PIM3* and *LKB1*	Mammalian expression plasmid for CRISPR editing	*LKB1* in II; *PIM1*, *PIM2* and *PIM3* in II and III

Table 5. Sequences of crRNAs for CRISPR/Cas9 editing

Target location	Sequence
***PIM1* Exon2**	CCGGCAAGTTGTCGGAGACG
***PIM1* Exon6**	TCGAAGGTTGGCCTATCTGA
***PIM2* Exon2**	TTCGAGGCCGAGTATCGACT
***PIM2* Exon6**	GGCCAGGCACCGGCGGATTA
***PIM3* Exon5**	GGGCGTGCTTCTCTACGATA
***PIM3* Exon6**	GCCGTCGCTGGATCAGATTG
***LKB1* Exon3**	CACCCTCAAAATCTCCGACC
***LKB1* Exon7**	CATGCTGCGCCACCGGTCCT

Table 6. gBlocks® gene fragments for ligation to BbsI-digested pSpCas9(BB)-2A-Puro (PX459) vector or pSpCas9(BB)-2A-GFP (PX458) vector. The gBlocks® gene fragments consist of several components: BbsI sites (highlighted in blue) for cloning into PX458 or PX459 plasmids, two crRNA sequences (highlighted in purple), and a gRNA scaffold consisting of tracRNA sequences (highlighted in green) and U6 promoter sequences (highlighted in yellow). The plasmid (PX458 or PX459) itself contains the U6 promoter sequence for the first gRNA and the gRNA scaffold sequence for the second gRNA. As the U6 promoter requires a G nucleotide as the start of a transcriptional signal, an additional G nucleotide (underlined in the sequence) was added for crRNA sequences that were not initiated by a G nucleotide.

Sequence	CCTTTTG**GAAGACCTCACC**G(crRNA sequence 1)GTTTTAGAGCTAGAAATAGCAAGTTAAAATAAGGCTAGTCCGTTATCAACTTGAAAAAGTGGCACCGAGTCGGTGCTTTTTTTCTAGACCCAGCTTTCTTGTTGTACAAAAAAGCAGGCTTTAAAGGAACCAATTCAGTCGACTGGATCCGGTACCAAGGTCGGGCAGGAAGAGGGCCTATTTCCCATGATTCCTTCATATTTGCATATACGATACAAGGCTGTTAGAGAGATAATTAGAATTAATTTGACTGTAAACACAAAGATATTAGTACAAAATACGTGACGTAGAAAGTAATAATTTCTTGGGTAGTTTGCAGTTTTAAAATTATGTTTTAAAATGGACTATCATATGCTTACCGTAACTTGAAAGTATTTCGATTTCTTGGCTTTATATATCTTGTGGAAAGGACGAAACACCG(crRNA sequence 2)**GTTTGGGTCTTC**GAGCTAG

Table 7. Primer sequences for site-directed mutagenesis

Protein	Muta-genesis	Primer type	Sequence	Article
Capza1	S106>A	Forward	GGAAAGAAGCAGCCGACCCGCAGCCAGAGG	I
	S106>A	Reverse	CCTCTGGCTGCGGGTCGGCTGCTTCTTTCC	I
	S106>E	Forward	GGAAAGAAGCAGAGGACCCGCAGCCAGAGG	I
	S106>E	Reverse	CCTCTGGCTGCGGGTCCTCTGCTTCTTTCC	I
	S126>A	Forward	GGAGGGAGTCGTGTGATGCTGCGCTGAGAGCC	I
	S126>A	Reverse	GGCTCTCAGCGCAGCATCACACGACTCCCTCC	I
	S126>E	Forward	GGGAGTCGTGTGATGAGGCGCTGAGAGCCTATG	I
	S126>E	Reverse	CATAGGCTCTCAGCGCCTCATCACACGACTCCC	I
Capzb2	S182>A	Forward	CTATGGCTGCAAACTAACAAGGCTGGCTCGGGCAC	I
	S182>A	Reverse	GTGCCCGAGCCAGCCTTGTTAGTTTGCAGCCATAG	I
	S182>E	Forward	GCAAACCAACAAAGAAGGCTCGGGCACCATGAAC	I
	S182>E	Reverse	GTTCATGGTGCCCGAGCCTTCTTTGTTGGTTTGC	I
	S192>A	Forward	GAACCTGGGAGGCGCACTAACGAGACAGATGG	I
	S192>A	Reverse	CCATCTGTCTCGTTAGTGCGCCTCCCAGGTTC	I
	S192>E	Forward	GAACCTGGGAGGCGAACTAACGAGACAGATGG	I
	S192>E	Reverse	CCATCTGTCTCGTTAGTTCGCCTCCCAGGTTC	I
	S226>A	Forward	GAAAACAAAATCCGGGCCACGCTGAATGAGATCTAC	I
	S226>A	Reverse	GTAGATCTCATTCAGCGTGGCCCGGATTTTGTTTTC	I
	S226>E	Forward	GGACATGGAAAACAAAATCCGAGAGACGCTGAATGAG	I
	S226>E	Reverse	CTCATTCAGCGTCTCTCGGATTTTGTTTTCCATGTC	I
LKB1	S334>A	Forward	CACCACAGTCATGGCGCGCCACCGGTCC	II
	S334>A	Reverse	GGACCGGTGGCGCGCCATGACTGTGGTG	II
	S428>A	Forward	GCTTGCAGGCCGCCAGCCGGCGG	II
	S428>A	Reverse	CCGCCGGCTGGCGGCCTGCAAGC	II
LDHA	S79>A	Forward	GAACACCAAAGATTGTCGCTGGCAAAGACTATAATGTAAC	III
	S79>A	Reverse	GTTACATTATAGTCTTTGCCAGCGACAATCTTTGGTGTTC	III
	S105>A	Forward	GTCAGCAAGAGGGAGAAGCCCGCCTTAATTTGGTCCAG	III
	S105>A	Reverse	CTGGACCAAATTAAGGCGGGCTTCTCCCTCTTGCTGAC	III
	S161>A	Forward	CCGTGTTATCGGAGCCGGTTGCAATCTGGATTC	III
	S161>A	Reverse	GAATCCAGATTGCAACCGGCTCCGATAACACGG	III
	S319>A	Forward	GAGGCCCGTTTGAAGAAGGCTGCAGATACACTTTGGGGG	III
	S319>A	Reverse	CCCCCAAAGTGTATCTGCAGCCTTCTTCAAACGGGCCTC	III

Table 8. **Primary antibodies.** Samples were stained overnight at +4°C in rotation in PBS or TBS Tween-20 according to the manufacturer´s protocols for western blotting (WB) or in a humidified chamber for immunofluorescence (IF) or proximity ligation assay (PLA).

Protein	Manufacturer	Product number	Dilution	Article
PIM1	Santa Cruz	12H8	1:500 (WB)	II,III
PIM1	Merck	MABC553	1:500 (WB,IF,PLA)	I,II,III
PIM2	Cell Signaling Technology	#4730	1:1000 (WB)	II,III
PIM3	Cell Signaling Technology	#4165	1:1000 (WB)	II,III
Capza1	Abcam	ab166892	1:1000 (WB)	I
CAZPA1/A2	Abcam	ab175378	1:1000 (WB), 1:500 (IF)	I
Capzb2	Sigma	HPA031531	1:500 (WB,IF)	I
LKB1	Cell Signaling Technology	#3047	1:1000 (WB)	II
AMPKα	Cell Signaling Technology	#2793	1:1000 (WB)	II
Phospho-AMPKα (Thr172)	Cell Signaling Technology	#2325	1:1000 (WB)	II
Phospho-Akt Substrate (RXXS/T)	Cell Signaling Technology	#9614	1:1000 (WB)	II
Phospho-AKT (Ser473)	Cell Signaling Technology	#4060	1:2000 (WB)	II
AKT	Cell Signaling Technology	#9272	1:2000 (WB)	II
Ubiquitin K-48	Sigma	ZRB2150	1:1000 (WB)	III
LDHA	Cell Signaling Technology	#3582	1:1000 (WB,PLA)	III
pan 14-4-3	Santa Cruz	sc-1657	1:2000 (WB,PLA)	III
β-Tubulin	Cell Signaling Technology	#86298	1:1000-5000 (WB)	I,II,III
Lamin A/C	Cell Signaling Technology	#4777	1:1000-5000 (WB)	I,II,III
Lamin A	Sigma	L2193	1:5000 (WB)	III
His-tag	Thermo Fisher Scientific	MAI_21315	1:2000 (WB), 1:500 (IF)	I
His-tag	Cell Signaling Technology	#12698	1:1000 (WB)	II
FLAG-tag	Sigma	F3165	1:500 (WB,IF)	I
FLAG-tag	Sigma	F7425	1:500 (PLA)	II
FLAG-tag	Sigma	F1804	1:1000 (WB)	II,III
ACTB	Cell Signaling Technology	#4970, #3700	1:1000-5000 (WB)	I,II,III

Table 9. Secondary antibodies. Samples were stained for 1 hour at room temperature for both western blot and immunofluorescence applications. Proximity ligation assays were performed according to the manufacturer's protocol.

Antibody	Manufacturer	Product number	Dilution	Article
horse anti-mouse	Cell Signaling Technology	#7076	1:5000 (WB)	I,II,III
goat anti-rabbit	Cell Signaling Technology	#7074	1:5000 (WB)	I,II,III
Duolink® In Situ Orange Starter Kit	Sigma-Aldrich	DUO92102	Manufacturer's protocol (PLA)	I,II,III

Table 10. Eukaryotic cell culture. Eukaryotic cells were cultured in Roswell Park Memorial Institute (RPMI-1640) medium or Dulbecco's Modified Eagles Medium (DMEM) supplemented with 2 mM L-glutamine, 10% fetal bovine serum, 50 U/ml penicillin and 50 µg/ml streptomycin. MEM Non-Essential Amino Acids (Gibco, #11140050; Thermo Fisher Scientific) and sodium pyruvate (Gibco, #11360070; Thermo Fisher Scientific) were further added to the RPMI-1640 medium to facilitate cell growth.

Cell line	Cell type	Culture medium	Article
A549	human lung carcinoma	DMEM	II
FDC-P1 (Stable cell lines FD/Neo, FD/Pim44)	murine myeloid cell precursors	RPMI-1640 supplemented with conditioned medium from WEHI3B cells	II
HeLa	human cervical adenocarcinoma	DMEM	II
MCF-7 (Wild type as well as CRISPR knock-out clones)	human breast adenocarcinoma	DMEM	II,III
PC3 (Wild type as well as CRISPR knock-out clones)	human prostate adenocarcinoma	RPMI-1640	I,II,III
WEHI3B	murine leukemia	RPMI-1640	II

Table 11. Bacterial cell culture. Bacterial cells were cultured in Luria Broth (LB) medium supplemented with kanamycin (50 µg/ml) or ampicillin (100 µg/ml).

E.Coli cells	Culture conditions and purposes	Article
DH5a	37 °C with constant shaking in shaker (Plasmids isolation)	I,II,III
BL21	30 °C/37 °C with constant shaking in shaker (Bacterial recombinant protein production, 30 °C for GST-tagged PIMs, 37 °C for GST/His-tagged LKB1 and GST-tagged LDHA)	I,II,III

Table 12. Transfer of nucleic acid to cells.

Cells	Methods	Article
Bacterial cells	Heat shock transformation (42°C for 1.5min)	I,II,III
Eukaryotic cells	Lipofection using FuGENE® HD Transfection Reagent	I,II,III

Table 13. *In vitro*, cellular and animal experiments

Experiment	Short protocol	Article
Cell adhesion	Electrical impedance-based method (xCelligence) on collagen and poly-L-lysine coated plates	I
Cell proliferation	Real-time measurement of cell confluence using an imaging machine (IncuCyte)	II
Wound healing assays	Pipette tips were used to manually scratch wounds into cell layers, and light microscopy was used to follow-up the time and extent of wound healing.	I
PIM1 substrate screening	Rat cortex was homogenized in kinase buffer and phosphorylated *in vitro* at 30 °C for 45 min, using recombinant murine PIM1 kinase in the presence of radioactive ATP. Proteins were separated in the first dimension by isoelectric focusing overnight at 3500 volts, followed by two-dimensional separation on 12% SDS-PAGE, silver staining and autoradiography. Extracted proteins were subjected to mass spectrometry analysis, and data were processed and matched to the SwissProt protein database.	I
Cellular protein phosphorylation	Immunoprecipitation followed by western blotting	I,II,III
***In vitro* kinase assays**	Reactions with radioactive or non-radioactive ATP, followed by autoradiography or western blotting	I,II,III
Protein localization and interactions	Fluorescence-lifetime imaging or proximity ligation assay. Subcellular fractionation followed by western blotting	I,II,III
Mass spectrometry	*In vitro* kinase assay followed by SDS-PAGE. *In gel* digestion of proteins with trypsin, followed by phosphopeptide enrichment and liquid chromatography–electrospray ionization–tandem mass spectrometry (LC-ESI-MS/MS)	III
Lactate dehydrogenase enzymatic assays	Cell lysates that had been normalized with protein were added into the reaction buffer, which consisted of NADH and pyruvate or sodium 2-ketobutyrate. LDHA activities were measured by the decrease in fluorescence (excitation: 350 nm, emission: 470 nm) with time, which corresponded to the conversion of NADH to NAD^+ at 25 °C	III

Experiment	Short protocol	Article
Protein crosslinking assay	Cell lysates that had been normalized with protein were incubated with glutaraldehyde for 10 min, followed by the addition of glycine to terminate the reactions. Protein oligomerisation status was monitored by western blotting.	III
Actin disassembly assays	Capping proteins produced in *E. coli* were mixed with both non-labelled and pyrene-labelled polymerized actin in the reaction buffer. Vitamin D-binding protein was added to sequester actin monomers and prevent the re-polymerisation of actin. The rate of actin disassembly was measured by the decrease in pyrene-actin signal through spectrophotometry (excitation: 365 nm, emission: 407 nm) at 25 °C with time.	I
Tumor growth in chicken eggs	Matrigel-mixed cells are implanted on the chorioallantoic membranes of fertilized eggs on embryonic development day 8 (EDD 8). Tumors were collected and weighted on EDD14.	II
Establishment of CRISPR knock out clones	crRNA sequences for desired genes were created using the CRISPOR online software. Plasmids encoding the Cas9 protein and gRNAs were transfected into the cells, and then single cells were sorted using a cell sorter into each well of 96-well plates. Genomic DNA extraction followed by PCR as well as western blotting were used to verify the validity of cell clones.	II
Quantitative PCR	RNA samples were extracted from cells lysed with Trizol reagent. RevertAid First Strand cDNA Synthesis Kit was used to synthesize cDNA from RNA. Quantitative PCR was performed using GoTaq® qPCR Master Mix (Promega) in Mic qPCR Cycler (Bio Molecular Systems).	III

Table 14. Statistical analyses and preparation of diagrams. Significant difference was defined as p value of 0.05 or lower. Standard deviation is represented by error bars.

Purposes	Software	Article
Student´s t-test	GraphPad Prism v.5.0	I,II,III
Preparation of diagrams	Corel Draw 2019 / Inkscape 1.2.1	I,II,III

5 Results

5.1 Identification of capping protein subunits as novel PIM substrates (I)

5.1.1 PIM1 phosphorylates and interacts with the capping protein in prostate cancer

The capping protein (CP) was identified by a phosphoproteomics screen of rat brain extracts as a potential PIM downstream target (I: Additional file 2: Table S5). This prompted us to study the functional relationship between CP and PIMs in more detail. Radioactive *in vitro* kinase assays were performed with bacterially produced recombinant proteins. While the coding sequences of *PIM1* and *CAPZA2* were of human origin, those of *Capza1* and *Capzb2* were derived from mice. However, no species-specific differences were expected, since human and murine CPs are highly homologous to each other at the amino acid level, with similarities of 97% between alpha1 subunits, 98% between alpha2 subunits and 100% between beta2 subunits.

For the generation of CP heterodimers, the coding sequences of CP alpha and beta subunits were inserted under two different CMV promoters in one single plasmid. The results of *in vitro* kinase assays with radioactive ATP indicated that PIM1 phosphorylates the CP heterodimer composed of Capza1 and Capzb2, which is hereafter abbreviated as Capza1/b2 (I: Fig. 1A). Mass spectrometry analysis coupled with the follow-up *in vitro* kinase assays confirmed that there are multiple PIM1 phosphorylation sites on both CP subunits: Ser106 and Ser126 in Capza1 as well as Ser182, Ser192 and Ser226 in Capzb2 (I: Fig. 1E). The cellular interactions between PIM1 and Capza1/b2 were investigated by co-immunoprecipitations in PC3 cells, where endogenous PIM1 protein was pulled down with FLAG-tagged Capzb2 protein (I: Fig. 1F), indicating that PIM1 physically interacts with the CP heterodimer in cells. Their physical interactions were further confirmed by immunofluorescence stainings of over-expressed proteins (I: Fig. 2A) as well as proximity ligation assays of endogenous proteins in PC3 cells (I: Fig. 2C).

5.1.2 Phosphorylation of the capping protein regulates cellular motility and formation of actin protrusions

Based on wound healing assays, PIM kinases had previously been demonstrated to promote cell migration in PC3 cells (Santio *et al*. 2010). Therefore, we now conducted wound healing assays to investigate the role of PIM1-mediated phosphorylation of CP subunits in cell motility. For this, a dual expression plasmid was used to simultaneously express both the alpha and beta subunits of CP. In addition to the wild type (WT) sequence, PIM1-targeted serine residues of CP subunits were mutated into alanine (SA) and glutamic acid (SE) to create phosphodeficient and phosphomimicking mutants, respectively. In addition to mutations of a single residue, mutations of two or three PIM phosphorylation sites were created, and these are referred to as 2X and 3X mutants. The functional consequences of these mutations were investigated in PC-3 prostate cancer cells. As judged by the extent of wound closure in the wound healing assay experiment that was followed up to 12 hours, migration of cells was decreased by over-expression of the SA mutants of Capza1 or Capzb2, but not by the corresponding WT proteins or SE mutants (I: Fig. 3A, B). In addition, inactivation of PIM activities by the pan-PIM inhibitor DHPCC9 significantly decreased cell migration, but its anti-migratory effects were rescued upon over-expression of the 3XSE Capzb2 mutant (I: Fig. 3C). All these data suggest that PIM promotes cell motility in part by phosphorylating CP subunits.

As CPs have been shown to modulate actin protrusion formation at the cell edges (Mejillano *et al*. 2004), this prompted us to investigate the effect of CP phosphorylation on the number and length of actin protrusions at the cell edges. Overexpression of the 3XSA Capzb2 mutant led to a significant increase in the number of protrusions but a decrease in their length, as compared to 3XSE Capzb2 mutant overexpression (I: Fig. 4A, B and C). The increase in the average number of protrusions at the cell edges was also observed in DHPCC9-treated cells compared to DMSO-treated control cells (I: Fig. 5D and E), but no significant difference in terms of the average length of protrusions was detected. Overall, these data suggest that the number of actin protrusions at the cell edges is in part regulated by PIM-mediated CP phosphorylation.

5.1.3 Phosphorylation of capping protein regulates cell adhesion and actin disassembly

When the effects of CP phosphorylation on PC3 cell adhesion were studied, over-expression of WT Capza1 and Capzb2 resulted in a modest increase in adhesion to collagen (I: Fig. 6A). Yet, cells with over-expression of SE mutants of Capza1 or Capzb2 adhered stronger to collagen than the corresponding SA mutants (I: Fig. 6B

and C). However, cells adhered to poly-L-lysine equally poorly regardless of the phosphorylation status of CP subunits (I: Additional file 3, Fig. S8A-C), suggesting that CP phosphorylation promotes cell adhesion to collagen but not poly-L-lysine.

To investigate the effect of CP phosphorylation on their actin-capping abilities, *in vitro* actin disassembly assays were performed. Pyrene-labelled actin was incubated with bacterially generated WT CP or the corresponding phosphomutants. Over time, actin monomers disassembled from pyrene-labeled actin filaments, and the degree of actin disassembly could be measured as the decrease of fluorescence. Of note, vitamin D-binding protein was added to the reaction mixture to prevent the reassembly of actin (Lees, Haddad, and Lin 1984; Otterbein *et al*. 2002). As expected, the incorporation of WT CPs prevented the disassembly of actin owing to their actin capping activities (I: Fig. 6D, E). While both WT and SA mutants of CPs effectively minimized actin disassembly, the incorporation of SE mutants was incapable of preventing actin disassembly at all (I: Fig. 6D, E). This demonstrates that phosphorylation at the PIM target sites of CPs hinders their actin capping activities.

5.2 Identification of LKB1 as a novel PIM substrate (II)

5.2.1 PIM inhibition increases LKB1-dependent phosphorylation

Both PIM and LKB1 kinases are serine/threonine kinases that phosphorylate multiple downstream targets to regulate cellular growth, albeit in opposite directions. While PIMs promote cell proliferation, LKB1 suppresses cellular growth. To find out whether there is any cross-talk between PIM and LKB1 to coordinate cellular growth, we used the CRISPR/Cas9-based genome editing system to knock out individual (PIM1KO, PIM2KO, and PIM3KO) or all three PIM family members (triple PIM kinase knock-out, TKO) in PC3 and MCF7 cells. Furthermore, we generated CRISPR/Cas9-edited clones lacking LKB1 (LKB1KO) as well as LKB1 plus all three PIM kinases (TKOLKB1) in both PC3 and MCF7 cells. The strategies of CRISPR design as well as their verification are depicted in schematic diagrams (II: Additional File 2, Fig. S1). The validity of knock-out cells was confirmed by both DNA gel electrophoresis (II: Additional File 2, Fig. S2) and western blotting (II: Fig. 2A).

To determine whether PIM kinases negatively regulate AMPK phosphorylation, we first used a pharmacological approach to inhibit PIM activity in cultured cell lines and performed Western blotting with antibodies against AMPK or its phosphorylated form.Treatments with two structurally distinct small molecule pan-PIM inhibitors,

DHPCC9 and AZD1208, at 10 μM for up to 24 hours significantly increased AMPK phosphorylation at the Thr183 residue in both PC3 and MCF7 WT cells (II: Fig. 1A), but not in LKB1-deficient Hela cells (II: Fig. 1A) or LKB1KO PC3 and MCF7 cells (II: Fig. 1B). By contrast, upon transient over-expression of FLAG-tagged LKB1 to restore LKB1 expression in Hela and LKB1KO cell lines, profound AMPK phosphorylation levels were detected with DHPCC9 treatment (II: Fig. 1C, Additional File2, Fig. S3). These data indicate that LKB1 is required for PIM inhibition-mediated AMPK phosphorylation.

5.2.2 Inactivation of all three PIM family members is necessary to trigger AMPK phosphorylation

We next evaluated the contribution of each PIM family member to regulating AMPK phosphorylation. The AMPK phosphorylation level was compared between WT and individual PIM KO clones of PC3 and MCF7 cells. Knocking out any individual PIM kinase did not trigger significant AMPK phosphorylation as compared to WT cells (II: Fig. 2B). By contrast, a remarkable increase in AMPK phosphorylation level was observed in PC3 and MCF7 cell clones deficient of all three PIM kinases (TKO) (II: Fig. 2C), while it returned to the basal level upon transient over-expression of His-tagged PIM1 (II: Fig. 2D). Additionally, the AMPK phosphorylation levels were significantly reduced in FDCP1 myeloid cells stably overexpressing PIM1 (FD/PIM1) compared to control cells (FD/NEO) (II: Fig. 2E). All these data suggest that inactivation of all three PIM kinases is required to trigger AMPK phosphorylation.

5.2.3 PIM family members are upstream kinases of LKB1

LKB1 is an upstream kinase of AMPK. As LKB1 expression is essential for PIM inhibition-mediated AMPK phosphorylation, this raises the hypothesis that PIMs are upstream kinases of LKB1 and thereby regulate AMPK phosphorylation via phosphorylating LKB1. To verify this hypothesis, radioactive *in vitro* kinase assays were performed with GST-tagged PIM and LKB1 proteins produced in bacteria. All three PIM family members were capable of phosphorylating LKB1 *in vitro*, while LKB1 did not auto-phosphorylate itself (II: Fig. 3A). The results were further confirmed by non-radioactive *in vitro* kinase assays (II: Fig. 3B), where phospho-AKT substrate (PAS) antibody was used to blot the phosphorylated proteins. The sequence that the PAS antibody recognizes (**RXXS/T**) not only matches well with the PIM-targeted consensus sequence (RX**RHXS/T**) (Peng *et al.* 2007), but also provided hints that Ser334 (D**RWRS**MTV) and Ser428 (I**RRLS**ACK) of LKB1 could be potential PIM phosphorylation sites (II: Fig. 3C). In the end, Ser334 residue

was identified as a PIM target site by using site-directed mutagenesis followed by *in vitro* kinase assays (II: Figs. 3D and E). However, the presence of residual signals in the LKB1 Ser334A phosphodeficient sample indicated that PIMs may phosphorylate LKB1 at other sites in addition to the Ser334 residue.

Having verified that PIMs are upstream kinases of LKB1 *in vitro*, follow-up cellular experiments were conducted. Firstly, their cellular interactions were verified by co-immunoprecipitation assays (II: Fig. 3F) and fluorescence-lifetime imaging microscopy (FLIM) (II: Fig. 3G). Secondly, cellular phosphorylation levels of LKB1 were found to be remarkably decreased in cells treated with DHPCC9 (II: Fig. 4A) as well as in TKO cells lacking all three PIM kinases (II: Fig. 4B), supporting the *in vitro* findings that PIMs are upstream kinases of LKB1. Of note, no significant difference in the phosphorylation levels of LKB1 S334A mutants was observed between WT and TKO cells (II: Fig. 4B), indicating that the S334 residue is the most prominent cellular PIM target site in LKB1. Thirdly, DHPCC9 treatment triggered a significant increase in AMPK phosphorylation levels in LKB1KO cells upon reintroduction of WT LKB1 but not the LKB1S334A mutant (II: Fig. 4C), indicating that phosphorylation of LKB1 at Ser334 is essential for the regulation of PIM inhibition-mediated AMPK phosphorylation.

Specifically, AKT has also been reported to phosphorylate LKB1 at the Ser334 residue, triggering nuclear sequestration of LKB1 (Liu *et al.* 2012). However, as revealed by the results of cellular fractionation experiments, there were no substantial differences between cytosolic and nuclear expression of FLAG-tagged LKB1WT and the S334A mutant in either PC3 or MCF7 cells (II: Additional File 2, Fig. S6A). Furthermore, the distributions of endogenous LKB1 protein between cytosolic and nuclear fractions were unaffected in cells treated with PIM inhibitors or in TKO cells lacking all three PIM kinases (II: Additional File, Fig. S6B and C), indicating that PIM-mediated phosphorylation of LKB1 has no effect on LKB1 subcellular compartmentalization. In addition, no compensatory AKT phosphorylation was observed in TKO cells, where AKT Ser473 phosphorylation levels were comparable to those of WT cells (II: Additional File 2, Fig. S6D).

5.2.4 Combined knock-out of LKB1 and PIM impair tumor growth

In addition to the regulation of AMPK signalling, the impact of LKB1 and PIMs on cellular proliferation was studied. Cellular confluence, serving as a proxy for cell proliferation, was recorded for up to 5 days by the IncuCyte live cell imaging system. The cellular growth rates of WT cells were similar to those of the LKB1KO clones, while DHPCC9 treatment imposed anti-proliferative effects on both WT and LKB1KO clones (II: Fig. 5A). The proliferation rates of TKO cells were lower than

those of WT cells, which was in line with observations of the effect of DHPCC9 (II: Fig. 5B). Surprisingly, cells lacking LKB1 as well as all three PIM family members (TKOLKB1) displayed a slower growth rate than TKO clones (II: Fig. 5B), even though the phosphorylation levels of AMPK in TKOLKB1 clones were lower than in TKO clones (II: Fig. 5C). This indicates that the phosphorylation level of AMPK is not necessarily linked to the cellular growth rate.

To further address the functional consequences of LKB1 phosphorylation, a chick embryonic chorioallantoic membrane (CAM) xenograft model was used to examine the *in vivo* characteristics of the WT versus knock-out cells (Deryugina and Quigley 2008). In contrast to the *in vitro* findings, no significant difference in the tumor mass was observed between WT and TKO clones (II: Fig. 5D). Notably, a significant increase in tumor mass of LKB1KO clones was observed in PC3 but not MCF7 cells, yet when combined with the loss of all three PIM family members, the tumor-promotive effect was abolished (II: Fig. 5D). Conversely, transient over-expression of PIM1 further promoted tumor growth in LKB1KO clones but not in WT samples (II: Fig. 5E), indicating that the activities of PIMs regulate the growth of tumors lacking LKB1.

5.3 Identification of LDHA as a novel PIM substrate (III)

5.3.1 Inactivation of all three PIM family members decreases nuclear LDHA expression and activities

Previous research suggested that LDHA is a potential PIM substrate (D. Hoover *et al*. 1991; Leverson *et al*. 1998), but the precise phosphorylation sites and their physiological significance were unknown. Therefore, we aimed to identify the PIM target sites in LDHA and investigate the functional consequences of the phosphorylation in more detail. We first looked at the mRNA and protein expression levels of LDHA in both WT and TKO cell clones of PC3 and MCF7 cell lines by qPCR analysis and western blotting, but no significant differences in either the mRNA or protein expression levels were found (III: Fig. 1A), indicating that inactivation of all three PIM kinases does not affect the steady state mRNA or protein expression of LDHA. However, subcellular fractionation experiments revealed that nuclear LDHA expression was consistently decreased in TKO clones, while no changes in cytosolic LDHA expression were observed as compared to WT cells (III: Fig.1B).

In line with the protein expression, nuclear LDHA activities in terms of production of lactate or αHB were consistently decreased in TKO clones compared to WT cells (III: Fig. 2B), while no significant differences in LDHA activities were

seen in the whole cell lysate or cytosolic fractions (III: Fig.2A, B). These data thus indicate that inactivation of all three PIM kinases specifically leads to a reduction in protein expression and enzymatic activity of nuclear LDHA.

5.3.2 PIMs phosphorylate LDHA and suppress its ubiquitination

We next verified that PIM1 physically interacts with LDHA in PC3 cells by proximity ligation assays (PLA) (III: Fig. 3A) and immunoprecipitation pull-down experiments (III: Fig. 3B, C). Even more importantly, serine phosphorylation levels of LDHA were dramatically decreased in TKO clones compared to WT cells (III: Fig. 3D), indicating that PIMs phosphorylate LDHA within cells. Radioactive *in vitro* kinase assays revealed that all three PIM kinases were capable of phosphorylating LDHA (III: Fig. 3E), and that both Ser161 and Ser319 residues of LDHA are targeted by PIM1 (III: Fig. 3F). However, while there was a significant difference in serine phosphorylation level between WT and TKO clones with over-expression of LDHA WT and the Ser319A phosphodeficient mutant, there was no difference in phosphorylation level with the Ser161A phosphodeficient mutant (III: Fig. 3G), indicating that Ser161 is the physiologically relevant PIM phosphorylation site on LDHA within cells.

In addition to the findings that PIM kinases phosphorylate LDHA at the Ser161 residue, it was observed that LDHA was heavily ubiquitinated in TKO clones but not in WT cells (III: Fig. 4A, B). Interestingly, subcellular fractionation experiments revealed that the majority of the ubiquitinated LDHA lied in the nuclear fraction (III: Fig. 4C), and that the extent of LDHA ubiquitination could be suppressed by transient over-expression of PIM1 in both PC3 and MCF7 TKO cells (III: Fig. 4D). This indicates that PIM kinases regulate the ubiquitination of nuclear LDHA. This was further confirmed by the finding that LDHA Ser161A mutation was sufficient to induce ubiquitination (II: Fig. 4E, F), indicating PIMs phosphorylate LDHA at the Ser161 residue to prevent LDHA from undergoing ubiquitination. Additionally, subsequent experiments were performed to show that LDHA is ubiquitinated by K48-linked ubiquitin (III: Fig. 4G, H). To find out whether PIM-mediated LDHA phosphorylation affects its conformation and thus increases its susceptibility to ubiquitination, protein crosslinking assays with glutaraldehyde were performed. The results revealed that the LDHA oligomerization status was not significantly different between WT and TKO clones, nor between FLAG-tagged LDHA WT and the Ser161A mutant (II: Fig. 4J). Hence, PIM-mediated phosphorylation is not involved in the regulation of LDHA oligomer formation.

5.3.3 PIMs promote phosphorylation-dependent interactions of LDHA with 14-3-3ε

Recently, 14-3-3 proteins have been reported to take part in the suppression of LDHA ubiquitination (Zhong *et al*. 2017). Given the examples of 14-3-3 proteins modulating cell signalling through interactions with phosphorylated proteins (Fu, Subramanian, and Masters 2000), it was tempting to speculate that 14-3-3 proteins regulate LDHA ubiquitination through interactions with PIM-phosphorylated LDHA. Strikingly, LDHA was found to be an interacting partner with 14-3-3 proteins in WT cells, and their interactions were dramatically abrogated in TKO cells (III: Fig. 5A, B). This demonstrates that PIM-mediated phosphorylation of LDHA facilitates interactions between LDHA and 14-3-3 proteins. Notably, the FLAG-tagged LDHA WT protein bound with HA-tagged 14-3-3ε protein strongly in WT cells but not in TKO clones, while the LDHA Ser161A mutation greatly abolished the interaction between LDHA and 14-3-3ε in both WT and TKO samples (III: Fig. 5C). This indicates that phosphorylation of LDHA at Ser161 increases its binding affinity to 14-3-3 proteins. Additionally, transient over-expression of HA-14-3-3ε partially suppressed LDHA ubiquitination (III: Fig. 5D), resulting in a modest increase in nuclear LDHA expression in TKO cells (II: Fig. 5E). While the partial suppression of LDHA ubiquitination is likely caused by the residual binding between HA-14-3-3ε and unphosphorylated LDHA, it underlines the importance of PIM phosphorylation in mediating nuclear LDHA ubiquitination as well as protein expression via 14-3-3 proteins.

6 Discussion

6.1 Actin capping protein as novel PIM substrates (I)

CPs are the actin-binding proteins that bind to the growing ends of actin filaments and thereby restrict the elongation of actin filaments. While PIMs have pro-migratory effects in cancer cells via phosphorylation of multiple downstream targets, as discussed in Section 2.3.3, the impact of PIMs on the regulation of actin cytoskeleton has received less attention. In this study, we have identified both the alpha 1 and beta 2 subunits of CP as novel PIM1 substrates. Additionally, we have demonstrated that PIM-dependent phosphorylation of CPs increases the adhesion and motility of PC3 cells while lowering their affinity for binding to actin filaments.

PIM inactivation was accomplished through pharmacological means, because the CRISPR/Cas9 knock-out clones were not yet available during the study period. Cells treated with the pan-PIM inhibitor DHPCC9 migrated less slowly in the wound healing assay experiments than the DMSO-treated control cells, but the anti-migratory effects of PIM inhibition could be countered by over-expressing the phosphomimicking mutant of Capzb2, highlighting the critical function of CP phosphorylation in controlling cell motility. It should be noted that poor cell viability was seen during sustained overexpression of CPs, which may have resulted from off-target effects (Mukherjee *et al*. 2016). Therefore, all over-expression experiments were initiated 12 hours after transfection.

Multiple PIM1-targeted phosphorylation sites of Capza1 and Capzb2 were identified (Ser106 and Ser126 for Capza1 and Ser182, Ser192 and Ser226 for Capzb2). The corresponding phosphorylation sites in human and mouse CP subunits are highly conserved (Hornbeck *et al*. 2015). According to one cryo-electron microscopy study (Narita *et al*. 2006), Ser226 in Capzb2 is predicted to be located in the binding interface between the CP heterodimer and the actin filament. With the experimental findings that phosphorylation of CP decreased its actin capping activity, it is tempting to speculate that phosphorylation at Ser226 of Capzb2 creates steric hindrance and thus directly interferes with the binding between the CP heterodimer and actin filament. While this hypothesis has yet to be validated, casein kinase II and protein kinase C epsilon are known to reduce CP actin capping

activities by phosphorylating CAPZA1 at Ser9 (Canton *et al*. 2005) and CAPZB1 Ser204 (Y. H. Lin *et al*. 2016) respectively, and that these two phosphorylation sites are not located at the interface of the CP heterodimer's actin binding domain.

A phosphoproteomics screen published two days before our manuscript identified PIM3 as a novel interacting partner for CAPZA1 and CAPZB2 (Buljan *et al*. 2020), supporting our findings. PIM family members are known to be functionally redundant and share many, although not all substrates (Nawijn, Alendar, and Berns 2011; Warfel and Kraft 2015; Santio and Koskinen 2017). Thus, even though our study focused on PIM1, it would not be surprising if other PIMs were also able to phosphorylate CPs. Of note, PIM3 is found primarily at the cell edges in lamellipodia and is co-localized with focal adhesion kinase (FAK) in human umbilical vein endothelial cells (HUVECs) (P. Zhang *et al*. 2009), implicating PIM3 as a regulator of actin dynamics. On the other hand, PIM1 has been demonstrated to take part in maintaining RAC1 (**Ra**s-related **C**3 botulinum toxin substrate **1**) expression during EGF-stimulated condition (S. Tanaka *et al*. 2009), in which RAC1 is involved in the regulation of actin polymerization for lamellipodia formation. All these findings demonstrate that PIM kinases are engaged in controlling actin dynamics, emphasizing the crucial function of PIMs in promoting cell motility. The results are also in line with a previous study from our group, where over-expression of PIM1 or PIM3 increased metastasis formation in an *in vivo* mouse model (Santio *et al*. 2015). However, further *in vivo* studies using phospho-deficient and phospho-mimicking CP knock-in mutant cells would be helpful, as they could provide a better understanding of the molecular pathways of PIMs in the regulation of tumor cell motility and migration. There one might use zebrafish, which is an emerging *in vivo* model organism to study actin dynamics. Not only do all three types of zebrafish muscle actins have 99% identity to their human counterparts, but there is also the possibility of microinjecting rhodamine-labeled actin into transparent zebrafish embryos, facilitating the study of actin dynamics using fluorescence microscopy (J. C. Cheng, Miller, and Webb 2004; Pinto, Mishima, and Sampath 2020).

6.2 LKB1 as a novel PIM substrate (II)

In this study, we illustrated how inhibiting the expression or activity of all three PIM kinases activates AMPK in cancer cells via LKB1-dependent phosphorylation at Thr172. This was demonstrated using both pharmacological and CRISPR/Cas9-based genomic editing methods. Furthermore, we showed that all three PIM kinases are upstream kinases of LKB1 and that Ser334 is the main PIM-targeted site in LKB1. The functional redundancy among PIMs on LKB1 was reflected in the requirement for all three PIM family members to be deleted to trigger AMPK phosphorylation.

Various subcellular localizations of LKB1 have been reported in the literature. While endogenously expressed LKB1 protein is entirely localized in the nucleus of non-transformed IMR90 fibroblasts, it is predominately found in the plasma membrane of polarized epithelial MDCK cells (Dogliotti *et al*. 2017). As revealed in our subcellular fractionation experiments, the endogenous LKB1 protein locates in the cytoplasm regardless of whether PIM expression or activity is inhibited in both PC3 and MCF7 WT cells, while overexpressed WT LKB1 and its S334A phosphodeficient mutant derivative are both primarily found in the nuclear fractions of PC3 and MCF7 LKB1KO cells. This is in contrast to an earlier study, which showed that nuclear sequestration of LKB1 in MDA-MB-231 breast cancer cells is caused by the phosphorylation of overexpressed LKB1 at Ser334 by AKT (L. Liu *et al*. 2012). Although the differences could be due to cell type-dependent variations in the subcellular localization of LKB1, the differences in cellular compartmentalization between endogenous and ectopically expressed LKB1 proteins revealed in our experimental data indicate the necessity of using knock-in mutant cell lines to properly study the physiological relevance of LKB1 phosphorylation.

The tumor-suppressive effects of LKB1 could be clearly observed in the three-dimensional CAM xenograft experiments, but not in the two-dimensional cell proliferation assays. In this regard, differences in the effects of LKB1 have been reported under *in vitro* and *in vivo* conditions (Hermanova *et al*. 2020). We took advantage of the CAM xenograft model to study the *in vivo* effects of LKB1 and PIM, because tumors on the CAM grow much faster than equivalent tumors implanted subcutaneously in mice, whereas the pattern of tumor growth and metastatic behavior of tumor cells in mice have been recapitulated in the CAM assay (M. Liu *et al*. 2013; Junhui Hu *et al*. 2019). According to our CAM data, knocking out LKB1 significantly increased tumor mass in PTEN-deficient PC3 cells but not in PTEN-expressing MCF7 cells. This was consistent with the findings that LKB1 inactivation alone is insufficient to drive tumorigenesis (Contreras *et al*. 2010; Hermanova *et al*. 2020), whereas an aggressive tumor phenotype is observed when the LKB1 mutation is combined with activation of an oncogene or inactivation of a tumor suppressor gene, such as PTEN (Hermanova *et al*. 2020; T.-T. Li and Zhu 2020). Particularly, PIM kinases play a crucial role in promoting tumor growth in LKB1-deficient PC3 cells, as demonstrated by the reduced tumor growth due to knocking out all three PIM family members or by the increased tumor mass due to upregulated PIM1 expression. Surprisingly, the increase in tumor mass of LKB1-deficient PC3 cells could be offset by PIM inactivation with no significant changes in AMPK phosphorylation level, implying that AMPK phosphorylation is not associated with the tumor suppressive effect accompanied with PIM inhibition in this case. In the $KRAS^{G12D}$ mutation-mediated non-small-cell lung carcinoma mouse

model, loss of LKB1 resulted in an increase in tumor growth, while loss of AMPK resulted in a decrease in tumor burden (Eichner *et al*. 2019), demonstrating that AMPK inactivation is not the determining factor for the constitutive tumor suppressive effect of LKB1. In fact, reports demonstrating AMPK is a tumor suppressor (Vila *et al.* 2017; Vara-Ciruelos *et al.* 2019) or a tumor promoter (Saito *et al.* 2015; Kishton *et al.* 2016) co-exist in the literature. These contradictory data may be caused by the differential roles of AMPK in tumor progression. AMPK serves as a tumor suppressor to prevent cancer formation, however, once the tumor has been established, AMPK acts as a tumor promoter by conferring to cancer cells adaptive resistance towards oxidative or metabolic stress (Vara-Ciruelos, Russell, and Hardie 2019).

Likewise, in the context of LKB1 knock-out, emerging data suggest that loss of salt-inducible kinases (SIKs), less-studied downstream targets of LKB1, is responsible for a significant portion of the transcriptional alterations and histological features of LKB1-deficient malignancies (Hollstein *et al.* 2019; Murray *et al.* 2019). In this regard, further studies are required to find out if PIM kinases affect the growth of LKB1-deficient cancers via regulation of SIKs and whether PIM inhibition can reduce the aggressive metastatic behaviour seen in tumors lacking both PTEN and LKB1. Furthermore, while significant AMPK phosphorylation was observed in TKO cells, the consequences for AMPK downstream effectors such as ACC or PGC-1α were not thoroughly investigated. This is of importance, as the elucidation of the effects of ACC or PGC-1α by the PIM/LKB1/AMPK axis may provide valuable information on how PIM kinases regulate energy metabolism in cancer cells.

6.3 LDHA as a novel PIM substrate (III)

Given that PIM kinases had been shown to promote glycolysis through direct phosphorylation of multiple glycolytic enzymes (Yu *et al.* 2013; Yang *et al.* 2018; Lu *et al.* 2021), it was expected that the same trend would apply to the phosphorylation of LDHA by PIM kinases. However, much to our surprise, it was found that there were no changes in mRNA or protein levels or enzymatic activities of LDHA in the whole cell lysate of PIM TKO cells as compared to wild-type cells. By contrast, we detected a reduction in protein expression and enzymatic activity of nuclear LDHA in TKO cells. LDHA has been conventionally depicted as a cytosolic enzyme, despite numerous reports of its presence in the nucleus (Ja *et al.* 1983; X H Zhong and B D Howard 1990; Koukourakis *et al.* 2003; Y. Liu *et al.* 2018). In particular, immunohistochemical stainings have shown that lung cancer cells express LDHA in both their cytoplasm and nucleus (Michael I. Koukourakis, Giatromanolaki, and Sivridis 2003). The presence of LDHA in the nucleus was further confirmed by transmission electron microscopy experiments conducted in

Hela cells (Y.-J. Chen *et al*. 2016). In PC3 prostate cancer cells and MCF7 breast cancer cells, we have seen that LDHA is expressed in both the cytosolic and nuclear fractions. The majority of LDHA proteins and their activities, however, are found in the cytosolic fractions, which is consistent with earlier findings from PC12 cells (X H Zhong and B D Howard 1990). The phosphorylation of LDHA at both serine and tyrosine residues has been reported in at least two separate reports to date (Ja *et al*. 1983; X H Zhong and B D Howard 1990). However, the majority of studies have addressed the effects of tyrosine phosphorylation on LDHA activity (J. Fan *et al*. 2011; L. Jin *et al*. 2017), leaving the effects of serine phosphorylation unexplored. In this study, we demonstrated that all three PIM kinases are upstream kinases of LDHA, and that Ser161 of LDHA is the physiologically most relevant PIM target site. Our observations suggest that this phosphorylation promotes interactions between LDHA and 14-3-3 proteins and thereby shields nuclear LDHA from undergoing degradation via K48-mediated ubiquitination.

Ubiquitination of LDHA has been observed and documented in different cell lines as well as in the skeletal muscles of rats (Onishi *et al.* 2005; Zhong *et al.* 2017; X. Li *et al.* 2020). Here, we demonstrated that K48-mediated ubiquitination of LDHA mostly takes place in the nuclear fractions of PC3 and MCF7 TKO cells. In accordance with the pattern of ubiquitination, knocking out all three PIM family members in PC3 and MCF7 cells reduced nuclear LDHA expression, but did not significantly alter cytosolic LDHA expression. It has been shown that in HEK293T cells, 14-3-3ζ shRNA knockdown caused robust LDHA ubiquitination, but the interaction between 14-3-3 proteins and LDHA prevented it from being ubiquitinated (Zhong *et al*. 2017). The phosphorylation status of LDHA was revealed to be a determining factor in the interaction between LDHA and 14-3-3 proteins, but the crucial phosphorylation site(s) and associated upstream kinase(s) were still unclear at that time. In this sense, we have solved the question by showing that PIM-dependent phosphorylation of LDHA on Ser161 residue promotes the interaction between LDHA and 14-3-3ε proteins. Of note, LDHA ubiquitination is partially suppressed by overexpression of 14-3-3ε proteins, but it is unable to entirely restore nuclear LDHA expression in PIM-deficient cells. This is most likely because of the dramatically diminished ability of 14-3-3ε proteins to bind to unphosphorylated LDHA. In the course of the manuscript preparation, it was discovered that LDHA was being ubiquitinated by a multi-subunit complex of E3 ligases (Maitland *et al*. 2021). Further studies are thus needed to investigate the connection between E3 ligases and PIM-mediated LDHA ubiquitination as well as the involvement of other 14-3-3 isoforms other than 14-3-3ε proteins.

Nuclear LDHA has been suggested to play several significant roles, despite being a small portion of total cellular LDHA proteins. It serves as a transcription factor in the nucleus to support histone H2B expression in the S phase of the cell

cycle (Dai *et al*. 2008; Hongpeng He *et al*. 2013). Furthermore, α-HB metabolites produced by nuclear LDHA protect cells from oxidative stress in part by increasing expression of anti-oxidant proteins (Y. Liu *et al*. 2018). Additionally, mice with induced nuclear LDHA expression develop larger tumors than mice with induced cytoplasmic LDHA expression (Y. Liu *et al*. 2018), highlighting the underappreciated contribution of nuclear LDHA to the development of tumors. In fact, the non-metabolic role of glycolytic enzymes has been gradually uncovered (X. Yu and Li 2017). For example, it was recently discovered that nuclear glycogenolysis serves as a carbon source for histone acetylation, which links glycogen metabolism to epigenetic regulation (Sun *et al*. 2019). Lactate has recently been discovered to be a substrate for histone lysine lactylation (D. Zhang *et al*. 2019), and high levels of histone lactylation have been linked to a poor prognosis in cancer patients (J. Yu *et al*. 2021). Increased histone lactylation causes the activation of genes related to arginine metabolism (D. Zhang *et al*. 2019), suggesting that PIMs may regulate gene expression by modulating the extent of histone lactylation through phosphorylation-dependent ubiquitnation of nuclear DHA. In fact, a previous study demonstrated that histone H3 is phosphorylated by PIM1 at serine 10, contributing to transcriptional activation of MYC-regulated genes (Zippo *et al*. 2007). Therefore, in the future it would be intriguing to investigate how PIM inhibition affects LDHA nuclear activities like histone methylation and histone lactylation, as it may enable the establishment of nuclear LDHA as a novel therapeutic target and increase our understanding of the roles of PIM kinases in the regulation of epigenetics. On the other hand, one recent study showed that phosphorylation of LDHB at serine 162 by Aurora-A kinase increases the enzymatic activity of LDHB and thereby promotes glycolysis (A. Cheng *et al*. 2019). Given that the phosphorylation motif in LDHB (KHRVIG**S**GCN) at serine 162 is very similar to that in LDHA (KNRVIG**S**GCN) at serine 161, further investigation into the effects of PIMs on LDHB may reveal another pathway through which PIM kinases act on glucose metabolism.

6.4 Functional redundancies between PIM and AKT kinases (II, III)

The functional redundancy of PIM kinase members has been well documented in the literature (Nawijn, Alendar, and Berns 2011; Warfel and Kraft 2015; Santio and Koskinen 2017). In proviral mutagenesis experiments, compensatory activation of PIM2 was observed in cells lacking PIM1 (van der Lugt *et al*. 1995), and activation of PIM3 was observed in cells lacking both PIM1 and PIM2 (Mikkers *et al*. 2002). As also revealed in this study, all three PIM kinases are capable of phosphorylating LKB1 and LDHA, and knocking out all three PIM kinases is necessary for LKB1 to

facilitate the phosphorylation of AMPK, illustrating the physiological relevance of the functional redundancies of PIMs.

Despite the functional redundancies amongst PIM family members, there are instances where other PIM family members are unable to offset the physiological impact of the loss of a specific PIM family member. For example, bone marrow-derived mast cells from PIM1 knock-out mice displayed a retarded growth rate compared to WT mice in response to IL3, despite the fact that IL3 induces expression of also PIM2 and PIM3 expressions (Domen, van der Lugt, Laird, Saris, Clarke, *et al.* 1993; Mikkers *et al.* 2004). Moreover, there are circumstances under which PIM members do not share substrates. The CXCR4 protein is phosphorylated at Ser339 by PIM1 and PIM3 but not PIM2, which increases the expression of CXCR4 on the cell surface and facilitates the migration of cancer cells towards the CXCL12 chemokine gradient (Grundler *et al.* 2009; Decker *et al.* 2014; Santio *et al.* 2015). Also, both PIM1 and PIM3 but not PIM2 phosphorylate viral protein X (VPX) at Ser 13 and thereby facilitate viral replication in hosts (Miyakawa *et al*. 2019). These findings thus warrant the necessity of studying the relative contribution of each PIM member on the specific target in the context of targeting PIMs for cancer therapy.

Similarly to PIMs, there are three AKT family kinases, each encoded by a separate gene. AKTs share both non-overlapping and overlapping roles with each other. Both AKT1 and AKT2 have been shown to positively regulate glucose uptake via facilitating translocation of glucose transporter into the plasma membranes in different cellular contexts (Calera *et al*. 1998; Boxer *et al*. 2006). Meanwhile, the findings of embryonic lethality of $AKT1^{-/-}$ mice, severe diabetes abnormalities in $AKT2^{-/-}$ mice, and reduced brain size rather than cognitive deficits in $AKT3^{-/-}$ mice provide substantial evidence of the nonredundant activities of ATK family members (Degan and Gelman 2021). Added to that, both $AKT1/2^{-/-}$ mice (X.-D. Peng *et al*. 2003) and $AKT1/3^{-/-}$ mice (Z.-Z. Yang *et al*. 2005) die shortly after birth, while $AKT2/3^{-/-}$ mice (Dummler *et al*. 2006) are viable but with a retarded growth rate. Phosphorylation motif (L/KRRXS*/T*) of PIM (Friedmann *et al*. 1992; Bullock *et al*. 2005) is very similar to that of AKT (RXRXXS*/T*) (Obata *et al*. 2000). Thereby, they share multiple overlapping downstream targets. For instance, they both phosphorylate the apoptotic BAD protein at different sites to prevent cell death (Del Peso *et al.* 1997; Aho *et al.* 2004). In addition, they both phosphorylate PRAS40 at the same site, releasing its inhibitory restraint on mTORC1 activity (Kovacina *et al.* 2003; F. Zhang *et al.* 2009). It should be noted that ectopically expressed PIM2 and AKT1 both increase protein synthesis, but only the increase in protein synthesis caused by AKT1 expression is inhibited by rapamycin administration (Hammerman *et al*. 2005), suggesting that PIM and AKT both have a non-redundant pro-survival role despite sharing overlapping target substrates. The estimation of the relative contributions of PIM and AKT kinases on phosphorylation of distinct targets has

been complicated by the fact that in many previous studies, the PI3K inhibitor LY294002 has been used as a way to inactivate AKT, while this compound has later been demonstrated to effectively inhibit also PIM kinases (Jacobs *et al*. 2005).

While PIM kinases are constitutively active in nature and their expression as well as activities are rapidly increased with cytokines and other growth factors, AKT kinases require the coordinated action of upstream kinases PI3K, PDK1 and mTORC2 to become activated (Alessi *et al*. 1997; Sarbassov *et al*. 2005). Thereby, despite the fact that both PIM and AKT share overlapping substrates, it is very likely that they elicit their biological functions via phosphorylation of their downstream targets under different physiological conditions. Intriguingly, increased PIM1 expression is observed in prostate cancer cells treated with AKT inhibitors (Cen *et al*. 2013), while there is no compensatory increase in AKT activation in cells lacking all three PIM family members (Narlik-Grassow *et al.* 2012; Mung *et al.* 2021). Nevertheless, it has been demonstrated that concurrent PIM and AKT inhibition is needed for complete inhibition of BAD and PRAS40 phosphorylation, whereas single agent inhibition fails to do so (X. Le *et al*. 2016).

6.5 Targeting PIM kinases for cancer therapy (I, II, III)

As shown in **Table 2**, PIMs are overexpressed in both solid tumors and haematological malignancies. Due to the presence of a proline residue in the hinge region at the site of the hydrogen donor, the mode of hydrogen bond formation between ATP and the ATP-binding pocket of PIM kinases is distinct from that of other kinases (Qian *et al*. 2005; Kumar *et al*. 2005), presenting an opportunity to develop PIM-selective ATP-competitive inhibitors. Nevertheless, all three PIM family members share a highly conserved ATP-binding pocket (Qian *et al*. 2005), making it difficult to create ATP-competitive inhibitors that target a particular PIM kinase member. Specific inhibitors have been developed that target both the ATP-binding pocket and the substrate binding site of PIM1; however, they also selectively target PIM3 in addition to PIM1 (Ekambaram *et al*. 2013; Nonga *et al*. 2021). Additionally, it is even more demanding to target PIM2, as its Km towards ATP (4 μmol/L) is much lower than that of PIM1 (400 μmol/L) and PIM3 (40 μmol/L) (Garcia *et al*. 2014), meaning that the inhibitor needs to be extremely potent in order to compete with the cellular ATP for the ATP-binding pocket of PIM2. Recently, researchers have overcome this hurdle through the development of a non-ATP competitive inhibitor. JP11646, a PIM2-specific inhibitor that facilitates selective proteasomal degradation of PIM2 but not PIM1 or PIM3, has been shown to have anti-tumor activity in a variety of cancer cell lines, including multiple myeloma (Nair *et al.* 2017; Katsuta *et al.* 2022). Furthermore, PP2A-activating drugs have

successfully promoted PIM1 proteasomal degradation in a variety of cell lines (Scarpa *et al*. 2021). While the effects on other PIM kinase members have not been studied, drugs promoting PIM degradation other than targeting their ATP binding pockets may be further investigated as a potent method for PIM inactivation.

Inhibiting all PIM isoforms will probably be the most effective approach in the context of cancer therapy due to their functional redundancies, as demonstrated by our findings that knocking out of all three PIM kinases is required for LKB1 to facilitate AMPK phosphorylation. AZD1208 and PIM477 are two of the several pan-PIM inhibitors that have entered clinical trials (Luszczak, Kumar, *et al*. 2020). PIM447 is a better candidate for PIM inhibition than AZD1208, since it has a stronger affinity for PIM kinases according to data from molecular docking simulations (Q. Chen *et al*. 2019). Phase I clinical studies of AZD1208 showed no significant clinical efficacy towards patients with acute myeloid leukaemia or advanced solid tumours (Cortes *et al*. 2018). While it may indicate that a more potent PIM inhibitor is needed, several lines of evidence indicate that dual inhibition of PIM and AKT is essential to exhibit robust anti-tumor effects (Meja *et al.* 2014; Le *et al.* 2016; Okada *et al.* 2018; Song *et al.* 2018; Lee *et al.* 2019). It has been specifically shown that over-expression of any PIM family member confers to cells resistance towards PI3K inhibitors in an AKT-independent manner (X. Le *et al*. 2016). While this can be in part explained by the fact that PIM and AKT share overlapping downstream substrates, it highlights the notion that targeting either of them alone is insufficient to have a substantial anti-tumor effect. Interestingly, AKT2 but not AKT1 has been shown to be crucial for survival and growth of PTEN-deficient prostate tumors (Chin *et al*. 2014). Our data confirmed that there were no significant changes in AKT Ser473 phosphorylation status in PC3 or MCF7 TKO cells, suggesting that there is no compensatory activation of AKT signalling in the absence of PIM signalling. As our antibody recognized all three phosphorylated AKT isoforms, the impact of PIM inactivation on each of them remained unknown. However, given that PC3 cells lacking both LKB1 and PTEN exhibit significant anti-tumor responses to PIM inhibition, it would be very interesting to investigate how co-inhibition of PIM and AKT2 would further affect tumor development in this context.

In fact, co-targeting PIM and other molecular pathways has been actively explored (Luszczak, Kumar, *et al*. 2020), and shown to have distinct advantages over monotherapies. Particularly, co-targeting of the PIM, PI3K and mTOR pathways has elicited pronounced anti-tumor effects on prostate and lung cancer (Luszczak, Simpson, *et al.* 2020; Moore *et al.* 2021) as well as neuroblastoma (Mohlin *et al*. 2019). Co-targeting of PIM and JAK/STAT pathways offers another therapeutic option, as demonstrated by the synergistic tumor-suppressive effects of a pan-PIM inhibitor and the JAK inhibitor ruxolitinib (Mazzacurati *et al*. 2015; 2019). The

therapeutic efficacy of co-targeting PIM and JAK/STAT pathway was even further increased by the addition of the CDK4/6 inhibitor LEE011 (Rampal *et al*. 2021). Furthermore, genetic screening analyses have revealed that enhanced p38α signalling is responsible for the resistance to PIM inhibition in certain cell lines, and that combined inhibition of PIM and p38α augments the anti-tumor response (Brunen *et al*. 2016). Along with targeting specific signalling pathways, treatments with PIM inhibitors together with an RNA polymerase I inhibitor (Rebello *et al*. 2016) or a proteasome inhibitor (Kunder *et al*. 2022) have resulted in synergistic reduction of tumor growth. Also, the concurrent use of PIM inhibitors permits lower dosages of chemotherapeutic agents such as cisplatin, doxorubicin, or etoposide to achieve equivalent tumor-suppressive effects (Mori *et al.* 2013; Mohlin *et al.* 2019). This is particularly crucial for such cancer patients that are experiencing cachexia-related symptoms as they are often intolerant to standard dosage of chemotherapies due to physical illness (Cleeland *et al.* 2012; Pin, Couch and Bonetto 2018). In addition, dexamethasone has been demonstrated to promote PIM1 expression, while it is recognized as a conventional treatment for T-cell acute lymphoblastic leukemia (T-ALL) and T-cell acute lymphoblastic lymphoma (T-LBL). To this end, combination treatment with the PIM inhibitor PIM447 and dexamethasone has significantly prolonged survival compared to single agents alone in preclinical models with patient-derived xenograft models (De Smedt *et al*. 2020). Also, some studies have demonstrated that PIM inhibition enhanced anticancer effects when combined with PD-L1 blockade (Xin *et al.* 2021; J.-C. Wang *et al.* 2022), supporting the idea that using PIM inhibitors may increase the functional outcomes of immunotherapy. Taken together, with numerous options for co-targeting PIMs with other pathways, it will be essential to develop companion diagnostics that forecast response to each co-targeted treatment option, as to determine which medications should be combined with PIM inhibitors for each patient.

7 Summary/Conclusions

PIM kinases are found in a wide range of hematological and solid cancers and they control networks of signaling pathways that are essential for tumorigenesis and development. Their unique binding modes in the ATP-binding pocket are atypical to most of the kinases, which makes them appealing drug targets. From a therapeutic standpoint, it is critical to understand the downstream targets of PIM kinases and to be able to estimate the on- and off-target effects of PIM inhibitors. In this study, three novel PIM downstream targets were identified (**Figure 8**): the CP actin capping proteins, the LKB1 tumor suppressor, and the LDHA metabolic enzyme. For validation of them, we used small molecule pan-PIM inhibitors as a pharmacological means of PIM inactivation, as well as CRISPR/Cas9 knock-out cells to inhibit PIM expression. The functional effects of PIM phosphorylation were investigated in addition to the identification of PIM-targeted sites on these new targets. Phosphorylation of CPs by PIM1 was shown to increase cell adhesion and migration, which is consistent with the pro-migratory roles of PIMs. LKB1 phosphorylation by PIM kinases was shown to inhibit AMPK phosphorylation, indicating that the oncogenic properties of PIMs and tumor-suppressive properties of LKB1 kinase are precisely regulated at the cellular level. Phosphorylation of LDHA by PIMs was shown to protect nuclear LDHA from undergoing K48-mediated ubiquitination and subsequent degradation, establishing the regulatory connections between PIM kinases and the glycolytic enzyme. According to this study, all three PIM kinases are capable of phosphorylating LKB1 and LDHA, and knocking out all three PIM kinases is required for LKB1 to be able to trigger AMPK phosphorylation in cancer cells, demonstrating the physiological significance of PIM functional redundancy.

The discovery of CPs as novel PIM targets shows a clear link between PIM kinases and actin dynamics, highlighting the importance of PIM family members in enhancing the motility and spreading behavior of cancer cells. Inactivation of both PIM kinases and LKB1 significantly slows tumor growth *in vivo*, which raises the possibility that LKB1-deficient cancers could be controlled with PIM-targeted pharmaceutical interventions. Nuclear LDHA expression is supported by PIM kinases, but further research is needed to understand how they affect LDHA nuclear activities such as histone methylation and lactylation, which may open up an

interesting avenue for future work on the impact of PIM kinases on the regulation of epigenetics. To sum up, all these data not only demonstrate the versatile roles of PIM kinases in regulation of cell motility, cell proliferation and cell metabolism, but also highlight the importance of co-targeting PIM kinases with other proteins or cellular pathways in the context of cancer therapy, as exemplified by the findings that the ensuing oncogenic insult in LKB1-deficient tumors could either be prevented by knocking down all three PIM kinase members or aggravated by increasing PIM1 expression.

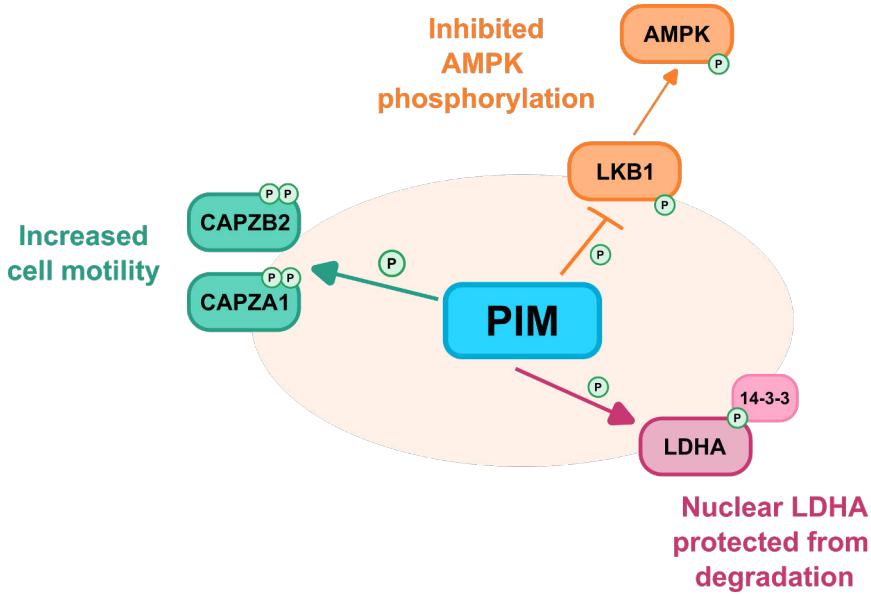

Figure 8. **Three novel PIM downstream targets identified in this study.** PIM1 increases cell motility by phosphorylating both CAPZA1 and CAPZB2. PIMs phosphorylate LKB1 and thereby inhibit AMPK phosphorylation. PIMs phosphorylate and prevent nuclear LDHA from undergoing ubiquitin-mediated degradation by promoting the phosphorylation-dependent interaction between LDHA and 14-3-3.

Acknowledgements

First of all, I would like to express my sincere thanks to my supervisor, Päivi Koskinen, as well as my supervisory board members, Cecilia Sahlgren, Adolfo Rivero-Müller and Katja Anttila. I would also like to thank both the reviewers of my thesis, Ville Hietakangas and Guillaume Jacquemet, for their constructive suggestions and comments to further improve the thesis. Without their excellent counsel and ongoing help, this thesis could not have been completed. I would also like to thank our collaborators Annika Meinander for providing technical advice and materials for ubiquitination experiments, as well as Pascale Moreau for her kind provision of the pan-PIM inhibitor DHPCC9.

Particularly, I want to express my gratitude to Päivi for her exceptional guidance, which combines trust and sympathy and allows me to pursue academic freedom without losing sight of my objectives. Throughout my PhD studies, especially during COVID19, your unconditional support from both the academic and non-academic sides has meant a lot to me. It enables me to focus entirely on my academic work without being distracted by countless daily concerns. Also, sincere thanks for the kind gift of the aquarium, the fish are still living happily at the time I am typing this paragraph! I would also like to thank Adolfo for taking care of me, especially in the early days when I arrived in Finland. The generation of CRISPR knock-out clones certainly could not be done efficiently without yours as well as Valeriy Paramonov's guidance and academic insight. The discussions among academics and non-academics are critically important to me. Also, a big thank you to William Eccleshall, who has been a great buddy and lab mate and has helped me with a lot of lab problems and research concerns over the course of the study. And Niina Santio, too, for supporting me through the study's technical challenges. In addition, I also thank the laboratories of Physiology and Genetics at the Department of Biology, University of Turku for research facilities and materials. The study could not be accomplished efficiently without the assistance of the Genome Biology Unit core facility at the University of Helsinki as well as the Biocenter Finland core facilities at Turku Bioscience. The technical advice and assistance on experiments provided by Sebastian Landor, Kai-Lan, Aravind Mohan, Natura 1/F members, and many others enable the studies to be conducted effectively.

I am also truly thankful for the financial support. This study was funded by the Drug Research Doctoral Programme, the Maud Kuistila Foundation, the Ida Montin Foundation, the Orion-Farmos Research Foundation and the Cancer Foundation Finland.

I would also like to thank my family in Hong Kong and friends, especially Tam, for the love and support in my daily life (Many stars over the head). I do not think that my father, mother, and brother will truly understand the other sections in this thesis except this part, so thank you for the support and patience in letting me study abroad to pursue my academic career!

01-12-2022
Kwan Long Mung

List of References

Adam, K. *et al.* (2015) 'Control of Pim2 kinase stability and expression in transformed human haematopoietic cells', *Bioscience Reports*, 35(6), p. e00274.

Adler, H.L. *et al.* (1999) 'Elevated levels of circulating interleukin-6 and transforming growth factor-beta1 in patients with metastatic prostatic carcinoma', *The Journal of Urology*, 161(1), pp. 182–187.

Adli, M. (2018) 'The CRISPR tool kit for genome editing and beyond', *Nature Communications*, 9(1), p. 1911.

Aho, T.L.T. *et al.* (2004) 'Pim-1 kinase promotes inactivation of the pro-apoptotic Bad protein by phosphorylating it on the Ser112 gatekeeper site', *FEBS Letters*, 571(1–3), pp. 43–49.

Ai, J. *et al.* (2016) 'Blockage of SSRP1/Ets-1/Pim-3 signalling enhances chemosensitivity of nasopharyngeal carcinoma to docetaxel in vitro', *Biomedicine & Pharmacotherapy*, 83, pp. 1022–1031.

Aksoy, I. *et al.* (2007) 'Self-renewal of murine embryonic stem cells is supported by the serine/threonine kinases Pim-1 and Pim-3', *Stem Cells* 25(12), pp. 2996–3004.

Akué-Gédu, R. *et al.* (2009) 'Synthesis, kinase inhibitory potencies, and in vitro antiproliferative evaluation of new pim kinase inhibitors', *The Journal of Medicinal Chemistry*, 52(20), pp. 6369–6381.

Alessi, D.R. *et al.* (1997) 'Characterization of a 3-phosphoinositide-dependent protein kinase which phosphorylates and activates protein kinase Balpha', *Current Biology*, 7(4), pp. 261–269.

Alimonti, A. *et al.* (2010) 'Subtle variations in Pten dose determine cancer susceptibility', *Nature Genetics*, 42(5), pp. 454–458.

Amson, R. *et al.* (1989) 'The human protooncogene product p33pim is expressed during fetal hematopoiesis and in diverse leukemias', *Proceedings of the National Academy of Sciences*, 86(22), pp. 8857–8861.

An, N., Kraft, A.S. and Kang, Y. (2013) 'Abnormal hematopoietic phenotypes in Pim kinase triple knockout mice', *Journal of Hematology & Oncology*, 6, p. 12.

Aragona, M. *et al.* (2013) 'A mechanical checkpoint controls multicellular growth through YAP/TAZ regulation by actin-processing factors', *Cell*, 154(5), pp. 1047–1059.

Ax, Z. *et al.* (2021) 'Final Overall Survival Efficacy Results of Ivosidenib for Patients With Advanced Cholangiocarcinoma With IDH1 Mutation: The Phase 3 Randomized Clinical ClarIDHy Trial', *JAMA Oncology*, 7(11).

Baas, A.F. *et al.* (2003) 'Activation of the tumour suppressor kinase LKB1 by the STE20-like pseudokinase STRAD', *The EMBO Journal*, 22(12), pp. 3062–3072..

Bachmann, M. *et al.* (2004) 'The oncogenic serine/threonine kinase Pim-1 phosphorylates and inhibits the activity of Cdc25C-associated kinase 1 (C-TAK1): a novel role for Pim-1 at the G2/M cell cycle checkpoint', *The Journal of Biological Chemistry*, 279(46), pp. 48319–48328.

Bachmann, M. *et al.* (2006) 'The oncogenic serine/threonine kinase Pim-1 directly phosphorylates and activates the G2/M specific phosphatase Cdc25C', *The International Journal of Biochemistry & Cell Biology*, 38(3), pp. 430–443.

Balinsky, D., Platz, C.E. and Lewis, J.W. (1984) 'Enzyme activities in normal, dysplastic, and cancerous human breast tissues', *Journal of the National Cancer Institute*, 72(2), pp. 217–224.

Balko, J.M. *et al.* (2014) 'Molecular profiling of the residual disease of triple-negative breast cancers after neoadjuvant chemotherapy identifies actionable therapeutic targets', *Cancer Discovery*, 4(2), pp. 232–245.

Barta, J.A. and McMahon, S.B. (2019) 'Lung-Enriched Mutations in the p53 Tumor Suppressor: A Paradigm for Tissue-Specific Gain of Oncogenic Function', *Molecular Cancer Research*, 17(1), pp. 3–9.

Beharry, Z. *et al.* (2011) 'The Pim protein kinases regulate energy metabolism and cell growth', *Proceedings of the National Academy of Sciences*, 108(2), pp. 528–533.

Beier, U.H. *et al.* (2007) 'Overexpression of Pim-1 in head and neck squamous cell carcinomas', *International Journal of Oncology*, 30(6), pp. 1381–1387.

Bellon, M., Lu, L. and Nicot, C. (2016) 'Constitutive activation of Pim1 kinase is a therapeutic target for adult T-cell leukemia', *Blood*, 127(20), pp. 2439–2450.

Ben-Sahra, I. and Manning, B.D. (2017) 'mTORC1 signaling and the metabolic control of cell growth', *Current Opinion in Cell Biology*, 45, pp. 72–82.

Bhattacharya, N. *et al.* (2002) 'Pim-1 associates with protein complexes necessary for mitosis', *Chromosoma*, 111(2), pp. 80–95.

Bhattacharya, N. *et al.* (2006) 'Binding of myotrophin/V-1 to actin-capping protein: implications for how capping protein binds to the filament barbed end', *The Journal of Biological Chemistry*, 281(41), pp. 31021–31030.

Białopiotrowicz, E. *et al.* (2018) 'Microenvironment-induced PIM kinases promote CXCR4-triggered mTOR pathway required for chronic lymphocytic leukaemia cell migration', *Journal of Cellular and Molecular Medicine*, 22(7), pp. 3548–3559.

Blanchoin, L. *et al.* (2014) 'Actin dynamics, architecture, and mechanics in cell motility', *Physiological Reviews*, 94(1), pp. 235–263.

Blanco, F.F. *et al.* (2016) 'The mRNA-binding protein HuR promotes hypoxia-induced chemoresistance through posttranscriptional regulation of the proto-oncogene PIM1 in pancreatic cancer cells', *Oncogene*, 35(19), pp. 2529–2541.

Boroughs, L.K. and DeBerardinis, R.J. (2015) 'Metabolic pathways promoting cancer cell survival and growth', *Nature Cell Biology*, 17(4), pp. 351–359.

Boudeau, J. *et al.* (2003) 'MO25α/β interact with STRADα/β enhancing their ability to bind, activate and localize LKB1 in the cytoplasm', *The EMBO Journal*, 22(19), pp. 5102–5114.

Boxer, R.B. *et al.* (2006) 'Isoform-specific requirement for Akt1 in the developmental regulation of cellular metabolism during lactation', *Cell Metabolism*, 4(6), pp. 475–490.

Brault, L. *et al.* (2012) 'PIM kinases are progression markers and emerging therapeutic targets in diffuse large B-cell lymphoma', *British Journal of Cancer*, 107(3), pp. 491–500.

Breuer, M.L., Cuypers, H.T. and Berns, A. (1989) 'Evidence for the involvement of pim-2, a new common proviral insertion site, in progression of lymphomas', *The EMBO Journal*, 8(3), pp. 743–748.

Brison, O. (1993) 'Gene amplification and tumor progression', *Biochimica Et Biophysica Acta*, 1155(1), pp. 25–41.

Brown, M.S. *et al.* (2022) 'Phenotypic heterogeneity driven by plasticity of the intermediate EMT state governs disease progression and metastasis in breast cancer', *Science Advances*, 8(31), p. eabj8002.

Brown, N.J. *et al.* (2013) 'Lactate Dehydrogenase-B Is Silenced by Promoter Methylation in a High Frequency of Human Breast Cancers', *PLOS ONE*, 8(2), p. e57697.

Brunen, D. *et al.* (2016) 'Intrinsic resistance to PIM kinase inhibition in AML through p38α-mediated feedback activation of mTOR signaling', *Oncotarget*, 7(25), pp. 37407–37419.

Bruno, A. *et al.* (2014) 'Mutational analysis of primary central nervous system lymphoma', *Oncotarget*, 5(13), pp. 5065–5075.

Buckley, A.R. *et al.* (1995) 'Rapid induction of pim-1 expression by prolactin and interleukin-2 in rat Nb2 lymphoma cells', *Endocrinology*, 136(12), pp. 5252–5259.

Buljan, M. *et al.* (2020) 'Kinase Interaction Network Expands Functional and Disease Roles of Human Kinases', *Molecular Cell*, 79(3), pp. 504-520.e9.

Bullock, A.N. *et al.* (2005) 'Structure and substrate specificity of the Pim-1 kinase', *The Journal of Biological Chemistry*, 280(50), pp. 41675–41682.

von Bülow, M. *et al.* (1997) 'CP beta3, a novel isoform of an actin-binding protein, is a component of the cytoskeletal calyx of the mammalian sperm head', *Experimental Cell Research*, 233(1), pp. 216–224.

Burger, M.T. *et al.* (2015) 'Identification of N-(4-((1R,3S,5S)-3-Amino-5-methylcyclohexyl)pyridin-3-yl)-6-(2,6-difluorophenyl)-5-fluoropicolinamide (PIM447), a Potent and Selective Proviral Insertion Site of Moloney Murine Leukemia (PIM) 1, 2, and 3 Kinase Inhibitor in Clinical Trials for Hematological Malignancies', *Journal of Medicinal Chemistry*, 58(21), pp. 8373–8386.

Caiola, E. *et al.* (2018) 'Co-occurring KRAS mutation/LKB1 loss in non-small cell lung cancer cells results in enhanced metabolic activity susceptible to caloric restriction: an in vitro integrated multilevel approach', *Journal of Experimental & Clinical Cancer Research*, 37(1), p. 302.

Caldwell, J.E. *et al.* (1989) 'Effects of CapZ, an actin capping protein of muscle, on the polymerization of actin', *Biochemistry*, 28(21), pp. 8506–8514.

Calera, M.R. *et al.* (1998) 'Insulin increases the association of Akt-2 with Glut4-containing vesicles', *The Journal of Biological Chemistry*, 273(13), pp. 7201–7204.

Canton, D.A. *et al.* (2005) 'The Pleckstrin Homology Domain-Containing Protein CKIP-1 Is Involved in Regulation of Cell Morphology and the Actin Cytoskeleton and Interaction with Actin Capping Protein', *Molecular and Cellular Biology*, 25(9), pp. 3519–3534.

Casella, J.F. *et al.* (1987) 'Cap Z(36/32), a barbed end actin-capping protein, is a component of the Z-line of skeletal muscle', *The Journal of Cell Biology*, 105(1), pp. 371–379.

Casella, J.F. *et al.* (1989) 'Isolation and characterization of cDNA encoding the alpha subunit of Cap Z(36/32), an actin-capping protein from the Z line of skeletal muscle', *Proceedings of the National Academy of Sciences*, 86(15), pp. 5800–5804.

Casillas, A.L. *et al.* (2021) 'Direct phosphorylation and stabilization of HIF-1α by PIM1 kinase drives angiogenesis in solid tumors', *Oncogene*, 40(32), pp. 5142–5152.

Cen, B. *et al.* (2010) 'Regulation of Skp2 levels by the Pim-1 protein kinase', *The Journal of Biological Chemistry*, 285(38), pp. 29128–29137.

Cen, B. *et al.* (2013) 'Elevation of receptor tyrosine kinases by small molecule AKT inhibitors in prostate cancer is mediated by Pim-1', *Cancer Research*, 73(11), pp. 3402–3411. 4619.

Cervantes-Gomez, F. *et al.* (2019) 'PIM kinase inhibitor, AZD1208, inhibits protein translation and induces autophagy in primary chronic lymphocytic leukemia cells', *Oncotarget*, 10(29), pp. 2793–2809.

Chatterjee, S. *et al.* (2019) 'Targeting PIM kinase with PD1 inhibition improves immunotherapeutic antitumor t-cell response', *Clinical Cancer Research*, 25(3), pp. 1036–1049.

Chen, Q. *et al.* (2019) 'Insights into the Interaction Mechanisms of the Proviral Integration Site of Moloney Murine Leukemia Virus (Pim) Kinases with Pan-Pim Inhibitors PIM447 and AZD1208: A Molecular Dynamics Simulation and MM/GBSA Calculation Study', *International Journal of Molecular Sciences*, 20(21), p. E5410.

Chen, T., Wang, L.H. and Farrar, W.L. (2000) 'Interleukin 6 activates androgen receptor-mediated gene expression through a signal transducer and activator of transcription 3-dependent pathway in LNCaP prostate cancer cells', *Cancer Research*, 60(8), pp. 2132–2135.

Chen, W.W. *et al.* (2005) 'Pim family kinases enhance tumor growth of prostate cancer cells', *Molecular Cancer Research*, 3(8), pp. 443–451.

Chen, X.P. *et al.* (2002) 'Pim serine/threonine kinases regulate the stability of Socs-1 protein', *Proceedings of the National Academy of Sciences*, 99(4), pp. 2175–2180.

Chen, Y.-J. *et al.* (2016) 'Lactate Metabolism is Associated with Mammalian Mitochondria', *Nature Chemical Biology*, 12(11), pp. 937–943.

Cheng, A. *et al.* (2019) 'Aurora-A mediated phosphorylation of LDHB promotes glycolysis and tumor progression by relieving the substrate-inhibition effect', *Nature Communications*, 10(1), p. 5566.

Cheng, J.C., Miller, A.L. and Webb, S.E. (2004) 'Organization and function of microfilaments during late epiboly in zebrafish embryos', *Developmental Dynamics*, 231(2), pp. 313–323.

Chiang, W.-F. *et al.* (2006) 'Up-regulation of a serine-threonine kinase proto-oncogene Pim-1 in oral squamous cell carcinoma', *International Journal of Oral and Maxillofacial Surgery*, 35(8), pp. 740–745.

Chin, Y.R. *et al.* (2014) 'PTEN-deficient tumors depend on AKT2 for maintenance and survival', *Cancer Discovery*, 4(8), pp. 942–955.

Chowdhury, R. *et al.* (2011) 'The oncometabolite 2-hydroxyglutarate inhibits histone lysine demethylases', *EMBO Reports*, 12(5), pp. 463–469.

Cibull, T.L. *et al.* (2006) 'Overexpression of Pim-1 during progression of prostatic adenocarcinoma', *Journal of Clinical Pathology*, 59(3), pp. 285–288.

Cilloni, D. and Saglio, G. (2012) 'Molecular pathways: BCR-ABL', *Clinical Cancer Research*, 18(4), pp. 930–937.

Cleeland, C.S. *et al.* (2012) 'Reducing the toxicity of cancer therapy: recognizing needs, taking action', *Nature Reviews Clinical Oncology*, 9(8), pp. 471–478.

Contreras, C.M. *et al.* (2010) 'Lkb1 inactivation is sufficient to drive endometrial cancers that are aggressive yet highly responsive to mTOR inhibitor monotherapy', *Disease Models & Mechanisms*, 3(3–4), pp. 181–193.

Conway, J.R.W. and Jacquemet, G. (2019) 'Cell matrix adhesion in cell migration', *Essays in Biochemistry*, 63(5), pp. 535–551.

Cooper, J.A. *et al.* (1991) 'Variant cDNAs encoding proteins similar to the alpha subunit of chicken CapZ', *Cell Motility and the Cytoskeleton*, 18(3), pp. 204–214.

Cooper, J.A. and Sept, D. (2008) 'New insights into mechanism and regulation of actin capping protein', *International Review of Cell and Molecular Biology*, 267, pp. 183–206.

Cortes, J. *et al.* (2018) 'Phase I studies of AZD1208, a proviral integration Moloney virus kinase inhibitor in solid and haematological cancers', *British Journal of Cancer*, 118(11), pp. 1425–1433.

Courtnay, R. *et al.* (2015) 'Cancer metabolism and the Warburg effect: the role of HIF-1 and PI3K', *Molecular Biology Reports*, 42(4), pp. 841–851.

Craig, A.L. *et al.* (2007) 'The MDM2 ubiquitination signal in the DNA-binding domain of p53 forms a docking site for calcium calmodulin kinase superfamily members', *Molecular and Cellular Biology*, 27(9), pp. 3542–3555.

Cui, J. *et al.* (2014) 'FOXM1 promotes the warburg effect and pancreatic cancer progression via transactivation of LDHA expression', *Clinical Cancer Research,*20(10), pp. 2595–2606.

Cuypers, H.T. *et al.* (1984) 'Murine leukemia virus-induced T-cell lymphomagenesis: integration of proviruses in a distinct chromosomal region.', *Cell*, 37(1), pp. 141–50.

Dai, R.-P. *et al.* (2008) 'Histone 2B (H2B) Expression Is Confined to a Proper NAD+/NADH Redox Status', *The Journal of Biological Chemistry*, 283(40), pp. 26894–26901.

Dang, L., Yen, K. and Attar, E.C. (2016) 'IDH mutations in cancer and progress toward development of targeted therapeutics', *Annals of Oncology*, 27(4), pp. 599–608.

Dautry, F. *et al.* (1988) 'Regulation of pim and myb mRNA accumulation by interleukin 2 and interleukin 3 in murine hematopoietic cell lines', *The Journal of Biological Chemistry*, 263(33), pp. 17615–17620.

De Smedt, R. *et al.* (2019) 'Pre-clinical evaluation of second generation PIM inhibitors for the treatment of T-cell acute lymphoblastic leukemia and lymphoma', *Haematologica*, 104(1), pp. e17–e20.

De Smedt, R. *et al.* (2020) 'Targeting cytokine- and therapy-induced PIM1 activation in preclinical models of T-cell acute lymphoblastic leukemia and lymphoma', *Blood*, 135(19), pp. 1685–1695.

DeBerardinis, R.J. *et al.* (2007) 'Beyond aerobic glycolysis: transformed cells can engage in glutamine metabolism that exceeds the requirement for protein and nucleotide synthesis', *Proceedings of the National Academy of Sciences*, 104(49), pp. 19345–19350.

DeBerardinis, R.J. and Chandel, N.S. (2020) 'We need to talk about the Warburg effect', *Nature Metabolism*, 2(2), pp. 127–129.

Decker, S. *et al.* (2014) 'PIM kinases are essential for chronic lymphocytic leukemia cell survival (PIM2/3) and CXCR4-mediated microenvironmental interactions (PIM1)', *Molecular Cancer Therapeutics*, 13(5), pp. 1231–1245.

Degan, S.E. and Gelman, I.H. (2021) 'Emerging Roles for AKT Isoform Preference in Cancer Progression Pathways', *Molecular Cancer Research*, 19(8), pp. 1251–1257.

Del Peso, L. *et al.* (1997) 'Interleukin-3-induced phosphorylation of BAD through the protein kinase Akt', *Science*, 278(5338), pp. 687–689.

Deng, D. *et al.* (2016) 'MicroRNA-124-3p regulates cell proliferation, invasion, apoptosis, and bioenergetics by targeting PIM1 in astrocytoma', *Cancer Science*, 107(7), pp. 899–907.

Dennison, J.B. *et al.* (2013) 'Lactate Dehydrogenase B: A Metabolic Marker of Response to Neoadjuvant Chemotherapy in Breast Cancer', *Clinical Cancer Research*, 19(13), pp. 3703–3713.

Deryugina, E.I. and Quigley, J.P. (2008) 'Chick embryo chorioallantoic membrane model systems to study and visualize human tumor cell metastasis', *Histochemistry and Cell Biology*, 130(6), pp. 1119–1130.

Dhanasekaran, S.M. *et al.* (2001) 'Delineation of prognostic biomarkers in prostate cancer', *Nature*, 412(6849), pp. 822–826.

Din, S. *et al.* (2013) 'Pim-1 preserves mitochondrial morphology by inhibiting dynamin-related protein 1 translocation.', *Proceedings of the National Academy of Sciences*, 110(15), pp. 5969–74.

Din, S. *et al.* (2014) 'Metabolic dysfunction consistent with premature aging results from deletion of Pim kinases.', *Circulation Research*, 115(3), pp. 376–87.

Ding, L. *et al.* (2008) 'Somatic mutations affect key pathways in lung adenocarcinoma', *Nature*, 455(7216), pp. 1069–1075.

Dogliotti, G. *et al.* (2017) 'Membrane-binding and activation of LKB1 by phosphatidic acid is essential for development and tumour suppression', *Nature Communications*, 8(1), pp. 1–12.

Domen, J. *et al.* (1987) 'Comparison of the human and mouse PIM-1 cDNAs: nucleotide sequence and immunological identification of the in vitro synthesized PIM-1 protein', *Oncogene Research*, 1(1), pp. 103–112.

Domen, J., van der Lugt, N.M., Laird, P.W., Saris, C.J. and Berns, A. (1993) 'Analysis of Pim-1 function in mutant mice', *Leukemia*, 7 Suppl 2, pp. S108-112.

Domen, J., van der Lugt, N.M., Laird, P.W., Saris, C.J., Clarke, A.R., *et al.* (1993) 'Impaired interleukin-3 response in Pim-1-deficient bone marrow-derived mast cells', *Blood*, 82(5), pp. 1445–1452.

Dong, W. *et al.* (2022) 'Long non-coding RNA (FALEC) promotes malignant behaviors of gastric cancer cells by regulating miR-203b/PIM3 axis', *Annals of Translational Medicine*, 10(10), p. 579.

Dummler, B. *et al.* (2006) 'Life with a single isoform of Akt: mice lacking Akt2 and Akt3 are viable but display impaired glucose homeostasis and growth deficiencies', *Molecular and Cellular Biology*, 26(21), pp. 8042–8051.

Edwards, M. *et al.* (2014) 'Capping protein regulators fine-tune actin assembly dynamics', *Nature Reviews Molecular Cell Biology*, 15(10), pp. 677–689.

Eerola, S.K. *et al.* (2019) 'Phosphorylation of NFATC1 at PIM1 target sites is essential for its ability to promote prostate cancer cell migration and invasion', *Cell Communication and Signaling*, 17(1), p. 148.

Eerola, S.K. *et al.* (2021) 'Expression and ERG regulation of PIM kinases in prostate cancer', *Cancer Medicine*, 10(10), pp. 3427–3436.

Eichmann, A. *et al.* (2000) 'Developmental expression of Pim kinases suggests functions also outside of the hematopoietic system', *Oncogene*, 19(9), pp. 1215–1224.

Eichner, L.J. *et al.* (2019) 'Genetic Analysis Reveals AMPK Is Required to Support Tumor Growth in Murine Kras-Dependent Lung Cancer Models', *Cell Metabolism*, 29(2), pp. 285-302.e7.

Ekambaram, R. *et al.* (2013) 'Selective bisubstrate inhibitors with sub-nanomolar affinity for protein kinase Pim-1', *ChemMedChem*, 8(6), pp. 909–913.

Elmore, S. (2007) 'Apoptosis: a review of programmed cell death', *Toxicologic Pathology*, 35(4), pp. 495–516.

Fan, J. *et al.* (2011) 'Tyrosine Phosphorylation of Lactate Dehydrogenase A Is Important for NADH/NAD+ Redox Homeostasis in Cancer Cells', *Molecular and Cellular Biology*, 31(24), pp. 4938–4950.

Fan, J. *et al.* (2013) 'Glutamine-driven oxidative phosphorylation is a major ATP source in transformed mammalian cells in both normoxia and hypoxia', *Molecular Systems Biology*, 9, p. 712.

Fares, J. *et al.* (2020) 'Molecular principles of metastasis: a hallmark of cancer revisited', *Signal Transduction and Targeted Therapy*, 5(1), p. 28.

Faubert, B., Solmonson, A. and DeBerardinis, R.J. (2020) 'Metabolic reprogramming and cancer progression', *Science*. American Association for the Advancement of Science.

Feldman, B.J. and Feldman, D. (2001) 'The development of androgen-independent prostate cancer', *Nature Reviews Cancer*, 1(1), pp. 34–45.

Feldman, J.D. *et al.* (1998) 'KID-1, a protein kinase induced by depolarization in brain', *The Journal of Biological Chemistry*, 273(26), pp. 16535–16543.

Feng, F. *et al.* (2022) 'Long non-coding RNA long intergenic non-protein coding RNA 1232 promotes cell proliferation, migration and invasion in bladder cancer via modulating miR-370-5p/PIM3 axis', *Journal of Tissue Engineering and Regenerative Medicine*, 16(6), pp. 575–585.

Fernandez, P.C. *et al.* (2003) 'Genomic targets of the human c-Myc protein', *Genes & Development*, 17(9), pp. 1115–1129.

Flick, M.J. and Konieczny, S.F. (2002) 'Identification of putative mammalian D-lactate dehydrogenase enzymes', *Biochemical and Biophysical Research Communications*, 295(4), pp. 910–916.

Forshell, L.P. *et al.* (2011) 'The direct Myc target Pim3 cooperates with other Pim kinases in supporting viability of Myc-induced B-cell lymphomas', *Oncotarget*, 2(6), pp. 448–460.

Foulkes, W.D., Smith, I.E. and Reis-Filho, J.S. (2010) 'Triple-negative breast cancer', *The New England Journal of Medicine*, 363(20), pp. 1938–1948.

Foulks, J.M. *et al.* (2014) 'A small-molecule inhibitor of PIM kinases as a potential treatment for urothelial carcinomas', *Neoplasia*, 16(5), pp. 403–412.

Fox, C.J. *et al.* (2003) 'The serine/threonine kinase Pim-2 is a transcriptionally regulated apoptotic inhibitor', *Genes & Development*, 17(15), pp. 1841–1854.

Friedmann, M. *et al.* (1992) 'Characterization of the proto-oncogene pim-1: kinase activity and substrate recognition sequence', *Archives of Biochemistry and Biophysics*, 298(2), pp. 594–601.

Fu, H., Subramanian, R.R. and Masters, S.C. (2000) '14-3-3 proteins: structure, function, and regulation', *Annual Review of Pharmacology and Toxicology*, 40, pp. 617–647.

Fujii, C. *et al.* (2005) 'Aberrant expression of serine/threonine kinase Pim-3 in hepatocellular carcinoma development and its role in the proliferation of human hepatoma cell lines', *International Journal of Cancer*, 114(2), pp. 209–218.

Gao, X. *et al.* (2019) 'PIM1 is responsible for IL-6-induced breast cancer cell EMT and stemness via c-myc activation', *Breast Cancer*, 26(5), pp. 663–671.

Gapter, L.A. *et al.* (2006) 'Pim-1 kinase expression during murine mammary development', *Biochemical and Biophysical Research Communications*, 345(3), pp. 989–997.

Garcia, P.D. *et al.* (2014) 'Pan-PIM kinase inhibition provides a novel therapy for treating hematologic cancers', *Clinical Cancer Research*, 20(7), pp. 1834–1845. 2062.

Giardiello, F.M. and Trimbath, J.D. (2006) 'Peutz-Jeghers syndrome and management recommendations', *Clinical Gastroenterology and Hepatology*, 4(4), pp. 408–415.

Glazova, M. *et al.* (2005) 'Pim-1 kinase enhances NFATc activity and neuroendocrine functions in PC12 cells', *Molecular Brain Research*, 138(2), pp. 116–123.

Goldberg, E. *et al.* (2010) 'LDHC: the ultimate testis-specific gene', *Journal of Andrology*, 31(1), pp. 86–94.
Gómez-Abad, C. *et al.* (2011) 'PIM2 inhibition as a rational therapeutic approach in B-cell lymphoma', *Blood*, 118(20), pp. 5517–5527.
Gong, J. *et al.* (2009) 'Serine/threonine kinase Pim-2 promotes liver tumorigenesis induction through mediating survival and preventing apoptosis of liver cell', *The Journal of Surgical Research*, 153(1), pp. 17–22.
Goodwin, J.M. *et al.* (2014) 'An AMPK-independent signaling pathway downstream of the LKB1 tumor suppressor controls Snail1 and metastatic potential', *Molecular Cell*, 55(3), pp. 436–450.
Gowans, G.J. *et al.* (2013) 'AMP is a true physiological regulator of AMP-activated protein kinase by both allosteric activation and enhancing net phosphorylation', *Cell Metabolism*, 18(4), pp. 556–566.
Grundler, R. *et al.* (2009) 'Dissection of PIM serine/threonine kinases in FLT3-ITD-induced leukemogenesis reveals PIM1 as regulator of CXCL12-CXCR4-mediated homing and migration', *The Journal of Experimental Medicine*, 206(9), pp. 1957–1970.
GTEx Consortium (2013) 'The Genotype-Tissue Expression (GTEx) project', *Nature Genetics*, 45(6), pp. 580–585.
Gu, J.J. *et al.* (2009) 'PIM1 phosphorylates and negatively regulates ASK1-mediated apoptosis', *Oncogene*, 28(48), pp. 4261–4271.
Guo, S. *et al.* (2010) 'Overexpression of Pim-1 in bladder cancer', *Journal of Experimental & Clinical Cancer Research*, 29, p. 161.
Ha, S. *et al.* (2013) 'Phosphorylation of the androgen receptor by PIM1 in hormone refractory prostate cancer', *Oncogene*, 32(34), pp. 3992–4000.
Hammerman, P.S. *et al.* (2004) 'Lymphocyte transformation by Pim-2 is dependent on nuclear factor-kappaB activation', *Cancer Research*, 64(22), pp. 8341–8348.
Hammerman, P.S. *et al.* (2005) 'Pim and Akt oncogenes are independent regulators of hematopoietic cell growth and survival', *Blood*, 105(11), pp. 4477–4483.
Han, W. *et al.* (2019) 'MicroRNA-26b-5p enhances T cell responses by targeting PIM-2 in hepatocellular carcinoma', *Cellular Signalling*, 59, pp. 182–190.
Hanahan, D. (2022) 'Hallmarks of Cancer: New Dimensions', *Cancer Discovery*, 12(1), pp. 31–46.
Hanahan, D. and Weinberg, R.A. (2011) 'Hallmarks of cancer: the next generation', *Cell*, 144(5), pp. 646–674.
Hardie, D.G. and Hawley, S.A. (2001) 'AMP-activated protein kinase: the energy charge hypothesis revisited', *BioEssays*, 23(12), pp. 1112–1119.
Hart, M.C. and Cooper, J.A. (1999) 'Vertebrate isoforms of actin capping protein beta have distinct functions In vivo', *The Journal of Cell Biology*, 147(6), pp. 1287–1298.
Hart, M.C., Korshunova, Y.O. and Cooper, J.A. (1997) 'Vertebrates have conserved capping protein alpha isoforms with specific expression patterns', *Cell Motility and the Cytoskeleton*, 38(2), pp. 120–132.
Hawley, S.A. *et al.* (2003) 'Complexes between the LKB1 tumor suppressor, STRADα/β and MO25α/β are upstream kinases in the AMP-activated protein kinase cascade', *Journal of Biology*, 2(4), p. 28.
Hay, E.D. (1995) 'An overview of epithelio-mesenchymal transformation', *Acta Anatomica*, 154(1), pp. 8–20.
He, H. *et al.* (2009) 'Real-time quantitative RT-PCR assessment of PIM-1 and hK2 mRNA expression in benign prostate hyperplasia and prostate cancer', *Medical Oncology*, 26(3), pp. 303–308.
He, H. *et al.* (2013) 'Integration of the metabolic/redox state, histone gene switching, DNA replication and S-phase progression by moonlighting metabolic enzymes', *Bioscience Reports*, 33(2), p. e00018.
Heinlein, C.A. and Chang, C. (2004) 'Androgen receptor in prostate cancer', *Endocrine Reviews*, 25(2), pp. 276–308.

Hemminki, A. *et al.* (1998) 'A serine/threonine kinase gene defective in Peutz-Jeghers syndrome', *Nature*, 391(6663), pp. 184–187.

Hermanova, I. *et al.* (2020) 'Genetic manipulation of LKB1 elicits lethal metastatic prostate cancer', *Journal of Experimental Medicine*, 217(6).

Hietakangas, V. and Cohen, S.M. (2009) 'Regulation of tissue growth through nutrient sensing', *Annual Review of Genetics*, 43, pp. 389–410.

Hollander, M.C., Blumenthal, G.M. and Dennis, P.A. (2011) 'PTEN loss in the continuum of common cancers, rare syndromes and mouse models', *Nature Reviews Cancer*, 11(4), pp. 289–301.

Hollstein, P.E. *et al.* (2019) 'The AMPK-related kinases SIK1 and SIK3 mediate key tumor-suppressive effects of LKB1 in NSCLC', *Cancer Discovery*, 9(11), pp. 1606–1627.

Hoosein, N. *et al.* (1995) 'Clinical significance of elevation in neuroendocrine factors and interleukin-6 in metastatic prostate cancer', *Urologic Oncology*, 1(6), pp. 246–251.

Hoover, D. *et al.* (1991) 'Recombinant human pim-1 protein exhibits serine/threonine kinase activity', *The Journal of Biological Chemistry*, 266(21), pp. 14018–14023.

Hoover, D.S. *et al.* (1997) 'Pim-1 protein expression is regulated by its 5'-untranslated region and translation initiation factor elF-4E', *Cell Growth & Differentiation*, 8(12), pp. 1371–1380.

Horiuchi, D. *et al.* (2016) 'PIM kinase inhibition presents a novel targeted therapy against triple-negative breast tumors with elevated MYC expression', *Nature Medicine*, 22(11), pp. 1321–1329.

Hornbeck, P.V. *et al.* (2015) 'PhosphoSitePlus, 2014: Mutations, PTMs and recalibrations', *Nucleic Acids Research*, 43(D1), pp. D512–D520.

Hospital, M.-A. *et al.* (2018) 'RSK2 is a new Pim2 target with pro-survival functions in FLT3-ITD-positive acute myeloid leukemia', *Leukemia*, 32(3), pp. 597–605.

Hu, J. *et al.* (2013) 'Heterogeneity of tumor-induced gene expression changes in the human metabolic network', *Nature Biotechnology*, 31(6), pp. 522–529.

Hu, J. *et al.* (2019) 'Establishment of xenografts of urological cancers on chicken chorioallantoic membrane (CAM) to study metastasis', *Precision Clinical Medicine*, 2(3), pp. 140–151.

Hu, X.F. *et al.* (2009) 'PIM-1-specific mAb suppresses human and mouse tumor growth by decreasing PIM-1 levels, reducing Akt phosphorylation, and activating apoptosis', *The Journal of Clinical Investigation*, 119(2), pp. 362–375.

Hu, Y.-L. *et al.* (2007) 'Evidence that the Pim1 kinase gene is a direct target of HOXA9', *Blood*, 109(11), pp. 4732–4738.

Huang, D. *et al.* (2019) 'Hypoxia induces actin cytoskeleton remodeling by regulating the binding of CAPZA1 to F-actin via PIP2 to drive EMT in hepatocellular carcinoma', *Cancer Letters*, 448, pp. 117–127.

Huang, H. and Tindall, D.J. (2007) 'Dynamic FoxO transcription factors', *Journal of Cell Science*, 120(Pt 15), pp. 2479–2487.

Huot, G. *et al.* (2014) 'CHES1/FOXN3 regulates cell proliferation by repressing PIM2 and protein biosynthesis', *Molecular Biology of the Cell*, 25(5), pp. 554–565.

Hüsemann, Y. *et al.* (2008) 'Systemic spread is an early step in breast cancer', *Cancer Cell*, 13(1), pp. 58–68.

Intlekofer, A.M. *et al.* (2017) 'L-2-Hydroxyglutarate production arises from noncanonical enzyme function at acidic pH', *Nature Chemical Biology*, 13(5), pp. 494–500.

Isakoff, S.J. (2010) 'Triple-negative breast cancer: role of specific chemotherapy agents', *Cancer Journal*, 16(1), pp. 53–61.

Isenberg, G., Aebi, U. and Pollard, T.D. (1980) 'An actin-binding protein from Acanthamoeba regulates actin filament polymerization and interactions', *Nature*, 288(5790), pp. 455–459.

Iyer, R.S. *et al.* (2017) 'A functional SUMO-motif in the active site of PIM1 promotes its degradation via RNF4, and stimulates protein kinase activity', *Scientific Reports*, 7(1), p. 3598.

Ja, C. *et al.* (1983) 'Three glycolytic enzymes are phosphorylated at tyrosine in cells transformed by Rous sarcoma virus', *Nature*, 302(5905), p. 1.

Jacobs, M.D. *et al.* (2005) 'Pim-1 ligand-bound structures reveal the mechanism of serine/threonine kinase inhibition by LY294002', *The Journal of Biological Chemistry*, 280(14), pp. 13728–13734.
James, O.J. *et al.* (2021) 'IL-15 and PIM kinases direct the metabolic programming of intestinal intraepithelial lymphocytes', *Nature Communications*, 12(1), p. 4290.
Jang, S.H. and Chung, H.Y. (2012) 'MYC and PIM2 co-expression in mouse bone marrow cells readily establishes permanent myeloid cell lines that can induce lethal myeloid sarcoma in vivo', *Molecules and Cells*, 34(2), pp. 201–208.
Jiménez-García, M.P. *et al.* (2016) 'The role of PIM1/PIM2 kinases in tumors of the male reproductive system', *Scientific Reports*, 6(1), p. 38079.
Jiménez-García, M.-P. *et al.* (2017) 'Inflammation and stem markers association to PIM1/PIM2 kinase-induced tumors in breast and uterus', *Oncotarget*, 8(35), pp. 58872–58886.
Jin, L. *et al.* (2017) 'Phosphorylation-mediated activation of LDHA promotes cancer cell invasion and tumour metastasis', *Oncogene*, 36(27), pp. 3797–3806.
Jin, Y. *et al.* (2012) 'Expressions of Osteopontin (OPN), αvβ3 and Pim-1 Associated with Poor Prognosis in Non-small Cell Lung Cancer (NSCLC)', *Chinese Journal of Cancer Research*, 24(2), pp. 103–108.
Jinek, M. *et al.* (2012) 'A programmable dual-RNA-guided DNA endonuclease in adaptive bacterial immunity', *Science,* 337(6096), pp. 816–821.
Julson, J.R. *et al.* (2022) 'The Role of PIM Kinases in Pediatric Solid Tumors', *Cancers*, 14(15), p. 3565.
Kalichamy, K.S. *et al.* (2019) 'PIM-Related Kinases Selectively Regulate Olfactory Sensations in Caenorhabditis elegans', *eNeuro*, 6(4), p. ENEURO.0003-19.2019.
Kalluri, R. and Weinberg, R.A. (2009) 'The basics of epithelial-mesenchymal transition', *The Journal of Clinical Investigation*, 119(6), pp. 1420–1428.
Kapelko-Słowik, K. *et al.* (2019) 'Expression of the PIM2 gene is associated with more aggressive clinical course in patients with chronic lymphocytic leukemia', *Advances in Clinical and Experimental Medicine*, 28(3), pp. 385–390.
Katsuta, E. *et al.* (2022) 'Targeting PIM2 by JP11646 results in significant antitumor effects in solid tumors', *International Journal of Oncology*, 61(4), p. 114.
Katti, A. *et al.* (2022) 'CRISPR in cancer biology and therapy', *Nature Reviews Cancer*, 22(5), pp. 259–279.
Kayser, G. *et al.* (2010) 'Lactate-dehydrogenase 5 is overexpressed in non-small cell lung cancer and correlates with the expression of the transketolase-like protein 1', *Diagnostic Pathology*, 5, p. 22.
Keeton, E.K. *et al.* (2014) 'AZD1208, a potent and selective pan-Pim kinase inhibitor, demonstrates efficacy in preclinical models of acute myeloid leukemia', *Blood*, 123(6), pp. 905–913.
Kim, E.-Y. *et al.* (2019) 'A Novel Lactate Dehydrogenase Inhibitor, 1-(Phenylseleno)-4-(Trifluoromethyl) Benzene, Suppresses Tumor Growth through Apoptotic Cell Death', *Scientific Reports*, 9(1), p. 3969.
Kim, J. *et al.* (2012) 'A mouse model of heterogeneous, c-MYC-initiated prostate cancer with loss of Pten and p53', *Oncogene*, 31(3), pp. 322–332.
Kim, K.-T. *et al.* (2005) 'Pim-1 is up-regulated by constitutively activated FLT3 and plays a role in FLT3-mediated cell survival', *Blood*, 105(4), pp. 1759–1767.
Kim, K.-T. *et al.* (2012) 'MicroRNA-16 is down-regulated in mutated FLT3 expressing murine myeloid FDC-P1 cells and interacts with Pim-1', *PLOS ONE*, 7(9), p. e44546.
Kim, O. *et al.* (2004) 'Synergism of cytoplasmic kinases in IL6-induced ligand-independent activation of androgen receptor in prostate cancer cells', *Oncogene*, 23(10), pp. 1838–1844.
Kishton, R.J. *et al.* (2016) 'AMPK Is Essential to Balance Glycolysis and Mitochondrial Metabolism to Control T-ALL Cell Stress and Survival', *Cell Metabolism*, 23(4), pp. 649–662.
Koppenol, W.H., Bounds, P.L. and Dang, C.V. (2011) 'Otto Warburg's contributions to current concepts of cancer metabolism', *Nature Reviews Cancer*, 11(5), pp. 325–337.

Koukourakis, M.I. *et al.* (2003) 'Lactate dehydrogenase-5 (LDH-5) overexpression in non-small-cell lung cancer tissues is linked to tumour hypoxia, angiogenic factor production and poor prognosis', *British Journal of Cancer*, 89(5), pp. 877–885.

Koukourakis, M.I. *et al.* (2014) 'Lactate dehydrogenase 5 isoenzyme overexpression defines resistance of prostate cancer to radiotherapy', *British Journal of Cancer*, 110(9), pp. 2217–2223.

Koukourakis, M.I., Giatromanolaki, A. and Sivridis, E. (2003) 'Lactate Dehydrogenase Isoenzymes 1 and 5: Differential Expression by Neoplastic and Stromal Cells in Non-Small Cell Lung Cancer and Other Epithelial Malignant Tumors', *Tumor Biology*, 24(4), pp. 199–202.

Kovacina, K.S. *et al.* (2003) 'Identification of a proline-rich Akt substrate as a 14-3-3 binding partner', *The Journal of Biological Chemistry*, 278(12), pp. 10189–10194.

Kuang, X. *et al.* (2019) 'PIM inhibitor SMI-4a induces cell apoptosis in B-cell acute lymphocytic leukemia cells via the HO-1-mediated JAK2/STAT3 pathway', *Life Sciences*, 219, pp. 248–256.

Kumar, A. *et al.* (2005) 'Crystal structures of proto-oncogene kinase Pim1: a target of aberrant somatic hypermutations in diffuse large cell lymphoma.', *Journal of Molecular Biology*, 348(1), pp. 183–93.

Kunder, R. *et al.* (2022) 'Synergistic PIM kinase and proteasome inhibition as a therapeutic strategy for MYC-overexpressing triple-negative breast cancer', *Cell Chemical Biology*, 29(3), pp. 358-372.e5.

Kuo, H.-P. *et al.* (2016) 'The role of PIM1 in the ibrutinib-resistant ABC subtype of diffuse large B-cell lymphoma', *American Journal of Cancer Research*, 6(11), pp. 2489–2501.

La Starza, R. *et al.* (2018) 'High PIM1 expression is a biomarker of T-cell acute lymphoblastic leukemia with JAK/STAT activation or t(6;7)(p21;q34)/TRB@-PIM1 rearrangement', *Leukemia*, 32(8), pp. 1807–1810.

Lamouille, S., Xu, J. and Derynck, R. (2014) 'Molecular mechanisms of epithelial–mesenchymal transition', *Nature reviews Molecular Cell Biology*, 15(3), pp. 178–196.

Le, A. *et al.* (2010) 'Inhibition of lactate dehydrogenase A induces oxidative stress and inhibits tumor progression', *Proceedings of the National Academy of Sciences*, 107(5), pp. 2037–2042.

Le Clainche, C. and Carlier, M.-F. (2008) 'Regulation of actin assembly associated with protrusion and adhesion in cell migration', *Physiological Reviews*, 88(2), pp. 489–513.

Le, X. *et al.* (2016) 'Systematic Functional Characterization of Resistance to PI3K Inhibition in Breast Cancer', *Cancer Discovery*, 6(10), pp. 1134–1147.

Ledet, R.J. *et al.* (2021) 'Identification of PIM1 substrates reveals a role for NDRG1 phosphorylation in prostate cancer cellular migration and invasion', *Communications Biology*, 4(1), p. 36.

Lee, M. *et al.* (2019) 'Pan-Pim Kinase Inhibitor AZD1208 Suppresses Tumor Growth and Synergistically Interacts with Akt Inhibition in Gastric Cancer Cells', *Cancer Research and Treatment*, 51(2), pp. 451–463.

Lee, S.-W. *et al.* (2015) 'Skp2-dependent ubiquitination and activation of LKB1 is essential for cancer cell survival under energy stress', *Molecular Cell*, 57(6), pp. 1022–1033.

Lee, W.J. *et al.* (2006) 'AMPK activation increases fatty acid oxidation in skeletal muscle by activating PPARalpha and PGC-1', *Biochemical and Biophysical Research Communications*, 340(1), pp. 291–295.

Lees, A., Haddad, J.G. and Lin, S. (1984) 'Brevin and vitamin D binding protein: comparison of the effects of two serum proteins on actin assembly and disassembly', *Biochemistry*, 23(13), pp. 3038–3047.

Leiblich, A. *et al.* (2006) 'Lactate dehydrogenase-B is silenced by promoter hypermethylation in human prostate cancer', *Oncogene*, 25(20), pp. 2953–2960.

Leung, C.O. *et al.* (2015) 'PIM1 regulates glycolysis and promotes tumor progression in hepatocellular carcinoma.', *Oncotarget*, 6(13), pp. 10880–92.

Leverson, J.D. *et al.* (1998) 'Pim-1 kinase and p100 cooperate to enhance c-Myb activity', *Molecular Cell*, 2(4), pp. 417–425.

Li, Q. *et al.* (2020) 'TAB3 upregulates PIM1 expression by directly activating the TAK1-STAT3 complex to promote colorectal cancer growth', *Experimental Cell Research*, 391(1), p. 111975.
Li, T.-T. and Zhu, H.-B. (2020) 'LKB1 and cancer: The dual role of metabolic regulation', *Biomedicine & Pharmacotherapy*, 132, p. 110872.
Li, X. *et al.* (2020) 'Lysine-222 succinylation reduces lysosomal degradation of lactate dehydrogenase a and is increased in gastric cancer', *Journal of Experimental & Clinical Cancer Research*, 39(1), p. 172.
Li, Y.-Y. *et al.* (2006) 'Pim-3, a proto-oncogene with serine/threonine kinase activity, is aberrantly expressed in human pancreatic cancer and phosphorylates bad to block bad-mediated apoptosis in human pancreatic cancer cell lines', *Cancer Research*, 66(13), pp. 6741–6747.
Li, Y.-Y. *et al.* (2009) 'Essential contribution of Ets-1 to constitutive Pim-3 expression in human pancreatic cancer cells', *Cancer Science*, 100(3), pp. 396–404.
Liang, Z. *et al.* (2005) 'Silencing of CXCR4 blocks breast cancer metastasis', *Cancer Research*, 65(3), pp. 967–971.
Lin, Y.-H. *et al.* (2013) 'CapZ and actin capping dynamics increase in myocytes after a bout of exercise and abates in hours after stimulation ends', *Journal of Applied Physiology*, 114(11), pp. 1603–1609.
Lin, Y.H. *et al.* (2016) 'Myofibril growth during cardiac hypertrophy is regulated through dual phosphorylation and acetylation of the actin capping protein CapZ', *Cellular Signalling*, 28(8), pp. 1015–1024.
Liu, H. *et al.* (2020) 'Inhibition of PIM1 attenuates the stem cell-like traits of breast cancer cells by promoting RUNX3 nuclear retention', *Journal of Cellular and Molecular Medicine*, 24(11), pp. 6308–6323.
Liu, J. *et al.* (2018) 'Aberrant FGFR Tyrosine Kinase Signaling Enhances the Warburg Effect by Reprogramming LDH Isoform Expression and Activity in Prostate Cancer', *Cancer Research*, 78(16), pp. 4459–4470.
Liu, L. *et al.* (2012) 'Akt blocks the tumor suppressor activity of LKB1 by promoting phosphorylation-dependent nuclear retention through 14-3-3 proteins.', *American Journal of Translational Research*, 4(2), pp. 175–86.
Liu, M. *et al.* (2013) 'The Histone Methyltransferase EZH2 Mediates Tumor Progression on the Chick Chorioallantoic Membrane Assay, a Novel Model of Head and Neck Squamous Cell Carcinoma', *Translational Oncology*, 6(3), pp. 273–281.
Liu, Y. *et al.* (2018) 'Nuclear lactate dehydrogenase A senses ROS to produce α-hydroxybutyrate for HPV-induced cervical tumor growth', *Nature Communications*, 9(1), p. 4429.
Long, Y.C. and Zierath, J.R. (2006) 'AMP-activated protein kinase signaling in metabolic regulation', *The Journal of Clinical Investigation*, 116(7), pp. 1776–1783.
Lou, L. *et al.* (2014) 'Differential expression of Pim-3, c-Myc, and p-p27 proteins in adenocarcinomas of the gastric cardia and distal stomach', *Tumour Biology*, 35(5), pp. 5029–5036.
Lu, C. *et al.* (2012) 'IDH mutation impairs histone demethylation and results in a block to cell differentiation', *Nature*, 483(7390), pp. 474–478.
Lu, C. *et al.* (2021) 'Positive regulation of PFKFB3 by PIM2 promotes glycolysis and paclitaxel resistance in breast cancer', *Clinical and Translational Medicine*, 11(4), p. e400.
Lu, J. *et al.* (2013) 'Pim2 is required for maintaining multiple myeloma cell growth through modulating TSC2 phosphorylation', *Blood*, 122(9), pp. 1610–1620.
van der Lugt, N.M. *et al.* (1995) 'Proviral tagging in E mu-myc transgenic mice lacking the Pim-1 proto-oncogene leads to compensatory activation of Pim-2', *The EMBO Journal*, 14(11), pp. 2536–2544.
Lum, J.J. *et al.* (2007) 'The transcription factor HIF-1α plays a critical role in the growth factor-dependent regulation of both aerobic and anaerobic glycolysis', *Genes & Development*, 21(9), pp. 1037–1049.

Luszczak, S., Simpson, B.S., *et al.* (2020) 'Co-targeting PIM and PI3K/mTOR using multikinase inhibitor AUM302 and a combination of AZD-1208 and BEZ235 in prostate cancer', *Scientific Reports*, 10(1), p. 14380.

Luszczak, S., Kumar, C., *et al.* (2020) 'PIM kinase inhibition: co-targeted therapeutic approaches in prostate cancer', *Signal Transduction and Targeted Therapy*, 5(1), p. 7.

M, S. *et al.* (2006) 'Dissecting the role of 5'-AMP for allosteric stimulation, activation, and deactivation of AMP-activated protein kinase', *The Journal of Biological Chemistry*, 281(43).

Ma, J. *et al.* (2007) 'Negative regulation of Pim-1 protein kinase levels by the B56beta subunit of PP2A', *Oncogene*, 26(35), pp. 5145–5153.

Ma, Jialin *et al.* (2020) 'A genetic predictive model for precision treatment of diffuse large B-cell lymphoma with early progression', *Biomarker Research*, 8, p. 33.

Macdonald, A. *et al.* (2006) 'Pim kinases phosphorylate multiple sites on Bad and promote 14-3-3 binding and dissociation from Bcl-XL', *BMC Cell Biology*, 7(1), p. 1.

Maekawa, M. *et al.* (2003) 'Promoter Hypermethylation in Cancer Silences LDHB, Eliminating Lactate Dehydrogenase Isoenzymes 1-4', *Clinical Chemistry*, 49(9), pp. 1518–1520.

Magistroni, V. *et al.* (2011) 'ERG Deregulation Induces PIM1 Over-Expression and Aneuploidy in Prostate Epithelial Cells', *PLOS ONE*, 6(11), p. e28162.

Maitland, M.E.R. *et al.* (2021) 'Proteomic analysis of ubiquitination substrates reveals a CTLH E3 ligase complex-dependent regulation of glycolysis', *The FASEB Journal*, 35(9), p. e21825.

Majewski, N. *et al.* (2004) 'Hexokinase-mitochondria interaction mediated by Akt is required to inhibit apoptosis in the presence or absence of Bax and Bak', *Molecular Cell*, 16(5), pp. 819–830.

Malinen, M. *et al.* (2013) 'Proto-oncogene PIM-1 is a novel estrogen receptor target associating with high grade breast tumors', *Molecular and Cellular Endocrinology*, 365(2), pp. 270–276.

Malumbres, M. (2014) 'Cyclin-dependent kinases', *Genome Biology*, 15(6), p. 122.

Mantovani, F., Collavin, L. and Del Sal, G. (2019) 'Mutant p53 as a guardian of the cancer cell', *Cell Death & Differentiation*, 26(2), pp. 199–212.

Marino, D. *et al.* (2022) 'High ETV6 Levels Support Aggressive B Lymphoma Cell Survival and Predict Poor Outcome in Diffuse Large B-Cell Lymphoma Patients', *Cancers*, 14(2), p. 338.

Markou, A. *et al.* (2020) 'PIM-1 Is Overexpressed at a High Frequency in Circulating Tumor Cells from Metastatic Castration-Resistant Prostate Cancer Patients', *Cancers*, 12(5), p. E1188.

Martinou, J.-C. and Youle, R.J. (2011) 'Mitochondria in Apoptosis: Bcl-2 family Members and Mitochondrial Dynamics', *Developmental Cell*, 21(1), pp. 92–101.

Maruyama, K. (1966) 'Effect of beta-actinin on the particle length of F-actin', *Biochimica Et Biophysica Acta*, 126(2), pp. 389–398.

Mary Photini, S. *et al.* (2017) 'PIM kinases 1, 2 and 3 in intracellular LIF signaling, proliferation and apoptosis in trophoblastic cells', *Experimental Cell Research*, 359(1), pp. 275–283.

Matikainen, S. *et al.* (1999) 'Interferon-alpha activates multiple STAT proteins and upregulates proliferation-associated IL-2Ralpha, c-myc, and pim-1 genes in human T cells', *Blood*, 93(6), pp. 1980–1991.

Mazzacurati, L. *et al.* (2015) 'The PIM inhibitor AZD1208 synergizes with ruxolitinib to induce apoptosis of ruxolitinib sensitive and resistant JAK2-V617F-driven cells and inhibit colony formation of primary MPN cells', *Oncotarget*, 6(37), pp. 40141–40157.

Mazzacurati, L. *et al.* (2019) 'The pan-PIM inhibitor INCB053914 displays potent synergy in combination with ruxolitinib in models of MPN', *Blood Advances*, 3(22), pp. 3503–3514.

McCleland, M.L. *et al.* (2012) 'An Integrated Genomic Screen Identifies LDHB as an Essential Gene for Triple-Negative Breast Cancer', *Cancer Research*, 72(22), pp. 5812–5823.

Meja, K. *et al.* (2014) 'PIM and AKT kinase inhibitors show synergistic cytotoxicity in acute myeloid leukaemia that is associated with convergence on mTOR and MCL1 pathways', *British Journal of Haematology*, 167(1), pp. 69–79.

Mejillano, M.R. *et al.* (2004) 'Lamellipodial Versus Filopodial Mode of the Actin Nanomachinery: Pivotal Role of the Filament Barbed End', *Cell*, 118(3), pp. 363–373.

Meyer, N. and Penn, L.Z. (2008) 'Reflecting on 25 years with MYC', *Nature Reviews Cancer*, 8(12), pp. 976–990.
Mikkers, H. *et al.* (2002) 'High-throughput retroviral tagging to identify components of specific signaling pathways in cancer', *Nature Genetics*, 32(1), pp. 153–159.
Mikkers, H. *et al.* (2004) 'Mice deficient for all PIM kinases display reduced body size and impaired responses to hematopoietic growth factors.', *Molecular and Cellular Biology*, 24(13), pp. 6104–6115.
Miles, K.A. and Williams, R.E. (2008) 'Warburg revisited: imaging tumour blood flow and metabolism', *Cancer Imaging*, 8(1), pp. 81–86.
Mitsuishi, Y. *et al.* (2012) 'Nrf2 Redirects Glucose and Glutamine into Anabolic Pathways in Metabolic Reprogramming', *Cancer Cell*, 22(1), pp. 66–79.
Miura, O. *et al.* (1994) 'Induction of tyrosine phosphorylation of Vav and expression of Pim-1 correlates with Jak2-mediated growth signaling from the erythropoietin receptor', *Blood*, 84(12), pp. 4135–4141.
Miyagawa, Y. *et al.* (2002) 'Molecular cloning and characterization of the human orthologue of male germ cell-specific actin capping protein alpha3 (cpalpha3)', *Molecular Human Reproduction*, 8(6), pp. 531–539.
Miyakawa, K. *et al.* (2019) 'PIM kinases facilitate lentiviral evasion from SAMHD1 restriction via Vpx phosphorylation', *Nature Communications*, 10(1), p. 1844.
Mochizuki, T. *et al.* (1999) 'Physical and functional interactions between Pim-1 kinase and Cdc25A phosphatase. Implications for the Pim-1-mediated activation of the c-Myc signaling pathway', *The Journal of Biological Chemistry*, 274(26), pp. 18659–18666.
Mohlin, S. *et al.* (2019) 'Anti-tumor effects of PIM/PI3K/mTOR triple kinase inhibitor IBL-302 in neuroblastoma', *EMBO Molecular Medicine*, 11(8), p. e10058.
Moody, S.E. *et al.* (2015) 'PRKACA mediates resistance to HER2-targeted therapy in breast cancer cells and restores anti-apoptotic signaling', *Oncogene*, 34(16), pp. 2061–2071.
Moore, G. *et al.* (2021) 'Co-Targeting PIM Kinase and PI3K/mTOR in NSCLC', *Cancers*, 13(9), p. 2139.
Mori, M. *et al.* (2013) 'A combination strategy to inhibit Pim-1: synergism between noncompetitive and ATP-competitive inhibitors', *ChemMedChem*, 8(3), pp. 484–496.
Morishita, D. *et al.* (2008) 'Pim kinases promote cell cycle progression by phosphorylating and down-regulating p27Kip1 at the transcriptional and posttranscriptional levels', *Cancer Research*, 68(13), pp. 5076–5085.
Motylewska, E., Braun, M. and Stępień, H. (2020) 'High Expression of NEK2 and PIM1, but Not PIM3, Is Linked to an Aggressive Phenotype of Bronchopulmonary Neuroendocrine Neoplasms', *Endocrine Pathology*, 31(3), pp. 264–273.
Mou, S. *et al.* (2016) 'Expression and function of PIM kinases in osteosarcoma', *International Journal of Oncology*, 49(5), pp. 2116–2126.
Mukherjee, K. *et al.* (2016) 'Actin capping protein CAPZB regulates cell morphology, differentiation, and neural crest migration in craniofacial morphogenesis†', *Human Molecular Genetics*, 25(7), pp. 1255–1270.
Müller, A. *et al.* (2001) 'Involvement of chemokine receptors in breast cancer metastasis', *Nature*, 410(6824), pp. 50–56.
Mullins, R.D., Heuser, J.A. and Pollard, T.D. (1998) 'The interaction of Arp2/3 complex with actin: nucleation, high affinity pointed end capping, and formation of branching networks of filaments', *Proceedings of the National Academy of Sciences*, 95(11), pp. 6181–6186.
Mung, K.L. *et al.* (2021) 'PIM kinases inhibit AMPK activation and promote tumorigenicity by phosphorylating LKB1', *Cell Communication and Signaling 2021 19:1*, 19(1), pp. 1–15.
Muraski, J.A. *et al.* (2007) 'Pim-1 regulates cardiomyocyte survival downstream of Akt', *Nature Medicine*, 13(12), pp. 1467–1475.

Murray, C.W. *et al.* (2019) 'An lkb1–sik axis suppresses lung tumor growth and controls differentiation', *Cancer Discovery*, 9(11), pp. 1590–1605.

Nair, J.R. *et al.* (2017) 'Novel inhibition of PIM2 kinase has significant anti-tumor efficacy in multiple myeloma', *Leukemia*, 31(8), pp. 1715–1726.

Narita, A. *et al.* (2006) 'Structural basis of actin filament capping at the barbed-end: a cryo-electron microscopy study', *The EMBO Journal*, 25(23), pp. 5626–5633.

Narlik-Grassow, M. *et al.* (2012) 'The essential role of PIM kinases in sarcoma growth and bone invasion', *Carcinogenesis*, 33(8), pp. 1479–1486.

Narlik-Grassow, M., Blanco-Aparicio, C. and Carnero, A. (2014) 'The PIM family of serine/threonine kinases in cancer', *Medicinal Research Reviews*, 34(1), pp. 136–159.

Nawijn, M.C., Alendar, A. and Berns, A. (2011) 'For better or for worse: the role of Pim oncogenes in tumorigenesis.', *Nature Reviews Cancer*, 11(1), pp. 23–34.

Newman, L.A. *et al.* (2015) 'The 2014 Society of Surgical Oncology Susan G. Komen for the Cure Symposium: triple-negative breast cancer', *Annals of Surgical Oncology*, 22(3), pp. 874–882.

Nguyen, D.X., Bos, P.D. and Massagué, J. (2009) 'Metastasis: from dissemination to organ-specific colonization', *Nature Reviews Cancer*, 9(4), pp. 274–284.

Nieborowska-Skorska, M. *et al.* (2002) 'Complementary functions of the antiapoptotic protein A1 and serine/threonine kinase pim-1 in the BCR/ABL-mediated leukemogenesis', *Blood*, 99(12), pp. 4531–4539.

Nihira, K. *et al.* (2010) 'Pim-1 controls NF-kappaB signalling by stabilizing RelA/p65', *Cell Death & Differentiation*, 17(4), pp. 689–698.

Nishimasu, H. *et al.* (2014) 'Crystal structure of Cas9 in complex with guide RNA and target DNA', *Cell*, 156(5), pp. 935–949.

Nonga, O.E. *et al.* (2021) 'Crystal Structure-Guided Design of Bisubstrate Inhibitors and Photoluminescent Probes for Protein Kinases of the PIM Family', *Molecules*, 26(14), p. 4353.

Obata, T. *et al.* (2000) 'Peptide and protein library screening defines optimal substrate motifs for AKT/PKB', *The Journal of Biological Chemistry*, 275(46), pp. 36108–36115.

Ocaña, O.H. *et al.* (2012) 'Metastatic colonization requires the repression of the epithelial-mesenchymal transition inducer Prrx1', *Cancer Cell*, 22(6), pp. 709–724.

Okada, K. *et al.* (2018) 'FLT3-ITD induces expression of Pim kinases through STAT5 to confer resistance to the PI3K/Akt pathway inhibitors on leukemic cells by enhancing the mTORC1/Mcl-1 pathway', *Oncotarget*, 9(10), pp. 8870–8886.

Onishi, Y. *et al.* (2005) 'Identification of mono-ubiquitinated LDH-A in skeletal muscle cells exposed to oxidative stress', *Biochemical and Biophysical Research Communications*, 336(3), pp. 799–806.

Otterbein, L.R. *et al.* (2002) 'Crystal structures of the vitamin D-binding protein and its complex with actin: Structural basis of the actin-scavenger system', *Proceedings of the National Academy of Sciences*, 99(12), pp. 8003–8008.

Padi, S.K.R. *et al.* (2019) 'Phosphorylation of DEPDC5, a component of the GATOR1 complex, releases inhibition of mTORC1 and promotes tumor growth', *Proceedings of the National Academy of Sciences*, 116(41), pp. 20505–20510.

Pandkar, M.R., Dhamdhere, S.G. and Shukla, S. (2021) 'Oxygen gradient and tumor heterogeneity: The chronicle of a toxic relationship', *Biochimica Et Biophysica Acta - Reviews on Cancer*, 1876(1), p. 188553.

Pantaloni, D., Le Clainche, C. and Carlier, M.F. (2001) 'Mechanism of actin-based motility', *Science*, 292(5521), pp. 1502–1506.

Parri, M. and Chiarugi, P. (2010) 'Rac and Rho GTPases in cancer cell motility control', *Cell Communication and Signaling*, 8, p. 23.

Peltola, K. *et al.* (2009) 'Pim-1 kinase expression predicts radiation response in squamocellular carcinoma of head and neck and is under the control of epidermal growth factor receptor.', *Neoplasia*, 11(7), pp. 629–36.

Peltola, K.J. *et al.* (2004) 'Pim-1 kinase inhibits STAT5-dependent transcription via its interactions with SOCS1 and SOCS3', *Blood*, 103(10), pp. 3744–3750.
Peng, C. *et al.* (2007) 'Pim kinase substrate identification and specificity', *Journal of Biochemistry*, 141(3), pp. 353–362.
Peng, X.-D. *et al.* (2003) 'Dwarfism, impaired skin development, skeletal muscle atrophy, delayed bone development, and impeded adipogenesis in mice lacking Akt1 and Akt2', *Genes & Development*, 17(11), pp. 1352–1365.
Perez-Garcia, V. *et al.* (2018) 'Placentation defects are highly prevalent in embryonic lethal mouse mutants', *Nature*, 555(7697), pp. 463–468.
Pin, F., Couch, M.E. and Bonetto, A. (2018) 'Preservation of muscle mass as a strategy to reduce the toxic effects of cancer chemotherapy on body composition', *Current Opinion in Supportive and Palliative Care*, 12(4), pp. 420–426.
Pinto, C.S., Mishima, M. and Sampath, K. (2020) 'Tools of the trade: studying actin in zebrafish', *Histochemistry and Cell Biology*, 154(5), pp. 481–493.
Podsypanina, K. *et al.* (2008) 'Seeding and propagation of untransformed mouse mammary cells in the lung', *Science*, 321(5897), pp. 1841–1844.
Pollard, T.D. and Borisy, G.G. (2003) 'Cellular motility driven by assembly and disassembly of actin filaments', *Cell*, 112(4), pp. 453–465.
Popivanova, B.K. *et al.* (2007) 'Proto-oncogene, Pim-3 with serine/threonine kinase activity, is aberrantly expressed in human colon cancer cells and can prevent Bad-mediated apoptosis', *Cancer Science*, 98(3), pp. 321–328.
Prior, I.A., Lewis, P.D. and Mattos, C. (2012) 'A comprehensive survey of Ras mutations in cancer', *Cancer Research*, 72(10), pp. 2457–2467.
Qian, K.C. *et al.* (2005) 'Structural basis of constitutive activity and a unique nucleotide binding mode of human Pim-1 kinase', *The Journal of Biological Chemistry*, 280(7), pp. 6130–6137.
Rainio, E.-M., Sandholm, J. and Koskinen, P.J. (2002) 'Cutting Edge: Transcriptional Activity of NFATc1 Is Enhanced by the Pim-1 Kinase', *The Journal of Immunology*, 168(4), pp. 1524–1527.
Ramachandran, J. *et al.* (2016) 'Pim2 is important for regulating DNA damage response in multiple myeloma cells', *Blood Cancer Journal*, 6(8), p. e462.
Rampal, R.K. *et al.* (2021) 'Therapeutic Efficacy of Combined JAK1/2, Pan-PIM, and CDK4/6 Inhibition in Myeloproliferative Neoplasms', *Clinical Cancer Research*, 27(12), pp. 3456–3468. - 4898.
Rang, Z. *et al.* (2016) 'miR-542-3p suppresses invasion and metastasis by targeting the proto-oncogene serine/threonine protein kinase, PIM1, in melanoma', *Biochemical and Biophysical Research Communications*, 474(2), pp. 315–320.
Rebello, R.J. *et al.* (2016) 'The Dual Inhibition of RNA Pol I Transcription and PIM Kinase as a New Therapeutic Approach to Treat Advanced Prostate Cancer', *Clinical Cancer Research*, 22(22), pp. 5539–5552.
Ren, C. *et al.* (2018) 'PIM2 interacts with tristetraprolin and promotes breast cancer tumorigenesis', *Molecular Oncology*, 12(5), pp. 690–704.
Ren, K. *et al.* (2013) 'The over-expression of Pim-2 promote the tumorigenesis of prostatic carcinoma through phosphorylating eIF4B', *The Prostate*, 73(13), pp. 1462–1469.
Rhim, A.D. *et al.* (2012) 'EMT and dissemination precede pancreatic tumor formation', *Cell*, 148(1–2), pp. 349–361.
Ritho, J., Arold, S.T. and Yeh, E.T.H. (2015) 'A Critical SUMO1 Modification of LKB1 Regulates AMPK Activity during Energy Stress', *Cell Reports*, 12(5), pp. 734–742.
Roberts, D.J. *et al.* (2013) 'Akt phosphorylates HK-II at Thr-473 and increases mitochondrial HK-II association to protect cardiomyocytes', *The Journal of Biological Chemistry*, 288(33), pp. 23798–23806.
Robey, R.B. and Hay, N. (2009) 'Is Akt the "Warburg kinase"?-Akt-energy metabolism interactions and oncogenesis', *Seminars in Cancer Biology*, 19(1), pp. 25–31.

Rong, Y. *et al.* (2013) 'Lactate dehydrogenase A is overexpressed in pancreatic cancer and promotes the growth of pancreatic cancer cells', *Tumour Biology*, 34(3), pp. 1523–1530.

Roy, S. *et al.* (2013) 'Suppression of Induced microRNA-15b Prevents Rapid Loss of Cardiac Function in a Dicer Depleted Model of Cardiac Dysfunction', *PLOS ONE*, 8(6), p. e66789.

Russell, F.M. and Hardie, D.G. (2020) 'AMP-Activated Protein Kinase: Do We Need Activators or Inhibitors to Treat or Prevent Cancer?', *International Journal of Molecular Sciences*, 22(1), p. E186.

Saha, A.K. and Ruderman, N.B. (2003) 'Malonyl-CoA and AMP-activated protein kinase: an expanding partnership', *Molecular and Cellular Biochemistry*, 253(1–2), pp. 65–70.

Saha, S.K. *et al.* (2014) 'Mutant IDH inhibits HNF-4α to block hepatocyte differentiation and promote biliary cancer', *Nature*, 513(7516), pp. 110–114.

Saito, Y. *et al.* (2015) 'AMPK Protects Leukemia-Initiating Cells in Myeloid Leukemias from Metabolic Stress in the Bone Marrow', *Cell Stem Cell*, 17(5), pp. 585–596.

Sanchez-Cespedes, MontserratParrella, P. *et al.* (2002) 'Inactivation of LKB1 / STK11 Is a Common Event in Adenocarcinomas of the Lung Inactivation of LKB1 / STK11 Is a Common Event in Adenocarcinomas of the Lung 1', *Cancer Research*, 62, pp. 3659–3662.

Santio, N.M. *et al.* (2010) 'Pim-selective inhibitor DHPCC-9 reveals Pim kinases as potent stimulators of cancer cell migration and invasion.', *Molecular Cancer*, 9, p. 279.

Santio, N.M. *et al.* (2015) 'Pim kinases promote migration and metastatic growth of prostate cancer xenografts', *PLOS ONE*, 10(6), p. e0130340.

Santio, N.M., Landor, S.K.-J., *et al.* (2016) 'Phosphorylation of Notch1 by Pim kinases promotes oncogenic signaling in breast and prostate cancer cells.', *Oncotarget*, 7(28), pp. 43220–43238.

Santio, N.M., Salmela, M., *et al.* (2016) 'The PIM1 kinase promotes prostate cancer cell migration and adhesion via multiple signalling pathways.', *Experimental Cell Research*, 342(2), pp. 113–24.

Santio, N.M. *et al.* (2020) 'PIM1 accelerates prostate cancer cell motility by phosphorylating actin capping proteins', *Cell Communication and Signaling*, 18(1), p. 121.

Santio, N.M. and Koskinen, P.J. (2017) 'PIM kinases: From survival factors to regulators of cell motility', *The International Journal of Biochemistry & Cell Biology*, 93, pp. 74–85.

Sarbassov, D.D. *et al.* (2005) 'Phosphorylation and regulation of Akt/PKB by the rictor-mTOR complex', *Science*, 307(5712), pp. 1098–1101.

Saris, C.J., Domen, J. and Berns, A. (1991) 'The pim-1 oncogene encodes two related protein-serine/threonine kinases by alternative initiation at AUG and CUG', *The EMBO Journal*, 10(3), pp. 655–664.

Sato, N. *et al.* (1993) 'Signal transduction by the high-affinity GM-CSF receptor: two distinct cytoplasmic regions of the common beta subunit responsible for different signaling', *The EMBO Journal*, 12(11), pp. 4181–4189.

Saurabh, K. *et al.* (2014) 'The PIM family of oncoproteins: small kinases with huge implications in myeloid leukemogenesis and as therapeutic targets', *Oncotarget*, 5(18), pp. 8503–8514.

Scarpa, M. *et al.* (2021) 'PP2A-activating Drugs Enhance FLT3 Inhibitor Efficacy through AKT Inhibition-Dependent GSK-3β-Mediated c-Myc and Pim-1 Proteasomal Degradation', *Molecular Cancer Therapeutics*, 20(4), pp. 676–690.

Schafer, D.A. *et al.* (1994) 'Differential localization and sequence analysis of capping protein beta-subunit isoforms of vertebrates', *The Journal of Cell Biology*, 127(2), pp. 453–465.

Schafer, D.A., Jennings, P.B. and Cooper, J.A. (1996) 'Dynamics of capping protein and actin assembly in vitro: uncapping barbed ends by polyphosphoinositides', *The Journal of Cell Biology*, 135(1), pp. 169–179.

Selmi, T. *et al.* (2012) 'ZFP36 expression impairs glioblastoma cell lines viability and invasiveness by targeting multiple signal transduction pathways', *Cell Cycle*, 11(10), pp. 1977–1987.

Selten, G. *et al.* (1986) 'The primary structure of the putative oncogene pim-1 shows extensive homology with protein kinases', *Cell*, 46(4), pp. 603–611.

Selten, G., Cuypers, H.T. and Berns, A. (1985) 'Proviral activation of the putative oncogene Pim-1 in MuLV induced T-cell lymphomas', *The EMBO Journal*, 4(7), pp. 1793–1798.

Semenza, G.L. *et al.* (1996) 'Hypoxia response elements in the aldolase A, enolase 1, and lactate dehydrogenase A gene promoters contain essential binding sites for hypoxia-inducible factor 1', *The Journal of Biological Chemistry*, 271(51), pp. 32529–32537.

Shackelford, D.B. and Shaw, R.J. (2009) 'The LKB1-AMPK pathway: metabolism and growth control in tumour suppression', *Nature Reviews Cancer*, 9(8), pp. 563–575.

Shannan, B. *et al.* (2016) 'PIM kinases as therapeutic targets against advanced melanoma', *Oncotarget*, 7(34), pp. 54897–54912.

Shay, K.P. *et al.* (2005) 'Pim-1 kinase stability is regulated by heat shock proteins and the ubiquitin-proteasome pathway', *Molecular Cancer Research*, 3(3), pp. 170–181.

Shi, M. *et al.* (2014) 'A novel KLF4/LDHA signaling pathway regulates aerobic glycolysis in and progression of pancreatic cancer', *Clinical Cancer Research*, 20(16), pp. 4370–4380.

Shim, H. *et al.* (1997) 'c-Myc transactivation of LDH-A: implications for tumor metabolism and growth', *Proceedings of the National Academy of Sciences*, 94(13), pp. 6658–6663.

Shirogane, T. *et al.* (1999) 'Synergistic roles for Pim-1 and c-Myc in STAT3-mediated cell cycle progression and antiapoptosis', *Immunity*, 11(6), pp. 709–719.

Short, M.L. *et al.* (1994) 'Analysis of the rat lactate dehydrogenase A subunit gene promoter/regulatory region.', *Biochemical Journal*, 304(Pt 2), pp. 391–398.

Sinnar, S.A. *et al.* (2014) 'Capping protein is essential for cell migration in vivo and for filopodial morphology and dynamics', *Molecular Biology of the Cell*, 25(14), pp. 2152–2160.

Song, J.H. *et al.* (2015) 'Deletion of Pim kinases elevates the cellular levels of reactive oxygen species and sensitizes to K-Ras-induced cell killing.', *Oncogene*, 34(28), pp. 3728–36.

Song, J.H. *et al.* (2016) 'Insulin receptor substrate 1 is a substrate of the Pim protein kinases.', *Oncotarget*, 7(15), pp. 20152–65.

Song, J.H. *et al.* (2018) 'Mechanisms Behind Resistance to PI3K Inhibitor Treatment Induced by the PIM Kinase', *Molecular Cancer Therapeutics*, 17(12), pp. 2710–2721.

Song, J.H. and Kraft, A.S. (2012) 'Pim Kinase Inhibitors Sensitize Prostate Cancer Cells to Apoptosis Triggered by Bcl-2 Family Inhibitor ABT-737', *Cancer Research*, 72(1), pp. 294–303.

Song, W. and Shi, C. (2021) 'LncRNA RGMB-AS1 facilitates pancreatic cancer cell proliferation and migration but inhibits cell apoptosis via miR-574-3p/PIM3 axis', *American Journal of Physiology. Gastrointestinal and Liver Physiology*, 321(5), pp. G477–G488.

Sousa, C.M. *et al.* (2016) 'Pancreatic stellate cells support tumour metabolism through autophagic alanine secretion', *Nature*, 536(7617), pp. 479–483.

Staal, S.P., Hartley, J.W. and Rowe, W.P. (1977) 'Isolation of transforming murine leukemia viruses from mice with a high incidence of spontaneous lymphoma.', *Proceedings of the National Academy of Sciences*, 74(7), pp. 3065–3067.

Stafman, L.L. *et al.* (2019) 'The presence of PIM3 increases hepatoblastoma tumorigenesis and tumor initiating cell phenotype and is associated with decreased patient survival', *Journal of Pediatric Surgery*, 54(6), pp. 1206–1213. 9.

Stambaugh, R. and Post, D. (1966) 'Substrate and Product Inhibition of Rabbit Muscle Lactic Dehydrogenase Heart (H4) and Muscle (M4) Isozymes', *The Journal of Biological Chemistry*, 241(7), pp. 1462–1467.

Stambolic, V. *et al.* (1998) 'Negative regulation of PKB/Akt-dependent cell survival by the tumor suppressor PTEN', *Cell*, 95(1), pp. 29–39.

Sun, R.C. *et al.* (2019) 'Nuclear Glycogenolysis Modulates Histone Acetylation in Human Non-Small Cell Lung Cancers', *Cell Metabolism*, 30(5), pp. 903-916.e7.

Svitkina, T. (2018) 'The actin cytoskeleton and actin-based motility', *Cold Spring Harbor Perspectives in Biology*, 10(1), p. a018267.

Szydłowski, M. *et al.* (2017) 'Expression of PIM kinases in Reed-Sternberg cells fosters immune privilege and tumor cell survival in Hodgkin lymphoma', *Blood*, 130(12), pp. 1418–1429.

Szydłowski, M., Garbicz, F., *et al.* (2021) 'Inhibition of PIM Kinases in DLBCL Targets MYC Transcriptional Program and Augments the Efficacy of Anti-CD20 Antibodies', *Cancer Research*, 81(23), pp. 6029–6043.

Szydłowski, M., Dębek, S., *et al.* (2021) 'PIM Kinases Promote Survival and Immune Escape in Primary Mediastinal Large B-Cell Lymphoma through Modulation of JAK-STAT and NF-κB Activity', *The American Journal of Pathology*, 191(3), pp. 567–574.

Takakuwa, T., Miyauchi, A. and Aozasa, K. (2009) 'Aberrant somatic hypermutations in thyroid lymphomas', *Leukemia Research*, 33(5), pp. 649–654.

Takeuchi, H. *et al.* (2022) 'PIM1 is a Poor Prognostic Factor for and Potential Therapeutic Target in Serous Carcinoma of the Endometrium', *International Journal of Gynecological Pathology*.

Talasniemi, J.P. *et al.* (2008) 'Analytical investigation: assay of D-lactate in diabetic plasma and urine', *Clinical Biochemistry*, 41(13), pp. 1099–1103.

Tanaka, H. *et al.* (1994) 'Isolation and characterization of cDNA clones specifically expressed in testicular germ cells', *FEBS letters*, 355(1), pp. 4–10.

Tanaka, S. *et al.* (2009) 'Pim-1 activation of cell motility induces the malignant phenotype of tongue carcinoma', *Molecular Medicine Reports*, 2(2), pp. 313–318.

Tang, X. *et al.* (2020) 'PIM2 promotes hepatocellular carcinoma tumorigenesis and progression through activating NF-κB signaling pathway', *Cell Death & Disease*, 11(7), p. 510.

Te Boekhorst, V., Preziosi, L. and Friedl, P. (2016) 'Plasticity of Cell Migration In Vivo and In Silico', *Annual Review of Cell and Developmental Biology*, 32, pp. 491–526.

Thomas, M. *et al.* (2012) 'The proto-oncogene Pim-1 is a target of miR-33a', *Oncogene*, 31(7), pp. 918–928.

Thompson, J. *et al.* (2003) 'Attenuation of androgen receptor-dependent transcription by the serine/threonine kinase Pim-1', *Laboratory Investigation*, 83(9), pp. 1301–1309.

Tiainen, M. *et al.* (2002) 'Growth arrest by the LKB1 tumor suppressor: Induction of p21WAF1/CIP1', *Human Molecular Genetics*, 11(13), pp. 1497–1504.

Tiainen, M., Ylikorkala, A. and Mäkelä, T.P. (1999) 'Growth suppression by Lkb1 is mediated by a G1 cell cycle arrest', *Proceedings of the National Academy of Sciences* 96(16), pp. 9248–9251.

Toth, R.K., Solomon, R. and Warfel, N.A. (2022) 'Stabilization of PIM Kinases in Hypoxia Is Mediated by the Deubiquitinase USP28', *Cells*, 11(6), p. 1006.

Tsai, J.H. *et al.* (2012) 'Spatiotemporal regulation of epithelial-mesenchymal transition is essential for squamous cell carcinoma metastasis', *Cancer Cell*, 22(6), pp. 725–736.

Ubellacker, J.M. *et al.* (2020) 'Lymph protects metastasizing melanoma cells from ferroptosis', *Nature*, 585(7823), pp. 113–118.

Uddin, N. *et al.* (2015) 'Persistent activation of STAT3 by PIM2-driven positive feedback loop for epithelial-mesenchymal transition in breast cancer', *Cancer Science*, 106(6), pp. 718–725.

Uren, A.G. *et al.* (2005) 'Retroviral insertional mutagenesis: past, present and future', *Oncogene*, 24(52), pp. 7656–7672.

Uruno, T., Remmert, K. and Hammer, J.A. (2006) 'CARMIL is a potent capping protein antagonist: identification of a conserved CARMIL domain that inhibits the activity of capping protein and uncaps capped actin filaments', *The Journal of Biological Chemistry*, 281(15), pp. 10635–10650.

Valdman, A. *et al.* (2004) 'Pim-1 expression in prostatic intraepithelial neoplasia and human prostate cancer', *The Prostate*, 60(4), pp. 367–371.

Valvona, C.J. *et al.* (2016) 'The Regulation and Function of Lactate Dehydrogenase A: Therapeutic Potential in Brain Tumor', *Brain Pathology*, 26(1), pp. 3–17.

Van Vu, T. *et al.* (2021) 'CRISPR/Cas-based precision genome editing via microhomology-mediated end joining', *Plant Biotechnology Journal*, 19(2), pp. 230–239.

Vander Heiden, M.G., Cantley, L.C. and Thompson, C.B. (2009) 'Understanding the Warburg effect: the metabolic requirements of cell proliferation', *Science*, 324(5930), pp. 1029–1033.

Vara-Ciruelos, D. *et al.* (2019) 'Phenformin, But Not Metformin, Delays Development of T Cell Acute Lymphoblastic Leukemia/Lymphoma via Cell-Autonomous AMPK Activation', *Cell Reports*, 27(3), pp. 690-698.e4.

Vara-Ciruelos, D., Russell, F.M. and Hardie, D.G. (2019) 'The strange case of AMPK and cancer: Dr Jekyll or Mr Hyde? †', *Open Biology*, 9(7), p. 190099.

Vila, I.K. *et al.* (2017) 'A UBE2O-AMPKα2 Axis that Promotes Tumor Initiation and Progression Offers Opportunities for Therapy', *Cancer Cell*, 31(2), pp. 208–224.

Vlacich, G. *et al.* (2010) 'Pim3 negatively regulates glucose-stimulated insulin secretion', *Islets*, 2(5), pp. 308–317.

Vogelstein, B. *et al.* (2013) 'Cancer genome landscapes', *Science*, 339(6127), pp. 1546–1558.

Wahba, H.A. and El-Hadaad, H.A. (2015) 'Current approaches in treatment of triple-negative breast cancer', *Cancer Biology & Medicine*, 12(2), pp. 106–116.

Wang, B.-W. *et al.* (2021) 'Pim1 Kinase Inhibitors Exert Anti-Cancer Activity Against HER2-Positive Breast Cancer Cells Through Downregulation of HER2', *Frontiers in Pharmacology*, 12, p. 614673.

Wang, F. *et al.* (2021) 'Long non-coding RNA SOX21-AS1 modulates lung cancer progress upon microRNA miR-24-3p/PIM2 axis', *Bioengineered*, 12(1), pp. 6724–6737.

Wang, J. *et al.* (2010) 'Pim1 kinase synergizes with c-MYC to induce advanced prostate carcinoma.', *Oncogene*, 29(17), pp. 2477–87.

Wang, J. *et al.* (2012) 'Pim1 kinase is required to maintain tumorigenicity in MYC-expressing prostate cancer cells', *Oncogene*, 31(14), pp. 1794–1803.

Wang, J.-C. *et al.* (2022) 'PIM2 Expression Induced by Proinflammatory Macrophages Suppresses Immunotherapy Efficacy in Hepatocellular Carcinoma', *Cancer Research*, 82(18), pp. 3307–3320.

Wang, L. *et al.* (2015) 'NFATc1 activation promotes the invasion of U251 human glioblastoma multiforme cells through COX-2', *International Journal of Molecular Medicine*, 35(5), pp. 1333–1340.

Wang, L. *et al.* (2021) 'PIM2-mediated phosphorylation contributes to granulosa cell survival via resisting apoptosis during folliculogenesis', *Clinical and Translational Medicine*, 11(3), p. e359.

Wang, S. *et al.* (2017) 'A positive feedback loop between Pim-1 kinase and HBP1 transcription factor contributes to hydrogen peroxide-induced premature senescence and apoptosis', *The Journal of Biological Chemistry*, 292(20), pp. 8207–8222.

Wang, W. *et al.* (2022) 'Long Noncoding RNA KCNQ1OT1 Confers Gliomas Resistance to Temozolomide and Enhances Cell Growth by Retrieving PIM1 From miR-761', *Cellular and Molecular Neurobiology*, 42(3), pp. 695–708.

Wang, Y. *et al.* (2021) 'Decreased expression of miR-3135b reduces sensitivity to 5-fluorouracil in colorectal cancer by direct repression of PIM1', *Experimental and Therapeutic Medicine*, 22(4), p. 1151.

Wang, Y., Liu, C. and Hu, L. (2019) 'Cholesterol regulates cell proliferation and apoptosis of colorectal cancer by modulating miR-33a-PIM3 pathway', *Biochemical and Biophysical Research Communications*, 511(3), pp. 685–692.

Wang, Y.-H. *et al.* (2014) 'Cell-state-specific metabolic dependency in hematopoiesis and leukemogenesis', *Cell*, 158(6), pp. 1309–1323.

Wang, Z. *et al.* (2010) 'Pim-2 phosphorylation of p21(Cip1/WAF1) enhances its stability and inhibits cell proliferation in HCT116 cells', *The International Journal of Biochemistry & Cell Biology*, 42(6), pp. 1030–1038.

Wang, Z., Weaver, M. and Magnuson, N.S. (2005) 'Cryptic promoter activity in the DNA sequence corresponding to the pim-1 5'-UTR', *Nucleic Acids Research*, 33(7), pp. 2248–2258.

Warfel, N.A. and Kraft, A.S. (2015) 'PIM kinase (and Akt) biology and signaling in tumors.', *Pharmacology & therapeutics*, 151, pp. 41–9.

Wasiak, S., Zunino, R. and McBride, H.M. (2007) 'Bax/Bak promote sumoylation of DRP1 and its stable association with mitochondria during apoptotic cell death', *The Journal of Cell Biology*, 177(3), pp. 439–450.

Waters, A.M. and Der, C.J. (2018) 'KRAS: The Critical Driver and Therapeutic Target for Pancreatic Cancer', *Cold Spring Harbor Perspectives in Medicine*, 8(9), p. a031435.

Wear, M.A. *et al.* (2003) 'How capping protein binds the barbed end of the actin filament', *Current Biology*, 13(17), pp. 1531–1537.

Weinberg, F. *et al.* (2010) 'Mitochondrial metabolism and ROS generation are essential for Kras-mediated tumorigenicity', *Proceedings of the National Academy of Sciences*, 107(19), pp. 8788–8793.

Wen, Q.-L. *et al.* (2021) 'Role of oncogene PIM-1 in the development and progression of papillary thyroid carcinoma: Involvement of oxidative stress', *Molecular and Cellular Endocrinology*, 523, p. 111144.

Wingett, D., Reeves, R. and Magnuson, N.S. (1991) 'Stability changes in pim-1 proto-oncogene mRNA after mitogen stimulation of normal lymphocytes', *Journal of Immunology*, 147(10), pp. 3653–3659.

Wingo, S.N. *et al.* (2009) 'Somatic LKB1 mutations promote cervical cancer progression', *PLOS ONE*, 4(4).

Wise, D.R. *et al.* (2008) 'Myc regulates a transcriptional program that stimulates mitochondrial glutaminolysis and leads to glutamine addiction', *Proceedings of the National Academy of Sciences*, 105(48), pp. 18782–18787.

Wojtaszewski, J.F.P. *et al.* (2002) 'Dissociation of AMPK activity and ACCbeta phosphorylation in human muscle during prolonged exercise', *Biochemical and Biophysical Research Communications*, 298(3), pp. 309–316.

Wolfson, R.L. *et al.* (2017) 'KICSTOR recruits GATOR1 to the lysosome and is necessary for nutrients to regulate mTORC1', *Nature*, 543(7645), pp. 438–442.

Woods, A. *et al.* (2003) 'LKB1 is the upstream kinase in the AMP-activated protein kinase cascade', *Current Biology*, 13(22), pp. 2004–2008.

Wu, Y.-B. *et al.* (2016) 'PIM1 polymorphism and PIM1 expression as predisposing factors of esophageal squamous cell carcinoma in the Asian population', *OncoTargets and Therapy*, 9, pp. 2919–2925.

X H Zhong and B D Howard (1990) 'Phosphotyrosine-containing lactate dehydrogenase is restricted to the nuclei of PC12 pheochromocytoma cells.', *Molecular and Cellular Biology*, 10(2), pp. 770–776.

Xia, X. *et al.* (2020) 'miR-410-5p promotes the development of diabetic cardiomyopathy by suppressing PIM1-induced anti-apoptosis', *Molecular and Cellular Probes*, 52, p. 101558.

Xie, H. *et al.* (2014) 'Targeting lactate dehydrogenase--a inhibits tumorigenesis and tumor progression in mouse models of lung cancer and impacts tumor-initiating cells', *Cell Metabolism*, 19(5), pp. 795–809.

Xie, Y. *et al.* (2006) 'The 44 kDa Pim-1 kinase directly interacts with tyrosine kinase Etk/BMX and protects human prostate cancer cells from apoptosis induced by chemotherapeutic drugs', *Oncogene*, 25(1), pp. 70–78.

Xie, Y. *et al.* (2008) 'The 44-kDa Pim-1 kinase phosphorylates BCRP/ABCG2 and thereby promotes its multimerization and drug-resistant activity in human prostate cancer cells', *The Journal of Biological Chemistry*, 283(6), pp. 3349–3356.

Xie, Y. *et al.* (2010) 'Pim-1 kinase protects P-glycoprotein from degradation and enables its glycosylation and cell surface expression', *Molecular Pharmacology*, 78(2), pp. 310–318.

Xie, Z. *et al.* (2008) 'Phosphorylation of LKB1 at serine 428 by protein kinase C-zeta is required for metformin-enhanced activation of the AMP-activated protein kinase in endothelial cells', *Circulation*, 117(7), pp. 952–962.

Xin, G. *et al.* (2021) 'Targeting PIM1-Mediated Metabolism in Myeloid Suppressor Cells to Treat Cancer', *Cancer Immunology Research*, 9(4), pp. 454–469.
Xin, H., Deng, Y. and Cao, J. (2018) 'Proviral insertion in murine lymphomas 2 promotes stomach cancer progression by regulating apoptosis via reactive oxygen species-triggered endoplasmic reticulum stress', *Biochemical and Biophysical Research Communications*, 506(1), pp. 145–152.
Xu, D. *et al.* (2011) 'The oncogenic kinase Pim-1 is modulated by K-Ras signaling and mediates transformed growth and radioresistance in human pancreatic ductal adenocarcinoma cells', *Carcinogenesis*, 32(4), pp. 488–495.
Xu, D. *et al.* (2013) 'Inhibition of oncogenic Pim-3 kinase modulates transformed growth and chemosensitizes pancreatic cancer cells to gemcitabine', *Cancer Biology & Therapy*, 14(6), pp. 492–501.
Xu, J. *et al.* (2016) 'PIM-1 contributes to the malignancy of pancreatic cancer and displays diagnostic and prognostic value', *Journal of Experimental & Clinical Cancer Research*, 35(1), p. 133.
Xu, W. *et al.* (2011) 'Oncometabolite 2-hydroxyglutarate is a competitive inhibitor of α-ketoglutarate-dependent dioxygenases', *Cancer Cell*, 19(1), pp. 17–30.
Xu, Y. *et al.* (2016) 'Pim-2 protects H9c2 cardiomyocytes from hypoxia/reoxygenation-induced apoptosis via downregulation of Bim expression', *Environmental Toxicology and Pharmacology*, 48, pp. 94–102.
Xue, C. *et al.* (2018) 'Downregulation of PIM1 regulates glycolysis and suppresses tumor progression in gallbladder cancer', *Cancer Management and Research*, 10, pp. 5101–5112.
Yadav, A.K. *et al.* (2019) 'AZD1208, a Pan-Pim kinase inhibitor, has anti-growth effect on 93T449 human liposarcoma cells via control of the expression and phosphorylation of Pim-3, mTOR, 4EBP-1, S6, STAT-3 and AMPK', *International Journal of Molecular Sciences*, 20(2).
Yamada, E. *et al.* (2010) 'Fyn-dependent regulation of energy expenditure and body weight is mediated by tyrosine phosphorylation of LKB1', *Cell Metabolism*, 11(2), pp. 113–124.
Yan, B. *et al.* (2012) 'Clinical and therapeutic relevance of PIM1 kinase in gastric cancer', *Gastric Cancer*, 15(2), pp. 188–197.
Yang, J. *et al.* (2013) 'eIF4B phosphorylation by pim kinases plays a critical role in cellular transformation by Abl oncogenes', *Cancer Research*, 73(15), pp. 4898–4908.
Yang, Q. *et al.* (2012) 'Transcription and translation are primary targets of Pim kinase inhibitor SGI-1776 in mantle cell lymphoma', *Blood*, 120(17), pp. 3491–3500.
Yang, T. *et al.* (2018) 'PIM2-mediated phosphorylation of hexokinase 2 is critical for tumor growth and paclitaxel resistance in breast cancer', *Oncogene*, 37(45), pp. 5997–6009.
Yang, T. *et al.* (2019) 'Phosphorylation of HSF1 by PIM2 Induces PD-L1 Expression and Promotes Tumor Growth in Breast Cancer', *Cancer Research*, 79(20), pp. 5233–5244.
Yang, Z.-Z. *et al.* (2005) 'Dosage-dependent effects of Akt1/protein kinase Balpha (PKBalpha) and Akt3/PKBgamma on thymus, skin, and cardiovascular and nervous system development in mice', *Molecular and Cellular Biology*, 25(23), pp. 10407–10418.
Yip-Schneider, M.T., Horie, M. and Broxmeyer, H.E. (1995) 'Transcriptional induction of pim-1 protein kinase gene expression by interferon gamma and posttranscriptional effects on costimulation with steel factor', *Blood*, 85(12), pp. 3494–3502.
Yu, J. *et al.* (2021) 'Histone lactylation drives oncogenesis by facilitating m6A reader protein YTHDF2 expression in ocular melanoma', *Genome Biology*, 22(1), p. 85.
Yu, X. and Li, S. (2017) 'Non-metabolic functions of glycolytic enzymes in tumorigenesis', *Oncogene*, 36(19), pp. 2629–2636.
Yu, Z. *et al.* (2013) 'Proviral Insertion in Murine Lymphomas 2 (PIM2) Oncogene Phosphorylates Pyruvate Kinase M2 (PKM2) and Promotes Glycolysis in Cancer Cells', *The Journal of Biological Chemistry*, 288(49), pp. 35406–35416.
Yuan, Y. *et al.* (2022) 'PIM1 promotes hepatic conversion by suppressing reprogramming-induced ferroptosis and cell cycle arrest', *Nature Communications*, 13(1), p. 5237.

Yuneva, M.O. *et al.* (2012) 'The metabolic profile of tumors depends on both the responsible genetic lesion and tissue type', *Cell Metabolism*, 15(2), pp. 157–170.

Ždralević, M. *et al.* (2018) 'Double genetic disruption of lactate dehydrogenases A and B is required to ablate the "Warburg effect" restricting tumor growth to oxidative metabolism', *The Journal of Biological Chemistry*, 293(41), pp. 15947–15961.

Zhang, D. *et al.* (2019) 'Metabolic regulation of gene expression by histone lactylation', *Nature*, 574(7779), pp. 575–580.

Zhang, F. *et al.* (2009) 'PIM1 protein kinase regulates PRAS40 phosphorylation and mTOR activity in FDCP1 cells', *Cancer Biology & Therapy*, 8(9), pp. 846–853.

Zhang, F. *et al.* (2013) 'A novel regulatory mechanism of Pim-3 kinase stability and its involvement in pancreatic cancer progression', *Molecular Cancer Research*, 11(12), pp. 1508–1520.

Zhang, H. (2017) 'Upregulation of PIM2 by Underexpression of MicroRNA-135-5p Improves Survival Rates of Skin Allografts by Suppressing Apoptosis of Fibroblast Cells', *Medical Science Monitor* 23, pp. 107–113.

Zhang, M. *et al.* (2018) 'Pim1 supports human colorectal cancer growth during glucose deprivation by enhancing the Warburg effect', *Cancer Science*, 109(5), pp. 1468–1479.

Zhang, P. *et al.* (2009) 'Pim-3 is expressed in endothelial cells and promotes vascular tube formation', *Journal of Cellular Physiology*, 220(1), pp. 82–90.

Zhang, R.-X. *et al.* (2017) 'Pim-3 as a potential predictor of chemoradiotherapy resistance in locally advanced rectal cancer patients', *Scientific Reports*, 7(1), p. 16043.

Zhang, X. *et al.* (2020) 'Inhibition of PIM1 kinase attenuates bleomycin-induced pulmonary fibrosis in mice by modulating the ZEB1/E-cadherin pathway in alveolar epithelial cells', *Molecular Immunology*, 125, pp. 15–22.

Zhang, Y. *et al.* (2008) 'Pim kinase-dependent inhibition of c-Myc degradation.', *Oncogene*, 27(35), pp. 4809–19.

Zhang, Y., Wang, Z. and Magnuson, N.S. (2007) 'Pim-1 kinase-dependent phosphorylation of p21Cip1/WAF1 regulates its stability and cellular localization in H1299 cells', *Molecular Cancer Research*, 5(9), pp. 909–922.

Zhang, Z. *et al.* (2020) 'LncRNA LUADT1 sponges miR-195 to prevent cardiac endothelial cell apoptosis in sepsis', *Molecular Medicine*, 26(1), p. 112.

Zhao, B. *et al.* (2018) 'PIM1 mediates epithelial-mesenchymal transition by targeting Smads and c-Myc in the nucleus and potentiates clear-cell renal-cell carcinoma oncogenesis', *Cell Death & Disease*, 9(3), p. 307.

Zhao, D. *et al.* (2013) 'Lysine-5 Acetylation Negatively Regulates Lactate Dehydrogenase A and Is Decreased in Pancreatic Cancer', *Cancer cell*, 23(4), pp. 464–476.

Zhao, Y. *et al.* (2008) 'Kruppel-like factor 5 modulates p53-independent apoptosis through Pim1 survival kinase in cancer cells', *Oncogene*, 27(1), pp. 1–8.

Zhao, Y.H. *et al.* (2009) 'Upregulation of lactate dehydrogenase A by ErbB2 through heat shock factor 1 promotes breast cancer cell glycolysis and growth', *Oncogene*, 28(42), pp. 3689–3701.

Zheng, H.-C. *et al.* (2008) 'Aberrant Pim-3 expression is involved in gastric adenoma-adenocarcinoma sequence and cancer progression', *Journal of Cancer Research and Clinical Oncology*, 134(4), pp. 481–488.

Zhong, X. *et al.* (2017) 'CUE domain-containing protein 2 promotes the Warburg effect and tumorigenesis', *EMBO Reports*, 18(5), pp. 809–825.

Zhou, J. *et al.* (2021) 'PDGF-BB promotes vascular smooth muscle cell migration by enhancing Pim-1 expression via inhibiting miR-214', *Annals of Translational Medicine*, 9(23), p. 1728.

Zhou, Z. *et al.* (2006) 'Synergy of p53 and Rb deficiency in a conditional mouse model for metastatic prostate cancer', *Cancer Research*, 66(16), pp. 7889–7898.

Zhu, N. *et al.* (2002) 'CD40 signaling in B cells regulates the expression of the Pim-1 kinase via the NF-kappa B pathway', *Journal of Immunology,* 168(2), pp. 744–754.

Zhu, Q. *et al.* (2019) 'Long non-coding RNA SNHG16 promotes proliferation and inhibits apoptosis of diffuse large B-cell lymphoma cells by targeting miR-497-5p/PIM1 axis', *Journal of Cellular and Molecular Medicine*, 23(11), pp. 7395–7405.

Zhu, Q. *et al.* (2022) 'Whole-Genome/Exome Sequencing Uncovers Mutations and Copy Number Variations in Primary Diffuse Large B-Cell Lymphoma of the Central Nervous System', *Frontiers in Genetics*, 13, p. 878618.

Zhu, X. *et al.* (2018) 'Expression of PIM-1 in salivary gland adenoid cystic carcinoma: Association with tumor progression and patients' prognosis', *Oncology Letters*, 15(1), pp. 1149–1156.

Zippo, A. *et al.* (2007) 'PIM1-dependent phosphorylation of histone H3 at serine 10 is required for MYC-dependent transcriptional activation and oncogenic transformation', *Nature Cell Biology*, 9(8), pp. 932–944.

Zu, X.L. and Guppy, M. (2004) 'Cancer metabolism: facts, fantasy, and fiction', *Biochemical and Biophysical Research Communications*, 313(3), pp. 459–465.

Original Publications

Santio NM, Vainio V, Hoikkala T, Mung KL, Lång M, Vahakoski R, Zdrojewska J, Coffey ET, Kremneva E, Rainio EM, Koskinen PJ. (2020)

PIM1 accelerates prostate cancer cell motility by phosphorylating actin capping proteins

Cell Communication and Signaling

I

Santio et al. Cell Communication and Signaling (2020) 18:121
https://doi.org/10.1186/s12964-020-00618-6

Cell Communication and Signaling

RESEARCH Open Access

PIM1 accelerates prostate cancer cell motility by phosphorylating actin capping proteins

Niina M. Santio[1], Veera Vainio[1], Tuuli Hoikkala[1], Kwan Long Mung[1], Mirka Lång[1], Riitta Vahakoski[1], Justyna Zdrojewska[2], Eleanor T. Coffey[2], Elena Kremneva[3], Eeva-Marja Rainio[1] and Päivi J. Koskinen[1*]

Abstract

Background: The PIM family kinases promote cancer cell survival and motility as well as metastatic growth in various types of cancer. We have previously identified several PIM substrates, which support cancer cell migration and invasiveness. However, none of them are known to regulate cellular movements by directly interacting with the actin cytoskeleton. Here we have studied the phosphorylation-dependent effects of PIM1 on actin capping proteins, which bind as heterodimers to the fast-growing actin filament ends and stabilize them.

Methods: Based on a phosphoproteomics screen for novel PIM substrates, we have used kinase assays and fluorescence-based imaging techniques to validate actin capping proteins as PIM1 substrates and interaction partners. We have analysed the functional consequences of capping protein phosphorylation on cell migration and adhesion by using wound healing and real-time impedance-based assays. We have also investigated phosphorylation-dependent effects on actin polymerization by analysing the protective role of capping protein phosphomutants in actin disassembly assays.

Results: We have identified capping proteins CAPZA1 and CAPZB2 as PIM1 substrates, and shown that phosphorylation of either of them leads to increased adhesion and migration of human prostate cancer cells. Phosphorylation also reduces the ability of the capping proteins to protect polymerized actin from disassembly.

Conclusions: Our data suggest that PIM kinases are able to induce changes in actin dynamics to support cell adhesion and movement. Thus, we have identified a novel mechanism through which PIM kinases enhance motility and metastatic behaviour of cancer cells.

Keywords: PIM kinases, Capping proteins, CAPZ, Actin, Migration, Prostate cancer

* Correspondence: paivi.koskinen@utu.fi
[1]Section of Physiology and Genetics, Department of Biology, University of Turku, Vesilinnantie 5, FI-20500 Turku, Finland
Full list of author information is available at the end of the article

Background

The hallmarks of malignant cancer cells that distinguish them from healthy cells include increased motility and an enhanced ability to invade other tissues and form metastatic colonies [1]. Cellular movements are normally strictly controlled by a network of intra- and extracellular components, which coordinate cell adhesion, spreading, polarity and locomotion. These include cadherin-like proteins that are responsible for adherent cell-cell junctions, and transmembrane integrins that connect the intracellular molecules to the extracellular matrix [2, 3]. However, the main forces driving cell locomotion are dependent on actin dynamics: the constant polymerization and depolymerization of actin filaments [4]. This leads to changes in cellular protrusions such as filopodia, lamellipodia as well as retraction fibers, which are important mediators of both normal and cancer cell movement [5].

Actin polymerization is regulated by several types of actin-binding proteins, such as the capping proteins (CPs) [5]. They bind as heterodimers to the fast-growing ends of the actin filaments, and thereby prevent both filament assembly and disassembly [6]. CP subunits are evolutionarily conserved, but their number varies between different species [7]. Originally, they were identified in the Z disks of striated muscles, but they have since been found in other muscle and non-muscle tissues as well [7–9]. CP alpha 1 and 2 subunits are expressed in both types of tissues, while alpha 3 is a germ cell-specific subunit [9–11]. Three different splice variants have been identified for the beta subunit, of which beta 1 is localized at the Z disks, and beta 2 at the intercalated disks and cell periphery in the muscles [12]. The third variant, beta 3, is a testis-specific isoform similar to alpha 3 [13]. Despite their importance in skeletal muscle, various functional roles have also been reported in other tissues, such as cardiac tissue, the nervous system and cancer [14–21].

The role of CPs in cancer has remained unclear due to contradictory results with different subunits. While the beta subunit has been reported to act as an oncogene, variable but mainly tumor suppressive roles have been suggested for the alpha subunits [17–21]. These opposite effects are surprising due to the heterodimeric mode of CP action. However, as the previous data are mostly based on silencing or overexpressing of individual subunits, they may not fully reflect the impact of the heterodimers. It is also likely that CP activity is context-dependent, as suggested by the differential expression of their distinct subunits. In addition, CPs are known to be targeted by post-translational modifications, such as phosphorylation by protein kinase Cε and casein kinase 2, both of which reduce actin capping activity [14, 22].

In this study, we have identified the CP alpha 1, alpha 2 and beta 2 subunits as novel substrates for the oncogenic PIM1 kinase. The three serine/threonine-specific PIM family kinases regulate cell growth, metabolism, and motility, and have also neuronal functions [23–26]. They have been implicated in both hematopoietic malignancies and solid cancers [23, 27, 28], and are therefore promising targets for cancer therapy. The effects of PIM kinases on cancer cell motility have been extensively studied in prostate cancer, where they have been shown to increase migration, invasion and adhesion of cultured cells, and enhance tumor angiogenesis and metastasis *in vivo* [29–32]. The pro-migratory effects of PIM kinases have been connected to phosphorylation-dependent activation of several substrates such as NOTCH1, NFATC1 and EIF4B, or inactivation of tumor suppressive factors such as FOXP3 [31, 33–36]. However, the previously identified PIM substrates do not regulate cellular movements by directly interacting with the actin cytoskeleton. Here we have used a dual expression plasmid to simultaneously study the phosphorylation-dependent effects of both CP alpha 1 and beta 2 subunits on prostate cancer cell motility. We demonstrate that their phosphorylation promotes adhesion and migration of cultured cells, and also decreases their ability to protect actin filament ends from disassembly in vitro. Thus, CP phosphorylation is expected to increase actin dynamics and thereby enhance the motility of prostate cancer cells.

Methods

Cloning and mutagenesis

To create cDNA libraries, total mRNA was isolated with Tri Reagent® (#T9424, Sigma-Aldrich, St Louis, MI, USA) from mouse tissue or human PC-3 prostate cancer cells, after which cDNA synthesis was performed using the first strand cDNA synthesis kit (#K1612, Thermo Fisher Scientific, Waltham, MA, USA). The cDNAs of interest were subcloned into pGEM-T-Easy vector (Promega, Madison, WI, USA) by using PCR with gene-specific primers. Further subclonings were performed either by PCR or by digestion with restriction enzymes. The gene-specific cloning and sequencing primers, and the detailed design of constructs are shown in Additional file 1: Tables S1 and S2.

For in vitro kinase assays with bacterially produced proteins, mouse *capza1* or human *CAPZA2* cDNAs were inserted together with mouse *capzb2* cDNA into the dual expression vector pRFSDuet-1 (shortened as "Duet", #71341, Merck Millipore, Burlington, MA, USA), so that alpha subunits were placed into the multiple cloning site (MCS) 1 and the beta subunit into MCS2. The *capzb2* cDNA was also subcloned into pGEX-6P-3 (GE Healthcare Life Sciences, Little Chalfont, UK).

For expression in mammalian cells, His-tagged *capza1* and *CAPZA2* constructs were prepared by subcloning the cDNAs from Duet to the MCS1 of PSF-CMV-CMV-SBFI-UB-PURO - DUAL CMV plasmid (shortened as "Dual-CMV" or "Dual"; #OGS597, Sigma-Aldrich, St. Louis, MI, USA). The *capzb2* cDNA was Flag-tagged by transferring it from pGEX-6P-3 to pFlag-CMV™-2 (#E7033, Sigma-Aldrich), after which it was further subcloned to Dual-CMV MCS2. For creation of GFP-tagged constructs, *capzb2* was transferred from pGEX-6P-3 to pEGFP-C1 (Clontech laboratories Inc., Takara Bio USA, Inc., Mountain View, CA, USA). In addition, GFP was subcloned from pEGFP-C1 into Dual-CMV prior to MCS2 to create a GFP-tagged Dual-CMV empty vector or a vector expressing Capza1 and GFP-tagged Capzb2.

Site-directed mutagenesis of mouse *capza1* and *capzb* genes was performed by Ultra Pfu DNA polymerase (Stratagene, San Diego, CA, USA) according to Manufacturer's protocol. The primers used are described in Additional file 1: Table S3.

The short isoform of the murine Pim1 protein cap away was expressed in bacterial cells from the pGEX-2T-Pim1 vector as previously described [34]. The human PIM1 protein was expressed in bacterial cells from the pGEX-6P-1-PIM1 vector or in mammalian cells from the pcDNA™3.1/PIM1-V5-His (from here on "pcDNA-PIM1") construct or Tag-PIM1-RFP (from here on "PIM1-RFP"), which along with the GST-tagged murine Notch1 intracellular domain (ICD) and the control plasmids have been described previously [33].

Protein production

For protein production, all bacterial constructs were expressed in the BL21 *E. coli* strain. Production of GST-tagged murine Pim1 or human PIM1 has been described previously [34, 37]. For production of heterodimers of Capza1 or CAPZA2 with Capzb2, cell pellets were suspended in ice-cold lysis buffer (50 mM Tris-HCl pH 7.5, 250 mM NaCl, 10 mM imidazole). Protease activity was inhibited by aprotinin (1 μg/ml) or PMSF (5 μM). Protein purification was performed by rotating the lysate for 30 min at + 4 °C with 50% HisLink™ resin (Promega). Thereafter samples were washed four times in washing buffer (10 mM Tris-HCl, pH 7.5, 20 mM imidazole) and rotated for 30 min at + 4 °C with elution buffer (10 mM Tris-HCl, pH 7.5, 300 mM Imidazole, 250 mM NaCl). The His-tagged alpha subunits formed heterodimers with the beta subunits, so both subunits could be simultaneously isolated. Protein samples were separated by SDS-PAGE and visualised by Page Blue™ Protein Staining Solution (Thermo Fisher Scientific).

PIM1 substrate screening, in vitro kinase assays and mass spectrometry

Potential Pim1 substrates were identified using an in vitro screen as previously described [38]. Briefly, rat cortex was homogenized in kinase buffer and phosphorylated in vitro at 30 °C for 45 min using recombinant murine Pim1 kinase in the presence of [γ-^{32}P] ATP (PerkinElmer Finland Oy, Turku, Finland). Protein extract was loaded onto a dry polyacrylamide gel strip with an immobilized pH gradient of 4–7, according to the manufacturer's instructions (Amersham Biosciences, Uppsala, Sweden). Proteins were separated in the first dimension by isoelectric focusing overnight at 3500 V, followed by two-dimensional separation on 12% SDS-PAGE, silver staining and autoradiography. Reduction, alkylation, and in-gel trypsin digestion of the proteins were performed as described previously [39]. Peptides were extracted into 5% HCOOH, 50% CAN, concentrated using SpeedVac vacuum and desalted with ZipTips with C18 resin (Millipore). After digestion, peptides were mixed 1:1 with matrix α-ciane-4-hydroxycinnamic acid (HCCA) dissolved in 70% ACN/0.1% TFA and spotted onto a stainless steel target plate. Mass spectrometry (MS) analysis was undertaken with a MALDI-TOF/TOF Ultraflex II mass spectrometer (Bruker Daltonics, Billerica, MA, USA). Spectra were internally calibrated with peptides from trypsin autolysis ($M + H^+ = 842.509$, $M + H^+ = 2211.104$). The most abundant peptide ions were then subjected to fragmentation analysis (MS/MS) to provide information for use in determining the peptide sequence. Data were processed by Analyst QS software (Applied Biosystems, Foster City, CA, USA) and matched to the SwissProt protein database using the MASCOT algorithm.

Phosphorylation of putative substrates by human PIM1 was validated by radioactive in vitro kinase assays, as described previously [37]. Shortly, 0.5–2.0 μg of PIM1 and its substrate were used in each reaction. Samples were separated by SDS-PAGE and stained by Page Blue™ protein staining solution (#24620, Thermo Fisher Scientific). Results were analysed by autoradiography and quantitated by the ChemiDoc™ MP Imaging System with Image Lab software Version 4.0 (Bio-Rad Laboratories, Inc., Hercules, CA, USA) and ImageJ/Fiji software (1.48 s, Fiji, Wayne Rashband, National Institutes of Health, Bethesda, MD, USA).

For mass spectrometry of phosphorylated substrates, in vitro kinase assays were prepared similarly to the radioactive assays, but without radiolabelled ATP. After SDS-PAGE, the ProQ® Diamond Phosphoprotein Gel Stain (Thermo Fisher Scientific) was used according to manufacturer's protocol. In-gel digestion of proteins with trypsin, liquid chromatography-electrospray ionization-tandem mass spectrometry (LC-ESI-MS/MS) with

phosphopeptide enrichment and analysis of data have been described previously [39–41]. Similar analyses were performed also with immunoprecipitated cellular proteins.

In silico analyses for mRNA and proteins

Phosphorylation sites were searched for from the in vitro kinase samples by the PhosphoMotif Finder in the Human Protein Reference Database (http://www.hprd.org/PhosphoMotif_finder/). The in vivo phosphorylation sites were searched for from the PhosphoSitePlus® database (phosphosite.org, Cell Signaling Technology, Inc., Danvers, MA, USA). Gene expression data were obtained from the IST Online™ (ist.medisapiens.com [42];) or betastasis database (betastasis.com; gene expression barblot) [43]. Correlation analyses were performed on gene expression data from the betastasis dataset [43]. Homology comparisons were performed by the Basic Local Alignment Search Tool (National Institutes of Health, Bethesda, MD, USA) using protein sequences from the National Center for Biotechnology Information (National Institutes of Health, Bethesda, MD, USA) and UniProt Knowledgebase [44].

Cell culture and transfections

The human prostate epithelial adenocarcinoma cell line PC-3 and the carcinoma cell lines DU-145 and LNCAP (from American Type Culture Collection) were maintained in RPMI-1640 medium supplemented with 10% fetal bovine serum, L-glutamine and antibiotics. For transient transfections, cells were plated 24 or 48 h earlier, cultured until ~ 80% confluence and then transfected with the FuGENE® HD Transfection Reagent (Promega) 1:3 to DNA. Approximately 0.5 μg of DNA was used to transfect 100,000 cells. The CP subunits were expressed either by cotransfecting His-tagged Capza1 (Dual-CMV) together with Flag-tagged Capzb2 (pFlag-CMV-2), or by transfecting the Dual-CMV vector encoding both His-tagged Capza1 or Capza2 and Flag-tagged Capzb2. The Capzb2 subunit alone was expressed by the Flag-tagged plasmid pFlag-CMV-2. To inhibit the catalytic activity of PIM kinases, cells were treated with the PIM-selective small molecule inhibitors DHPCC-9 [29, 45], AZD-1208 (Astra Zeneca, Cambridge, UK) or SGI-1776 (#526528, Sigma-Aldrich) at 10 μM concentration in 0.1% DMSO, which alone was used in control samples.

Nuclear fractionation

Cells cultured on 10 cm plates were lysed in 500 μl of lysis buffer: 10 mM Tris-HCL pH 7.5, 10 mM NaCl, 3 mM $MgCl_2$, 0.5% Nonidet P-40, 1 mM PMSF and mini EDTA- free protease inhibitor tablet (Roche, Basel, Switzerland) according to the manufacturer's protocol. 100 μl of lysate was stored as a whole cell lysate control and heated with 5x Laemmli sample buffer (LSB) for 5 min at + 95 °C. After centrifugation at 500 x g for 5 min at + 4 °C, the supernatant contained the cytoplasm, while the nuclei were in the pellet. The pellets were washed three times with lysis buffer and centrifuged each time at 500 x g for 5 min at + 4 °C, after which they were suspended to 200 μl of lysis buffer. The cytoplasm-containing solution was centrifuged at 12000 x g for 15 min at + 4 °C, after which the supernatant was collected. Nuclear and cytoplasmic lysates were heated for 5 min at + 95 °C with 5x LSB. 30 μl aliquots of samples were loaded to each well on SDS-PAGE and samples were analysed by Western blotting, using nuclear A/C laminin and cytoplasmic beta-tubulin as fraction-specific positive controls (Additional file 1: Table S4).

Western blotting

Cultured cells were directly lysed into 75–120 μl of hot 2x LSB or lysed for co-immunoprecipitation analyses as described below. In both cases, LSB-containing samples were heated for 5 min at 95 °C. Proteins (20–50 μl/ well) were separated by 10–12% SDS-PAGE. After blotting onto PVDF membrane, samples were stained with primary antibodies (Additional file 1: Table S4) at + 4 °C overnight. Secondary antibody staining (1:1000) was performed for 30 min at RT with HRP-linked goat anti-mouse IgG #7076 or goat anti-rabbit IgG #7074 antibodies (Cell Signaling Technology, Beverly, MA, USA).

Immunoprecipitations and immunofluorescence

Cellular protein interactions were measured by co-immunoprecipitation (CO-IP) and colocalization analyses, after which they were confirmed by proximity ligation assays (PLA) and fluorescence-lifetime imaging microscopy (FLIM). For IP and CO-IP, PC-3 cells were cotransfected with pcDNA-PIM1, His-tagged Capza1 and Flag-tagged Capzb2. After 48 h, cells were scraped into sterile PBS, centrifuged 300 x g for 3–4 min and re-suspended into 5x volume of lysis buffer: 50 mM Tris pH 7.5, 10% glycerol, 100 mM NaCl, 1 mM EDTA, 1% NP-40, 50 mM NaF, 250 μM β-glycerophosphate, 1 mM Na_3VO_4 and mini EDTA-free protease inhibitor tablet (Roche) according to the manufacturer's protocol. Samples were incubated on ice for 60 min, vortexed occasionally and centrifuged for 10 min at 4 °C and 14,000 rpm. Supernatants were collected and protein concentrations were measured using the Bio-Rad Protein Assay Dye Reagent Concentrate (#5000006, Bio-Rad laboratories Inc.) according to the manufacturer's protocol. For immunoprecipitation of Flag-tagged proteins, 0.5–1 mg of protein lysate was combined with 50 μl of anti-Flag® M2 affinity agarose gel (#A2220, Sigma-Aldrich) in 1 ml of lysis buffer. After 1 h rotation at + 4 °C, the agarose gel was washed four times with the lysis buffer. Samples were prepared by adding preheated 2x LSB, vortexing and heating for 5 min at + 95 °C. Coprecipitated proteins

and lysate controls (50–100 μg) were analysed by Western blotting. For mass spectrometry, ~ 2.5 mg of protein was used for immunoprecipitation, after which CP subunits were separated by SDS-PAGE and stained by Page Blue.

For colocalization imaging, PLA and FLIM, PC-3 cells were transiently co-transfected on coverslips or left untransfected. After 24–48 h, samples were fixed at RT for 15 min with 4% PFA. For colocalization, cells were blocked in 10% BSA/PBS, followed by overnight incubation with the primary antibodies (Additional file 1: Table S4). On the following day, Alexa Fluor 488 goat anti-mouse (#A11001) or Alexa Fluor 647 goat anti-rabbit (#A21245) IgG secondary antibodies (Thermo Fisher Scientific) were used 1:1000 for 1 h at RT. During the secondary antibody staining, cells were simultaneously stained with DAPI (4′,6-diamidino-2-phenylindole dihydrochloride, #D9542, Sigma-Aldrich, 300 nM) and/or Alexa Fluor™ 546 Phalloidin (#A22283, Thermo Fisher Scientific, 150 nM) for visualization of the nuclei and/or actin cytoskeleton. For PIM inhibitor-treated, untransfected samples, Phalloidin–Atto 647 N (#65906, Sigma Aldrich, 100 nM) was used to stain actin filaments. Samples were imaged by the Zeiss LSM 780 confocal microscope with ZEN lite/Zen Black 2.3 software with 63x Zeiss C-Apochromat objective, numerical aperture: 1.2 (Carl Zeiss, Oberkochen, Germany) or the 3i CSU-W1 spinning disk confocal microscope with SlideBook 6 software, 63x Zeiss Plan-Apochromat objective, numerical aperture: 1.4 and Hamamatsu sCMOS Orca Flash4 v2 C11440-22CU camera (Intelligent, Imaging Innovations, Denver, CO, USA; Hamamatsu Photonics, Hamamatsu City, Shizuoka Pref., Japan). Colocalization was confirmed by Pearson's correlation coefficiency test and Costes Threshold regression by ImageJ Coloc2 analysis. PLA was performed according to the manufacturer's protocol using the Duolink® In Situ Orange Starter Kit Mouse/Rabbit (DUO92102, Sigma-Aldrich). PLA samples were imaged by the Nikon fluorescent microscope with NIS-Elements AR software (Nikon, Tokyo, Japan). Samples and figures were analysed and prepared using the respective microscopy software and ImageJ/Fiji. Samples for FLIM were directly mounted, while samples for the other assays were permeabilized in 0.1–0.2% Triton-X-100 for 15 min. FLIM was carried out as previously described [31, 33] using the Lambert Instruments LIFA FLIM system with the Carl Zeiss AxioImager microscope and LI-FLIM software (Lambert Instruments BV, Groningen, The Netherlands). All imaging was performed at room temperature. Actin filament length and number was manually measured in a double-blinded fashion using ImageJ/Fiji and calculating protrusions that were at least 3 μm long.

Cell motility, attachment and viability assays

Cell migration, cell adhesion and cell viability assays were performed as described previously [29, 31]. For wound healing assays to measure cell migration, wounds were scratched by a 10 μl tip, after which they were imaged by light microscopy with Basler Microscopy Software 2.0 (Basler AG, Ahrensburg, Germany) and analysed by ImageJ/Fiji. Single cell tracking was performed at 37 °C, 5% CO_2 by automated imaging with the Nikon Eclipse Ti2-E microscope and NIS-Elements AR 5.11.00 64-bit software with the 10x Nikon CFI Plan-Fluor objective, numerical aperture: 0.3., and the Hamamatsu sCMOS Orca Flash4.0 v3 C13440-20CU camera. Cell movement was tracked manually by ImageJ/Fiji from the .nd2 data files. Cell attachment was studied using the electrical impedance-based Roche xCelligence method with 15,000–25,000 cells plated per well. Cell viability was measured by the MTT assay [29]. Western blotting samples were prepared after the experiments to control for protein levels.

Actin disassembly assays

Actin polymerization and disassembly assays as well as muscle actin production were performed as previously described [46]. 10 μM non-labelled (95%) and pyrene-labelled (5%) muscle actin were polymerized in a reaction mix containing 1 mM EGTA, 100 mM NaCl, 5 mM MgCl2. 0.2 mM ATP, 5 mM Tris-HCl pH 7.5, 0.2 mM DTT, 0.2 mM CaCl2. The solution was gently mixed and incubated first 15 min at RT and then 40 min at + 4 °C. Thereafter the disassembly assay was performed at RT in a reaction mix containing 1 mM EGTA, 100 mM NaCl, 5 mM MgCl2. 0.2 mM ATP, 5 mM Tris-HCl pH7.5, 1.2 mM DTT, 0.05 μM capping proteins produced in *E. coli* or the elution buffer (a negative control) and 4 μM of polymerized actin. The buffer and CPs were mixed gently by rotating a pipette tip in the tube and incubating for 5 min at RT. Thereafter, 4 μM vitamin D-binding protein (Human DBP, G8764, Sigma-Aldrich) was added to sequester actin monomers. Samples were carefully transferred into a cuvette, after which the decrease in pyrene-actin signal was measured by spectrophotometry (excitation 365 nm, emission 407 nm) for 4000 s. Average signal intensities were calculated by comparing each value to the first peak. The START time-point represents an average of values of 100 s time scale after the first peak. Similarly, average values from 100 s time scales were calculated for the other time-points as well: 1000 s (900–1000 s average), 2000 s (1900–2000 s average), 3000 s (2900–3000 s average) and 4000 s (3900–4000 s average).

Statistical analysis and figure preparation

The student's t-test was used to compare the difference between groups, while correlations were analysed by the

Pearson's correlation coefficiency. Significant differences ($P < 0.05$) are marked with asterisks in figures and supplementary files. Correlation coefficiencies (r [2]) were interpreted as very weak (0.00–0.19), weak (0.20–0.39), moderate (0.40–0.59), strong (0.60–0.79) or very strong (0.80–1.00). Error bars represent standard deviations. Corel Draw 2019 was used for figure preparation.

Results

Capping proteins are phosphorylated by PIM1 in prostate cancer cells

The initial aim of our study was to identify novel neuronal PIM substrates, as we have previously observed that *pim* family mRNAs are prominently expressed in the central nervous system [24] and that PIM kinases are active in neuron-like cells [25]. For this purpose, we used an in vitro phosphoproteomics-based method [38] and recombinant mouse Pim1 kinase to screen for target proteins from rat brain extracts. From this screen, we identified five potential Pim1 substrates: capping protein alpha 2 (Capza2), dihydropyrimidinase like 2 (Dpysl), enolase 1 (Eno1), endocytosis-associated protein 1 (Necap1) and prohibitin (Phb) (Additional file 2: Table S5). We next decided to focus our validation efforts on the capping protein (CP) family members, the phosphorylation of which could potentially allow PIM kinases to directly regulate actin dynamics and thereby cell motility.

To analyse phosphorylation of CP subunits by human PIM1, radioactive in vitro kinase assays were performed targeting human CAPZA2 or mouse Capza1 together with mouse Capzb2. While these subunits had been selected for the study based on their availability, no species-specific differences were expected, as human and murine CPs are highly homologous to each other (amino acid identity for alpha 1 97%, alpha 2 98% and beta 2 100%) [44, 47]. The CPs were produced in bacteria as heterodimers, and incubated with wild-type (WT) or kinase-deficient (KD) human PIM1. As shown in Fig. 1a, WT, but not KD PIM1 was able to phosphorylate Capza1 and CAPZA2, although not as strongly as the Notch1 intracellular domain (ICD) used as a positive control. According to the relative signal intensities, Capza1 subunit was more efficiently phosphorylated by PIM1 than CAPZA2. Interestingly, however, Capzb2 was phosphorylated only when it formed a heterodimer with Capza1, but not with CAPZA2. These data validated the Capza1/b2 heterodimer as a prominent direct target of PIM1.

As we have previously shown that PIM kinases promote PC-3 prostate cancer cell motility [29–31, 36], we were interested in determining whether CPs are involved in this process. We therefore searched for *CP* mRNA expression levels from the IST Online™ database [42], according to which relatively high levels of *CAPZA1* and *CAPZB* had been observed in PC-3 cells as compared to *CAPZA2* or *CAPZA3* (Fig. 1b). For this reason, as well as for the absence of in vitro phosphorylation of Capzb2 with CAPZA2, our further studies focused on the functional consequences of phosphorylation of the Capza1/b2 heterodimer.

To evaluate whether CPs and PIM kinases are coexpressed in clinically relevant samples, we analysed the *PIM* and *CP* mRNA expression levels in prostate tumors of varying severity. According to data from the Betastasis database [43], both *CAPZA1* and *CAPZB* mRNA levels positively correlated with *PIM1* in primary prostate cancer patient samples (Fig. 1c-d). Positive correlations were also detected in metastatic tissues as well as between different *CP* and *PIM* isoforms (Additional file 2: Table S6). While *CAPZA1*, *CAPZA2* and *CAPZB*, but not *CAPZA3* levels correlated well with *PIM1* levels in all tumor tissues, similar correlations were also observed for PIM2 and PIM3 in the samples with high Gleason scores. By contrast, no correlations were seen in healthy prostate tissues. These data imply that PIMs and CPs are both present in the cancer tissues, suggesting that PIM-dependent phosphorylation of CPs can occur in this setting.

Both CP subunits interact with and are phosphorylated by PIM1

To identify the PIM1 target residues, Capza1 and Capzb2 phosphorylation sites were analysed by mass spectrometry from in vitro kinase assays as well as from PC-3 cell co-immunoprecipitation assays. From those samples, several in vitro and in vivo sites were detected in both CP subunits (Fig. 1e, Additional file 2: Table S7). In addition, in silico analysis [48] of the Capzb2 amino acid sequence suggested that phosphorylation occurs at S226. Mass spectrometry also identified phosphorylation of Capzb2 at S2, but due to its close proximity to the N-terminus of the protein, it was expected to be an artefact and was not included in further studies. In addition, Capzb2 was found to be phosphorylated at T186 in vivo, but not in vitro, suggesting that it is targeted by a kinase other than PIM1. To validate the phosphorylation sites, the targeted serine residues were mutated to alanines (SA) and tested by in vitro kinase assays. Mutagenesis of the sites S106 and S126 in Capza1 and S182, S192 and S226 in Capzb2 decreased the phosphorylation signal efficiently and confirmed these sites as PIM1 target sites (Fig. 1e).

To analyse the interactions between PIM1 and the CP heterodimer, co-immunoprecipitation assays were performed. For this purpose, PC-3 cells were transiently transfected with different combinations of PIM1, Capza1 and Capzb2. When Flag-tagged Capzb2 was precipitated with Flag agarose, both Capza1 and PIM1 were co-

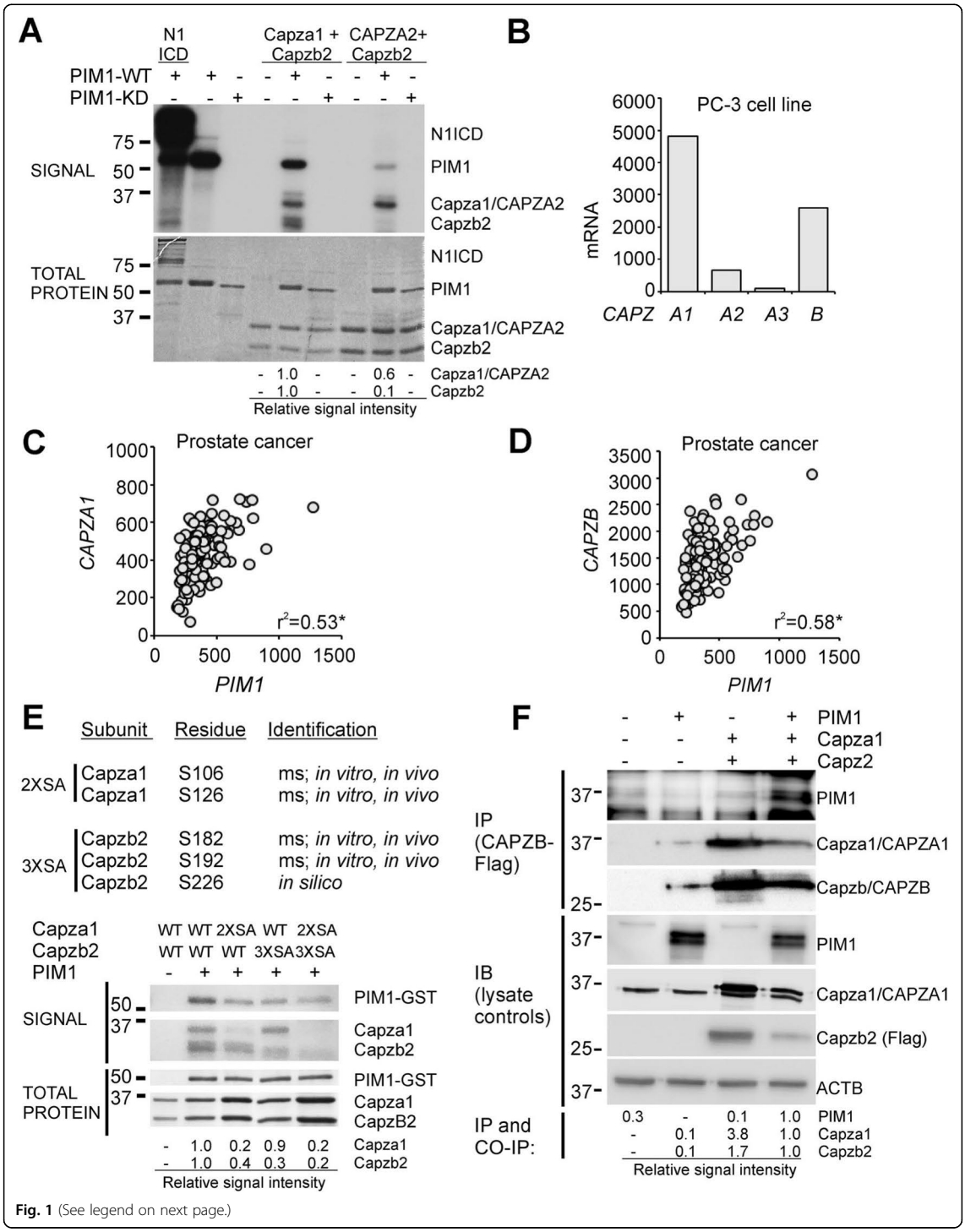

Fig. 1 (See legend on next page.)

(See figure on previous page.)
Fig. 1 CPs are phosphorylated by and co-expressed with PIM1 in prostate cancer. **a** Radioactive in vitro kinase assays were performed by incubating human GST-tagged wild-type (WT) or kinase-deficient (KD) PIM1 with murine Notch1 intracellular domain (N1ICD, a positive control) or with murine His-Capza1 or human His-CAPZA2 together with murine Capzb2. Shown are results from one representative experiment out of three assays. Relative phosphorylation signal intensities as compared to loaded amounts of protein are shown under the blots. **b** *CAPZ* mRNA levels expressed in human PC-3 prostate cancer cells were obtained from the IST Online™ database. **c-d** Pearson's correlation coefficiencies were determined to *PIM* and *CAPZA1* or *CAPZB* mRNA levels in human prostate cancer patient samples obtained from the Betastasis database. Shown are correlations (r^2) along with significance (P) values. **e** Mass spectrometry (ms) of in vitro and in vivo phosphorylated CP samples as well as in silico analysis were used to predict PIM kinase target sites. In vitro kinase assays were performed with GST-tagged PIM1 and either wild-type (WT) CP or serine to alanine (SA) mutants, where two alpha sites (2X; S106, S126) or three beta sites (3X; S182, S192, S226) had been mutated. Shown are representative figures with relative signal intensities. **f** Proteins interacting with Flag-Capzb2 were analysed from lysates of transiently transfected PC-3 cells. Shown are examples of immunoprecipitation (IP), immunoblotting (IB) and and co-immunoprecipitation (CO-IP). Note that the PIM1 antibody non-specifically detects also other proteins, most likely immunoglobulins

precipitated with it (Fig. 1f), indicating that PIM1 and CPs physically interact with each other.

CP subunits colocalize with PIM1 in the cytoplasm

To obtain information on CP localization in PC-3 prostate cancer cells, we analysed the subcellular distribution of endogenously expressed CAPZA1, CAPZA2 and CAPZB2 from fractionated cells by Western blotting. As controls for the CP-specific antibodies, PC-3 cells were transfected with His-tagged alpha subunits and Flag-tagged beta subunit, while lamin A/C and tubulin stainings were used as nuclear and cytoplasmic controls, respectively. Interestingly, both CAPZA1 and CAPZB proteins were mainly found from the cytoplasmic lysates, while CAPZA2 was mostly nuclear (Additional file 3: Fig. S1A-B).

Immunofluorescent stainings of transiently transfected PC-3 cells confirmed that His-tagged Capza1 colocalizes with Capzb2 in the cytoplasm (Additional file 3: Fig. S2A). Colocalization of PIM1 with the CP heterodimer was also observed in the cytoplasm at multiple positions (Fig. 2a). Negative controls for primary and secondary antibodies used in these assays are shown in the Additional file 3: Fig. S2B. In addition, we analysed colocalization of PIM1 with either ectopically or endogenously expressed alpha subunits. While in Western blotting, the CAPZA1 and CAPZA2 antibodies detected both subunits equally well (Additional file 3: Fig. S2C), only the CAPZA2 antibody worked in the immunofluorescent stainings. However, most likely it was unable to penetrate into the nuclei, as only cytoplasmic signals were observed that most likely were derived from the CAPZA1 subunit (Additional file 3: Fig. S2D).

Interactions between PIM1 and CPs were then analysed by proximity ligation assay (PLA), which confirmed interactions between overexpressed Capza1, Capzb2 and PIM1 (Fig. 2b), but revealed interactions also between endogenously expressed proteins (Fig. 2c). Additional controls for PLA assays with statistical analyses are shown in Additional file 3: Fig. S3A-B.

Additional confirmatory data on cellular interactions were obtained by fluorescence-lifetime imaging microscopy (FLIM). For that purpose, Capzb2 was N-terminally tagged with GFP, and expressed either alone or together with His-tagged Capza1. When these plasmids were co-overexpressed in PC-3 cells with RFP-tagged PIM1, the lifetime of GFP fluorescence was reduced, indicating the presence of physical interactions between PIM1 and Capzb2 (Additional file 3: Fig. S4A-B). However, addition of the large fluorescent tag increased the nuclear localization of Capzb2 (Additional file 3: Fig. S4C-D), which is why the more cytoplasmic Flag-tagged version of Capzb2 was chosen for further functional assays.

CP phosphorylation promotes PC-3 prostate cancer cell motility

As we have previously performed wound healing assays to demonstrate the pro-migratory effects of PIM kinases in PC-3 cells [29], we now wanted to analyse the role of CP phosphorylation in this setting. For this purpose, we used a dual expression vector to simultaneously overexpress different combinations of wild-type (WT) and phosphomutant forms of both CP subunits. For phosphodeficient mutants, PIM-targeted serine residues were mutated to alanines (SA) and for phosphomimicking mutants, they were mutated to glutamic acids (SE). From here on, the SA or SE mutants are referred to with the mutated residue number or with double (2X; S106 and S126 in Capza1, or S182 and S192 in Capzb2) or triple (3X; S182, S192, S226 in Capzb2) mutations. To facilitate interpretation of the results, the graphs have been colour-coded: non-transfected or mock-transfected samples (grey), wild-type CPs (black), Capza1 SA/SE mutants (orange/yellow), Capzb2 SA/SE mutants (purple/blue), and combined Capza1/b2 SA/SE mutants (dark green/light green).

In the wound healing assays, both wild-type CPs and the phosphomimicking mutants promoted PC-3 cell migration as compared to controls or the phosphodeficient

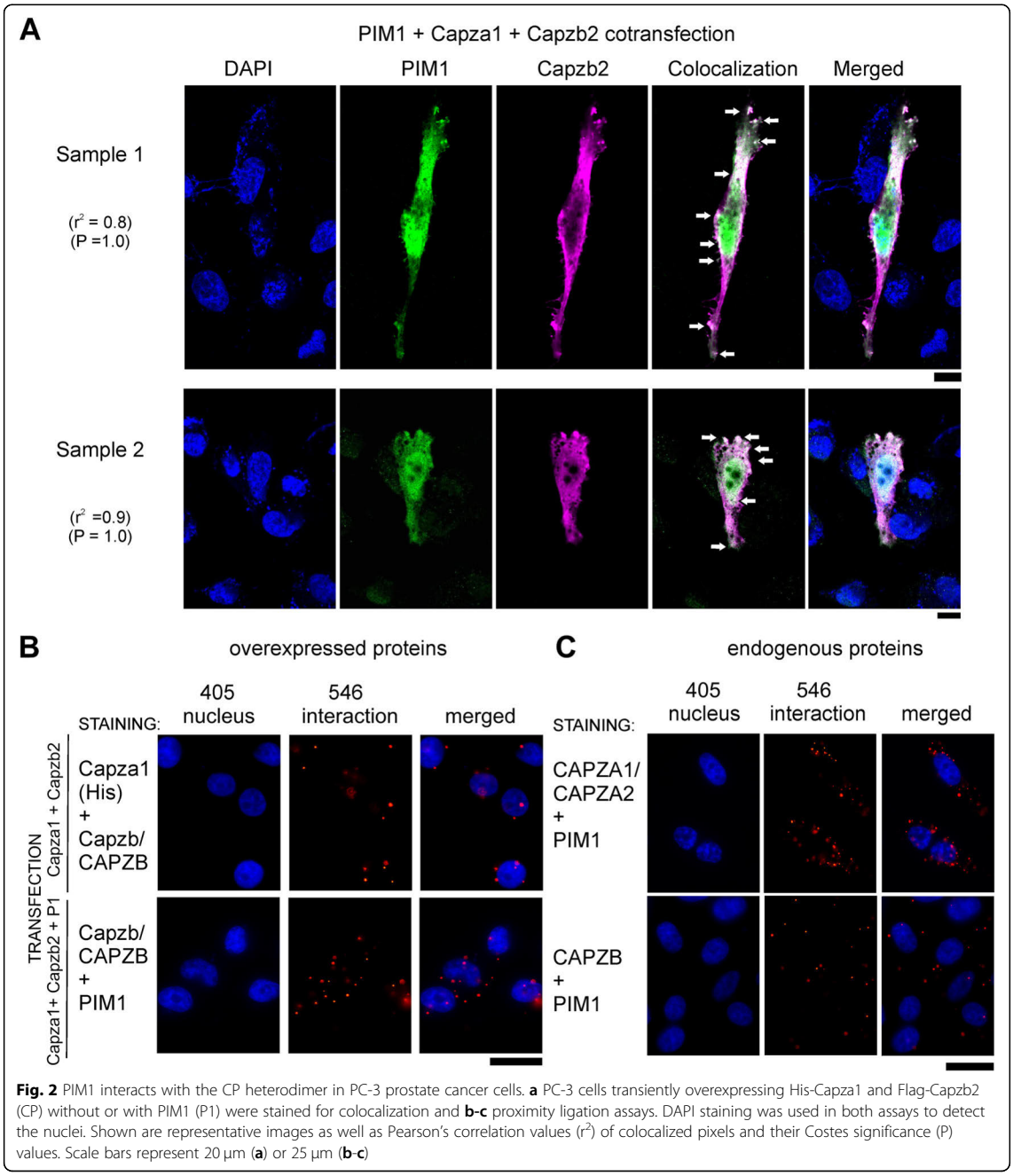

Fig. 2 PIM1 interacts with the CP heterodimer in PC-3 prostate cancer cells. **a** PC-3 cells transiently overexpressing His-Capza1 and Flag-Capzb2 (CP) without or with PIM1 (P1) were stained for colocalization and **b-c** proximity ligation assays. DAPI staining was used in both assays to detect the nuclei. Shown are representative images as well as Pearson's correlation values (r^2) of colocalized pixels and their Costes significance (P) values. Scale bars represent 20 μm (**a**) or 25 μm (**b**-**c**)

mutants (Fig. 3a-b). In the case of the alpha subunit, quite similar results were obtained after mutagenesis of either one of the PIM target sites. The equivalent effects of the double and triple mutants of Capzb2 indicated that lack of the two identified in vivo sites was sufficient to inhibit cell migration. Furthermore, the 2XSE mutant of Capzb2 was sufficient to support wound healing also in the absence of co-overexpressed Capza1, while the 2XSA mutant of Capzb2 alone reduced cell motility. This implies that the ectopically expressed beta subunits dimerize with the endogenous alpha subunits to regulate cell movements. As the pan-PIM inhibitor DHPCC-9

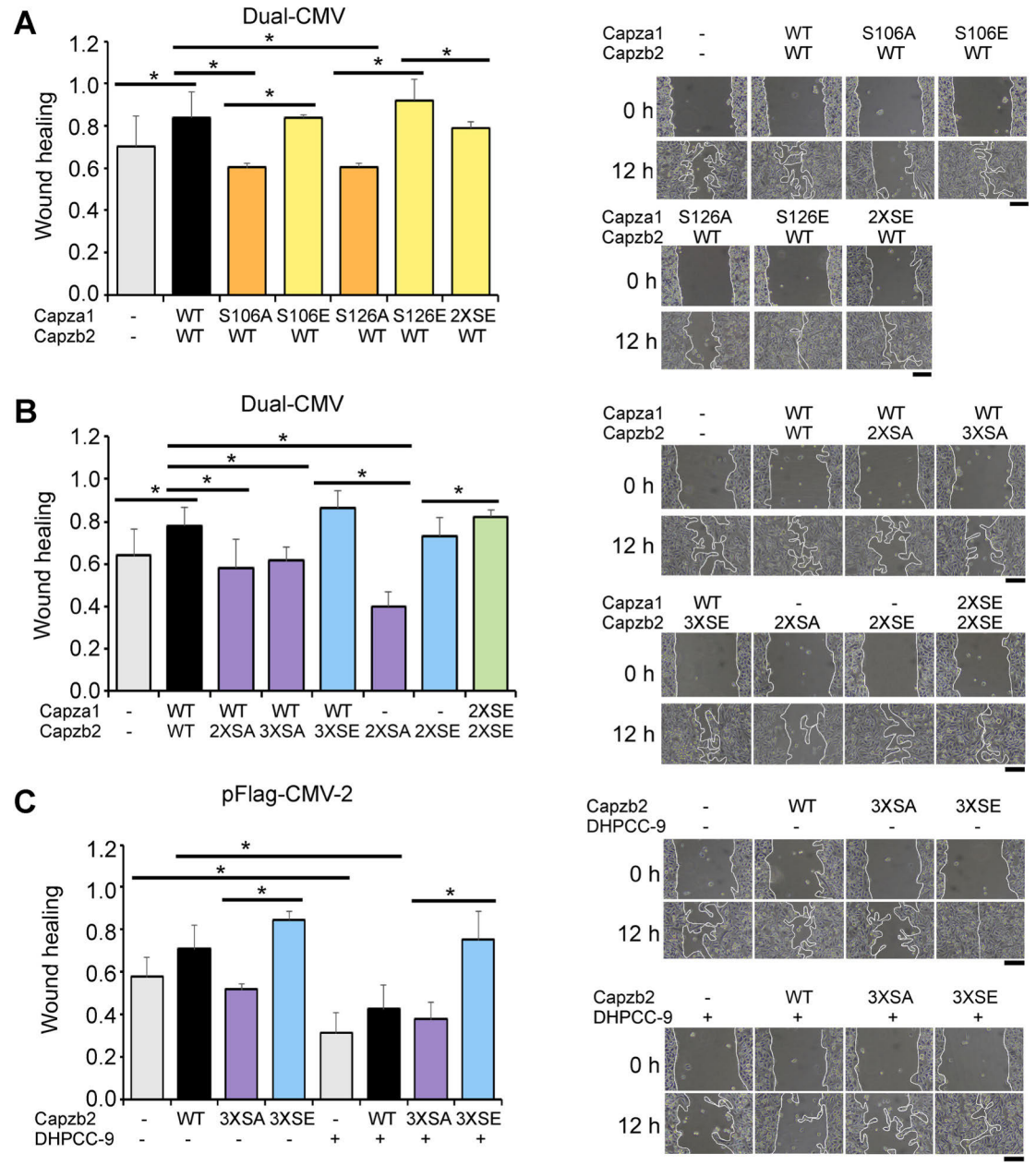

Fig. 3 CP phosphorylation promotes PC-3 cell migration. **a**-**b** Wound healing assays were performed with PC-3 cells transiently overexpressing Capza1/b2 wild-type (WT) proteins and/or phosphodeficient (SA) or phosphomimicking (SE), single, double (2X) or triple (3X) mutants. **c** Similar assays were performed with cells that overexpressed only Capzb2 variants and were treated with DMSO (0.1%) or 10 μM PIM inhibitor DHPCC-9. Shown are averages from at least three independent experiments with three parallel samples along with representative images. Wound edges are lined in white. Scale bars represent 20 μm. Expression plasmid names are shown on top of the graph bars

not only efficiently and selectively inhibits catalytic activities of all three PIM family kinases, but also slows down PC-3 cell migration [29], we tested its effects in cells transfected with Flag-tagged Capzb2. In the DMSO-treated control samples, Capzb2 WT and 3XSE increased cell motility in an expected fashion, while

DHPCC-9 treatment resulted in significantly decreased migration in all other samples except for the sample expressing the 3XSE mutant (Fig. 3c). Thus, the ability of this phosphomimicking mutant to rescue the anti-migratory effects of the PIM inhibitor strongly suggests that phosphorylation of CPs is essential for PIM-induced changes in cell motility.

To confirm that the above data were not due to differences in CP expression or cell viability, these parameters were analysed. No major changes were detected in WT versus mutant CP expression levels (Additional file 3: Fig. S5A-D). However, the levels of Capzb2 SA or SE mutants were reduced, when they were overexpressed alone without Capza1 (Additional file 3: Fig. S5C). MTT assays in turn showed that the CP mutants did not have major effects on cell viability, while the PIM inhibitor DHPCC-9 slightly decreased it in the transfected cells (Additional file 3: Fig. S6A-C).

Phosphorylation of CPs regulates formation of actin protrusions

As CPs regulate actin polymerization and have previously been reported to regulate actin protrusion formation at the cell edges [49], we wanted to measure the effects of CP phosphorylation on the formation of actin filopodia at the leading edge and retraction fibers at the lagging edge. For this purpose, actin filaments were stained by phalloidin and imaged in transiently transfected PC-3 cells. Overexpression of the phosphodeficient (3XSA) Capzb2 led to significantly increased protrusion numbers, while the protrusions were also slightly shorter than in the other samples (Fig. 4a-c, Additional file 3: Fig. S7). We counted both leading edge filopodia and lagging edge retraction fibers, provided they were over 3 μm long. By contrast, both single phosphomutants of Capza1 as well as the triple phosphomimicking (3XSE) mutant of Capzb2 slightly reduced the protrusion number as compared to wild-type, but did not affect their length.

When the effects of three structurally distinct PIM inhibitors (DHPCC-9, AZD-1208 and SGI-1776) were compared by single cell tracking in wound healing assays, all inhibitors reduced PC-3 cell migration, but DHPCC-9 was most efficient (Fig. 5a, b). Data from MTT assays indicated that both DHPCC-9 and AZD-1208 were well tolerated within the 24 h follow-up period, whereas SGI-1776 showed significant cytotoxicity (Fig. 5c). When DHPCC-9-treated cells were stained with phalloidin, the number of actin protrusions was dramatically increased, but without major effects on their length (Fig. 5d-e). Altogether, these data suggest that CP phosphorylation by PIM kinases restricts the ability of cells to form actin protrusions at cell edges.

CP phosphorylation increases cell adhesion

We have previously observed that PIM inhibition by DHPCC-9 inhibits cell adhesion to collagen and fibronectin matrices [31]. To analyse the effects of CP phosphorylation on cell adhesion, we used xCelligence to measure PC-3 cell attachment according to the electrical impedance (resistance to alternating current). Cell adhesion to collagen was slightly enhanced by overexpression of WT Capza1 and Capzb2 (Fig. 6a), and was further enhanced by the phosphomimicking mutants (9–24% increase as compared to the wild-type protein), while the phosphodeficient mutants had an opposite effect (8–16% decrease as compared to the wild-type protein) (Fig. 6b-c). By contrast, all cells adhered equally poorly to poly-L-lysine, which was used as a negative control surface (Additional file 3: Fig. S8A-C).

PIM-mediated CP phosphorylation increases actin disassembly

To mechanistically analyse the effects of PIM-mediated phosphorylation on CP actin capping activity, actin disassembly assays were performed with or without wild-type or mutant CPs. After actin polymerization, the decrease in pyrene-labelled actin fluorescence was followed up for more than an hour (4000 s). Vitamin D-binding protein was added to prevent actin re-assembly, as it has been shown to sequester actin monomers, allowing us to follow actin depolymerization and CP effects on the process [50, 51]. While actin by itself slowly started to disassemble over time, wild-type CPs prevented actin disassembly, but the phosphomimicking mutants did not (Fig. 6d-e). Here it should be noted that the bacterially produced wild-type protein was non-phosphorylated, and was thereby expected to behave similarly to the phosphodeficient mutant. These results indicate that phosphorylation indeed interferes with the actin capping activity.

Phosphorylation of CPs also promote the motility of DU-145 prostate cancer cells

Finally, we wanted to compare the effects of PIM kinases on the motility of other prostate cancer cell lines. For this purpose, we used qPCR to measure relative *PIM* mRNA levels in PC-3, DU-145 and LNCAP cell lines (Additional file 3: Fig. S9A-C). *PIM1* mRNA expression was lower in LNCAP cells as compared to the others, while no significant differences were detected in *PIM2* and *PIM3* mRNA levels between the cell lines. When we performed wound healing assays, we found that DU-145 cells migrated faster than PC-3 cells, and that also their motility could be reduced by a treatment with the DHPCC-9 PIM inhibitor (Additional file 3: Fig. S9D-E). By contrast, the migration rate of LNCAP cells was very

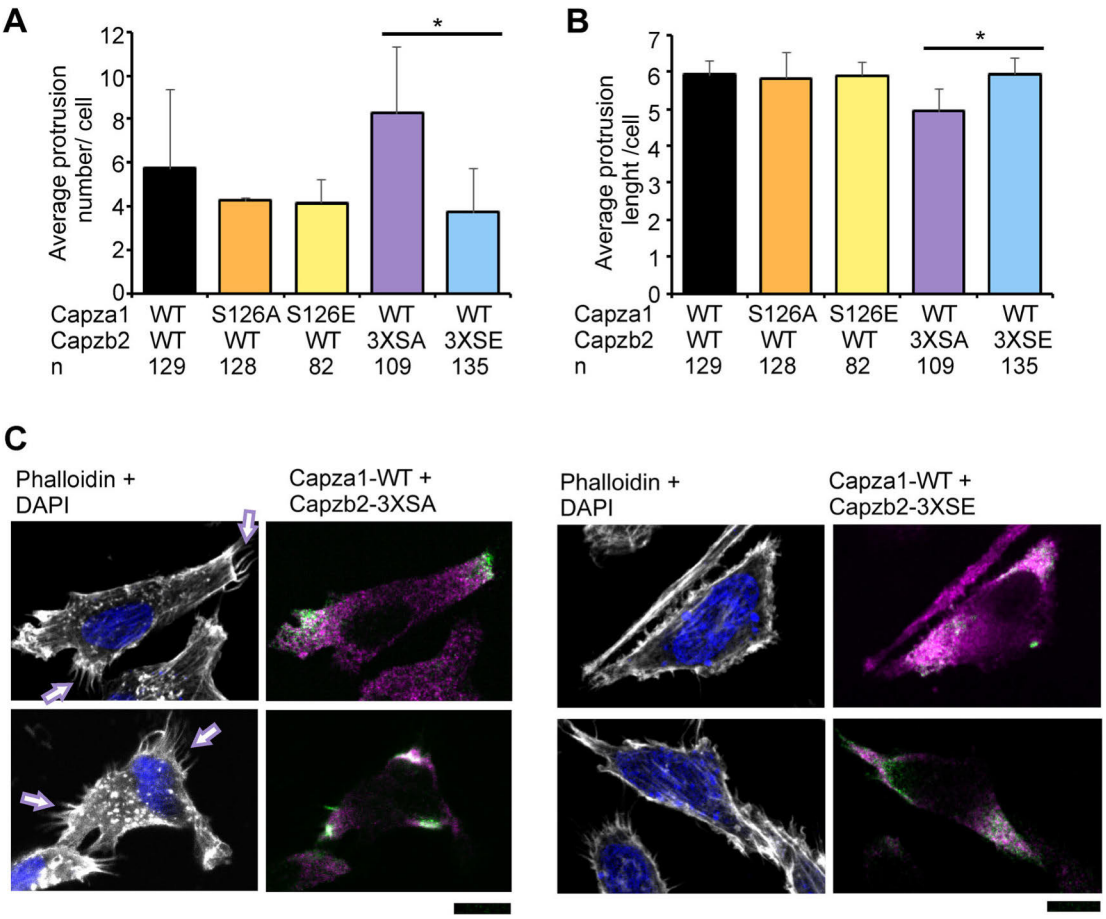

Fig. 4 CP dephosphorylation increases actin protrusion numbers at cell edges. **a**-**c** PC-3 cells plated on coverslips were transiently transfected to overexpress wild-type (WT) Capza1 and Capzb2 or their phosphodeficient (SA) or phosphomimicking (SE) mutants. Actin filaments were stained by phalloidin, and actin protrusion numbers and lengths were measured. Shown are averages from at least three individual samples along with representative images for the Capzb2 phosphomutants. The increase in actin protrusion numbers in SA samples is pointed out by arrows. Scale bars represent 10 μm

low and not affected by PIM inhibition (Additional file 3: Fig. S9F).

When we compared CP expression in different prostate cancer cell lines by Western blotting, we observed slightly lower levels of CAPZA1 in PC-3 cells as compared to the other lines, while CAPZB levels were highest in DU-145 cells (Additional file 3: Fig. S10A). To analyse the role of CP phosphorylation in the rapidly migrating DU-145 cells, wound healing assays were carried out with cells that had been transiently transfected to overexpress wild-type Capza1 with wild-type or mutant Capzb2. No major changes were detected between the expression levels of wild-type and phosphomutant proteins (Additional file 3: Fig. S10B). Similarly to the data from PIM inhibitor-treated cells, migration of DU-145 cells was affected by CP phosphorylation, but in a less pronounced fashion (Additional file 3: Fig. S10C-D). When adhesion of DU-145 cells was analysed, PIM inhibition by DHPCC-9 reduced adhesion to collagen in a similar manner as observed in PC-3 cells (Additional file 3: Fig. S10E). Furthermore, transient overexpression of wild-type Capzb2 or its phosphomimicking (3XSE) mutant significantly promoted cell adhesion as compared to control cells or those overexpressing the phosphodeficient (3XSA) mutant (Additional file 3: Fig. S10F-G). Data from MTT assays indicated that even though DHPCC-9 slightly reduced viability of LNCAP cells, it had no effects in DU-145 cells, the viability of which was also only marginally affected by CP overexpression (Additional file 3: Fig. S11A-C).

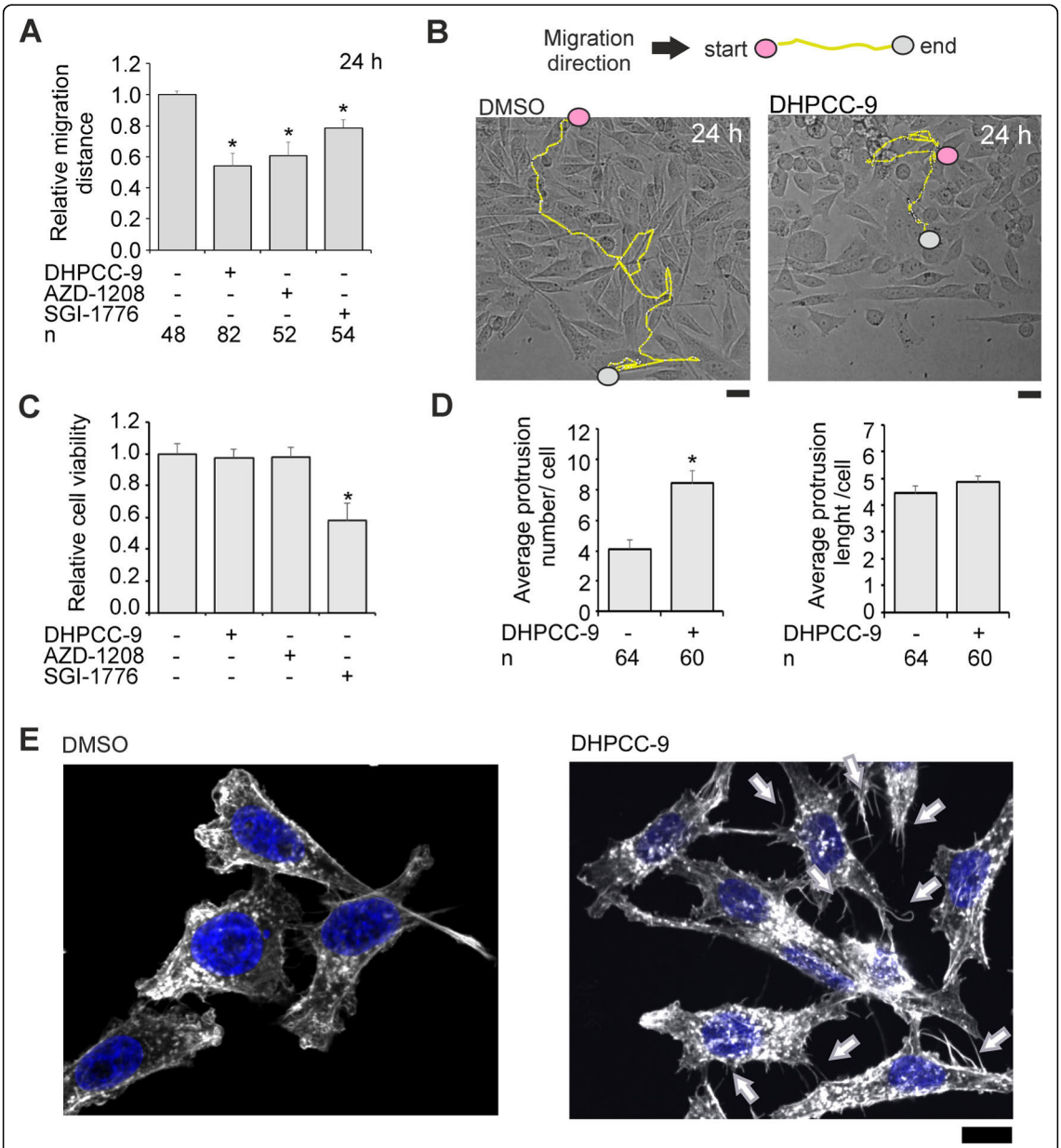

Fig. 5 PIM inhibition increases the number of actin protrusions at cell edges. PC-3 cells were treated for 24 h with 10 μM DHPCC-9, AZD-1208 or SGI-1776. Single cell tracking was performed to visualize the migration route and distance after PIM inhibition. **a** Shown are averages of indicated numbers (n) of cells along with **b** representative images of cells treated with DMSO or DHPCC-9. Scale bars represent 20 μm. **c** MTT assays were used to determine the relative viability of PC-3 cells after 24 h treatments with PIM inhibitors. Shown are averages from three independent experiments with three parallel samples. **d** PC-3 cells were plated on coverslips and treated with DMSO or DHPCC-9 for 24 h, after which actin filaments were stained by phalloidin, and the number of actin protrusions and their length were measured. Shown are averages of indicated numbers (n) of cells along with **e** representative images for actin protrusions. Scale bars represent 10 μm. The increase in actin protrusion numbers in DHPCC-9-treated samples is pointed out by arrows

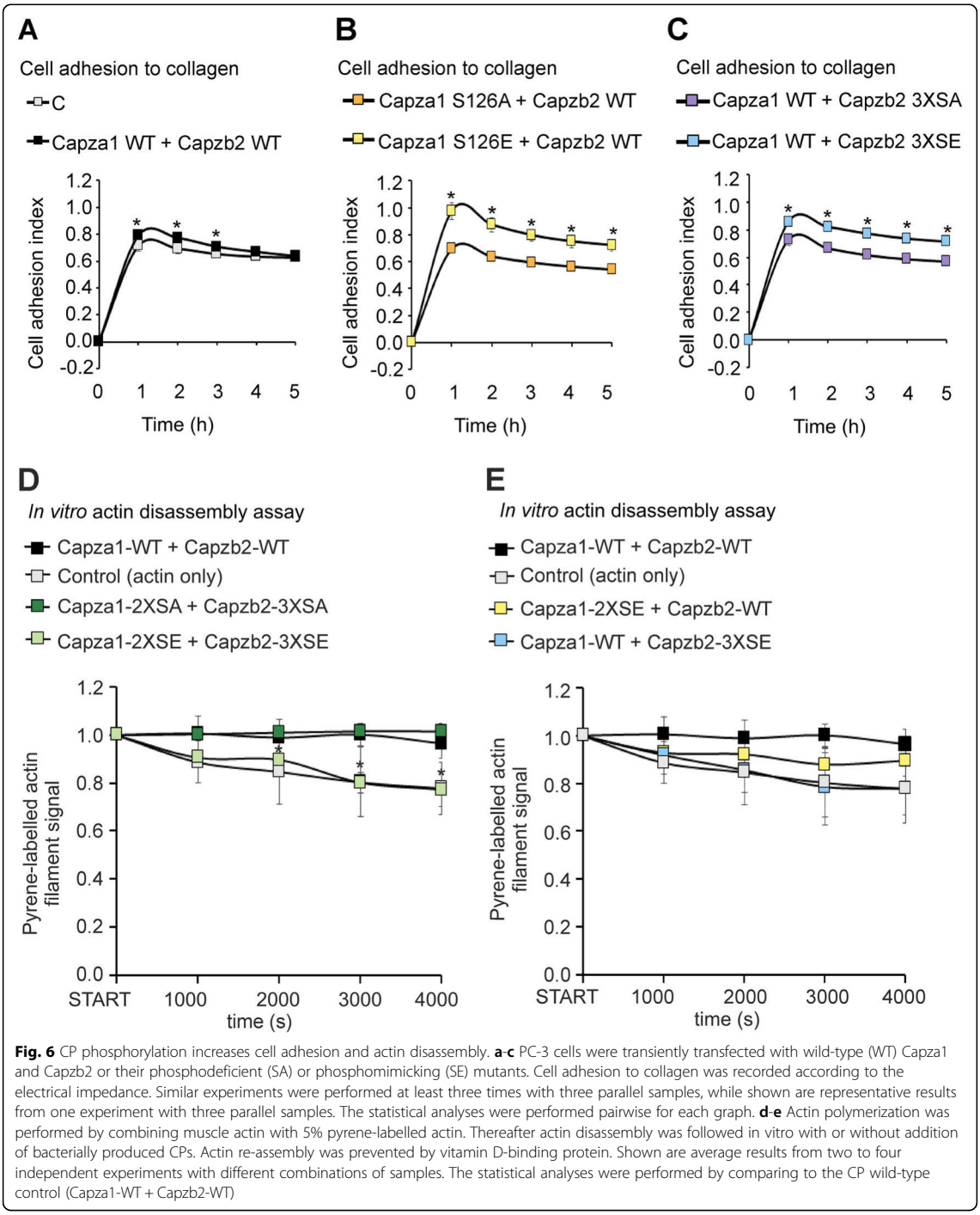

Fig. 6 CP phosphorylation increases cell adhesion and actin disassembly. **a**-**c** PC-3 cells were transiently transfected with wild-type (WT) Capza1 and Capzb2 or their phosphodeficient (SA) or phosphomimicking (SE) mutants. Cell adhesion to collagen was recorded according to the electrical impedance. Similar experiments were performed at least three times with three parallel samples, while shown are representative results from one experiment with three parallel samples. The statistical analyses were performed pairwise for each graph. **d**-**e** Actin polymerization was performed by combining muscle actin with 5% pyrene-labelled actin. Thereafter actin disassembly was followed in vitro with or without addition of bacterially produced CPs. Actin re-assembly was prevented by vitamin D-binding protein. Shown are average results from two to four independent experiments with different combinations of samples. The statistical analyses were performed by comparing to the CP wild-type control (Capza1-WT + Capzb2-WT)

Discussion

The oncogenic PIM kinases support tumor growth as well as cancer cell adhesion, migration, invasion and the formation of metastases through multiple signalling pathways [23]. Here we have identified capping proteins as novel PIM substrates and demonstrate that PIM-

dependent phosphorylation of the CP heterodimers inhibits their actin capping activity and thereby enhances actin dynamics and prostate cancer cell motility. To investigate the impact of phosphorylation, the CP subunits or their phosphomimicking (SE) or phosphodeficient (SA) mutants were simultaneously overexpressed using a dual plasmid. To reduce potential off-target effects, which have previously been associated with high expression levels [52, 53], all overexpression experiments were initiated 12 h after transfection.

In our study, we observed that both subunits of the Capza1/b2 heterodimer are phosphorylated by PIM1, while in the other heterodimer formed by human CAPZA2 and mouse Capzb2, only CAPZA2 was phosphorylated. This cannot be explained by species-specific differences, as the beta subunits in mouse and human are identical (Additional file 3: Fig. S12). Furthermore, also the two alpha 1 phosphorylation sites and their surrounding sequences are fully conserved between mouse and human proteins (Additional file 3: Fig. S12). Based on mRNA expression levels [42], the CAPZA1/B2 heterodimer is more prominently expressed than the CAPZA2/B2 in the PC-3 prostate cancer cells, which were used in most of our cellular assays. However, according to our Western blotting data, both CAPZA1 and CAPZA2 proteins are expressed in PC-3 cells, but have distinct subcellular localizations. Alpha 1 is cytoplasmic, but alpha 2 mostly nuclear, hinting at distinct functions for the CAPZA1/B2 and CAPZA2/B2 heterodimers. Based on our imaging and immunoprecipitation data, PIM1 colocalizes and interacts with the CP heterodimer mainly in the cytoplasmic regions, and promotes both cell adhesion and migration in a phosphorylation-dependent fashion. On the other hand, phosphorylation of CAPZA2 was not studied in more detail and it may therefore play an as of yet unknown role in the regulation of e.g. nuclear actin dynamics in prostate cancer cells.

Previously, capping protein activity has been reported to be inhibited by multiple factors, while no activators have been discovered. Proteins such as formins and Ena/VASP proteins regulate CP function indirectly, while myotrophin, phosphoinositides and CARMIL proteins inhibit CPs directly by binding to them [6]. Very little is known about post-translational modification of CPs, except that Capza1 can be phosphorylated by the casein kinase CK-2 at S9 [22], and CAPZB1 acetylated at K199 and phosphorylated by PKCε at S204 [14]. All these modifications reduce capping activity. Here we have shown that both CP alpha and beta subunits are phosphorylated by PIM1: Capza1 at S106 and S126, and Capzb2 at S182, S192 and S226. Phosphorylation decreases the ability of CPs to protect actin filament ends and thereby increases dynamical changes in actin filament organization. This promotes the shortening or elongation of filamentous actin. Here, in the phosphodeficient samples, the filament dynamics is blocked, and increased numbers of slightly shortened filaments are seen. The continuous changes in actin organization are known to be needed for proper cell adhesion and migration [54]. As expected, we observed increases in both cell adhesion and motility by overexpressing the phosphomimicking mutants. The balance of CP activity is expected to be crucial for proper actin dynamics and cell shape formation. For instance, CP beta silencing has been shown to increase the number of filopodia on cell edges [49], while complete silencing or overexpressing CPs leads to embryonic death [53].

All other PIM phosphorylation sites were identified from cellular samples, except for S226 in Capzb2. However, phosphorylation of this residue may be context-dependent, as it has previously been observed to be phosphorylated in colorectal cancer samples [48]. It should also be noted that some of the PIM phosphorylation sites, as well as the additional T186 site of Capzb2, may be targeted by other kinases as well. Furthermore, the PIM consensus sequences (K/R-K/R-R-K/R-L-S/T-X [55], K/R-K/R-K/R-X-S/T-X [56] and R-X-R-H-X-S [57]) do not completely match with the CP target sites, which is also the case with several other previously identified PIM kinase substrates [36, 58–61]. Therefore, it may be worth re-evaluating the PIM1 consensus sequence in the future.

Our data may also have clinical implications. Here we show positive correlations between *PIM1* and either *CAPZA1*, *CAPZA2* or *CAPZB* mRNAs in prostate cancer samples with different Gleason grades, but not in the healthy control tissues. Also, *PIM2* and *PIM3* mRNA expression levels correlate with those of CPs in more advanced tumors. Thus, the similar expression patterns of PIM kinases and CPs at different cancer stages suggest that their interactions may affect prostate cancer progression via phosphorylation-dependent regulation of the capping activity. This is supported by our comparative studies with additional prostate cancer cell lines. Interestingly, the hormone-independent prostate cancer cell lines PC-3 and DU-145 behave quite similarly, while no major phosphorylation-dependent changes are detected in the androgen-dependent LNCAP cells with relatively low PIM1 levels. Thus, the higher PIM1 levels and increased activity of PIM-mediated signalling pathways in PC-3 and DU-145 cells may be connected to their increased motility as compared to LNCAP cells.

From a therapeutic perspective, it is crucial to know the downstream targets of PIM kinases and to be able to estimate the on- and off-target effects of PIM inhibitors. According to our results, PIM inhibition is expected to increase CP activity, resulting in decreased cancer cell

migration. However, it would be important to analyse the effects of PIM kinases and their inhibitors on other CP subunits to confirm that PIM inhibition does not cause any unexpected changes in healthy tissues, such as muscle, testis or the nervous system, from where we originally identified the Capza2 subunit as a neuronal substrate for PIM1.

Conclusions

To summarize, CP alpha and beta subunits have previously been reported to behave in an opposite fashion [17–21], leading to contradictory interpretations of the role CPs play in cancer progression. Here we have demonstrated that it is essential to simultaneously analyse the effects of both CP subunits as a heterodimer, which is the functional unit protecting the ends of actin filaments. We have shown that phosphorylation of the alpha 1 and beta 2 subunits by PIM1 reduces the actin capping activity of the CP heterodimer, resulting in increased prostate cancer cell motility. This is also the first study linking PIM kinases directly to the regulation of actin dynamics, highlighting the importance of PIM family members in enhancing motility and metastatic behaviour of cancer cells.

Supplementary information

Supplementary information accompanies this paper at https://doi.org/10.1186/s12964-020-00618-6.

Additional file 1. Additional protocols tables. Tables S1-S4 show detailed data related to the methods of the study.

Additional file 2. Additional results tables. Tables S5-S7 show additional data related to the results shown in the main figures.

Additional file 3 Additional results figures. Figures S1-S12 show additional data related to the results shown in the main figures.

Abbreviations

2X: double mutant (S106 and S126 in Capza1 or S182 and S192 in Capzb2); 3X: triple mutant (S182, S192, S226 in Capzb2); CP: capping protein; DHPCC-9: 1,10-dihydropyrrolo [2,3-a]carbazole-3-carbaldehyde, compound 9 (PIM inhibitor); Dual-CMV: PSF-CMV-CMV-SBFI-UB-PURO - DUAL CMV; Duet : pRFSDuet-1; ICD: intracellular domain (of Notch receptor); KD: kinase-deficient; MCS: multiple cloning site; pcDNA-PIM1: pcDNA™3.1/PIM1-V5-His; SA: serine (S) to alanine (A) phosphomutant (phosphodeficient); SE: serine (S) to glutamic acid (E) phosphomutant (phosphomimicking); WT: wild-type

Acknowledgements

We thank P Lappalainen (University of Helsinki) for advice, V Paavilainen (University of Helsinki) for the murine Capza1-Capzb2-pRFS-Duet expression plasmid, J Jokinen, S Hakala, L Hokkanen, M Hyttinen, L Parkkali, J Rikkinen, N Tulonen, M Nevala and S Sysmelin for technical assistance, and W Eccleshall for checking the English language. We also thank the Biocenter Finland core facilities of Turku Bioscience for assistance in microscopy (Cell Imaging and Cytometry Core with J Sandholm) and mass spectrometry analyses (Proteomics facility with A Rokka). The LNCAP and DU-145 cell lines were kind gifts from J Heino (University of Turku, Finland) and J Tuomela (University of Turku, Finland), respectively.

Authors' contributions

PIM kinase substrate identification was performed in collaboration between R.V., E.M.R., J.Z., E.C. and P.J.K. Other experiments and cloning were performed by N.M.S., V.V., T.H., K.L.M. and M.L. The actin disassembly assays were designed by E.K. The study was mainly designed and the manuscript written by N.M.S. and P.J.K. All authors have read and approved the manuscript.

Funding

This study was financially supported by the Academy of Finland grants 111820 and 287040 to P.J.K. and grant 111870 to E.C.

Availability of data and materials

The databases used for in silico analysis are the following: PhosphoMotif Finder (www.hprd.org/PhosphoMotif_finder/), the PhosphoSitePlus® database (phosphosite.org), IST Online™ database (ist.medisapiens.com), Betastasis database (betastasis.com; gene expression barblot and Taylor et al. dataset), the Basic Local Alignment Search Tool (blast.ncbi.nlm.nih.gov/Blast.cgi), the National Center for Biotechnology Information (www.ncbi.nlm.nih.gov/) and UniProt Knowledgebase (www.uniprot.org/help/uniprotkb). Plasmid backbones are the following: pGEM-T-Easy (#A1360, Promega, https://fi.promega.com), pRFSDuet-1 (#71341, Merck Millipore; www.merckmillipore.com), GST vectors (GE Healthcare Life Sciences; www.fishersci.com), PSF-CMV-CMV-SBFI-UB-PURO and pFlag-CMVTM-2 (#OGS597 and # E7033, Sigma-Aldrich; www.sigmaaldrich.com), pEGFP-C1 (Clontech laboratories Inc.; www.addgene.org), pcDNATM3.1/V5-His (#V81020, Thermo Fisher Scientific, www.thermofisher.com), Tag-RFP-N (#FP142, Evrogen; evrogen.com).

Ethics approval and consent to participate

Not applicable.

Consent for publication

Not applicable (study does not contain any individual person's data).

Competing interests

No potential competing interest.

Author details

[1]Section of Physiology and Genetics, Department of Biology, University of Turku, Vesilinnantie 5, FI-20500 Turku, Finland. [2]Turku Bioscience, University of Turku and Åbo Akademi University, 20520 Turku, Finland. [3]Institute of Biotechnology, University of Helsinki, 00014 Helsinki, Finland.

Received: 25 March 2020 Accepted: 27 June 2020
Published online: 08 August 2020

References

1. Hanahan D, Weinberg RA. The hallmarks of cancer. Cell. 2000. https://doi.org/10.1016/S0092-8674(00)81683-9.
2. Kourtidis A, Lu R, Pence LJ, Anastasiadis P. Z. A central role for cadherin signaling in cancer. Exp Cell Res. 2017; doi:https://doi.org/10.1016/j.yexcr.2017.04.006.
3. Conway JRW, Jacquemet G. Cell matrix adhesion in cell migration. Essays Biochem. 2019. https://doi.org/10.1042/ebc20190012.
4. Christopher RA, Guan JL. To move or not: how a cell responds (review). Int J Mol Med. 2000;5:575–81. https://doi.org/10.3892/ijmm.5.6.575.
5. Svitkina T. The actin cytoskeleton and actin-based motility. Cold Spring Harb Perspect Biol. 2018. https://doi.org/10.1101/cshperspect.a018267.
6. Edwards M, Zwolak A, Schafer DA, Sept D, Dominguez R, Cooper JA. Capping protein regulators fine-tune actin assembly dynamics. Nat Rev Mol Cell Biol. 2014. https://doi.org/10.1038/nrm3869.
7. Cooper JA, Sept D. New insights into mechanism and regulation of actin capping protein. Int Rev Cell Mol Biol. 2008. https://doi.org/10.1016/S1937-6448(08)00604-7.
8. Maruyama K, Kmura S, Ishii T, Kuroda M, Ohashi K, Muramatsu S. β-Actinin, a regulatory protein of muscle: purification, characterization, and function. J Biochem. 1977. https://doi.org/10.1093/oxfordjournals.jbchem.a131438.
9. Casella JF, Casella SJ, Hollands JA, Caldwell JE, Cooper JA. Isolation and characterization of cDNA encoding the α subunit of cap Z (36/32), an actin-capping protein from the Z line of skeletal muscle. Proc Natl Acad Sci U S A. 1989. https://doi.org/10.1073/pnas.86.15.5800.
10. Cooper JA, Caldwell JE, Gattermeir DJ, Torres MA, Amatruda JF, Casella JF. Variant cDNAs encoding proteins similar to the α subunit of chicken CapZ. Cell Motil Cytoskeleton. 1991. https://doi.org/10.1002/cm.970180306.

11. Tanaka H, Yoshimura Y, Nishina Y, Nozaki M, Nojima H, Nishimune Y. Isolation and characterization of cDNA clones specifically expressed in testicular germ cells. FEBS Lett. 1994. https://doi.org/10.1016/0014-5793(94)01155-9.
12. Schafer DA, Korshunova YO, Schroer TA, Cooper JA. Differential localization and sequence analysis of capping protein beta-subunit isoforms of vertebrates. J Cell Biol. 1994. https://doi.org/10.1083/jcb.127.2.453.
13. Von Bülow M, Rackwitz HR, Zimbelmann R, Franke WW. CPβ3, a novel isoform of an actin-binding protein, is a component of the cytoskeletal calyx of the mammalian sperm head. Exp Cell Res. 1997. https://doi.org/10.1006/excr.1997.3564.
14. Lin YH, Warren CM, Li J, McKinsey TA, Russell B. Myofibril growth during cardiac hypertrophy is regulated through dual phosphorylation and acetylation of the actin capping protein CapZ. Cell Signal. 2016. https://doi.org/10.1016/j.cellsig.2016.05.011.
15. Davis DA, Wilson MH, Giraud J, Xie Z, Tseng HC, England C, et al. Capzb2 interacts with β-tubulin to regulate growth cone morphology and neurite outgrowth. PLoS Biol. 2009. https://doi.org/10.1371/journal.pbio.1000208.
16. Mukaihara K, Suehara Y, Kohsaka S, Kubota D, Toda-Ishii M, Akaike K, et al. Expression of F-actin-capping protein subunit beta, CAPZB, is associated with cell growth and motility in epithelioid sarcoma. BMC Cancer. 2016. https://doi.org/10.1186/s12885-016-2235-z.
17. Sun D, Zhou M, Kowolik CM, Trisal V, Huang Q, Kernstine KH, et al. Differential expression patterns of capping protein, protein phosphatase 1, and casein kinase 1 may serve as diagnostic markers for malignant melanoma. Melanoma Res. 2011. https://doi.org/10.1097/CMR.0b013e328346b715.
18. Lee YJ, Jeong SH, Hong SC, Cho BI, Ha WS, Park ST, et al. Prognostic value of CAPZA1 overexpression in gastric cancer. Int J Oncol. 2013. https://doi.org/10.3892/ijo.2013.1867.
19. Huang D, Cao L, Zheng S. CAPZA1 modulates EMT by regulating actin cytoskeleton remodelling in hepatocellular carcinoma. J Exp Clin Cancer Res. 2017. https://doi.org/10.1186/s13046-016-0474-0.
20. Kwon MJ, Kim RN, Song K, Jeon S, Jeong HM, Kim JS, et al. Genes co-amplified with ERBB2 or MET as novel potential cancer-promoting genes in gastric cancer. Oncotarget. 2017; doi:https://doi.org/10.18632/oncotarget.21150.
21. Ohishi T, Yoshida H, Katori M, Migita T, Muramatsu Y, Miyake M, et al. Tankyrase-binding protein TNKS1BP1 regulates actin cytoskeleton rearrangement and cancer cell invasion. Cancer Res. 2017. https://doi.org/10.1158/0008-5472.CAN-16-1846.
22. Canton DA, Olsten ME, Kim K, Doherty-Kirby A, Lajoie G, Cooper JA, et al. The pleckstrin homology domain-containing protein CKIP-1 is involved in regulation of cell morphology and the actin cytoskeleton and interaction with actin capping protein. Mol Cell Biol. 2005. https://doi.org/10.1128/mcb.25.9.3519-3534.2005.
23. Santio NM, Koskinen PJ. PIM kinases: from survival factors to regulators of cell motility. Int J Biochem Cell Biol. 2017. https://doi.org/10.1016/j.biocel.2017.10.016.
24. Eichmann A, Yuan L, Bréant C, Alitalo K, Koskinen PJ. Developmental expression of Pim kinases suggests functions also outside of the hematopoietic system. Oncogene. 2000. https://doi.org/10.1038/sj.onc.1203355.
25. Glazova M, Aho TL, Palmetshofer A, Murashov A, Scheinin M, Koskinen PJ. Pim-1 kinase enhances NFATc activity and neuroendocrine functions in PC12 cells. Mol Brain Res. 2005. https://doi.org/10.1016/j.molbrainres.2005.04.003.
26. Kalichamy KS, Ikkala K, Pörsti J, Santio NM, Tuomaala J, Jha S, et al. PIM-related kinases selectively regulate olfactory sensations in *Caenorhabditis elegans*. eNeuro. 2019. https://doi.org/10.1523/eneuro.0003-19.2019.
27. Brault L, Gasser C, Bracher F, Huber K, Knapp S, Schwaller J. Pim serine/threonine kinases in the pathogenesis and therapy of hematologic malignancies and solid cancers. Haematologica. 2010. https://doi.org/10.3324/haematol.2009.017079.
28. Nawijn MC, Alendar A, Berns A. For better or for worse: the role of Pim oncogenes in tumorigenesis. Nat Rev Cancer. 2011. https://doi.org/10.1038/nrc2986.
29. Santio NM, Vahakoski RL, Rainio EM, Sandholm JA, Virtanen SS, Prudhomme M, et al. Pim-selective inhibitor DHPCC-9 reveals Pim kinases as potent stimulators of cancer cell migration and invasion. Mol Cancer. 2010;9:279. https://doi.org/10.1186/1476-4598-9-279.
30. Santio NM, Eerola SK, Paatero I, Yli-Kauhaluoma J, Anizon F, Moreau P, et al. Pim kinases promote migration and metastatic growth of prostate cancer xenografts. PLoS One. 2015. https://doi.org/10.1371/journal.pone.0130340.
31. Santio NM, Salmela M, Arola H, Eerola SK, Heino J, Rainio EM, et al. The PIM1 kinase promotes prostate cancer cell migration and adhesion via multiple signalling pathways. Exp Cell Res. 2016. https://doi.org/10.1016/j.yexcr.2016.02.018.
32. Rebello RJ, Kusnadi E, Cameron DP, Pearson HB, Lesmana A, Devlin JR, et al. The dual inhibition of RNA pol I transcription and PIM kinase as a new therapeutic approach to treat advanced prostate cancer. Clin Cancer Res. 2016. https://doi.org/10.1158/1078-0432.CCR-16-0124.
33. Santio NM, Landor SK, Vahtera L, Ylä-Pelto J, Paloniemi E, Imanishi SY, et al. Phosphorylation of Notch1 by Pim kinases promotes oncogenic signaling in breast and prostate cancer cells. Oncotarget. 2016; doi:https://doi.org/10.18632/oncotarget.9215.
34. Rainio EM, Sandholm J, Koskinen PJ. Cutting edge: transcriptional activity of NFATc1 is enhanced by the Pim-1 kinase. J Immunol. 2002. https://doi.org/10.4049/jimmunol.168.4.1524.
35. Cen B, Xiong Y, Song JH, Mahajan S, DuPont R, McEachern K, et al. The Pim-1 protein kinase is an important regulator of MET receptor tyrosine kinase levels and signaling. Mol Cell Biol. 2014. https://doi.org/10.1128/mcb.00147-14.
36. Eerola SK, Santio NM, Rinne S, Kouvonen P, Corthals GL, Scaravilli M, et al. Phosphorylation of NFATC1 at PIM1 target sites is essential for its ability to promote prostate cancer cell migration and invasion. Cell Commun Signal. 2019. https://doi.org/10.1186/s12964-019-0463-y.
37. Kiriazis A, Vahakoski RL, Santio NM, Arnaudova R, Eerola SK, Rainio EM, et al. Tricyclic benzo [cd] azulenes selectively inhibit activities of Pim kinases and restrict growth of Epstein-Barr virus-transformed cells. PLoS One. 2013. https://doi.org/10.1371/journal.pone.0055409.
38. Björkblom B, Ostman N, Hongisto V, Komarovski V, Filén JJ, Nyman TA, et al. Constitutively active cytoplasmic c-Jun N-terminal kinase 1 is a dominant regulator of dendritic architecture: role of microtubule-associated protein 2 as an effector. J Neurosci. 2005. https://doi.org/10.1523/JNEUROSCI.1517-05.2005.
39. Shevchenko A, Wilm M, Vorm O, Mann M. Mass spectrometric sequencing of proteins from silver-stained polyacrylamide gels. Anal Chem. 1996. https://doi.org/10.1021/ac950914h.
40. Imanishi SY, Kochin V, Eriksson JE. Optimization of phosphopeptide elution conditions in immobilized Fe (III) affinity chromatography. Proteomics. 2007. https://doi.org/10.1002/pmic.200600571.
41. Kauko O, Laajala TD, Jumppanen M, Hintsanen P, Suni V, Haapaniemi P, et al. Label-free quantitative phosphoproteomics with novel pairwise abundance normalization reveals synergistic RAS and CIP2A signaling. Sci Rep. 2015. https://doi.org/10.1038/srep13099.
42. Kilpinen S, Autio R, Ojala K, Iljin K, Bucher E, Sara H, et al. Systematic bioinformatic analysis of expression levels of 17,330 human genes across 9,783 samples from 175 types of healthy and pathological tissues. Genome Biol. 2008. https://doi.org/10.1186/gb-2008-9-9-r139.
43. Taylor BS, Schultz N, Hieronymus H, Gopalan A, Xiao Y, Carver BS, et al. Integrative genomic profiling of human prostate cancer. Cancer Cell. 2010. https://doi.org/10.1016/j.ccr.2010.05.026.
44. Bateman A. UniProt: a worldwide hub of protein knowledge. Nucleic Acids Res. 2019. https://doi.org/10.1093/nar/gky1049.
45. Akué-Gédu R, Rossignol E, Azzaro S, Knapp S, Filippakopoulos P, Bullock AN, et al. Synthesis, kinase inhibitory potencies, and *in vitro* antiproliferative evaluation of new Pim kinase inhibitors. J Med Chem. 2009. https://doi.org/10.1021/jm901018f.
46. Kremneva E, Makkonen MH, Skwarek-Maruszewska A, Gateva G, Michelot A, Dominguez R, et al. Cofilin-2 controls actin filament length in muscle sarcomeres. Dev Cell. 2014. https://doi.org/10.1016/j.devcel.2014.09.002.
47. Altschul SF, Gish W, Miller W, Myers EW, Lipman DJ. Basic local alignment search tool. J Mol Biol. 1990. https://doi.org/10.1016/S0022-2836(05)80360-2.
48. Shiromizu T, Adachi J, Watanabe S, Murakami T, Kuga T, Muraoka S, et al. Identification of missing proteins in the neXtProt database and unregistered phosphopeptides in the PhosphoSitePlus database as part of the chromosome-centric human proteome project. J Proteome Res. 2013. https://doi.org/10.1021/pr300825v.
49. Mejillano MR, Kojima S, Applewhite DA, Gertler FB, Svitkina TM, Borisy GG. Lamellipodial versus filopodial mode of the actin nanomachinery: pivotal role of the filament barbed end. Cell. 2004. https://doi.org/10.1016/j.cell.2004.07.019.
50. Lees A, Lin S, Haddad JG. Brevin and vitamin D-binding protein: comparison of the effects of two serum proteins on actin assembly and disassembly. Biochemistry. 1984. https://doi.org/10.1021/bi00308a030.

51. Otterbein LR, Cosio C, Graceffa P, Dominguez R. Crystal structures of the vitamin D-binding protein and its complex with actin: structural basis of the actin-scavenger system. Proc Natl Acad Sci U S A. 2002. https://doi.org/10.1073/pnas.122126299.
52. Hopmann R, Cooper JA, Miller KG. Actin organization, bristle morphology, and viability are affected by actin capping protein mutations in *Drosophila*. J Cell Biol. 1996. https://doi.org/10.1083/jcb.133.6.1293.
53. Mukherjee K, Ishii K, Pillalamarri V, Kammin T, Atkin JF, Hickey SE, et al. Actin capping protein CAPZB regulates cell morphology, differentiation, and neural crest migration in craniofacial morphogenesis. Hum Mol Genet. 2016. https://doi.org/10.1093/hmg/ddw006.
54. Shekhar S, Pernier J, Carlier MF. Regulators of actin filament barbed ends at a glance. J Cell Sci. 2016. https://doi.org/10.1242/jcs.179994.
55. Palaty CK, Clark-Lewis I, Leung D, Pelech SL. Phosphorylation site substrate specificity determinants for the Pim-1 protooncogene-encoded protein kinase. Biochem Cell Biol. 1997. https://doi.org/10.1139/o97-026.
56. Friedmann M, Nissen MS, Hoover DS, Reeves R, Magnuson NS. Characterization of the proto-oncogene Pim-1: kinase activity and substrate recognition sequence. Arch Biochem Biophys. 1992. https://doi.org/10.1016/0003-9861(92)90454-5.
57. Peng C, Knebel A, Morrice NA, Li X, Barringer K, Li J, Jakes S, et al. Pim kinase substrate identification and specificity. J Biochem. 2007. https://doi.org/10.1093/jb/mvm040.
58. Yuan LL, Green AS, Bertoli S, Grimal F, Mansat-De Mas V, Dozier C, et al. Pim kinases phosphorylate Chk1 and regulate its functions in acute myeloid leukemia. Leukemia. 2014. https://doi.org/10.1038/leu.2013.168.
59. Zippo A, De Robertis A, Serafini R, Oliviero S. PIM1-dependent phosphorylation of histone H3 at serine 10 is required for MYC-dependent transcriptional activation and oncogenic transformation. Nat Cell Biol. 2007. https://doi.org/10.1038/ncb1618.
60. Nihira K, Ando Y, Yamaguchi T, Kagami Y, Miki Y, Yoshida K. Pim-1 controls NF-B signalling by stabilizing RelA/p65. Cell Death Differ. 2010. https://doi.org/10.1038/cdd.2009.174.
61. Kim H, Oh B, Choi JK, Bae SC. Pim-1 kinase phosphorylates and stabilizes RUNX3 and alters its subcellular localization. J Cell Biochem. 2008. https://doi.org/10.1002/jcb.21906.

Publisher's Note

Table S1 – Primers used for cloning and sequencing

Shortenings: pRFSDuet-1 (Duet), pGEM-T-Easy (Easy), pGEX-6P-3 (GST), PSF-CMV-CMV-SBFI-UB-PURO - DUAL CMV (Dual) and pFlag-CMV-2 (Flag); multiple cloning site (MCS), cloning primer (c), sequencing primer(s), bacterial expression vector (be), bacterial cloning vector (bc) or mammalian expression vector (me).

Vector	Insert	Primer	Primer sequence 5´- 3´
Duet (be)	Capza1 (MCS 1)	Forward (s)	GGATCTCGACGCTCTCCCT
Duet (be)	Capza1 (MCS 1)	Reverse (s)	GATTATGCGGCCGTGTACAA
Duet (be)	Capzb2 (MCS 2)	Forward (s)	TTGTACACGGCCGCATAATC
Duet (be)	Capzb2 (MCS 2)	Reverse (s)	GCTAGTTATTGCTCAGCGG
Easy (bc)	CAPZA2	Forward (c)	AGGCTTATGGCGGATCTGGAGGAGCAG
Easy (bc)	CAPZA2	Reverse (c)	GCGGCCGCTCATGCATTCTGCATCTCTTT
Easy (bc)	Capzb2	Foward (c)	GCCGCCCCATGAGCGATCAGCAG
Easy (bc)	Capzb2	Reverse (s)	TCTTCAACACTGCTGCTTTCTCTTCAAGGC
Easy (bc)	CAPZA2	Forward (s)	GTAATACGACTCACTATAGGGC
GST (be)	Capzb2	Forward (s)	ATAGCATGGCCTTTGCAGGGCTG
Dual (me)	Capza1/ CAPZA2	Forward (s)	GGATCTCGACGCTCTCCCT
Dual (me)	Capza1/ CAPZA2	Reverse (s)	GATTATGCGGCCGTGTACAA
Dual (me)	Capzb2	Forward (s)	TTGTACACGGCCGCATAATC
Dual (me)	Capzb2	Reverse (s)	GCTAGTTATTGCTCAGCGG
To Dual from Flag (me)	Capzb2	Forward (s)	GGCATGTCGACATGGACTACAAAGAC
To Dual from Flag (me)	Capzb2	Reverse (s)	CCTCTAGAGTCGATCGACTGGTACC

Table S2 – Plasmid design

Shortenings: pRFSDuet-1 (Duet), pGEM-T-Easy (Easy), pGEX-6P-3 (GST), PSF-CMV-CMV-SBFI-UB-PURO - DUAL CMV (Dual), pFlag-CMV-2 (Flag) and pEGFP-C1 (GFP); multiple cloning site (MCS), digestion prior to insert (Digestion 1) and digestion after the insert (Digestion2), blunt end generation with Klenow fragment or digestion (italics), disruption of digestion site (overlining), insert (i), vector (v) and N-terminal (N-).

Vector	**Insert**	**Digestion 1**	**Digestion 2**	**MCS 1 or 2**	**(N-)Tag**
Duet	Capza1	NcoI	~~BamHI~~	**1**: Capza1 **2**: Capzb2	His
Duet	Capzb2	NdeI	~~BglII~~	**1**: Capza1 or CAPZA2 **2**: Capzb2	-
Duet	CAPZA2	EcoRI	NotI	**1**: Capza2 **2**: Capzb2	His
Easy	CAPZA2	EcoRI	SpeI	**1**	-
Easy	Capzb2	EcoRI	SpeI	**1**	-
GST	Capzb2	EcoRI	EcoRI	**1**	GST
Dual	Capza1	NcoI	*i: EcoRI or NotI* *v: EcoRV*	**1**: Capza1 **2**: Capzb2	His
Dual	CAPZA2	NcoI	*i: NotI* *v: EcoRV*	**1**: CAPZA2 **2**: Capzb2	His
Flag	Capzb2	EcoRI	EcoRI	**1**	Flag
Dual	Capzb2	SalI	SpeI	**1**: Capza1 or CAPZA2 **2**: Capzb2	Flag
GFP	Capzb2	EcoRI	EcoRI	**1**	GFP
Dual	GFP-Capzb2	*i: NheI,* *v: PciI*	*i: KpnI* *v: SpeI*	**1**: Capza1 **2**: Capzb2	GFP

Table S3 – Primers for mutagenesis

Amino acid residues of wild-type or mutant proteins: serine (S), alanine (A) and glutamic acid (E).

Protein	Mutagenesis	Primer type	Primer sequence
Capza1	S106>A	Forward	GGAAAGAAGCAGCCGACCCGCAGCCAGAGG
Capza1	S106>A	Reverse	CCTCTGGCTGCGGGTCGGCTGCTTCTTTCC
Capza1	S106>E	Forward	GGAAAGAAGCAGAGGACCCGCAGCCAGAGG
Capza1	S106>E	Reverse	CCTCTGGCTGCGGGTCCTCTGCTTCTTTCC
Capza1	S126>A	Forward	GGAGGGAGTCGTGTGATGCTGCGCTGAGAGCC
Capza1	S126>A	Reverse	GGCTCTCAGCGCAGCATCACACGACTCCCTCC
Capza1	S126>E	Forward	GGGAGTCGTGTGATGAGGCGCTGAGAGCCTATG
Capza1	S126>E	Reverse	CATAGGCTCTCAGCGCCTCATCACACGACTCCC
Capzb2	S182>A	Forward	CTATGGCTGCAAACTAACAAGGCTGGCTCGGGCAC
Capzb2	S182>A	Reverse	GTGCCCGAGCCAGCCTTGTTAGTTTGCAGCCATAG
Capzb2	S182>E	Forward	GCAAACCAACAAAGAAGGCTCGGGCACCATGAAC
Capzb2	S182>E	Reverse	GTTCATGGTGCCCGAGCCTTCTTTGTTGGTTTGC
Capzb2	S192>A	Forward	GAACCTGGGAGGCGCACTAACGAGACAGATGG
Capzb2	S192>A	Reverse	CCATCTGTCTCGTTAGTGCGCCTCCCAGGTTC
Capzb2	S192>E	Forward	GAACCTGGGAGGCGAACTAACGAGACAGATGG
Capzb2	S192>E	Reverse	CCATCTGTCTCGTTAGTTCGCCTCCCAGGTTC
Capzb2	S226>A	Forward	GAAAACAAAATCCGGGCCACGCTGAATGAGATCTAC
Capzb2	S226>A	Reverse	GTAGATCTCATTCAGCGTGGCCCGGATTTTGTTTTC
Capzb2	S226>E	Forward	GGACATGGAAAACAAAATCCGAGAGACGCTGAATGAG
Capzb2	S226>E	Reverse	CTCATTCAGCGTCTCTCGGATTTTGTTTTCCATGTC

Table S4 – Primary antibodies

Samples were stained overnight at +4°C in rotation in PBS or TBS Tween-20 according to manufacturer´s protocols for Western blotting (WB) or in a humidified chamber for immunofluorescence (IF).

Protein or tag	**Company**	**Product number**	**Dilution for WB**	**Dilution for IF**
PIM1	Merck	MABC553	1:500	1:500
Capza1	Abcam	ab166892	1:1000	-
CAZPA1/A2	Abcam	ab175378	1:1000	1:500
Capzb2	Sigma	HPA031531	1:500	1:500
His	Thermo Fisher Scientific	MAI_21315	1:2000	1:500
Flag	Sigma	F3165	1:500	1:500
Tubulin	Cell Signaling Technology	#86298	1:1000	-
Lamin A/C	Cell Signaling Technology	#4777	1:1000	-
ACTB	Cell Signaling Technology	#4970, #3700	1:1000	-

Table S5 – Identification of potential Pim1 substrates by mass spectrometry

Rat proteins phosphorylated by murine Pim1 in an *in vitro* phosphoproteomics screen were identified by mass spectrometry. The recognized peptides are shown alongside their UniProt identifiers.

UniProt entry code	**Rat protein**	**Identified peptides**
Q3T1K5	Capza2	FIIHAPPGEFNEVFNDVR; EATDPRPYEAENAIESWR; NFWNGR
P47942	Dpysl2	MVIPGGIDVHTR; FQMPDQGMTSADDFFQGTK; GTVVYGEPITASLGTDGSH; DNFTLIPEGTNGTEER; VFNLYPR
P04764	Eno1	AAVPSGASTGIYEALELR; GVPLYR; LAMQEFMILPVGASSFR; AGYTDQVVIGMDVAASEFYR; FTASAGIQVVGDDLTVTNPK
P69682	Necap1	ASDWKLDQPDWTGR; LDQPDWTGR; VSGELFAQAPVEQYPGIAVETVTD; SAFIGIGFTDR; SAFIGIGFTDRGDAFDFNVSLQDH; GDAFDFNVSLQDHFK
P67779	Phb	FDAGELITQR; DLQNVNITLR; VLPSITTEILK; IYTSIGEDYDER; KLEAAEDIAYQLSR; AAELIANSLATAGDGLIELR; AATFGLILDDVSLTHLTFGK; FGLALAVAGGVVNSALYNVDAGHR

Table S6 – Correlation of PIM and CAPZ levels in prostate tissues

Pearson´s correlation coefficiencies and their statistical significance (*) in human samples.

Gene	*PIM1*	*PIM2*	*PIM3*	Tissue type
CAPZA1	0,53*	0,28	0,26	**Primary tumor**
CAPZA2	0,59*	0,27	0,20	
CAPZA3	-0,08	0,03	0,03	
CAPZB	0,58*	0,36	0,39	
CAPZA1	0,58*	-0,13	0,22	**Metastasis**
CAPZA2	0,62*	-0,03	0,28	
CAPZA3	-0,46*	0,16	-0,23	
CAPZB	0,52*	0,16	0,50*	
CAPZA1	0,69*	0,27	0,17	**Gleason score <7**
CAPZA2	0,70*	0,25	0,22	
CAPZA3	-0,23	-0,15	-0,07	
CAPZB	0,63*	0,34	0,36	
CAPZA1	0,42*	0,18	0,22	**Gleason score 7**
CAPZA2	0,51*	0,18	0,14	
CAPZA3	0,04	0,22	0,12	
CAPZB	0,56*	0,33	0,41*	
CAPZA1	0,72*	0,60*	0,47*	**Gleason score >7**
CAPZA2	0,82*	0,66*	0,32*	
CAPZA3	-0,17	-0,02	-0,02	
CAPZB	0,76*	0,58*	0,43*	
CAPZA1	0,02	-0,20	0,16	**Healthy prostate tissue**
CAPZA2	0,20	-0,23	0,16	
CAPZA3	0,03	0,05	-0,05	
CAPZB	0,18	-0,12	0,10	

Table S7 – Identification of CAPZ phosphorylation sites

Phosphorylation of Capza1 and Capzb2 by PIM1 was analysed by *in vitro* kinase assays. For cellular *in vivo* analyses, Capza1 and Capzb2 were co-overexpressed with PIM1 in PC-3 prostate cancer cells, and Capza1 was co-immunoprecipitated with Capzb2. In both cases, proteins separated by SDS-PAGE were cut out, and subjected to trypsin digestion and mass spectrometry analysis with TiO_2 enrichment. Shown are protein names, codes and identified phosphopeptides along with other observed modifications.

Protein (Uniprot code)	**Residue**	**Peptide**	**Modifications**	***in vitro***	***in vivo***
Capza1 (P47753)	S106	KEASDPQPEDVDGGLK	S4-Phospho	x	x
Capza1 (P47753)	S126	ESCDSALR	C3-Carbamidomethyl, S5-Phospho	x	x
Capzb2 (P47757)	S2	SDQQLDCALDLMR	S1-Phospho, C7-Carbamidomethyl, M12-Oxidation	x	-
Capzb2 (P47757)	S182	SGSGTMNLGGSLTR	S1-Phospho, M6-Oxidation	x	x
Capzb2 (P47757)	T186	SGSGTMNLGGSLTR	T5-Phospho	-	x
Capzb2 (P47757)	S192	SGSGTMNLGGSLTR	M6-Oxidation, S11-Phospho	x	x

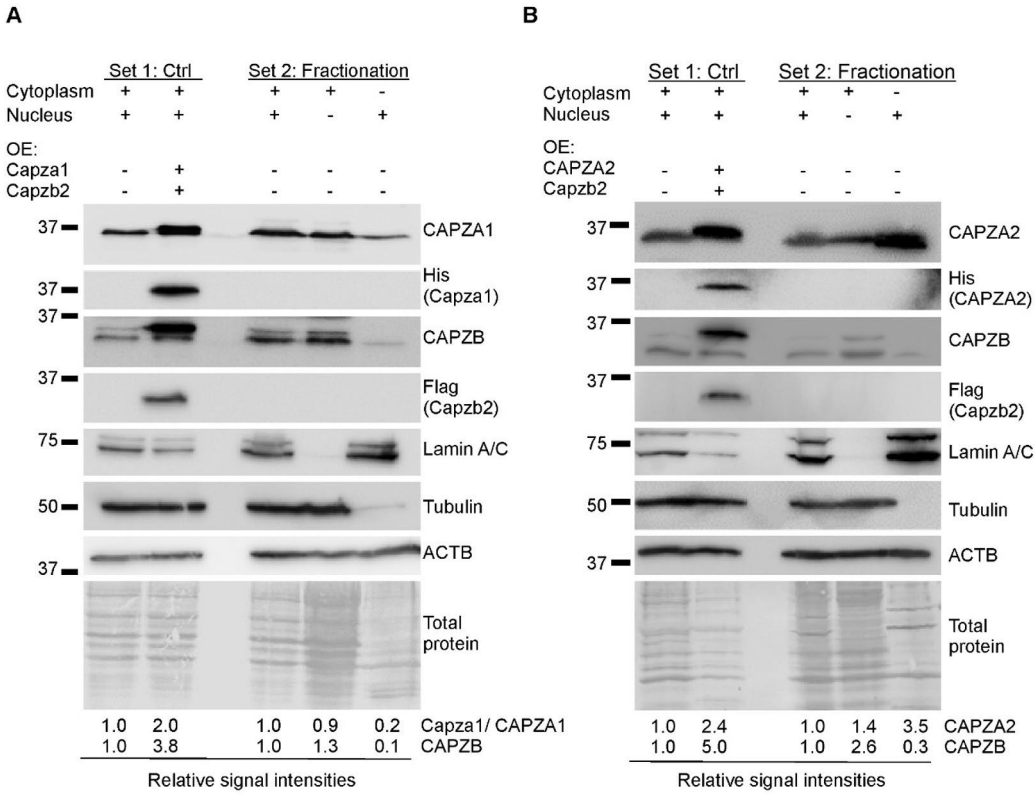

Figure S1 – CAPZA1 and CAPZB2 are expressed mainly in the cell cytoplasm, unlike CAPZA2

(A-B) Untransfected PC-3 cells were fractionated into nuclear and cytoplasmic fractions and stained with antibodies against CP proteins, while lysates from PC-3 cells overexpressing His- and Flag-tagged Capza1/b2 **(A)** or CAPZA2/b2 **(B)** were used as positive controls. Lamin A/C, Tubulin, ACTB and total protein staining were used as localization and loading controls.

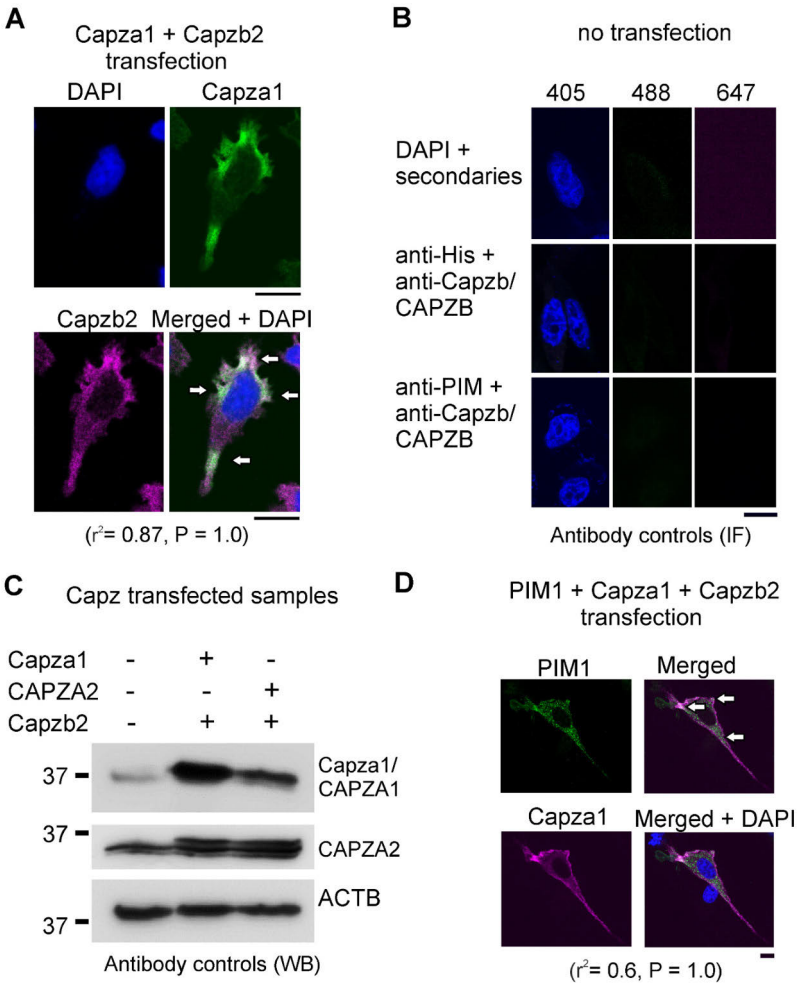

Figure S2 – Immunofluorescence controls and additional colocalization assays

(A) PC-3 cells transiently overexpressing His-Capza1 and Flag-Capzb2 were stained with His and Capzb antibodies. **(B)** Untransfected cells were used as controls for immunofluorescence, where adjusted signal intensity and laser power for the overexpression were too low to detect the endogenous proteins. **(C)** Capza/CAPZA antibody specificity was tested with transfected PC-3 cell samples. **(D)** Transfected PC-3 cells were stained with Capza2 and PIM1 antibodies to measure the co-localization between PIM1 and Capza1. Colocalization is shown in white in the merged images and pointed-out by arrows. Scale bars represent 20 µm (A-B) or 10 µm (D). Shown are also Pearson´s correlations (r^2) of colocalized pixels and their Costes significance (P) values.

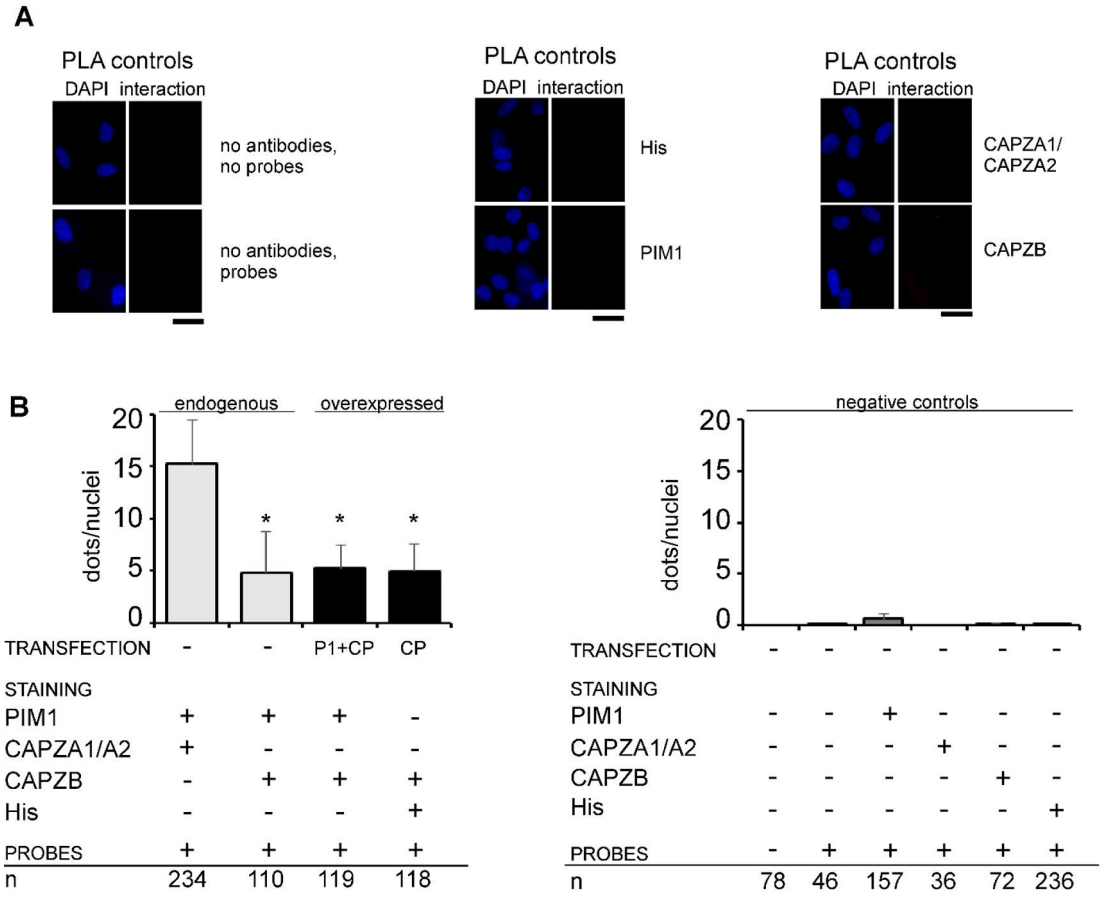

Figure S3 – Controls and analysis of proximity ligation assays

(A) Untransfected PC-3 cells were used as negative controls for the indicated antibodies in proximity ligation assays (PLA). Antibodies are shown in the right. DAPI staining was used to visualize nuclei. Scale bars represent 25 µm. **(B)** Summary of PLA data with analysed cell numbers (n). Shown are stainings for endogenous proteins or ectopically overexpressed PIM1 (P1) and/ or Capza1 + Capzb2 (CP). As negative controls, we used both samples with probes and without probes to confirm that we did not have any background signals.

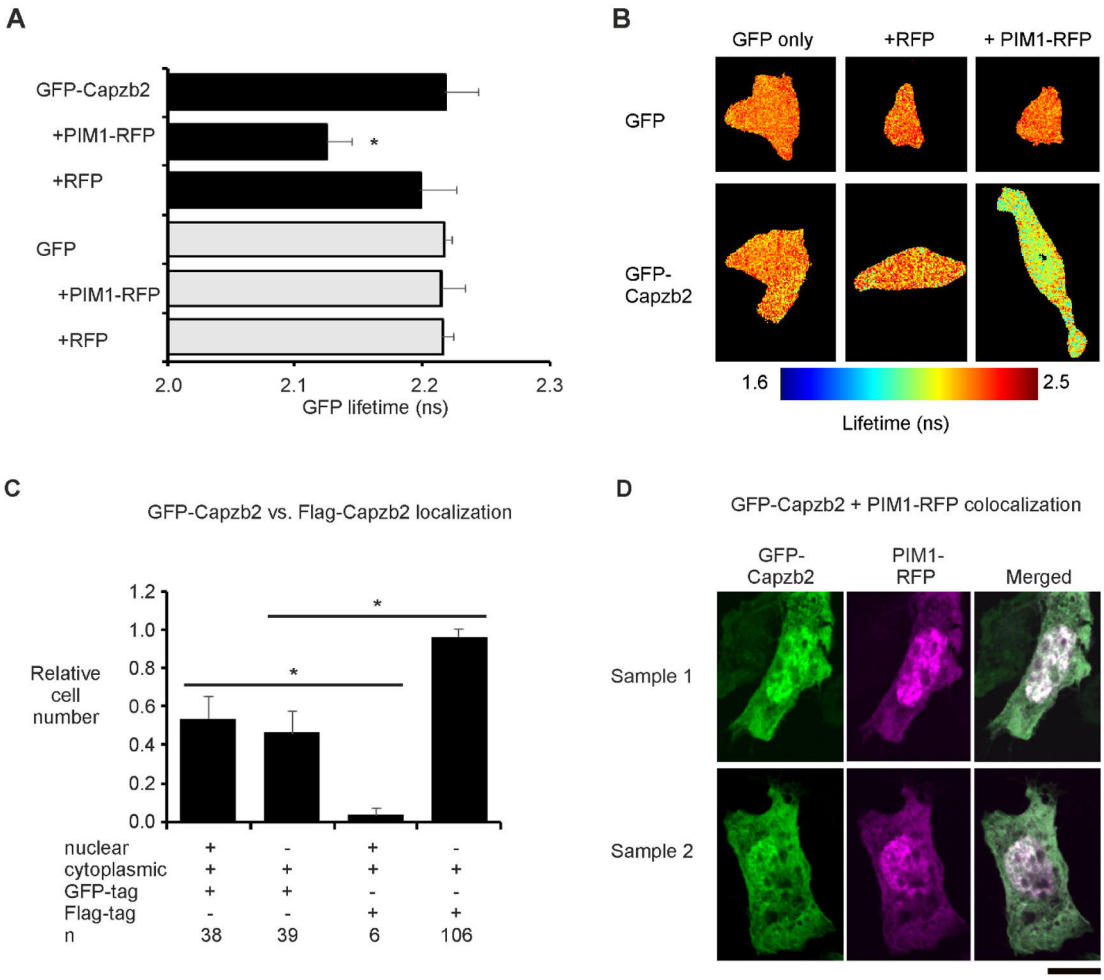

Figure S4 – GFP-Capzb2 and PIM1-RFP interact and colocalize in cells

(A) PC-3 cells were plated on coverslips and transfected with empty vectors or vectors overexpressing GFP-tagged mouse Capzb2 or RFP-tagged human PIM1 followed by fixation and fluorescence-lifetime imaging. Shown are average GFP lifetimes along with analysed cell numbers inside the bars. Lifetimes are combined from two individual experiments with parallel samples, with either GFP-tagged Capzb2 alone or in combination with His-tagged Capza1. **(B)** Representative figures show the decreased GFP lifetime due to protein-protein interaction. **(C)** The localization of GFP- versus Flag-tagged Capzb2 was analysed from control samples without PIM1 overexpression. Both GFP- and Flag-tagged Capzb2 proteins were co-overexpressed with the wild-type Capza1 subunit. **(D)** Representative figures show colocalization of GFP-Capzb2 and PIM1-RFP in both nuclei and cytoplasm. For visualization, the RFP red color has been turned into magenta. Scale bar represents 10 µm.

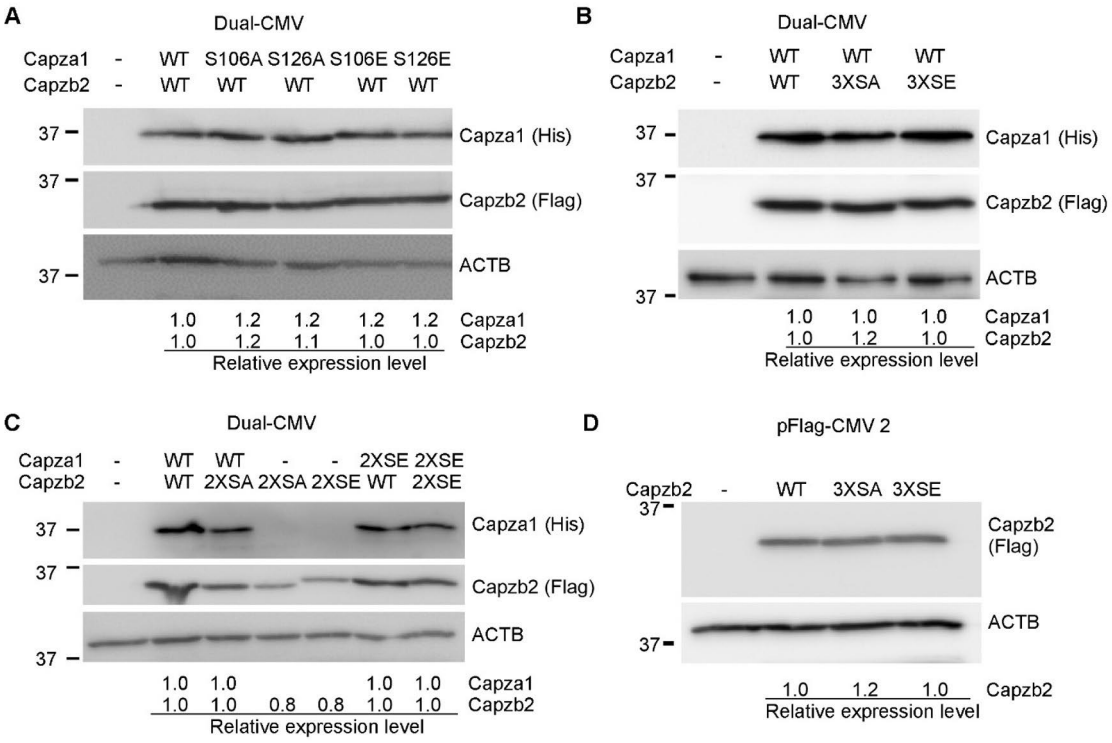

Figure S5 – CP mutants are expressed similarly to the wild-type proteins

(A-D) Wild-type (WT) Capza1 and Capzb2 or phosphomimicking (SE) or phosphodeficient (SA) single, double (2X) or triple (3X) phosphomutants were transiently overexpressed in PC-3 cells from plasmids indicated above the blots. Samples were prepared for Western blotting after wound healing assays, and overexpression was confirmed by targeting CP tags with antibodies.

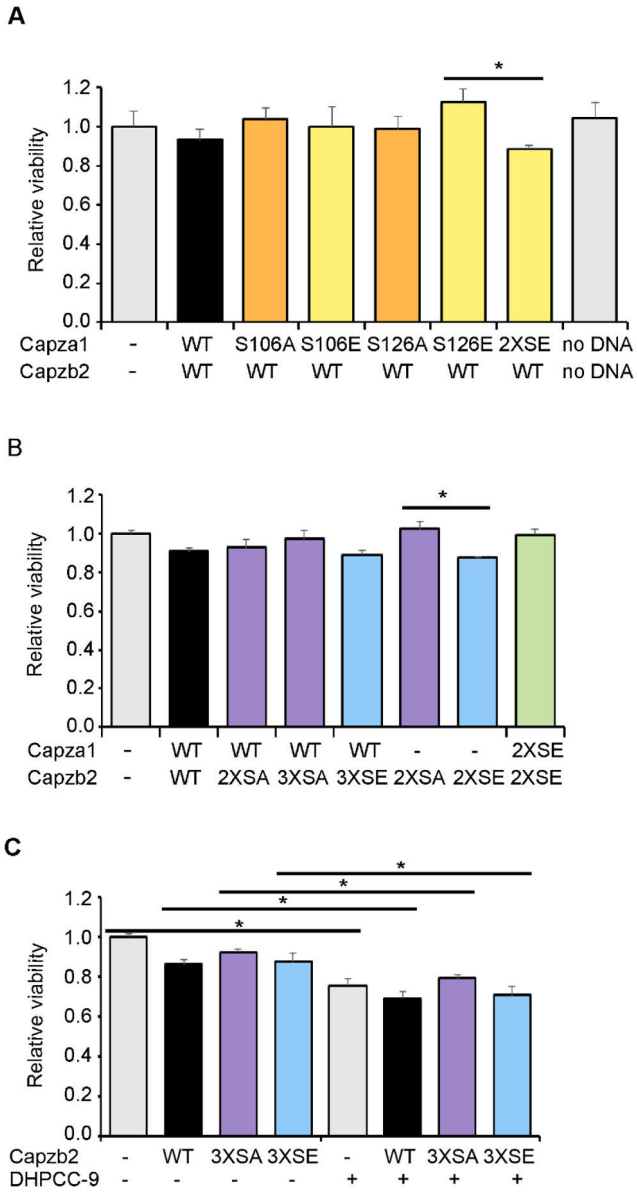

Figure S6 – CP phosphorylation does not have major effects on cell survival

(A-C) Wild-type (WT) Capza1 and Capzb2 or single phosphomimicking (SE) or phosphodeficient (SA) mutants or double (2X) or triple (3X) phosphomutants were transiently overexpressed in PC-3 cells. Cell motility was analysed by wound healing assays, which were initiated 12 h after transfection, and followed up for another 12 h, as shown in Figure 3. Cell viability was then measured by MTT assays. Shown are average viabilities from at least three independent assays.

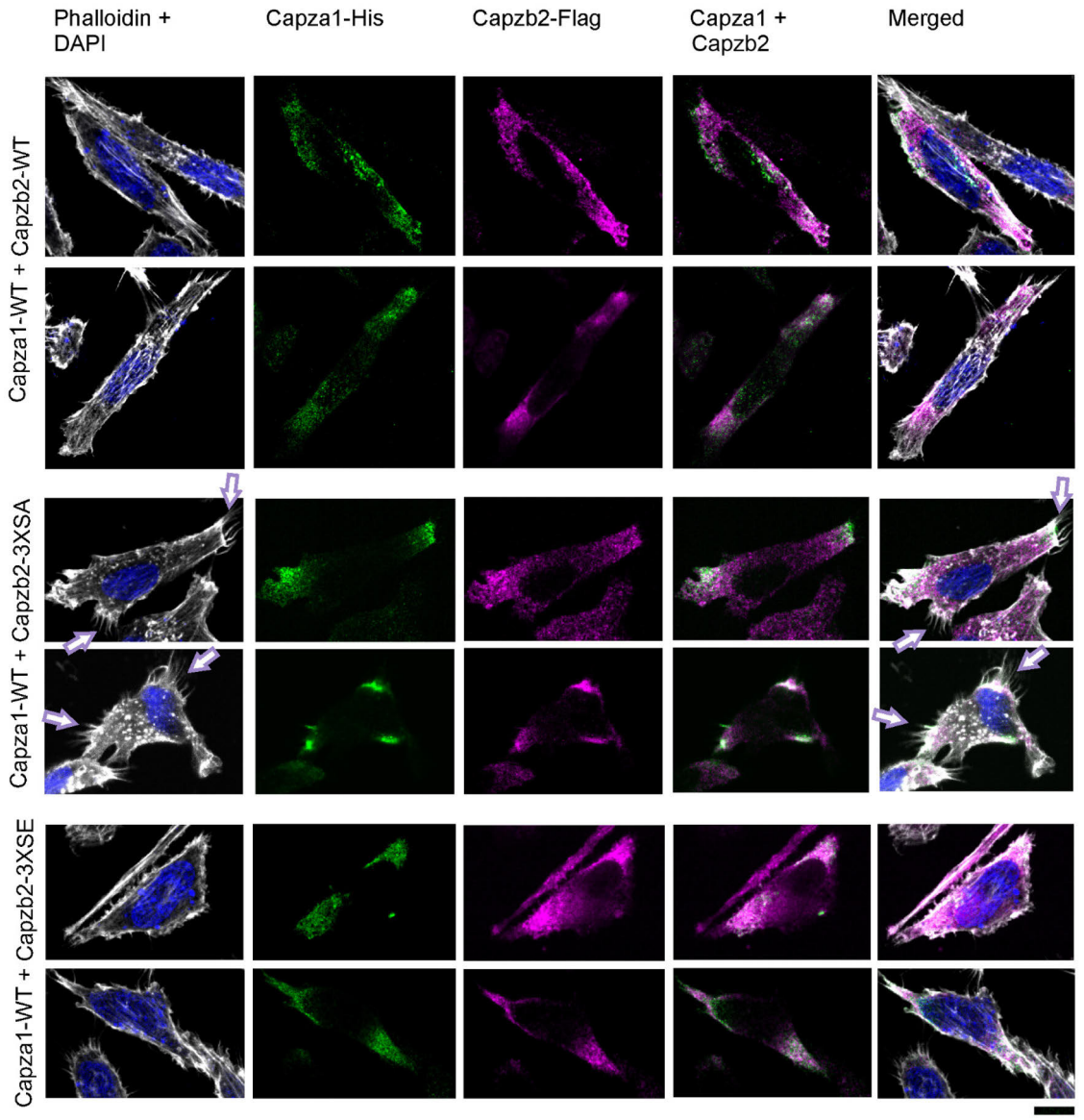

Figure S7 – CP dephosphorylation increases the number of actin protrusions

(A-C) PC-3 cells were transiently transfected to overexpress wild-type (WT) Capza1 and Capzb2 or their phosphodeficient (SA) or phosphomimicking (SE) mutants. Shown are images for the wild-type proteins as well as the phosphomutants. The increase in the number of actin protrusions in SA samples is pointed out by arrows. Scale bars represent 10 µm.

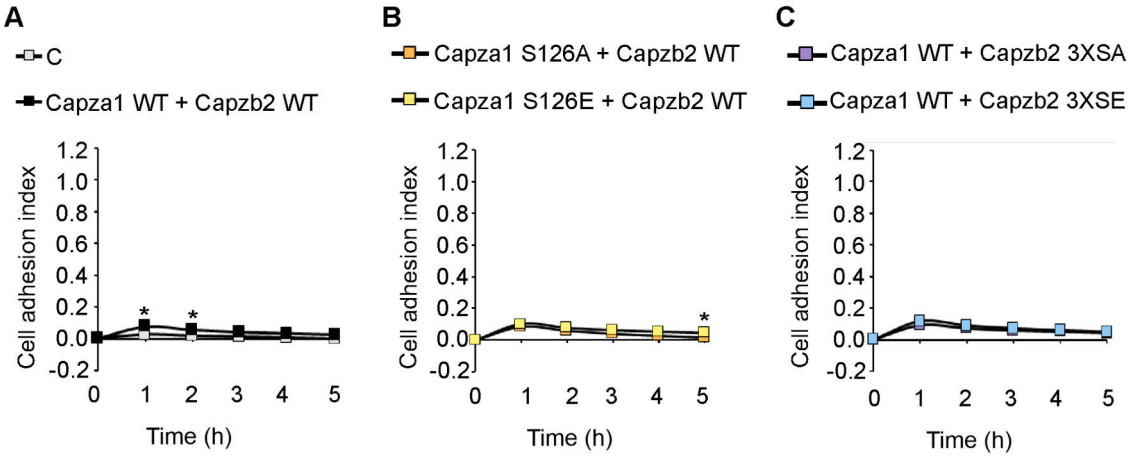

Figure S8 – Cell adhesion assay controls

(A-C) PC-3 cells were transiently transfected with wild-type (WT), phosphodeficient (SA) or phosphomimicking (SE) CPs. Cell adhesion to poly-L-lysine was measured according to electrical impedance. Three experiments were performed, while shown are results from one representative experiment with three parallel samples.

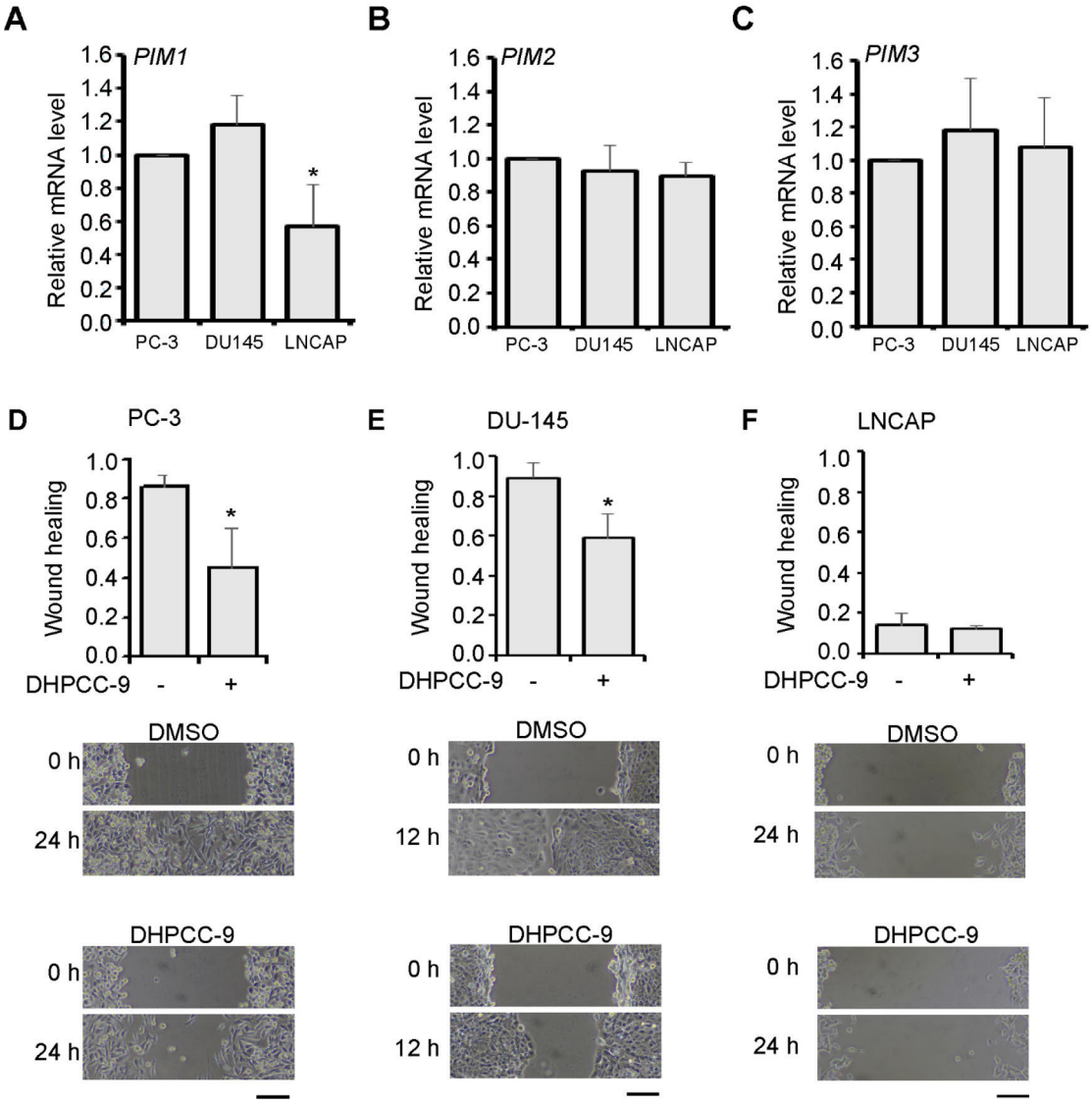

Figure S9 – Prostate cancer cell migration is reduced by PIM inhibition in a cell line-dependent manner

(A-C) *PIM* mRNA levels were measured in untransfected prostate cancer cell lines by RT-PCR and compared to those of PC-3 cells. **(D-F)** Wound healing assays were performed with the same cell lines treated with DMSO or 10 µM DHPCC-9. Wound closure was followed for 12 to 24 h, and shown are average results from at least three independent experiments with two or three parallel samples along with representative examples. Scale bars represent 20 µm.

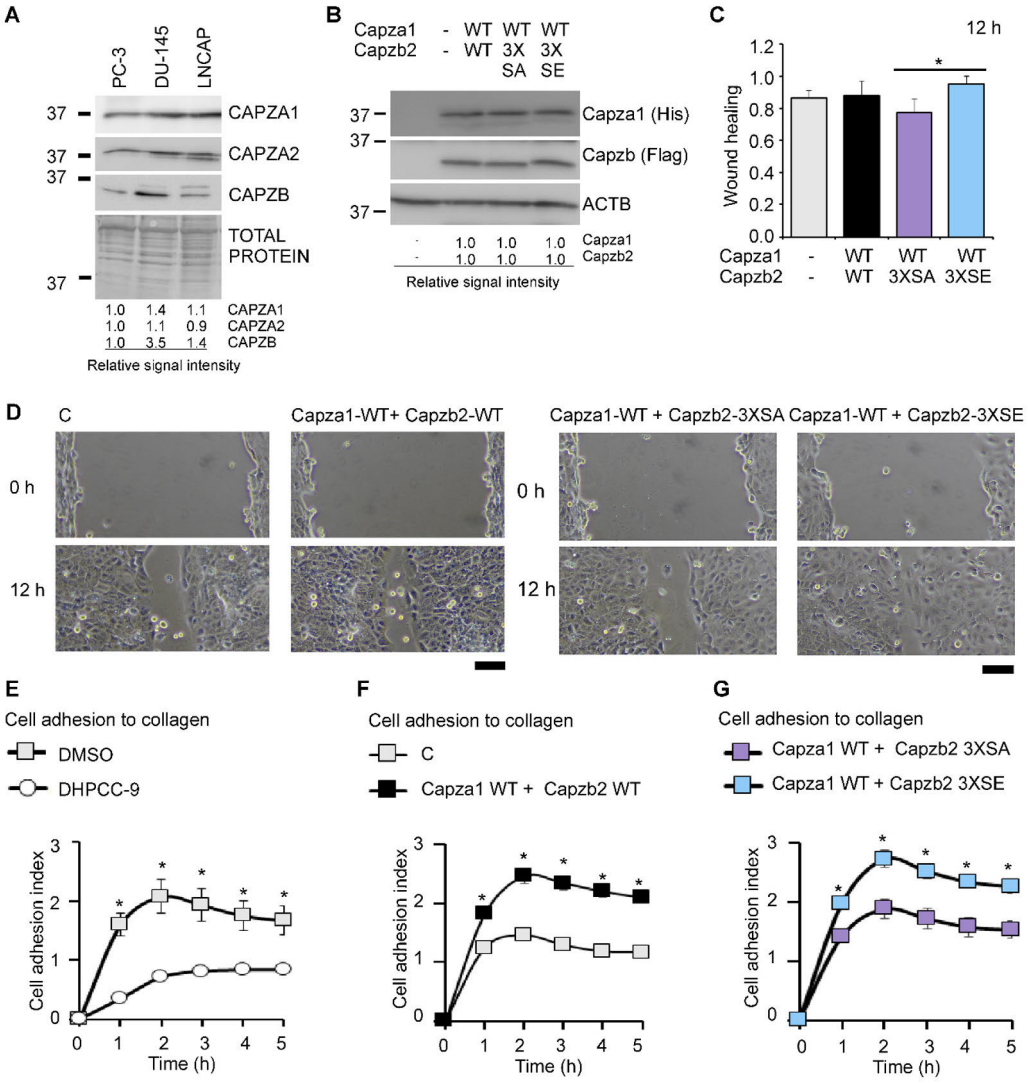

Figure S10 – CP phosphorylation promotes DU-145 cell migration and adhesion

(A-B) Western blotting was used to detect endogenous CPs in prostate cancer cell lines and transiently transfected CPs in DU-145 cells. **(C-D)** Cell migration was measured by wound healing assays from DU-145 cells overexpressing wild-type (WT) or phosphomutant (3XSA or 3XSE) CPs. Shown are average results from three independent experiments with representative images. Scale bars represent 20 µm. **(E)** Cell adhesion of untransfected or transiently transfected DU-145 cells was measured according to electrical impedance. PIM activity was inhibited by 10 µM DHPCC-9 starting 12 h prior to the assays. **(F-G)** The adhesion of transfected cells was measured starting 12 h after transfection. Similar experiments were performed at least three times with three parallel samples, while shown are representative results from one experiment.

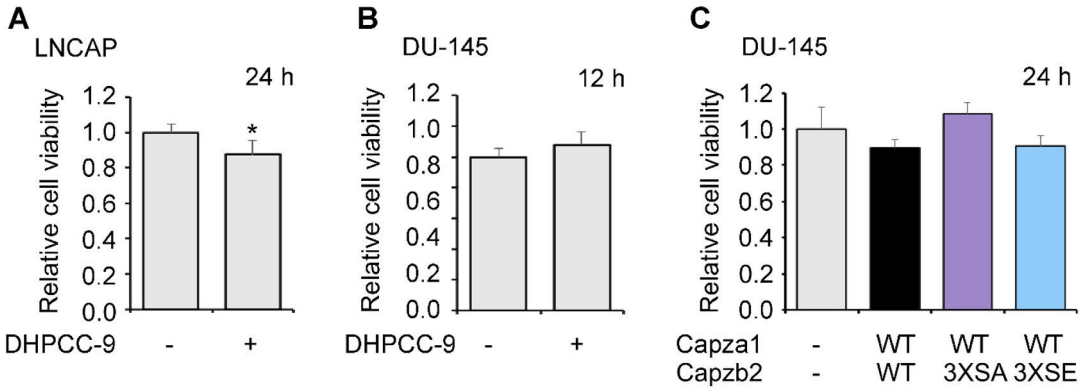

Figure S11 – Prostate cancer cell survival after different treatments or transfections

MTT assays were performed to the wound healing assay samples used for Figure S10. **(A-B)** Non-transfected LNCAP or DU-145 cells were measured 24 or 12 hours after the beginning of the treatment depending on the length of the wound healing assay**. (C)** Similarly, MTT assays were performed to transiently transfected DU-145 cells 24 hours after transfection.

A. Capza1 vs CAPZA1 sequence similarity

```
Mouse   1    MADFEDRVSDEEKVRIAAKFITHAPPGEFNEVFNDVRLLLNNDNLLREGAAHAFAQYNMD  60
             MADF+DRVSDEEKVRIAAKFITHAPPGEFNEVFNDVRLLLNNDNLLREGAAHAFAQYNMD
Human   1    MADFDDRVSDEEKVRIAAKFITHAPPGEFNEVFNDVRLLLNNDNLLREGAAHAFAQYNMD  60
                                                        S106
Mouse   61   QFTPVKIEGYDDQVLITEHGDLGNSRFLDPRNQISFKFDHLRKEASDPQPEDVDGGLKSW  120
             QFTPVKIEGY+DQVLITEHGDLGNSRFLDPRN+ISFKFDHLRKEASDPQPE+ DGGLKSW
Human   61   QFTPVKIEGYEDQVLITEHGDLGNSRFLDPRNKISFKFDHLRKEASDPQPEEADGGLKSW  120
                  S126
Mouse   121  RESCDSALRAYVKDHYSNGFCTVYAKTIDGQQTIIACIESHQFQPKNFWNGRWRSEWKFT  180
             RESCDSALRAYVKDHYSNGFCTVYAKTIDGQQTIIACIESHQFQPKNFWNGRWRSEWKFT
Human   121  RESCDSALRAYVKDHYSNGFCTVYAKTIDGQQTIIACIESHQFQPKNFWNGRWRSEWKFT  180

Mouse   181  ITPPSAQVVGVLKIQVHYYEDGNVQLVSHKDVQDSVTVSNEIQTTKEFIKIIESAENEYQ  240
             ITPP+AQVVGVLKIQVHYYEDGNVQLVSHKDVQDS+TVSNE QT KEFIKIIE+AENEYQ
Human   181  ITPPTAQVVGVLKIQVHYYEDGNVQLVSHKDVQDSLTVSNEAQTAKEFIKIIENAENEYQ  240

Mouse   241  TAISENYQTMSDTTFKALRRQLPVTRTKIDWNKILSYKIGKEMQNA  286
             TAISENYQTMSDTTFKALRRQLPVTRTKIDWNKILSYKIGKEMQNA
Human   241  TAISENYQTMSDTTFKALRRQLPVTRTKIDWNKILSYKIGKEMQNA  286
```

Uniprot identifier P47753-1 for mouse and P52907-1 for human

B. Capzb vs CAPZB sequence similarity

```
Mouse   1    MSDQQLDCALDLMRRLPPQQIEKNLSDLIDLVPSLCEDLLSSVDQPLKIARDKVVGKDYL  60
             MSDQQLDCALDLMRRLPPQQIEKNLSDLIDLVPSLCEDLLSSVDQPLKIARDKVVGKDYL
Human   1    MSDQQLDCALDLMRRLPPQQIEKNLSDLIDLVPSLCEDLLSSVDQPLKIARDKVVGKDYL  60

Mouse   61   LCDYNRDGDSYRSPWSNKYDPPLEDGAMPSARLRKLEVEANNAFDQYRDLYFEGGVSSVY  120
             LCDYNRDGDSYRSPWSNKYDPPLEDGAMPSARLRKLEVEANNAFDQYRDLYFEGGVSSVY
Human   61   LCDYNRDGDSYRSPWSNKYDPPLEDGAMPSARLRKLEVEANNAFDQYRDLYFEGGVSSVY  120

Mouse   121  LWDLDHGFAGVILIKKAGDGSKKIKGCWDSIHVVEVQEKSSGRTAHYKLTSTVMLWLQTN  180
             LWDLDHGFAGVILIKKAGDGSKKIKGCWDSIHVVEVQEKSSGRTAHYKLTSTVMLWLQTN
Human   121  LWDLDHGFAGVILIKKAGDGSKKIKGCWDSIHVVEVQEKSSGRTAHYKLTSTVMLWLQTN  180
             S182      S192                                  S226
Mouse   181  KSGSGTMNLGGSLTRQMEKDETVSDCSPHIANIGRLVEDMENKIRSTLNEIYFGKTKDIV  240
             KSGSGTMNLGGSLTRQMEKDETVSDCSPHIANIGRLVEDMENKIRSTLNEIYFGKTKDIV
Human   181  KSGSGTMNLGGSLTRQMEKDETVSDCSPHIANIGRLVEDMENKIRSTLNEIYFGKTKDIV  240

Mouse   241  NGLRSVQTFADKSKQEALKNDLVEALKRKQQC  272
             NGLRSVQTFADKSKQEALKNDLVEALKRKQQC
Human   241  NGLRSVQTFADKSKQEALKNDLVEALKRKQQC  272
```

Uniprot identifier P47757-2 for mouse and P47756-2 for human

Figure S12 – Comparison of human and mouse CP sequences

(A-B) BLAST was used to compare sequence similarities between mouse and human CP subunits at the PIM1 phosphorylation target sites (in bold and marked above the sequences) and their surrounding areas (inside squares).

Mung KL, Eccleshall WB, Santio NM, Rivero-Müller A, Koskinen PJ. (2021)

PIM kinases inhibit AMPK activation and promote tumorigenicity by phosphorylating LKB1

Cell Communication and Signaling

II

Mung *et al. Cell Commun Signal* (2021) 19:68
https://doi.org/10.1186/s12964-021-00749-4

Cell Communication and Signaling

RESEARCH Open Access

PIM kinases inhibit AMPK activation and promote tumorigenicity by phosphorylating LKB1

Kwan Long Mung[1], William B. Eccleshall[1,2], Niina M. Santio[1], Adolfo Rivero-Müller[1,2,3] and Päivi J. Koskinen[1*]

Abstract

Background: The oncogenic PIM kinases and the tumor-suppressive LKB1 kinase have both been implicated in the regulation of cell growth and metabolism, albeit in opposite directions. Here we investigated whether these kinases interact with each other to influence AMPK activation and tumorigenic growth of prostate and breast cancer cells.

Methods: We first determined how PIM and LKB1 kinases affect AMPK phosphorylation levels. We then used in vitro kinase assays to demonstrate that LKB1 is phosphorylated by PIM kinases, and site-directed mutagenesis to identify the PIM target sites in LKB1. The cellular functions of PIM and LKB1 kinases were evaluated using either pan-PIM inhibitors or CRISPR/Cas9 genomic editing, with which all three PIM family members and/or LKB1 were knocked out from PC3 prostate and MCF7 breast cancer cell lines. In addition to cell proliferation assays, we examined the effects of PIM and/or LKB1 loss on tumor growth using the chick embryo chorioallantoic membrane (CAM) xenograft model.

Results: We provide both genetic and pharmacological evidence to demonstrate that inhibition of PIM expression or activity increases phosphorylation of AMPK at Thr172 in both PC3 and MCF7 cells, but not in their derivatives lacking LKB1. This is explained by our observation that all three PIM family kinases can phosphorylate LKB1 at Ser334. Wild-type LKB1, but not its phosphodeficient derivative, can restore PIM inhibitor-induced AMPK phosphorylation in LKB1 knock-out cells. In the CAM model, loss of LKB1 enhances tumorigenicity of PC3 xenografts, while cells lacking both LKB1 and PIMs exhibit slower proliferation rates and form smaller tumors.

Conclusion: PIM kinases are novel negative regulators of LKB1 that affect AMPK activity in an LKB1-dependent fashion. The impairment of cell proliferation and tumor growth in cells lacking both LKB1 and PIMs indicates that these kinases possess a shared signaling role in the context of cancer. These data also suggest that PIM inhibitors may be a rational therapeutic option for LKB1-deficient tumors.

Keywords: PIM kinases, LKB1, AMPK, Phosphorylation, Prostate cancer, Breast cancer, CAM model

*Correspondence: paivi.koskinen@utu.fi
[1] Department of Biology, University of Turku, Vesilinnantie 5, 20500 Turku, Finland
Full list of author information is available at the end of the article

Background

The three serine/threonine-specific PIM family members (PIM1, PIM2, and PIM3) are highly homologous and in part functionally redundant [1–3]. As PIM kinases are constitutively active in cells [4], their catalytic activities correlate well with their protein expression levels. These oncogenic kinases are often overexpressed in solid tumors or haematological malignancies, in which they promote cell proliferation, survival, motility and metabolism via phosphorylation-dependent activation or inactivation of a wide variety of substrates, such as the NFATC1 and NOTCH1 transcriptional regulators, the CDKN1A and CDKN1B cell cycle inhibitors, the BAD pro-apoptotic protein, the CXCR4 chemokine receptor, the CAPZ actin capping proteins, and the AKT1S1 and EIF4EBP1 translational inhibitors [1–3, 5]. Accordingly, PIM kinases have emerged as attractive targets for cancer therapy, especially as they possess a structurally unique ATP-binding pocket [4], and as PIM triple knock-out (TKO) mice are viable and fertile with only a mild reduction in body size [6]. This phenotype may at least partially be due to reduced cytokine responses [7] and a diminished glycolytic phenotype [8].

The serine/threonine-specific liver kinase B1 (LKB1), encoded by the *STK11* gene, is a tumor suppressor, which is mutated in patients with the hereditary Peutz-Jeghers syndrome [9, 10]. Somatic inactivating mutations have also been found in sporadic tumors: 5–17% of non-small cell lung carcinomas [11–13], 5% of pancreatic cancers and melanomas [14–16] and around 20% of cervical cancers [17, 18]. Furthermore, *STK11* has been identified as the third most frequently mutated gene in human lung adenocarcinoma, following *TP53* and *KRAS* [19]. By contrast, LKB1 mutations have rarely been reported from breast, colorectal or gastric cancer [9]. The tumor suppressor function of LKB1 is largely attributed to its ability to phosphorylate the AMP-activated protein kinase (AMPK) [20–22] and 12 other closely related kinases [23]. AMPK in turn is a heterotrimeric protein comprising of a catalytic α subunit and regulatory β and γ subunits [24]. In response to changes in the AMP/ATP ratio resulting e.g. from energy deprivation, LKB1 phosphorylates the α subunit of AMPK at a conserved threonine site (commonly stated as Thr172 because of its pivotal finding in rats [25], while the corresponding site in the human protein is Thr183). Phosphorylation of AMPK increases its catalytic activity more than 100-fold in vitro [26], and in cells this allows it to inhibit anabolic biosynthetic pathways and to promote catabolic processes to restore the energy balance in favour of ATP production [24, 27]. Remarkably, failure to activate AMPK in response to energy stress has been proposed as an explanation for the massive cell death that occurs in LKB1-deficient tumors after treatment with metabolic inhibitors, such as metformin or phenformin [28, 29]. Interestingly, inhibition of PIM expression or activity has been shown to increase AMPK phosphorylation, possibly via LKB1 [30], but the exact mechanism behind this phenomenon has remained unclear.

As cancer cell growth and metabolism are regulated by the balance between oncogenic (e.g. PIM) and tumor-suppressive (e.g. LKB1) kinases, both overexpression of PIM kinases and loss of LKB1 expression are expected to promote tumorigenesis. In the present study with prostate and breast cancer cell lines expressing PIM and LKB1 kinases, we demonstrate that PIM kinases act as upstream kinases of LKB1 and that Ser334 in LKB1 is their phosphorylation target site. Both pharmacological and CRISPR/Cas9-based approaches reveal that inhibition of expression or activity of all three PIM family members upregulates AMPK activity in an LKB1-dependent manner. Finally, double knock-out of both LKB1 and PIM kinases led to a striking reduction in cell proliferation and tumor growth, raising possibilities for PIM-targeted pharmaceutical interventions in suppressing the growth of LKB1-deficient tumors.

Methods

Cell culture, reagents and DNA constructs

MCF7 breast cancer, HeLa cervical cancer and PC3 prostate cancer cells were obtained from American Type Culture Collection (Manassas, VA). Construction and maintenance of FDCP1-derived myeloid cell lines have been described previously [31]. MCF7 and HeLa cells were cultured in Dulbecco's modified Eagle's medium (DMEM), and PC3 and FDCP1 cells in RPMI-1640 medium (Sigma-Aldrich, St. Louis, MI, USA). Both media were supplemented with L-glutamine, 10% fetal bovine serum and antibiotics. MEM Non-Essential Amino Acids (Gibco, #11140050; Thermo Fisher Scientific, Waltham, MA, USA) and sodium pyruvate (Gibco, #11360070; Thermo Fisher Scientific) were further added to RPMI-1640 medium to facilitate cell growth. To study effects of nutrient deprivation, glucose-free medium was supplemented with different concentrations of glucose. FuGENE® HD Transfection Reagent (Promega, Madison, WI, USA) was used for plasmid transfection according to the manufacturer's protocol. PIM-selective small molecule inhibitors DHPCC9 [32, 33] and AZD1208 (AstraZeneca, Cambridge, UK) were diluted in DMSO. Expression vectors pcDNA™3.1/V5-His-C, pGEX-6P-1 and pTagRFP-N for wild-type (WT) human PIM kinases have been described previously [34]. Expression vectors pcDNA™6.2/N-EmGFP-DEST-LKB1 and pDEST™15-LKB1 were acquired from the Genome Biology Unit core facility (HiLIFE Helsinki Institute of Life Science,

Helsinki, Finland). His-tagged LKB1 construct was prepared by subcloning the LKB1 coding region from pcDNA™6.2/N-EmGFP-DEST-LKB1 to pRFSDuet-1 vector. Site-directed mutagenesis of LKB1 was performed by Ultra Pfu DNA Polymerase (Stratagene, San Diego, CA, USA) according to the manufacturer's protocol. The primers used are described in Supplementary material (Additional file 1: Table S1).

Establishment of stable knock-out cell lines

The CRISPR-Cas9 genome editing technique [35] was used to create stable knock-out cell lines. CRISPOR (http://crispor.tefor.net/) online software was used to design single guide RNA (sgRNA) sequences. These sequences were acquired as gBlocks® gene fragments (Integrated DNA Technologies, Coralville, Iowa, USA) and ligated into the BbsI-digested pSpCas9(BB)-2A-Puro (PX459) vector or pSpCas9(BB)-2A-GFP (PX458) to simultaneously express two sgRNAs. Transfected cells were either selected for 3–7 days with puromycin or by single cell sorting of GFP-positive cells into 96-well plates with the FACSAria cell sorter (Becton Dickinson, Franklin Lakes, NJ, USA). Knock-out cell screening was done by PCR amplification of the genomic DNA regions surrounding the CRISPR/Cas9 target sites. Genomic DNA extraction and PCR amplification were performed by using Mouse Direct PCR Kit (B40013; Bio-Connect, TE Huissen, The Netherlands) according to the manufacturer´s protocol, with PCR annealing temperature set to 60 °C and extension time to 1 min. The sequencing strategies and gel electrophoresis results are presented in Supplementary material (Additional file 2: Figure S1 and S2), as are also the sgRNA sequences and sequencing primers (Additional file 1: Table S2 and S3). After knocking out individual PIM family members, triple PIM kinase knock-out (TKO) cell lines were generated by sequentially knocking out additional genes.

Expression of GST-tagged or His-tagged fusion proteins in *Escherichia coli*

pDEST™15 plasmids (expressing GST-LKB1), pGEX-6P-1 plasmids (expressing GST-PIMs) and pRFSDuet-1 plasmid (expressing His-LKB1) were transformed into BL21 *E. coli* strain for protein production. Overnight bacterial cultures were grown at 30 °C until OD_{600} of 0.6. Isopropyl-β-D-galactosidase (250 μM; Sigma-Aldrich) was added to induce protein expression, and the cells were cultured for another 4 h (GST-PIMs) or 24 h (GST-LKB1, His-LKB1). The follow-up purification steps of GST-tagged and His-tagged protein have been described previously [5].

Western blotting

Cells were lysed for 10 min in ice-cold 50 mM Tris–HCl, pH 8.0 buffer containing 150 mM NaCl, 2 mM EDTA, 1% NP-40, 5 mM NaF, 1 mM Na_3VO_4, 1 mM PMSF and Mini EDTA-free protease inhibitor tablet (Roche, Basel, Switzerland). Supernatants were collected after 10 s centrifugation at 21,000 × g. Protein concentrations were determined using the Bio-Rad Protein Assay Dye Reagent or Pierce™ BCA Protein Assay Kit according to manufacturers' protocols. Protein aliquots (20-60 μg) were separated by 10% SDS-PAGE and transferred onto a PVDF membrane (Millipore, Burlington, MA, USA). The membranes were incubated overnight at + 4 °C with primary antibodies (Additional file 1: Table S4). Secondary antibody staining (1:5000) was performed for 1 h at RT with HRP-linked goat anti-mouse IgG #7076 or goat anti-rabbit IgG #7074 antibodies (Cell Signaling Technology, Beverly, MA, USA). For immunoprecipitation of Flag-tagged proteins, 0.2–1 mg of protein lysate was incubated with 10 μl of anti-Flag® M2 affinity agarose gel (#A2220, Sigma-Aldrich). After 1 h rotation at + 4 °C, the agarose gel was washed three times with the lysis buffer. Samples were prepared for Western blotting by adding of 2 × Laemmli Sample Buffer directly to the agarose gel and by heating the samples for 10 min at + 95 °C prior to gel loading. Chemiluminescence was detected by Bio-Rad Clarity or Clarity Max ECL Western Blotting Substrates. Results were visualised with the ChemiDoc™ MP Imaging System and analysed with Image Lab software Version 5.2.1 (Bio-Rad Laboratories, Inc., Hercules, CA, USA).

Nuclear/cytoplasmic fractionation

Nearly confluent cells (~ 80% confluence) were collected from 10 cm plates by scraping them into 1 ml aliquots of PBS. After 10 s centrifugation at 21,000 × g, supernatants were discarded and the pellets were lysed for 15 min in 500 μl of lysis buffer: 10 mM Tris–HCl, pH 7.5, 10 mM NaCl, 3 mM $MgCl_2$, 0.5% Nonidet P-40, 5 mM NaF, 1 mM PMSF and mini EDTA-free protease inhibitor tablet. After centrifugation at 500 × g for 5 min at + 4 °C, the supernatants contained the cytoplasmic compartments, while the nuclei were in the pellets. The pellets were washed three times with 500 μl lysis buffer and centrifuged each time at 500 × g for 5 min at + 4 °C, after which they were suspended in 200 μl of lysis buffer and sonicated for 30 s. After an additional centrifugation at 500 × g for 1 min, the supernatants were collected which contained nuclear fractions. The cytoplasm-containing solutions were centrifuged at 12,000 × g for 15 min at + 4 °C, after which the supernatant was collected. Laminin A/C and beta-tubulin were used as nuclear and

cytosolic markers, respectively, to evaluate fractionation efficiency.

In vitro kinase assays

The procedure for performing radioactive in vitro kinase assays has been described previously [36]. Briefly, 0.5–2.0 μg of PIM kinase and its substrate were used in each reaction. Samples were separated by SDS-PAGE and stained by Page Blue™ protein staining solution (#24620, Thermo Fisher Scientific). Additional in vitro kinase assays were performed similarly, but without radioactivity. Band intensities were quantitated by the Image Lab software Version 5.2.1 (Bio-Rad).

Fluorescence-lifetime imaging microscopy (FLIM)

FLIM was carried out as previously described [34] to probe for intracellular protein–protein interactions. Briefly, cells were plated on coverslips and transiently transfected with RFP- or GFP-tagged expression vectors. After 24 h, samples were fixed with 4% paraformaldehyde, washed with PBS and mounted with Mowiol. Samples were imaged by using the Lambert Instruments LIFA FLIM system with the Carl Zeiss AxioImager microscope and LI-FLIM software (Lambert Instruments BV, Groningen, The Netherlands). All imaging was performed at room temperature.

Proximity ligation assay (PLA)

Cell samples seeded on coverslips were fixed for 10 min with 4% paraformaldehyde, washed twice with PBS, permeabilised with 0.1% Triton X-100 in PBS for 10 min and then washed twice with PBS. Thereafter, the assays were continued using the Duolink® In Situ Detection Reagent kit (DUO9207, Sigma-Aldrich) according to manufacturer's instructions. Samples were imaged by the Nikon fluorescent microscope with NIS-Elements AR software (Nikon, Tokyo, Japan) and analysed by ImageJ/Fiji.

Chick chorioallantoic membrane (CAM) model

The chick embryo chorioallantoic membrane (CAM) model [37] was used for in vivo study of tumor development. PC3 and MCF7 cells ($0.5–2 \times 10^6$) were trypsinised from cell plates, washed with ice-cold PBS twice and mixed 1:1 with Matrigel (356,231; Corning™, NY, USA). A 20 μl aliquot of the solution was added onto each CAM of a fertilized chicken egg on embryonal development day 8 (EDD8). On EDD14, the tumors were excised and weighed immediately.

IncuCyte analysis

Cells were seeded in a 96-well plate at a density of 3500 cells per well. After an overnight incubation, they were treated with DMSO or DHPCC-9 and imaged every 2 h using the IncuCyte S3 Live-Cell Analysis System (Essen BioScience, Ltd., Newark, United Kingdom). Phase images were acquired and the percentage of confluence of the cell layers was analysed using the IncuCyte® Software (v2019B) Basic Analyzer module.

In silico analysis

The PhosphoSitePlus® database (https://phosphosite.org, Cell Signaling Technology, Inc., Danvers, MA, USA) was used to search for potential phosphorylation sites. IST Online™ (https://ist.medisapiens.com/) was used to generate gene expression data derived from patient samples.

Statistical analysis and figure preparation

Bar graphs or scatter plots were produced by GraphPad Prism 6.0 and results were analysed by Student's t-test. Significant differences ($p < 0.05$ and $p < 0.01$) were marked by * and **, respectively. Error bars represent standard deviations. Inkscape was used for figure preparation.

Results

PIM inhibition increases LKB1-dependent phosphorylation of AMPK

To investigate in more detail whether PIM kinases negatively regulate AMPK phosphorylation and activation, we used a pharmacological approach to inhibit PIM activity in PC3 prostate cancer, HeLa cervical cancer and MCF7 breast cancer cell lines. Cells were treated with either DMSO or 10 μM concentrations of two structurally distinct small molecule pan-PIM inhibitors, DHPCC9 or

(See figure on next page.)

Fig. 1 AMPK phosphorylation is enhanced by PIM inhibitors in an LKB1-dependent fashion. **a** PC3, Hela and MCF7 cells were treated for 24 h with DMSO (0.1%) or either DHPCC9 or AZD1208 pan-PIM inhibitor (10 μM in 0.1% DMSO) and subjected to Western blotting with antibodies against phospho-AMPK (Thr172), AMPK or LKB1. ACTB staining was used as a loading control. Shown in the graph are representative images together with graphs, where the relative levels of phosphorylated versus total AMPK were quantitated in comparison to DMSO-treated control samples (average values ± SD, n = 3). **b** Wild-type (WT) PC3 or MCF7 cells or their knock-out derivatives lacking LKB1 (LKB1KO) were treated for 24 h with DMSO or 10 μM DHPCC9, and subjected to Western blotting. Shown in the graphs are relative AMPK phosphorylation levels in comparison to DMSO-treated WT samples (average values ± SD, n = 3). **c** LKB1KO derivatives of PC3 or MCF7 cells were transiently transfected with FLAG or FLAG-LKB1 plasmids, treated for 24 h with DMSO or 10 μM DHPCC9, and subjected to Western blotting. Shown in the graphs are relative AMPK phosphorylation levels in comparison to DMSO-treated FLAG-transfected samples (average values ± SD, n = 3)

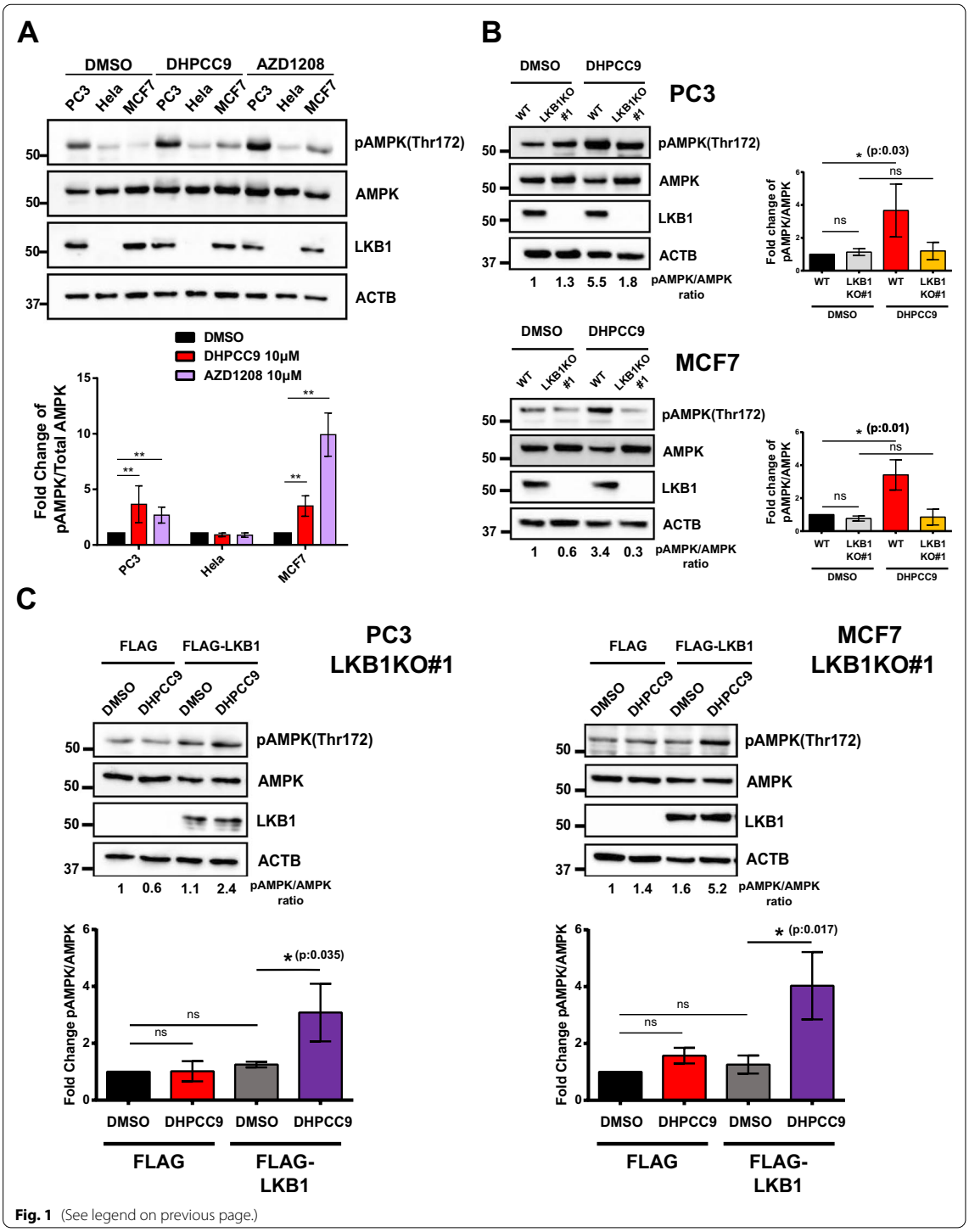

Fig. 1 (See legend on previous page.)

AZD1208, which inhibit the catalytic activity of all three PIM family members [33, 38]. The relative phosphorylation level of AMPK was determined 24 h later by Western blotting with antibodies against AMPK or its phosphorylated Thr172 residue. As shown in Fig. 1a, AMPK was expressed at a similar level in all three cell lines, but it was more prominently phosphorylated in PC3 cells than in the others. When PIM activity was inhibited by either DHPCC9 or AZD1208, AMPK phosphorylation was significantly enhanced in both PC3 and MCF7 cells, but not in HeLa cells. These results could be explained by the observed expression of the AMPK upstream kinase LKB1 in PC3 and MCF7 cells, but not in HeLa cells. Indeed, restoration of LKB1 expression in HeLa cells resulted in increased AMPK phosphorylation in response to treatment with DHPCC9 (Additional file 2: Figure S3). To further verify the role of LKB1 in PIM-mediated AMPK phosphorylation, we used the CRISPR/Cas9-based genomic editing technique to knock out LKB1 from both PC3 and MCF7 cells (Additional file 2: Figure S1A). As demonstrated by DNA gel electrophoresis (Additional file 2: Figure S2) and Western blotting (Fig. 1b), there was no LKB1 expression in the knock-out cells. When AMPK phosphorylation levels were analysed, no significant differences were observed between wild-type and LKB1-deficient cells that had been treated with DMSO (Fig. 1b). By contrast, treatment with the PIM inhibitor DHPCC9 induced a profound increase in AMPK phosphorylation in wild-type, but not knock-out cells. Furthermore, transient expression of FLAG-tagged LKB1 in LKB1-deficient PC3 or MCF7 cells restored the response to DHPCC9 (Fig. 1c). Altogether, these data indicate that LKB1 is necessary for the PIM inhibition-induced increase in AMPK phosphorylation.

AMPK phosphorylation levels are inversely correlated with PIM expression levels

In order to analyse the respective contribution of the different PIM family members in regulating AMPK phosphorylation and activity, we used the CRISPR/Cas9 technique to generate both individual and combined PIM knock-out cells (Additional file 2: Figure S1B-D). As confirmed by DNA gel electrophoresis (Additional file 2: Figure S2) and Western blotting (Fig. 2a), single (KO) as well as triple (TKO) knock-out lines were successfully produced from both PC3 and MCF7 cells. Lack of any single PIM protein did not result in notable changes in AMPK phosphorylation in either cell line (Fig. 2b). By contrast, significantly elevated levels of phosphorylation were observed in the two independent PC3 and MCF7 TKO cell clones (Fig. 2c), while transient expression of His-tagged PIM1 in these cells reduced AMPK phosphorylation back to its basal level (Fig. 2d). Furthermore, FDCP1 myeloid cells stably overexpressing PIM1 (FD/PIM1) exhibited significantly lower levels of AMPK phosphorylation than the corresponding control cells (FD/NEO) (Fig. 2e). Taken together, our data indicate that either pharmacological inactivation or knock-out of all three PIM family members results in increased AMPK phosphorylation.

As AMPK is activated upon nutrient deprivation, we wanted to determine whether this response is affected by lack of PIM or LKB1 proteins. Therefore, we cultivated PC3-derived WT, PIM TKO and LKB1 KO cells in glucose-free medium supplemented with different concentrations of glucose and then analysed AMPK phosphorylation levels. As compared to WT cells, AMPK was more phosphorylated in PIM TKO cells and less phosphorylated in LKB1 KO cells (Additional file 2: Figure S4). However, glucose deprivation increased AMPK phosphorylation in all cells, suggesting that under such conditions, other kinases in addition to LKB1 regulate AMPK activity.

LKB1 is a novel substrate for PIM kinases

As LKB1 was indispensable for the PIM inhibitor-induced phosphorylation of AMPK in both PC3 and MCF7 cells, this raised the question of whether PIM kinases downregulate LKB1 activity by directly phosphorylating it. To address this question, we subjected GST-tagged PIM family members, LKB1 or their combinations to radioactive in vitro kinase assays. Visualisation of ^{32}P-labeled phosphoproteins by autoradiography revealed that all three PIM kinases phosphorylate LKB1 in vitro, and that LKB1 does not undergo autophosphorylation (Fig. 3a). Thus, our data indicate that LKB1 indeed is a novel substrate targeted by all three PIM kinases. These data were further confirmed by a non-radioactive in vitro

(See figure on next page.)

Fig. 2 PIM expression levels inversely correlate with AMPK phosphorylation levels. PIM family members were knocked out in PC3 and MCF7 cells. **a** PIM expression levels in wild-type (WT) cells or their knock-out derivatives lacking individual (PIM1, PIM2, PIM3 KO) or all three (TKO) PIM kinases were examined by Western blotting. ACTB staining was used as a loading control. NS refers to non-specific staining observed with the PIM1 antibody. Phospho-AMPK (Thr172) versus AMPK levels were measured from WT cells in comparison to cells lacking individual **b** or all **c** PIM family members (average values ± SD, n = 3). **d** WT or TKO cells were transiently transfected with His or His-PIM1 plasmids, lysed 24 h later and subjected to Western blotting to determine relative AMPK phosphorylation levels (average values ± SD, n = 3). **e** Lysates of stably transfected FD/NEO and FD/PIM1 cell lines were subjected to Western blotting to determine relative AMPK phosphorylation levels

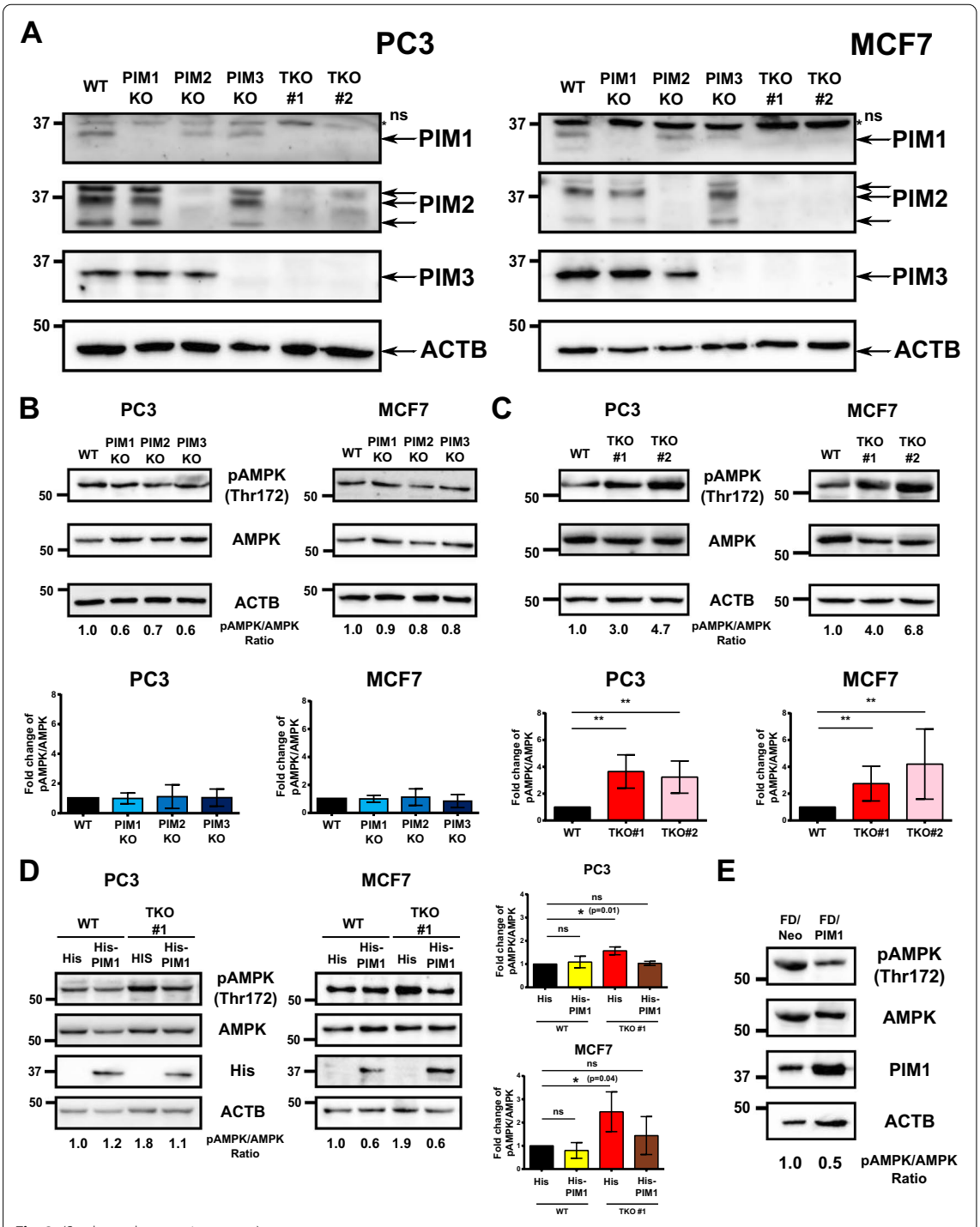

Fig. 2 (See legend on previous page.)

kinase assay (Fig. 3b), where phosphoproteins were visualised by Western blotting with the phospho-AKT substrate (PAS) antibody. This antibody recognises not only the AKT-targeted sequence RXXS/T, but also the PIM-targeted consensus sequence RXRHXS/T [39] (Fig. 3c).

For LKB1, multiple phosphorylation sites have been identified [40, 41]. However, only a few of them, including Ser334 and Ser428, resemble PIM target sites that can be recognised by the PAS antibody. To determine whether one or both of them are PIM target sites, we mutated them separately to alanine residues and subjected the mutant proteins to in vitro kinase assays. When His-tagged wild-type (WT) or mutant proteins were incubated in the presence of GST-PIM1, there was a 40% decrease in the intensity of the ^{32}P-labeled signal for the S334A mutant as compared to the WT protein, while no significant changes were observed for the S428A mutant (Fig. 3d), indicating that Ser334 is a prominent PIM target site. This was confirmed by non-radioactive in vitro kinase assays followed by Western blotting with the PAS antibody (Fig. 3e). However, as the S334A mutation did not completely remove the residual signals in either assay, it remains possible that PIM kinases target also other sites in LKB1.

Having established PIM proteins as upstream kinases of LKB1, we examined their intracellular interactions. In co-immunoprecipitation assays, His-tagged PIM1 could be captured by FLAG-tagged LKB1 from both cell lines (Fig. 3f). In fluorescence-lifetime imaging microscopy (FLIM) analysis, significantly reduced GFP lifetimes were observed when GFP-tagged LKB1 and RFP-tagged PIM1 were co-expressed in either MCF7 or PC3 cells (Fig. 3g). Furthermore, in a proximity ligation assay (PLA) with anti-PIM1 and anti-FLAG antibodies, we observed significantly more colocalisation dots in PC3 cells between endogenously expressed PIM1 and ectopically expressed FLAG-tagged LKB1 than between PIM1 and FLAG (Additional file 2: Figure S5). All these data suggest that PIM1 and LKB1 physically interact with each other in cells.

PIM kinases target Ser334 in LKB1 to regulate AMPK phosphorylation

To verify that PIM kinases phosphorylate LKB1 in cells, we transiently expressed FLAG-tagged LKB1 in both PC3 and MCF7 cells. At 24 h after transfection, cells were treated with DMSO or 10 μM DHPCC9 for another 24 h, after which cells were lysed, FLAG-LKB1 proteins were pulled down with the FLAG antibody and their phosphorylation levels were analysed by Western blotting with the PAS antibody. As shown in Fig. 4a, the relative phosphorylation levels of LKB1 were significantly reduced by PIM inhibition in both types of cells. In addition to the pharmacological approach, we analysed LKB1 phosphorylation in WT and TKO MCF7 cells transiently expressing either FLAG-tagged LKB1 or the corresponding S334A mutant. In line with our data on PIM inhibition, LKB1 phosphorylation was dramatically decreased in TKO cells lacking all three PIM kinases (Fig. 4b). Notably, there was no significant difference between the phosphorylation level of the S334A mutant in WT and TKO cells, suggesting that Ser334 is a prominent PIM target site in LKB1.

To explore the impact of Ser334 phosphorylation of LKB1 on AMPK phosphorylation, FLAG-tagged LKB1 or the corresponding S334A mutant were transiently expressed in LKB1 KO derivatives of PC3 and MCF7 cells, and the cells were treated with either DMSO or 10 μM DHPCC9. As expected, DHPCC9 treatment did not trigger any considerable increase in AMPK phosphorylation in either type of FLAG-transfected cells lacking LKB1 (Fig. 4c). By contrast, reintroduction of WT LKB1, but not the phosphorylation-deficient S334A mutant restored the response of cells to DHPCC-9, resulting in a significant increase in AMPK phosphorylation. These data suggest that phosphorylation of LKB1 at Ser334 is involved in the regulation of AMPK phosphorylation by PIM kinases and their inhibitors.

AKT has been reported to phosphorylate LKB1 at Ser334, resulting in its nuclear sequestration by the 14–3–3 protein [42]. To determine whether

(See figure on next page.)

Fig. 3 PIM kinases phosphorylate LKB1 in vitro and LKB1 interacts with PIM1 in cells. **a** Radioactive in vitro kinase assays were performed by incubating GST, GST-PIMs and/or GST-LKB1 in the presence of ^{32}P-ATP. Phosphorylation signals were analysed by autoradiography (upper panel), while protein loading was visualised by Page Blue staining (lower panel). Shown is a representative image out of two repeated experiments. **b** Similar non-radioactive in vitro kinase assays were analysed by Western blotting with phospho-AKT substrate (PAS) antibody (upper panel), while protein loading was visualised by stain-free technology (lower panel). **c** Shown are the PIM kinase consensus phosphorylation motif, the PAS antibody recognition site, and the LKB1 sequences around residues Ser334 and Ser428. **d** Radioactive in vitro kinase assays (n = 2) were performed by incubating GST-PIM1 with His-tagged wild-type (WT) or mutant (S334A or S428A) LKB1. **e** Similar non-radioactive in vitro kinase assays (n = 2) were performed using GST-tagged PIM1 and LKB1 (WT or S334A) proteins. **f** MCF7 and PC3 cells were transiently transfected with FLAG-tagged LKB1 and His or His-tagged PIM1 plasmids. After 24 h, 10% of cell lysates were stained with FLAG antibody (input), while the rest was immunoprecipitated with FLAG M2 affinity gel and stained with His antibody (IP: FLAG). **g** MCF7 and PC3 cells were transiently transfected with GFP, GFP-tagged LKB1, RFP and/or RFP-tagged PIM1 plasmids. After 24 h, cells were fixed and analysed by fluorescence-lifetime imaging microscopy (FLIM). Shown are representative FLIM images as well as graphs (average value ± SD), where numbers of counted cells have been indicated

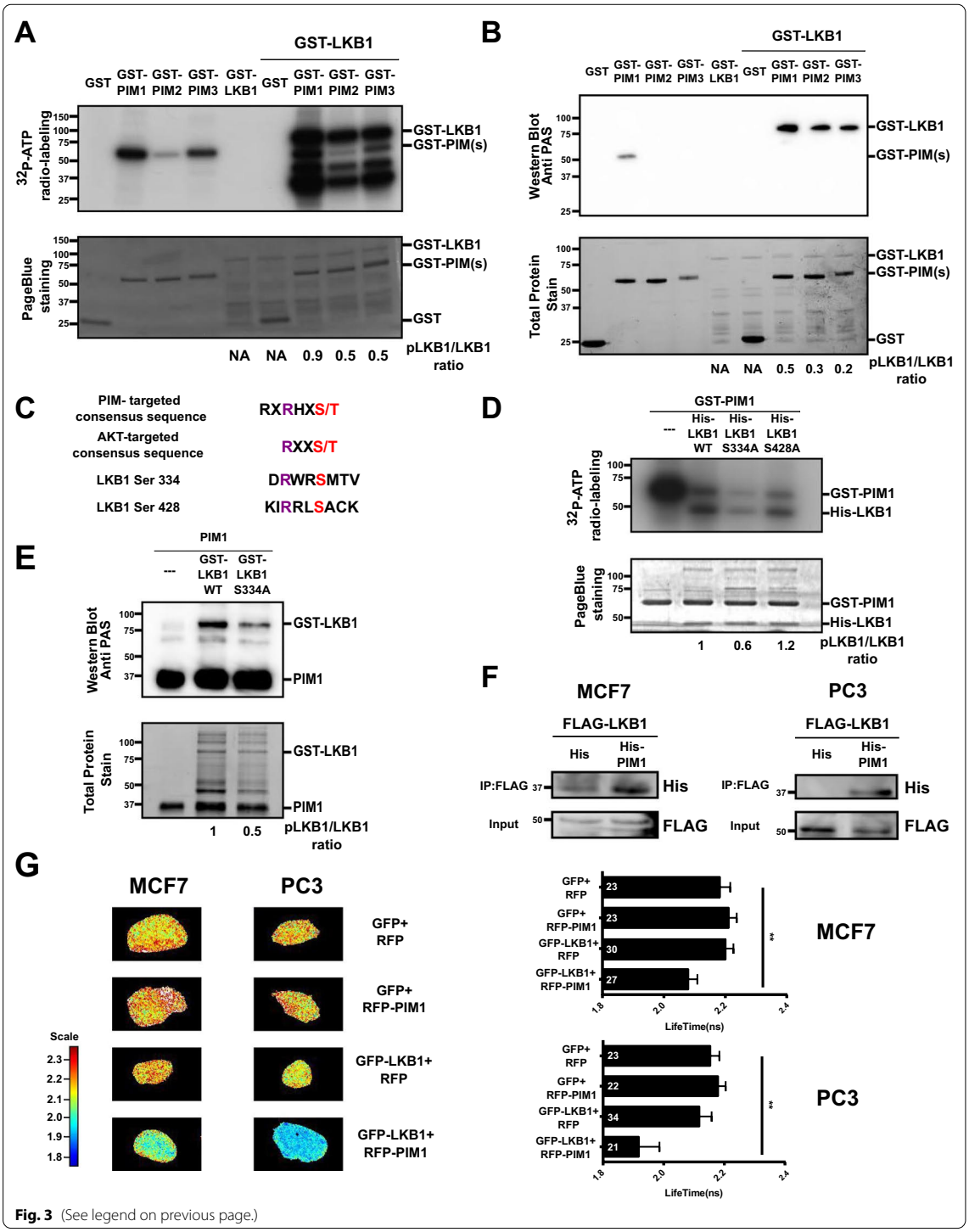

Fig. 3 (See legend on previous page.)

PIM-dependent phosphorylation of this site has similar consequences in PC3 or MCF7 cells, we fractionated LKB1KO cells transiently expressing FLAG-tagged WT LKB1 or the phosphodeficient S334A mutant. According to our analyses, both WT and mutant proteins were mainly localised in the nuclear fractions of both PC3 and MCF7 derivatives (Additional file 2: Figure S6A). By contrast, the endogenous LKB1 in parental cells was mostly localised in the cytosolic fractions, and this was not influenced by pharmacological PIM inhibition (Additional file 2: Figure S6B) or by knocking out of all three PIM kinase members (Additional file 2: Figure S6C). However, the level of AMPK phosphorylation in the cytoplasmic fraction was increased in both cases. To confirm that there is no compensatory activation of AKT in the PIM TKO cells, we analysed AKT Ser473 phosphorylation levels from them, but did not observe any major changes as compared to WT cells (Additional file 2: Figure S6D).

Combined knock-out of LKB1 and PIM kinases impairs cell proliferation and tumor growth

We next performed an in silico analysis of mRNA expression levels in patient-derived samples and observed that in prostate carcinomas and certain breast carcinomas, *PIM* expression was elevated and *LKB1/STK11* expression was reduced (Additional file 2: Figure S7). However, in the breast medullary carcinoma dataset, both *PIM* and *LKB1* expression levels were highly upregulated. As LKB1 expression and LKB1-dependent AMPK activation are often associated with cell growth suppression [43], this prompted us to evaluate the proliferation rates for WT PC3 or MCF7 cells or their LKB1-deficient derivatives in response to treatment with DMSO or 10 μM DHPCC9. Proliferation was followed for 5 days by measuring cell confluence with the IncuCyte live cell imaging system, where the two independent LKB1 KO clones behaved similarly to the WT cells (Fig. 5a). All the DMSO-treated cells proliferated well with sigmoidal growth curves, while the DHPCC9 treatment retarded cell growth.

The proliferation rates of TKO cells lacking all PIM kinases were reduced (Fig. 5b), which was in line with what we observed following the DHPCC9 treatment of WT cells. Surprisingly, cells lacking both LKB1 and PIM kinases (TKOLKB1 KO) grew even slower than TKO clones. As shown in Fig. 5c, increased AMPK phosphorylation levels in TKO clones correlated well with their slower proliferation rates as compared to their WT counterparts. On the other hand, due to the absence of LKB1, the phosphorylation levels of AMPK in TKOLKB1 KO clones were lower than in TKO clones, yet the proliferation rates of TKOLKB1 KO clones were slower. These data suggest that under the conditions of PIM inhibition, changes in AMPK phosphorylation levels are not directly connected to the proliferation properties of LKB1 KO cells.

We next employed the chick embryo chorioallantoic membrane (CAM) xenograft model [37] to investigate the in vivo behaviour of the knock-out cells lacking both PIM and LKB1. WT MCF7 and PC3 cells or their KO and/or TKO derivatives were implanted onto the CAM of eggs on day 7 of incubation to allow the development of tumors. On day 14, tumors were excised from the CAM and weighed. Interestingly, there was a significant increase in the mass of tumors derived from LKB1 KO clones in PC3 but not MCF7 cells (Fig. 5d), but there was no significant difference between WT and TKO clones in either cell type. However, the mass of TKOLKB1KO MCF7 tumor cells was significantly lower than that of WT or LKB1KO samples. Intriguingly, while loss of LKB1 alone in PC3 cells increased tumor load, this effect was abolished, when combined with the loss of PIM kinases. Conversely, transient over-expression of PIM1 triggered further increases in tumor mass in two independent PC3 LKB1KO clone xenografts but not in WT samples (Fig. 5e). These data indicate that LKB1 and PIM kinases cooperate in the regulation of tumorigenic growth.

Discussion

To our knowledge, this is the first report combining both pharmacological and CRISPR/Cas9-based genomic editing approaches to show that inhibition of the expression or activity of all three PIM kinases activates AMPK in cancer cells via LKB1-dependent phosphorylation at Thr172. Notably, knocking out of any particular PIM family member is not sufficient to trigger AMPK activation, reflecting the previously observed functional redundancy

(See figure on next page.)

Fig. 4 Ser334 is a PIM target site in LKB1 and is essential for increased AMPK phosphorylation in response to PIM inhibition. **a** PC3 and MCF7 cells were transiently transfected with the FLAG-LKB1 plasmid. After 24 h, cells were treated with either DMSO or 10 μM DHPCC9 for another 24 h. 10% of cell lysates were stained with FLAG antibody (Input), while the rest was immunoprecipitated with FLAG M2 affinity gel and stained with PAS antibody (IP:FLAG). Shown are representative images as well as graphs with relative differences in phosphorylation levels of LKB1 as compared to the DMSO-treated control samples (average values ± SD, n = 3). **b** MCF7 WT and TKO cells were transiently transfected with WT or S334A FLAG-LKB1 plasmids. After 48 h, relative phosphorylation levels of LKB1 were determined (average values ± SD, n = 3). **c** LKB1 KO derivatives of PC3 and MCF7 cells were transiently transfected with FLAG or FLAG-LKB1 (WT or S334A) plasmids. After 24 h, cells were treated with either DMSO or 10 μM DHPCC9 for another 24 h before Western blotting with pAMPK (Thr172), AMPK and LKB1 antibodies. Shown are representative images as well as graphs with relative phosphorylation levels of AMPK as compared to DMSO-treated control samples (average values ± SD, n = 3)

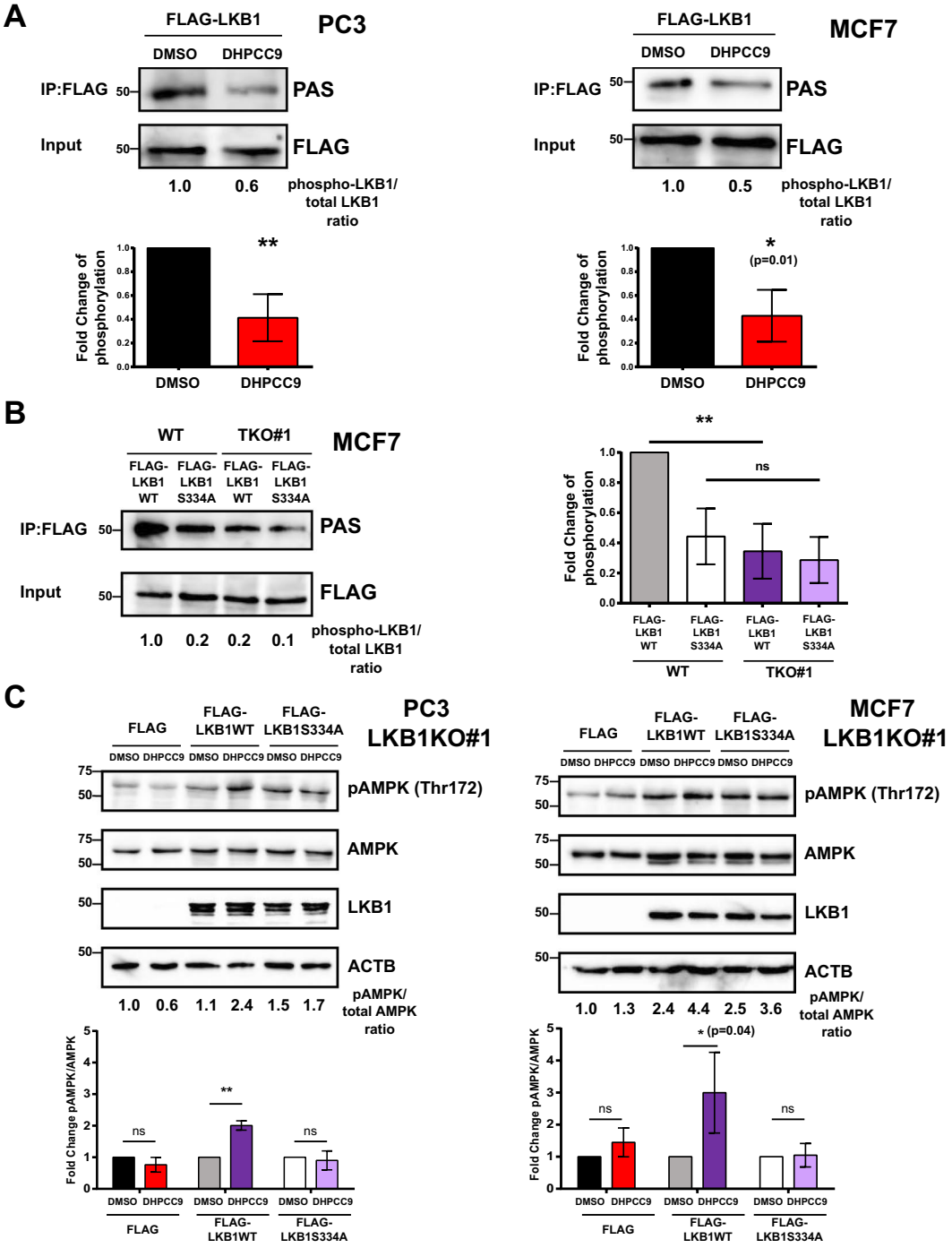

Fig. 4 (See legend on previous page.)

of PIM kinases and the fact that all three PIM kinases are capable of phosphorylating LKB1 and thereby inhibiting its ability to phosphorylate AMPK. Besides demonstrating that PIM kinases are upstream regulators of LKB1, we have also identified Ser334 as the major, although possibly not the sole PIM target site in LKB1.

In MDA-MB-231 breast cancer cells, phosphorylation of LKB1 at Ser334 by AKT has been reported to block the tumor suppressor activity of overexpressed LKB1 via nuclear sequestration by the 14–3–3 protein [42]. However, there may be cell type-specific differences in the subcellular localisation of LKB1. While endogenously expressed LKB1 protein is exclusively localised in the nucleus of non-transformed IMR90 fibroblasts, it is predominantly located in the plasma membrane of polarised epithelial MDCK cells [43]. According to our fractionation data, overexpressed LKB1 and its S334A phospho-deficient mutant derivative are both mostly found in the nuclear fractions of PC3 and MCF7 LKB1KO cells, while the endogenously expressed LKB1 protein of the parental cells resides in the cytoplasm, irrespective of whether PIM expression or activity is inhibited. These discrepancies in the cellular compartmentalisation between endogenous and ectopically expressed proteins warrants the usage of knock-in mutant cell lines to properly examine the physiological consequences of LKB1 phosphorylation.

It is not surprising that both PIM and AKT kinases target LKB1, as they also share several other substrates [2, 3]. For example, both PIM and AKT protect cells from apoptosis by phosphorylating the pro-apoptotic BAD protein, albeit at different but proximate sites [44, 45]. In addition, both PIM and AKT promote mTOR- and cap-dependent protein synthesis by phosphorylating the AKT1S1 and EIF4EBP1 translational inhibitors [2, 3]. However, these kinases also have cell type-specific non-redundant roles, as we did not detect any compensatory increase in AKT activity in PC3 or MCF7 PIM TKO cells.

In terms of cell proliferation and tumor growth, the tumor-suppressive effects of LKB1 could be readily seen in the chick embryo CAM xenograft experiments, but not in the two-dimensional cell proliferation assays. Similar discrepancies with respect to the effects of LKB1 between in vitro and in vivo models have also recently been demonstrated [46]. Co-deletion of PTEN and LKB1 from prostate cancer cells results in aggressive tumors and lung metastases, while deletion of LKB1 alone has no such effect. This finding is in line with our CAM data, in which knocking out LKB1 elicited a robust increase in tumor mass in PTEN-deficient PC3 cells, but not in PTEN-expressing MCF7 cells. In PC3 cells, the resulting oncogenic insult could be either suppressed by knocking out all three PIM kinase members or exacerbated by upregulating PIM1 expression, highlighting the integral role of PIM kinases in supporting tumor growth in this setting. Notably, the combined PIM and LKB1 knock-out slowed the rate of cell proliferation and tumor growth as compared to the LKB1 knock-out alone, but without considerable changes in AMPK phosphorylation levels. Even though a decrease in AMPK activity is conventionally associated with the enhanced growth of tumors lacking LKB1, this idea has recently been challenged by findings in K-Ras-driven models of non-small-cell lung carcinoma which indicated that loss of LKB1 and AMPK suppresses tumorigenesis [47]. In addition, emerging data have revealed that loss of salt-inducible kinases (SIKs), which are less-well studied LKB1 downstream targets, accounts for a significant proportion of the transcriptional changes and histological features of LKB1-deficient tumors [48, 49]. Further studies are therefore needed to determine whether PIM kinases share signaling pathways with SIKs in affecting the growth of LKB1-deficient tumors as well as whether PIM inhibition can suppress the aggressive metastatic behaviour observed in tumors lacking both PTEN and LKB1.

Conclusions

Catabolic events invoked by the LKB1/AMPK signalling pathway are expected to antagonise the oncogenicity of PIM kinases. Our novel finding that PIM kinases

(See figure on next page.)

Fig. 5 Lack of both LKB1 and PIM kinases impairs cell proliferation and tumor growth**. a** WT PC3 or MCF7 cells or their LKB1-deficient KO derivatives were grown overnight on 96-well plates, after which they were treated with DMSO or 10 μM DHPCC9, and their proliferation was followed for 5 days using the IncuCyte live cell imaging system. Shown are average percentages of confluence at indicated time-points (± SD of a representative experiment, n = 3). **b** Proliferation assays were performed with WT PC3 or MCF7 cells or their KO or TKO derivatives lacking LKB1 and/or all PIM kinases, respectively (n = 3). **c** Phospho-AMPK (Thr172) versus AMPK levels were measured from WT cells in comparison to cells lacking all PIM family members or LKB1 or both PIM and LKB1 in PC3 and MCF7 cells (average values ± SD, n = 3). **d** WT PC3 and MCF7 cells or their KO and/or TKO derivatives were grown for 7 days on the chorioallantoic membranes (CAM) of chick embryos. Shown are scatter plots of tumor mass at the end of the experiment. Numbers of the samples are listed at the bottom of the graphs. **e** PC3 cells and their LKB1KO derivatives were transiently transfected with His or His-PIM1 plasmids for 48 h before being grown for 7 days on CAM. Parts of the xenograft samples were subjected to Western blotting to examine PIM1 and LKB1 expression levels. Shown are scatter plots of tumor mass at the end of the experiment. Numbers of the samples are listed at the bottom of the graphs

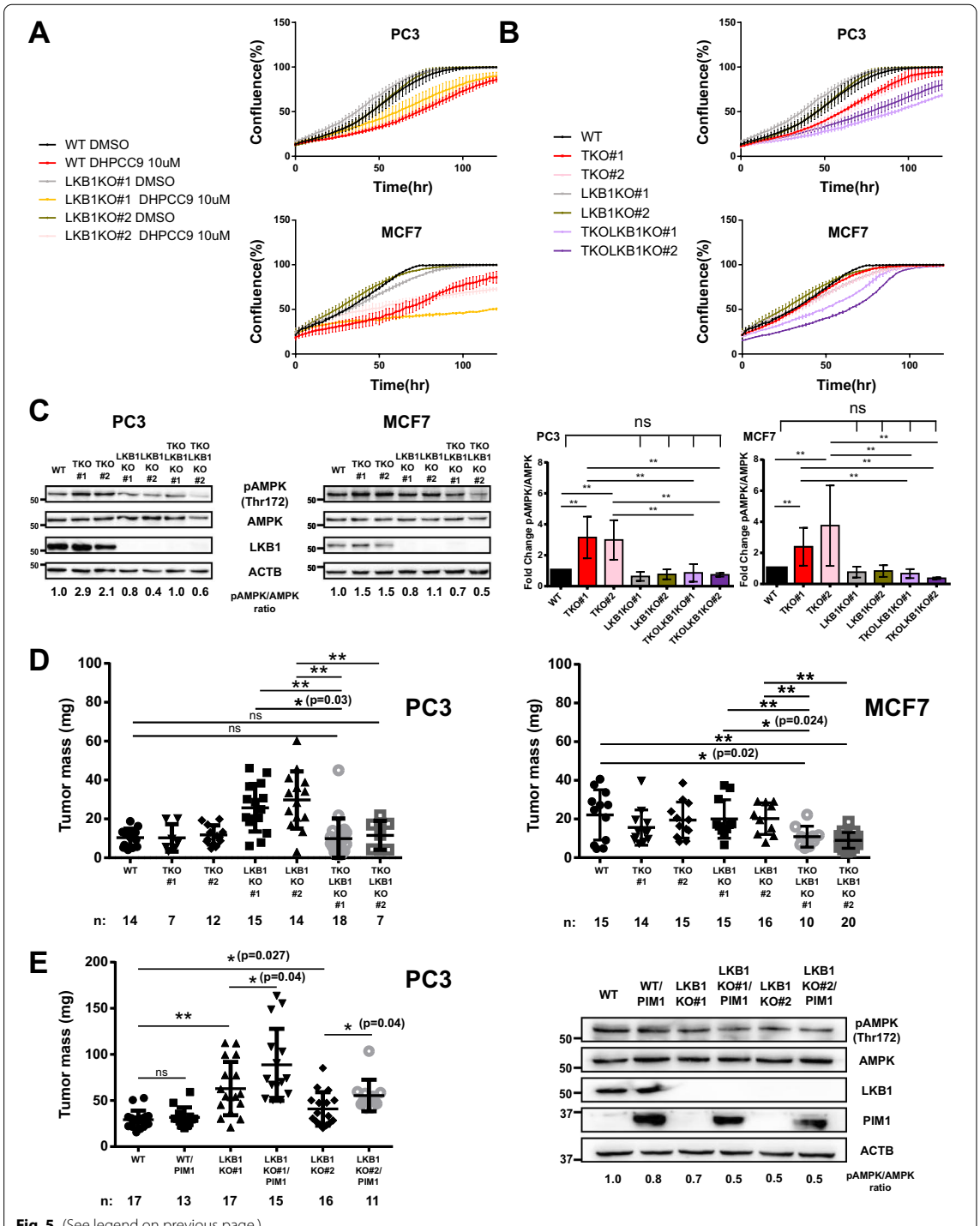

Fig. 5 (See legend on previous page.)

act as upstream regulators of LKB1 uncovers a molecular pathway that allows the tumor-suppressive function of LKB1 and the oncogenic functions of PIM kinases to be tightly and precisely controlled. Inactivation of both PIM kinases and LKB1 results in a significant decrease in cell proliferation in vitro and tumor growth in vivo, suggesting that PIM-targeted pharmaceutical interventions could be exploited to suppress the growth of LKB1-deficient tumors.

Abbreviations

AMPK: AMP-activated protein kinase; CAM: chorioallantoic membrane; FLIM: fluorescence-lifetime imaging microscopy; PLA: proximity ligation assay; KO: knock-out; LKB1: liver kinase B1; PAS: phosphorylated AKT substrate; SA: serine (S) to alanine (A) phosphomutant; TKO: triple knock-out; WT: wild-type.

Supplementary Information

The online version contains supplementary material available at https://doi.org/10.1186/s12964-021-00749-4.

Additional file 1: Table S1. Primers for mutagenesis. **Table S2**. CRISPR sgRNA sequences. **Table S3**. Primers for verification of CRISPR knock-out clones. **Table S4**. Antibodies.

Additional file 2: Figure S1 Schematic diagram for the strategies of CRISPR/Cas9 design and verification. **Figure S2**. DNA gel electrophoresis results for wild-type and knock-out clones. **Figure S3**. LKB1 is needed for PIM-dependent regulation of AMPK phosphorylation. **Figure S4**. Glucose deprivation increases AMPK phosphorylation in an LKB1-independent fashion. **Figure S5**. Proximity ligation assay (PLA) to demonstrate the physical interactions between PIM1 and LKB1. **Figure S6**. Analyses of LKB1 subcellular localisation and AKT phosphorylation levels. **Figure S7**. Expression of PIM family members and LKB1(STK11) in distinct types of breast or prostate cancer.

Acknowledgements

We thank P. Moreau (University of Clermont Auvergne, France) for DHPCC9, Genome Biology Unit core facility (HiLIFE Helsinki Institute of Life Science, Biocenter Finland) for preparation of expression vectors**,** S. K. J. Landor and K. L. Lin (Åbo Akademi University) for technical advice and assistance on CAM experiments, C. Sahlgren (Åbo Akademi University) for helpful discussions, and the Biocenter Finland core facilities of Turku Bioscience for assistance in microscopy (Cell Imaging and Cytometry Core with J. Sandholm).

Authors' contributions

The study was mainly designed and written by KLM and PJK. Experiments were mainly performed by KLM, but with help from WBE, NMS and ARM. All authors have read and approved the manuscript.

Funding

This study was financially supported by the Academy of Finland grant 287040 and the Turku University Foundation to PJK. and by the Drug Research Doctoral Programme of the University of Turku and the Maud Kuistila Foundation to KLM and WBE. The funding bodies had no influence on the design or execution of the studies or on the preparation of the manuscript.

Availability of data and materials

PhosphoSitePlus® database (https://phosphosite.org) and IST Online™ database (https://ist.medisapiens.com) were used for in silico analyses.

Declarations

Ethics approval and consent to participate

Not applicable (study does not contain such animal experimentation that would require an ethical permit).

Consent for publication

Not applicable (study does not contain any individual person's data).

Competing interests

No potential competing interest.

Author details

[1]Department of Biology, University of Turku, Vesilinnantie 5, 20500 Turku, Finland. [2]Faculty of Science and Engineering/Cell Biology, Åbo Akademi University, Turku, Finland. [3]Present Address: Department of Biochemistry and Molecular Biology, Medical University of Lublin, Lublin, Poland.

Received: 14 January 2021 Accepted: 14 May 2021
Published online: 30 June 2021

References

1. Nawijn MC, Alendar A, Berns A. For better or for worse: the role of Pim oncogenes in tumorigenesis. Nat Rev Cancer. 2011;11:23–34. https://doi.org/10.1038/nrc2986.
2. Warfel NA, Kraft AS. PIM kinase (and Akt) biology and signaling in tumors. Pharmacol Ther. 2015;151:41–9. https://doi.org/10.1016/j.pharmthera.2015.03.001.
3. Santio NM, Koskinen PJ. PIM kinases: from survival factors to regulators of cell motility. Int J Biochem Cell Biol. 2017;93:74–85. https://doi.org/10.1016/j.biocel.2017.10.016.
4. Qian KC, Wang L, Hickey ER, Studts J, Barringer K, Peng C, et al. Structural basis of constitutive activity and a unique nucleotide binding mode of human Pim-1 kinase. J Biol Chem. 2005;280:6130–7. https://doi.org/10.1074/jbc.M409123200.
5. Santio NM, Vainio V, Hoikkala T, Mung KL, Lång M, Vahakoski R, et al. PIM1 accelerates prostate cancer cell motility by phosphorylating actin capping proteins. Cell Commun Signal. 2020;18:121. https://doi.org/10.1186/s12964-020-00618-6.
6. Mikkers H, Nawijn M, Allen J, Brouwers C, Verhoeven E, Jonkers J, et al. Mice deficient for all PIM kinases display reduced body size and impaired responses to hematopoietic growth factors. Mol Cell Biol. 2004;24:6104–15. https://doi.org/10.1128/MCB.24.13.6104-6115.2004.
7. Rainio EM, Sandholm J, Koskinen PJ. Cutting edge: transcriptional activity of NFATc1 is enhanced by the Pim-1 kinase. J Immunol. 2002;168:1524–7. https://doi.org/10.4049/jimmunol.168.4.1524.
8. Song JH, An N, Chatterjee S, Kistner-Griffin E, Mahajan S, Mehrotra S, et al. Deletion of Pim kinases elevates the cellular levels of reactive oxygen species and sensitizes to K-Ras-induced cell killing. Oncogene. 2015;34:3728–36. https://doi.org/10.1038/onc.2014.306.
9. Sanchez-Cespedes M. A role for LKB1 gene in human cancer beyond the Peutz–Jeghers syndrome. Oncogene. 2007;26:7825–32. https://doi.org/10.1038/sj.onc.1210594.
10. Hemminki A, Markie D, Tomlinson I, Avizienyte E, Roth S, Loukola A, et al. A serine/threonine kinase gene defective in Peutz–Jeghers syndrome. Nature. 1998;391:184–7. https://doi.org/10.1038/34432.
11. Sanchez-Cespedes M, Parrella P, Esteller M, Nomoto S, Trink B, Engles JM, et al. Inactivation of LKB1/STK11 is a common event in adenocarcinomas of the lung. Cancer Res. 2002;62:3659–62.
12. Zhong D, Guo L, de Aguirre I, Liu X, Lamb N, Sun SY, et al. LKB1 mutation in large cell carcinoma of the lung. Lung Cancer. 2006;53:285–94. https://doi.org/10.1016/j.lungcan.2006.05.018.
13. Matsumoto S, Iwakawa R, Takahashi K, Kohno T, Nakanishi Y, Matsuno Y, et al. Prevalence and specificity of LKB1 genetic alterations in lung cancers. Oncogene. 2007;26:5911–8. https://doi.org/10.1038/sj.onc.1210418.

14. Avizienyte E, Loukola A, Roth S, Hemminki A, Tarkkanen M, Salovaara R, et al. LKB1 somatic mutations in sporadic tumors. Am J Pathol. 1999;154:677–81. https://doi.org/10.1016/S0002-9440(10)65314-X.
15. Guldberg P, Straten PT, Ahrenkiel V, Seremet T, Kirkin AF, Zeuthen J. Somatic mutation of the Peutz–Jeghers syndrome gene, LKB1/STK11, in malignant melanoma. Oncogene. 1999;18:1777–80. https://doi.org/10.1038/sj.onc.1202486.
16. Su GH, Hruban RH, Bansal RK, Bova GS, Tang DJ, Shekher MC, et al. Germline and somatic mutations of the STK11/LKB1 Peutz–Jeghers gene in pancreatic and biliary cancers. Am J Pathol. 1999;154:1835–40. https://doi.org/10.1016/S0002-9440(10)65440-5.
17. Wingo SN, Gallardo TD, Akbay EA, Liang MC, Contreras CM, Boren T, et al. Somatic LKB1 mutations promote cervical cancer progression. PLoS ONE. 2009;4:e5137. https://doi.org/10.1371/journal.pone.0005137.
18. Kuragaki C, Enomoto T, Ueno Y, Sun H, Fujita M, Nakashima R, et al. Mutations in the STK11 gene characterize minimal deviation adenocarcinoma of the uterine cervix. Lab Invest. 2003;83:35–45. https://doi.org/10.1097/01.LAB.0000049821.16698.D0.
19. Ding L, Getz G, Wheeler DA, Mardis ER, McLellan MD, Cibulskis K, et al. Somatic mutations affect key pathways in lung adenocarcinoma. Nature. 2008;455:1069–75. https://doi.org/10.1038/nature07423.
20. Hong SP, Leiper FC, Woods A, Carling D, Carlson M. Activation of yeast Snf1 and mammalian AMP-activated protein kinase by upstream kinases. Proc Natl Acad of Sci USA. 2003;100:8839–43. https://doi.org/10.1073/pnas.1533136100.
21. Woods A, Johnstone SR, Dickerson K, Leiper FC, Fryer LGD, Neumann D, et al. LKB1 is the upstream kinase in the AMP-activated protein kinase cascade. Current Biol. 2003;13:2004–8. https://doi.org/10.1016/j.cub.2003.10.031.
22. Hawley SA, Boudeau J, Reid JL, Mustard KJ, Udd L, Mäkelä TP, et al. Complexes between the LKB1 tumor suppressor, STRADα/β and MO25α/β are upstream kinases in the AMP-activated protein kinase cascade. J Biol. 2003;2:28. https://doi.org/10.1186/1475-4924-2-28.
23. Lizcano JM, Göransson O, Toth R, Deak M, Morrice NA, Boudeau J, et al. LKB1 is a master kinase that activates 13 kinases of the AMPK subfamily, including MARK/PAR-1. EMBO J. 2004;23:833–43. https://doi.org/10.1038/sj.emboj.7600110.
24. Hardie DG, Ross FA, Hawley SA. AMPK: a nutrient and energy sensor that maintains energy homeostasis. Nat Rev Mol Cell Biol. 2012;13:251–62. https://doi.org/10.1038/nrm3311.
25. Hawley SA, Davison M, Woods A, Davies SP, Beri RK, Carling D, et al. Characterization of the AMP-activated protein kinase kinase from rat liver and identification of threonine 172 as the major site at which it phosphorylates AMP-activated protein kinase. J Biol Chem. 1996;271:27879–87. https://doi.org/10.1074/jbc.271.44.27879.
26. Suter M, Riek U, Tuerk R, Schlattner U, Wallimann T, Neumann D. Dissecting the role of 5′-AMP for allosteric stimulation, activation, and deactivation of AMP-activated protein kinase. J Biol Chem. 2006;281:32207–16. https://doi.org/10.1074/jbc.M606357200.
27. Garcia D, Shaw RJ. AMPK: Mechanisms of cellular energy sensing and restoration of metabolic balance. Mol Cell. 2017;66:789–800. https://doi.org/10.1016/j.molcel.2017.05.032.
28. Shackelford DB, Abt E, Gerken L, Vasquez DS, Seki A, Leblanc M, et al. LKB1 inactivation dictates therapeutic response of non-small cell lung cancer to the metabolism drug phenformin. Cancer Cell. 2013;23:143–58. https://doi.org/10.1016/j.ccr.2012.12.008.
29. Shaw RJ, Kosmatka M, Bardeesy N, Hurley RL, Witters LA, DePinho RA, et al. The tumor suppressor LKB1 kinase directly activates AMP-activated kinase and regulates apoptosis in response to energy stress. Proc Natl Acad of Sci USA. 2004;101:3329–35. https://doi.org/10.1073/pnas.0308061100.
30. Beharry Z, Mahajan S, Zemskova M, Lin Y-W, Tholanikunnel BG, Xia Z, et al. The Pim protein kinases regulate energy metabolism and cell growth. Proc Natl Acad of Sci USA. 2011;108:528–33. https://doi.org/10.1073/pnas.1013214108.
31. Lilly M, Sandholm J, Cooper JJ, Koskinen PJ, Kraft A. The PIM-1 serine kinase prolongs survival and inhibits apoptosis-related mitochondrial dysfunction in part through a *bcl-2*-dependent pathway. Oncogene. 1999;18:4022–31. https://doi.org/10.1038/sj.onc.1202741.
32. Akué-Gédu R, Rossignol E, Azzaro S, Knapp S, Filippakopoulos P, Bullock AN, et al. Synthesis, kinase inhibitory potencies, and in vitro antiproliferative evaluation of new pim kinase inhibitors. J Med Chem. 2009;52:6369–81. https://doi.org/10.1021/jm901018f.
33. Santio NM, Vahakoski RL, Rainio E-M, Sandholm JA, Virtanen SS, Prudhomme M, et al. Pim-selective inhibitor DHPCC-9 reveals Pim kinases as potent stimulators of cancer cell migration and invasion. Mol Cancer. 2010;9:279. https://doi.org/10.1186/1476-4598-9-279.
34. Santio NM, Landor SK-J, Vahtera L, Ylä-Pelto J, Paloniemi E, Imanishi SY, et al. Phosphorylation of Notch1 by Pim kinases promotes oncogenic signaling in breast and prostate cancer cells. Oncotarget. 2016;7:43220–38. https://doi.org/10.18632/oncotarget.9215.
35. Ran FA, Hsu PD, Wright J, Agarwala V, Scott DA, Zhang F. Genome engineering using the CRISPR-Cas9 system. Nat Protoc. 2013;8:2281–308. https://doi.org/10.1038/nprot.2013.143.
36. Kiriazis A, Vahakoski RL, Santio NM, Arnaudova R, Eerola SK, Rainio EM, et al. Tricyclic benzo[cd]azulenes selectively inhibit activities of Pim kinases and restrict growth of Epstein-Barr virus-transformed cells. PLoS ONE. 2013;8:e55409. https://doi.org/10.1371/journal.pone.0055409.
37. Deryugina EI, Quigley JP. Chick embryo chorioallantoic membrane model systems to study and visualize human tumor cell metastasis. Histochem Cell Biol. 2008;130:1119–30. https://doi.org/10.1007/s00418-008-0536-2.
38. Keeton EK, McEachern K, Dillman KS, Palakurthi S, Cao Y, Grondine MR, et al. AZD1208, a potent and selective pan-Pim kinase inhibitor, demonstrates efficacy in preclinical models of acute myeloid leukemia. Blood. 2014;123:905–13. https://doi.org/10.1182/blood-2013-04-495366.
39. Peng C, Knebel A, Morrice NA, Li X, Barringer K, Li J, et al. Pim kinase substrate identification and specificity. J Biochem. 2007;141:353–62. https://doi.org/10.1093/jb/mvm040.
40. Alessi DR, Sakamoto K, Bayascas JR. LKB1-dependent signaling pathways. Annu Rev Biochem. 2006;75:137–63. https://doi.org/10.1146/annurev.biochem.75.103004.142702.
41. Hornbeck PV, Zhang B, Murray B, Kornhauser JM, Latham V, Skrzypek E. PhosphoSitePlus, 2014: mutations, PTMs and recalibrations. Nucleic Acids Res. 2015;43:D512–20. https://doi.org/10.1093/nar/gku1267.
42. Liu L, Siu FM, Che CM, Xu A, Wang Y. Akt blocks the tumor suppressor activity of LKB1 by promoting phosphorylation-dependent nuclear retention through 14-3-3 proteins. Am J Transl Res. 2012;4:175–86.
43. Dogliotti G, Kullmann L, Dhumale P, Thiele C, Panichkina O, Mendl G, et al. Membrane-binding and activation of LKB1 by phosphatidic acid is essential for development and tumour suppression. Nat Commun. 2017;8:1–12. https://doi.org/10.1038/ncomms15747.
44. del Peso L, González-García M, Page C, Herrera R, Nuñez G. Interleukin-3-induced phosphorylation of BAD through the protein kinase Akt. Science. 1997;278:687–9. https://doi.org/10.1126/science.278.5338.687.
45. Aho TLT, Sandholm J, Peltola KJ, Mankonen HP, Lilly M, Koskinen PJ. Pim-1 kinase promotes inactivation of the pro-apoptotic Bad protein by phosphorylating it on the Ser112 gatekeeper site. FEBS Lett. 2004;571:43–9. https://doi.org/10.1016/j.febslet.2004.06.050.
46. Hermanova I, Zúñiga-García P, Caro-Maldonado A, Fernandez-Ruiz S, Salvador F, Martín-Martín N, et al. Genetic manipulation of LKB1 elicits lethal metastatic prostate cancer. J Exp Med. 2020. https://doi.org/10.1084/jem.20191787.
47. Eichner LJ, Brun SN, Herzig S, Young NP, Curtis SD, Shackelford DB, et al. Genetic analysis reveals AMPK is required to support tumor growth in murine Kras-dependent lung cancer models. Cell Metab. 2019;29:285-302.e7. https://doi.org/10.1016/j.cmet.2018.10.005.
48. Murray CW, Brady JJ, Tsai MK, Li C, Winters IP, Tang R, et al. An LKB1–SIK axis suppresses lung tumor growth and controls differentiation. Cancer Discov. 2019;9:1590–605. https://doi.org/10.1158/2159-8290.CD-18-1237.
49. Hollstein PE, Eichner LJ, Brun SN, Kamireddy A, Svensson RU, Vera LI, et al. The AMPK-related kinases SIK1 and SIK3 mediate key tumor-suppressive effects of LKB1 in NSCLC. Cancer Discov. 2019;9:1606–27. https://doi.org/10.1158/2159-8290.CD-18-1261.

Publisher's Note

Table S1. Primers for mutagenesis

Target	Primer Type	Sequence
LKB1S334A	Forward	CACCACAGTCATGGCGCGCCACCGGTCC
LKB1S334A	Backward	GGACCGGTGGCGCGCCATGACTGTGGTG
LKB1S428A	Forward	GCTTGCAGGCCGCCAGCCGGCGG
LKB1S428A	Backward	CCGCCGGCTGGCGGCCTGCAAGC
LKB1Sequencing Primer	Forward	GAAGGGGACAACATCTACAAGT

Table S2. CRISPR sgRNA sequences

Target Location	Sequence
PIM1 Exon2	CCGGCAAGTTGTCGGAGACG
PIM1 Exon6	TCGAAGGTTGGCCTATCTGA
PIM2 Exon2	TTCGAGGCCGAGTATCGACT
PIM2 Exon6	GGCCAGGCACCGGCGGATTA
PIM3 Exon5	GGGCGTGCTTCTCTACGATA
PIM3 Exon6	GCCGTCGCTGGATCAGATTG
LKB1 Exon3	CACCCTCAAAATCTCCGACC
LKB1 Exon7	CATGCTGCGCCACCGGTCCT

Table S3. Primers for verification of CRIPSR knock-out clones

Target	Primer Type	Sequence
PIM1 Exon2(P1E2)	Forward	ATGCTCTTGTCCAAAATCAACTCG
PIM1 Exon6(P1E6)	Forward	ATGCTTGGCCTCCCTGG
PIM1 Exon6(P1E6)	Backward	GAGAGTCACTCTTCCCCACTGTT
PIM2 Exon2(P2E2)	Forward	CAAGCCTCTACAGGGGC
PIM2 Exon2(P2E2)	Backward	TCCTCTACACACTCTGCAGG
PIM2 Exon6(P2E6)	Backward	GTAAAACCAAGTCAACAAATGTCC
PIM3	Forward	GGTGATGACGAGCAGGATTT
PIM3	Backward	TTTGGACAGACAGAGCTTGAG
LKB1	Forward	CAAAGGGGACCCCTGTGAG
LKB1	Backward	GTCCGGCAGGTGTCGTC

Table S4. Antibodies

Protein or tag	Company	Product Code	Dilution
PIM1	Santa Cruz	12H8	1:500
PIM2	Cell Signaling Technology	#4730	1:1000
PIM3	Cell Signaling Technology	#4165	1:1000
PIM1 (PLA assay)	Merck	MABC553	1:500
FLAG-tag (PLA assay)	Sigma	F7425	1:500
Beta-actin	Cell Signaling Technology	#3700	1:5000
Phospho-AMPKα (Thr172)	Cell Signaling Technology	#2325	1:1000
AMPKα	Cell Signaling Technology	#2793	1:1000
LKB1	Cell Signaling Technology	#3047	1:1000
His-tag	Cell Signaling Technology	#12698	1:1000
FLAG-tag	Sigma	F1804	1:1000
Phospho-Akt Substrate (RXXS/T)	Cell Signaling Technology	#9614	1:1000
β-Tubulin	Cell Signaling Technology	#86298	1:5000
Lamin A/C	Cell Signaling Technology	#4777	1:5000
Phospho-Akt (Ser473)	Cell Signaling Technology	#4060	1:2000
Akt	Cell Signaling Technology	#9272	1:2000

Figure S1

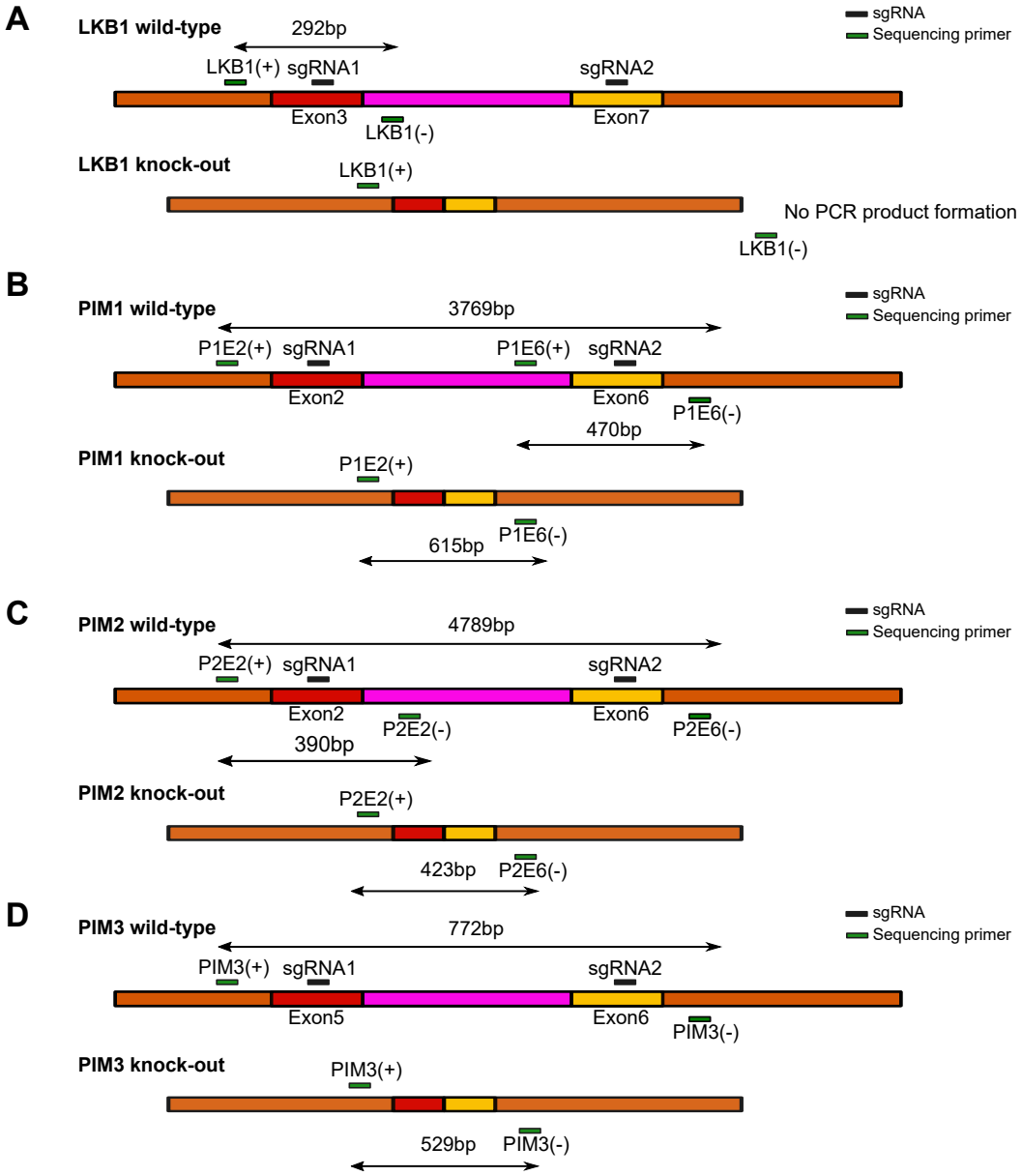

Figure S1. Schematic diagram for the strategies of CRISPR/Cas9 design and verification. To knock out desired genes, two sgRNAs (coloured in blue) were chosen that targeted genomic DNA within exon 2 and 6 of PIM1 (**A**), exon 2 and 6 of PIM2 (**B**), exon 5 and 6 of PIM3 (**C**), or exon 3 and 7 of LKB1(**D**). Sequencing primers (coloured in green) were chosen for nearby sites to be able to verify the wild-type (WT) and the corresponding knock-out (KO) clones.

Figure S2

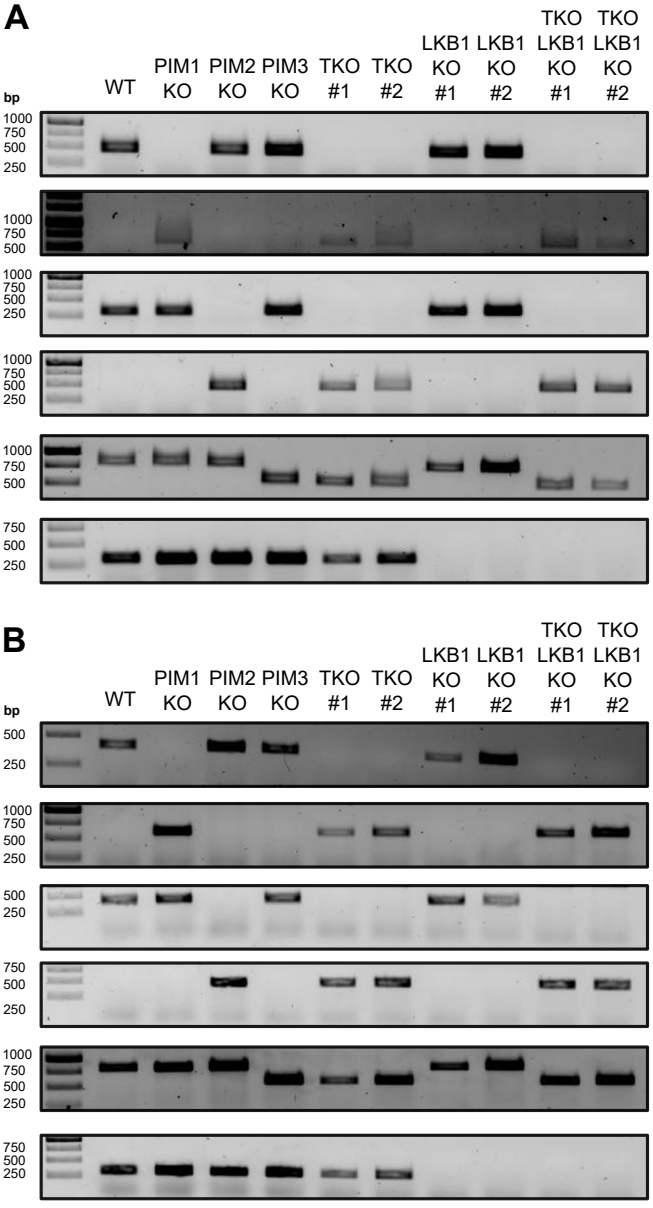

PC3	Expected product size
(+):PIM1E6 (-) :PIM1E6	WT:470bp
(+):PIM1E2 (-) :PIM1E6	KO:615bp
(+):PIM2E2 (-) :PIM2E2	WT:390bp
(+):PIM2E2 (-) :PIM2E6	KO:423bp
(+):PIM3 (-) :PIM3	WT:772bp KO:529bp
(+):LKB1 (-) :LKB1	WT:292bp

MCF7	Expected product size
(+):PIM1E6 (-) :PIM1E6	WT:470bp
(+):PIM1E2 (-) :PIM1E6	KO:615bp
(+):PIM2E2 (-) :PIM2E2	WT:390bp
(+):PIM2E2 (-) :PIM2E6	KO:423bp
(+):PIM3 (-) :PIM3	WT:772bp KO:529bp
(+):LKB1 (-) :LKB1	WT:292bp

Figure S2. DNA gel electrophoresis results for wild-type and knock-out clones. Pairs of indicated sequencing primers were used to amplify genomic DNA from PC3 (**A**) and MCF7 (**B**) wild-type (WT) cells, their knock-out derivatives lacking individual (PIM1, PIM2, PIM3 KO) or all three PIM kinases (TKO), LKB1 (LKB1KO) or LKB1 plus all three PIM kinases (TKOLKB1KO). Amplicons with expected product sizes are listed. Products longer than 2 kb were not amplified, as PCR extension time was set to 1 min (2kb/min) in each amplification cycle.

Figure S3

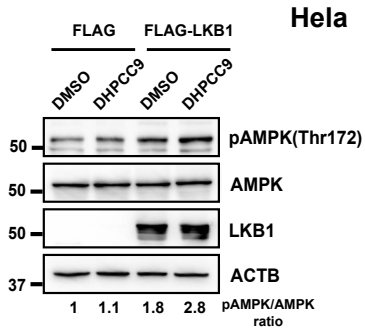

Figure S3. LKB1 is needed for PIM-dependent regulation of AMPK phosphorylation. Hela cells transiently expressing FLAG or FLAG-tagged LKB1 were treated for 24h with DMSO or 10μM DHPCC9, and subjected to Western blotting with antibodies against phospho-AMPK (Thr172), AMPK or LKB1. ACTB staining was used as a loading control. Shown below the graph are the relative levels of phosphorylated versus total AMPK that were quantitated in comparison to DMSO-treated control samples.

Figure S4

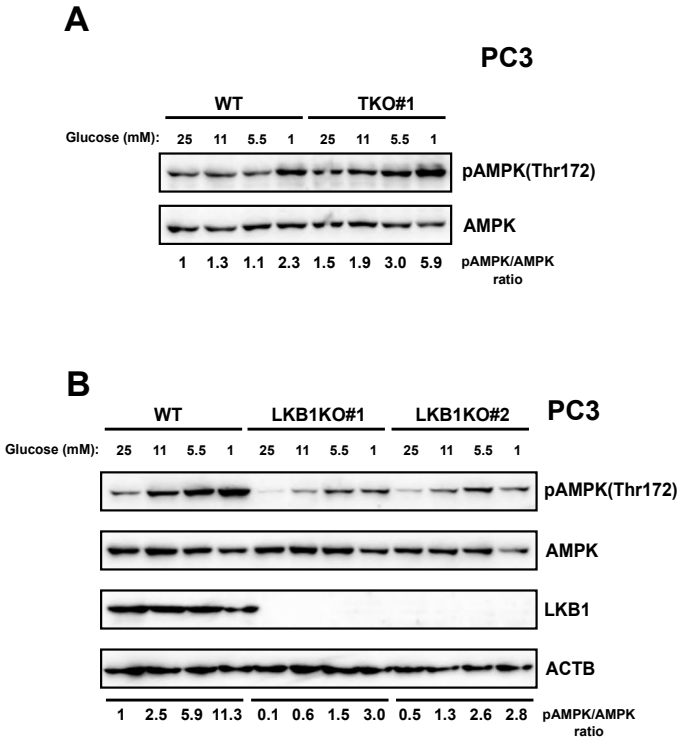

Figure S4. Glucose deprivation increases AMPK phosphorylation also in an LKB1-independent fashion. **A**) PC3 WT and TKO cells were incubated with indicated glucose concentrations for 24h, and subjected to Western blotting. **B**) PC3 WT and LKB1KO cells were incubated with indicated glucose concentrations for 48h, and subjected to Western blotting. ACTB staining was used as a loading control. Shown below the graphs are the relative levels of phosphorylated versus total AMPK that were quantitated in comparison to control samples of WT cells grown in the presence of 25 mM glucose.

Figure S5

A

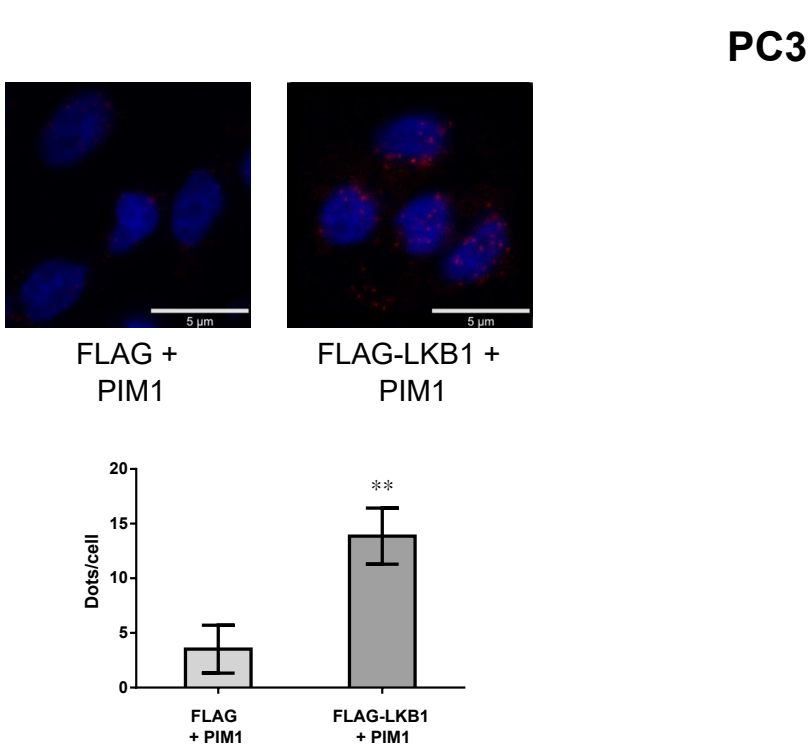

Figure S5. Proximity ligation assay (PLA) to demonstrate the physical interactions between PIM1 and LKB1. PC3 cells transiently expressing FLAG or FLAG-tagged LKB1 plasmids were imaged 24h after transfection. Shown are representative images and quantification from the PLA assays with anti-PIM1 and anti-FLAG antibodies.

Figure S6

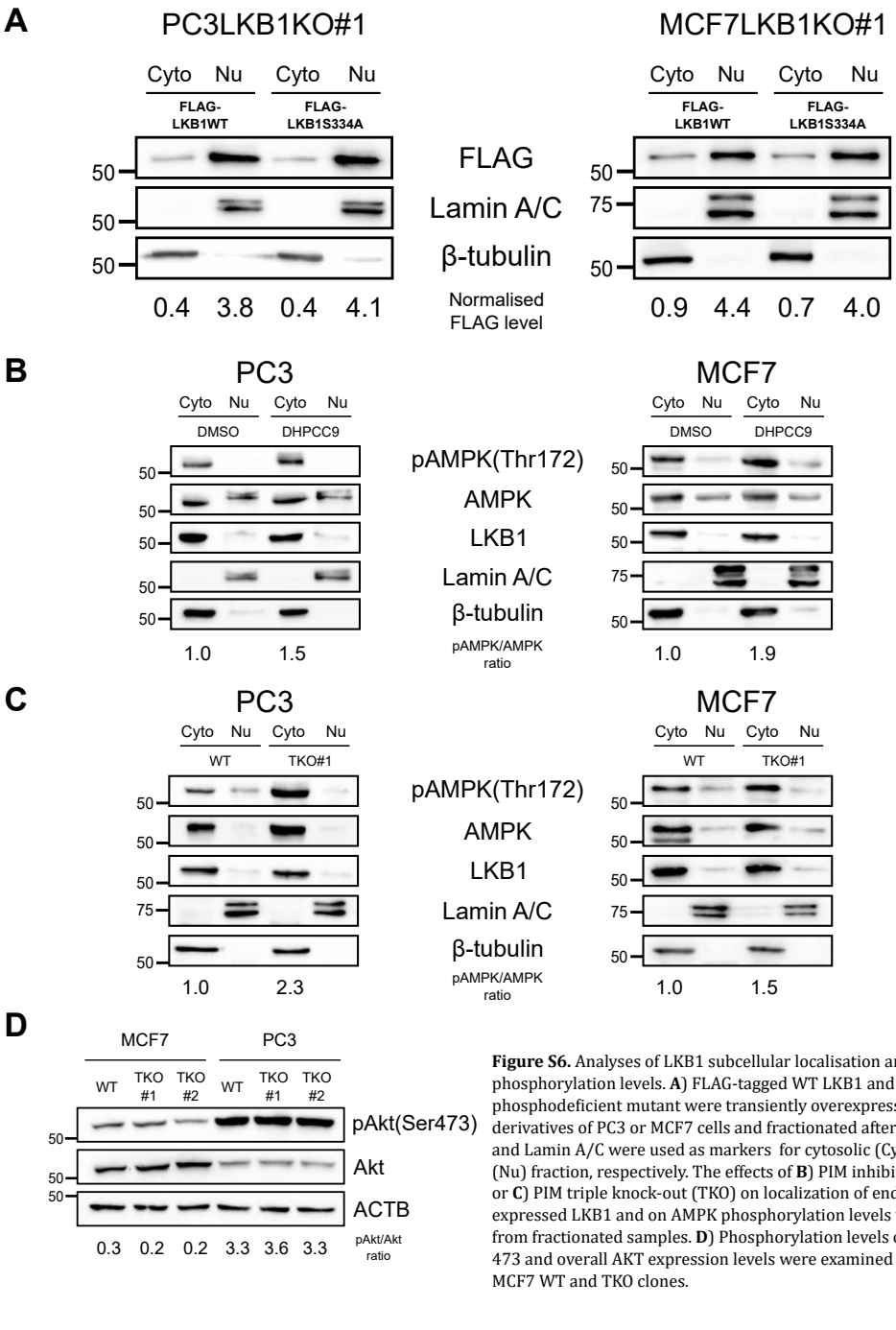

Figure S6. Analyses of LKB1 subcellular localisation and AKT phosphorylation levels. **A**) FLAG-tagged WT LKB1 and its Ser334A phosphodeficient mutant were transiently overexpressed in LKB1KO derivatives of PC3 or MCF7 cells and fractionated after lysis. β-Tubulin and Lamin A/C were used as markers for cytosolic (Cyto) and nuclear (Nu) fraction, respectively. The effects of **B**) PIM inhibition by DHPCC9 or **C**) PIM triple knock-out (TKO) on localization of endogenously expressed LKB1 and on AMPK phosphorylation levels were analysed from fractionated samples. **D**) Phosphorylation levels of AKT at Ser 473 and overall AKT expression levels were examined in both PC3 and MCF7 WT and TKO clones.

Figure S7

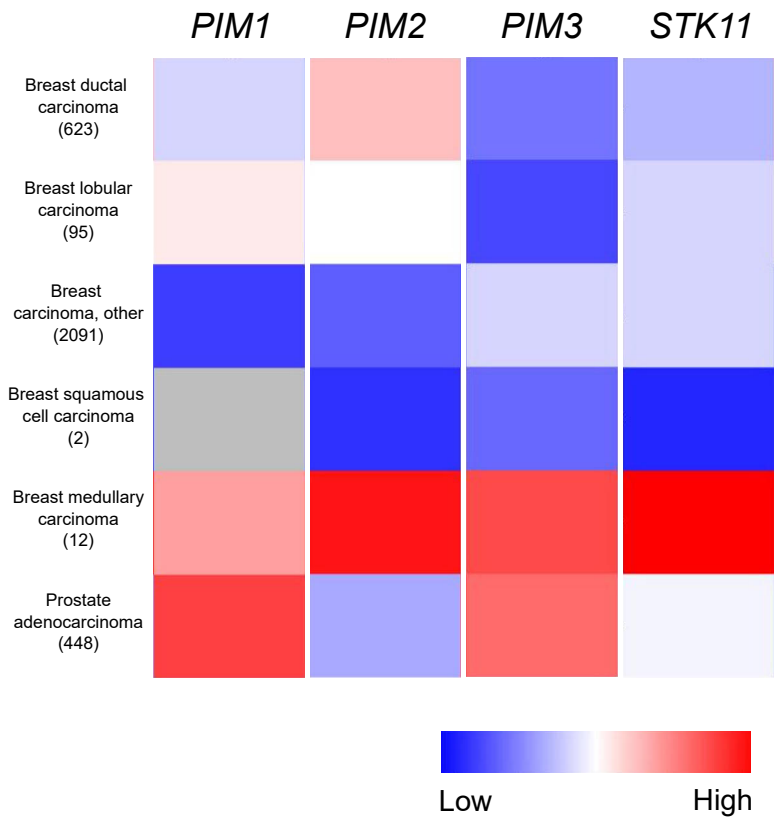

Figure S7. Expression of *PIM* family members and *LKB1(STK11)* in distinct types of breast or prostate cancer. Gene expression heatmap for *PIM1, PIM2, PIM3* and *LKB1(STK11)* in breast and prostate cancer subtypes were generated from IST Online™ database (ist.medisapiens.com). The colour in the heatmap refers to the mean mRNA expression values. Numbers in the brackets stand for the number of patient-derived samples available for analysis.

Mung KL, Meinander A, Koskinen PJ. (2022)

PIM kinases phosphorylate lactate dehydrogenase A at serine 161 and suppress its nuclear ubiquitination

The FEBS Journal

III

The FEBS Journal

FEBS PRESS science publishing by scientists

PIM kinases phosphorylate lactate dehydrogenase A at serine 161 and suppress its nuclear ubiquitination

Kwan Long Mung[1], Annika Meinander[2] and Päivi J. Koskinen[1]

1 Department of Biology, University of Turku, Finland
2 Faculty of Science and Engineering, Cell Biology, BioCity, Åbo Akademi University, Turku, Finland

Keywords
14-3-3; LDHA; phosphorylation; PIM kinases; ubiquitination

Correspondence
Päivi J. Koskinen, Department of Biology, University of Turku, Vesilinnantie 5, FI-20500 Turku, Finland
Tel: +358 29 450 4218
E-mail: paivi.koskinen@utu.fi

(Received 23 June 2022, revised 14 September 2022, accepted 13 October 2022)

doi:10.1111/febs.16653

Lactate dehydrogenase A (LDHA) is a glycolytic enzyme catalysing the reversible conversion of pyruvate to lactate. It has been implicated as a substrate for PIM kinases, yet the relevant target sites and functional consequences of phosphorylation have remained unknown. Here, we show that all three PIM family members can phosphorylate LDHA at serine 161. When we investigated the physiological consequences of this phosphorylation in PC3 prostate cancer and MCF7 breast cancer cells, we noticed that it suppressed ubiquitin-mediated degradation of nuclear LDHA and promoted interactions between LDHA and 14-3-3 proteins. By contrast, in CRISPR/Cas9-edited knock-out cells lacking all three PIM family members, ubiquitination of nuclear LDHA was dramatically increased followed by its decreased expression. Our data suggest that PIM kinases support nuclear LDHA expression and activities by promoting phosphorylation-dependent interactions of LDHA with 14-3-3ε, which shields nuclear LDHA from ubiquitin-mediated degradation.

Introduction

PIM kinases are a family of serine–threonine kinases with three highly homologous family members (PIM1, PIM2 and PIM3) that are often over-expressed in haematological or solid tumours [1–3] and that contribute to tumorigenesis there [4–6]. The PIM kinases are constitutively active [7] and regulate cell survival, motility, proliferation and metabolism by phosphorylating a wide range of substrates including BAD [8], NFATC1 [9], NOTCH1 [10], NOTCH3 [11], CAPZ [12] and LKB1 [13]. Knocking out all three members of the PIM family results in LKB1-dependent AMPK activation [13,14], increased production of reactive oxygen species as well as altered expression of several metabolic enzymes involved in glycolysis, pentose phosphate pathway or oxidative phosphorylation [15,16]. There is also increasing evidence on the ability of PIM kinases to directly phosphorylate metabolic enzymes, such as lactate dehydrogenase (LDH) [17], enolase [12,17], pyruvate kinase M2 [18], hexokinase 2 [19] and hypoxia-inducible factor 1 [20]. Furthermore, we have previously identified LDH as a putative PIM1-interacting protein in a yeast two-hybrid screen [21]. However, the exact PIM target site(s) in LDH and the functional consequences of PIM-dependent phosphorylation have remained unknown.

Lactate dehydrogenase is a tetrameric enzyme that catalyses the inter-conversion of pyruvate to lactate and NADH to NAD^+, enabling sustained glycolysis through NAD^+ regeneration [22]. It also catalyses the conversion of α-ketobutyrate (α-KB) to α-hydroxybutyrate (α-HB) with the expense of NADH to NAD^+ [23]. The homo- or heterotetrameric LDH complex is composed of protein products encoded by two different genes: LDHA and LDHB. LDHA is also

Abbreviations
KO, knock-out; LDH, lactate dehydrogenase; NAD, nicotinamide adenine dinucleotide; PLA, proximity ligation assay; pSer, phosphoserine; SA, serine (S)-to-alanine (A) phosphomutant; TKO, triple knock-out; Ub, ubiquitin; WT, wild-type; αHB, α-hydroxybutyrate; αKB, α-ketobutyrate.

called the M isoform, as it is the dominant isoform found in skeletal muscle, while LDHB is called the H isoform and is predominantly found in the heart [24]. Over-expression of LDHA is observed in various cancers [22,25,26], where it contributes to resistance towards chemotherapies [27,28]. Upregulation of LDHB is found in aggressive basal-like and triple-negative breast cancers [29,30]. However, in several cases, silencing of LDHB expression via promoter methylation is also observed [22].

Cellular activities of LDHA are heavily regulated by post-translational modifications. Acetylation of LDHA at K5 residue promotes LDHA degradation via autophagy through interaction with HSC70 [31]. On the contrary, succinylation of LDHA at K222 decreases its lysosomal degradation [32]. FGFR1 increases LDHA enzymatic activities through phosphorylation of Y10 and Y83, promoting the formation of active LDHA tetramers and increasing the binding of the NADH substrate, respectively [33]. In addition, both HER2 and SRC phosphorylate LDHA at Y10 and thereby contribute to the metastatic potential of tumours [34].

Lactate dehydrogenase A has been suggested to be protected by 14-3-3 proteins from ubiquitin-dependent degradation [35]. The 14-3-3 protein family consists of seven isoforms (β, γ, ε, η, σ, τ and ζ) that interact with phosphorylated proteins and subsequently modulate cellular signalling [36–38]. For example, PIM-dependent phosphorylation of BAD prevents its pro-apoptotic effects as it becomes sequestered by 14-3-3 [8,39]. In this study, we analysed phosphorylation of LDHA in more detail and identified Ser161 as the major target site for PIM kinases. We also observed that PIM-induced phosphorylation of LDHA is essential for its interaction with 14-3-3 and for its protection from ubiquitination. By contrast, knocking out all three PIM kinase members by CRISPR/Cas9-based editing increased ubiquitination and decreased nuclear LDHA expression in both PC3 prostate and MCF7 breast cancer cells. All these data suggest that nuclear LDHA expression is modulated by activities of both the PIM and 14-3-3ε proteins.

Results

Nuclear LDHA expression and activities are decreased in the absence of PIM kinases

As we and others had previously reported that PIM kinases bind to LDHA and phosphorylate it *in vitro* [17,21], we wanted to investigate the putative physiological effects of PIM kinases on LDHA expression or activity in a cellular context. For this purpose, we used both PC3 prostate and MCF7 breast cancer cells as well as their derivatives, from which we had knocked out the expression of all three PIM family members by CRISPR/Cas9 genomic editing [13]. For both cell lines, we had established two independent triple knock-out clones (TKO#1 and TKO#2) that provide useful models to study PIM-dependent cellular functions.

When we analysed LDHA protein and mRNA expression levels by western blotting and quantitative PCR, respectively, we did not observe any statistically significant differences between whole-cell lysates of wild-type (WT) and TKO clones of either PC3 or MCF7 cells (Fig. 1A). However, when we performed subcellular fractionations to separate whole-cell lysates into cytosolic and nuclear fractions, significant differences in expression of nuclear LDHA were observed in both PC3 and MCF7 cells (Fig. 1B). There LDHA protein expression was consistently decreased in the nuclear, but not cytosolic fractions of TKO clones as compared to WT cells.

We then analysed the activity of LDHA by measuring its abilities to convert pyruvate to lactate as well as α-ketobutyrate (αKB) to α-hydroxybutyrate (αHB) with the exchange of NADH to NAD^+ (Fig. 2A). In line with the protein expression levels, we did not observe any statistically significant changes in either lactate or αHB production between whole-cell lysates of WT and TKO clones (Fig. 2A). By contrast, when we compared LDHA activities between cytosolic and nuclear fractions, we detected dramatically decreased LDHA activities in terms of production of lactate and αHB in nuclear, but not cytoplasmic fractions of TKO clones as compared to WT cells (Fig. 2B). The cytosolic LDHA activities were on average 25- to 50-fold higher than those of nuclear fractions, which correlated well with the observations that prolonged exposures were required to detect LDHA protein in nuclear fractions (Fig. 1C). Therefore, due to the overwhelming amount of LDHA present in cytosolic fractions compared to nuclear fractions, it was evident that examination of whole-cell lysates did not enable detection of any nuclear-level changes in LDHA activity. Ultimately, the aforementioned results indicate that both expression and activity of nuclear LDHA are reduced in PIM-deficient cells.

PIM kinases phosphorylate LDHA at serine 161 residue

Having observed PIM-dependent physiological effects on LDHA activities, we proceeded to examine cellular interactions between PIM kinases and LDHA in more

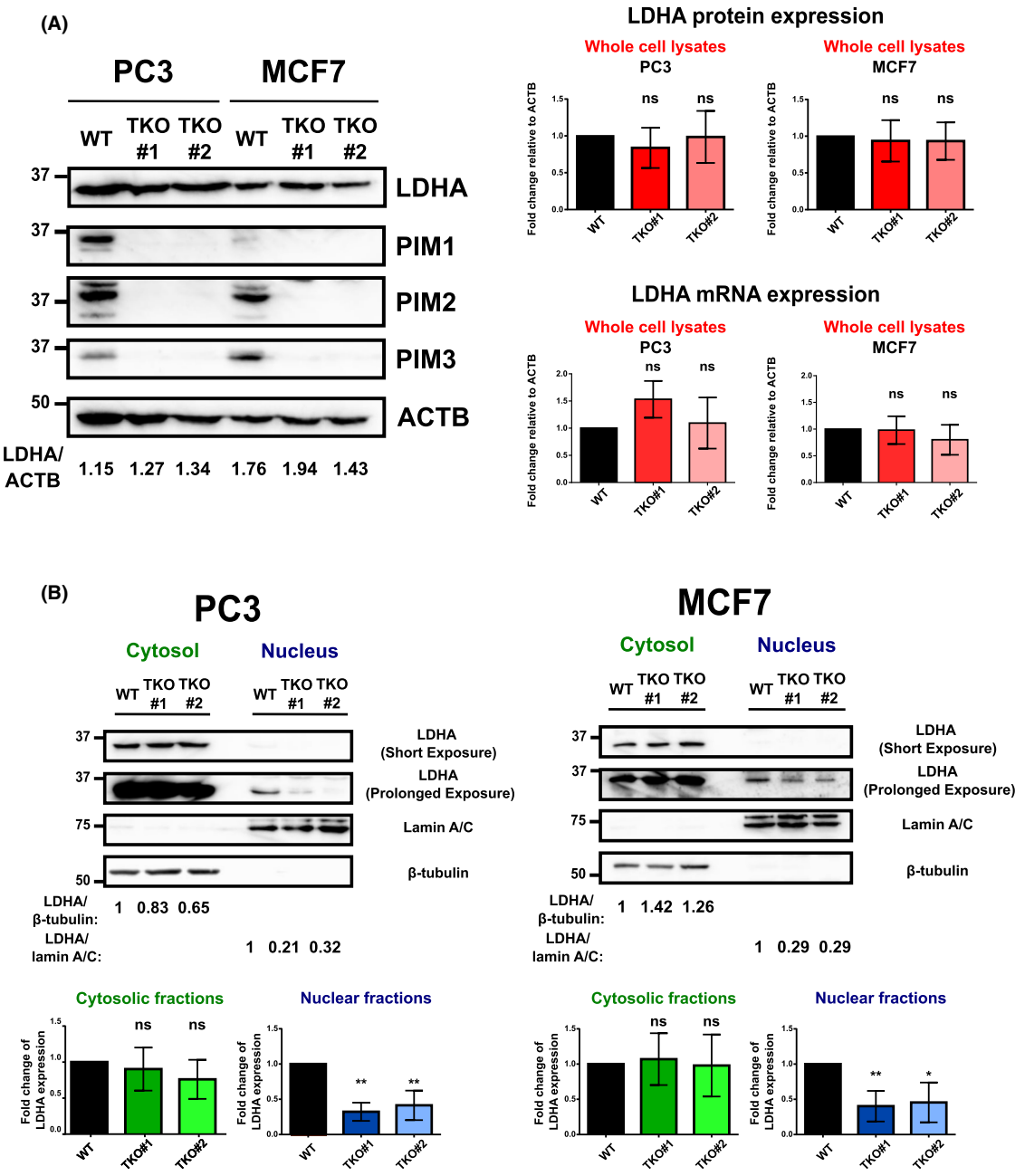

Fig. 1. Inactivation of PIM kinases decreases nuclear LDHA expression. (A) LDHA and PIM protein expression levels were examined by western blotting from wild-type (WT) PC3 and MCF7 cells and their triple knock-out (TKO#1 and TKO#2) derivatives lacking all three PIM kinases, while LDHA mRNA expression levels were measured by quantitative PCR. (B) Cytosolic and nuclear LDHA protein expression levels were similarly analysed. β-tubulin and lamin A/C were used as markers for the cytosolic and nuclear fractions, respectively. Shown are representative images as well as bar charts with relative expression levels of LDHA in TKO cells as compared to WT cells (average values ± SD, $n = 3$). Student's *t*-test was used to determine the statistical significance. Significant differences ($P < 0.05$ and $P < 0.01$) were marked with * and **, respectively; ns refers to no significance. Error bars represent standard deviations.

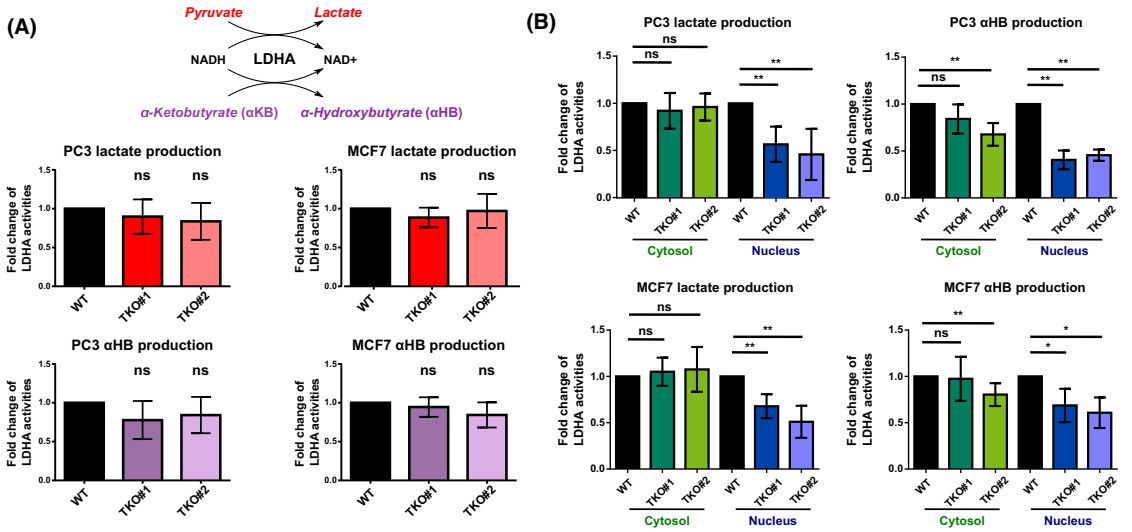

Fig. 2. Inactivation of PIM kinases decreases nuclear LDHA activities. (A) Cellular LDHA activities corresponding to the rate of conversion from pyruvate to lactate or from α-ketobutyrate (αKB) to α-hydroxybutyrate (αHB) were measured from cell lysates of PC3 or MCF7 WT and TKO cells. Results were normalized with total protein and plotted as bar charts with relative activities of TKO cells as compared to WT cells (average values ± SD, $n = 3$). (B) Bar charts with relative cytosolic and nuclear LDHA activities in TKO cells as compared to WT cells (average values ± SD, $n = 3$). Student's *t*-test was used to determine the statistical significance. Significant differences ($P < 0.05$ and $P < 0.01$) were marked with * and **, respectively; ns refers to no significance. Error bars represent standard deviations.

detail. Using both proximity ligation assays (Fig. 3A) and co-immunoprecipitation experiments (Fig. 3B,C) with PC3 cell samples, we demonstrated that endogenously expressed PIM1 and LDHA physically interact with each other in WT, but not TKO cells. Moreover, we observed that serine phosphorylation levels of immunoprecipitated LDHA were significantly lower in TKO clones of both PC3 and MCF7 cells as compared to WT cells (Fig. 3D), suggesting that the serine/threonine-specific PIM kinases phosphorylate LDHA within cells. To confirm this conclusion, we performed radioactive *in vitro* kinase assays with PIM and LDHA proteins. For this purpose, both types of proteins were produced in bacteria as fusions with glutathione S-transferase (GST), but the GST-tag was later removed from LDHA. The results of the kinase assays indicated that all three PIM kinases are capable of phosphorylating LDHA *in vitro*, while LDHA does not autophosphorylate itself (Fig. 3E).

To reveal the PIM target sites, we performed in-gel digestion of *in vitro* phosphorylated LDHA followed by mass spectrometry analysis. Based on this analysis, serine residues 79, 105 and 161 were identified as potential PIM target sites on LDHA. In addition, *in silico* analysis of LDHA indicated that the amino acid sequence around serine 319 (LKKSA) aligns relatively well with the PIM1-targeted consensus sequence (K/R-K/R-R-K/R-L-**S/T**-a; a = a small = 0 chain amino acid) [40]. Therefore, we used site-directed mutagenesis to change the four putative PIM-targeted serine residues to alanines. Radioactive kinase assays with phospho-deficient mutants revealed that S161 and S319 are the major *in vitro* target sites for PIM1 on LDHA (Fig. 3F).

Next, we pursued verifying the PIM target sites on LDHA within cells. For this purpose, PC3 WT and TKO#1 cells were transfected with plasmids expressing either WT LDHA tagged with the green fluorescent protein (GFP), or one of the corresponding phospho-deficient mutants, S161A or S319A. When cell lysates were immunoprecipitated with GFP antibodies and immunoblotted with phosphoserine antibodies, there was a significant decrease in the level of LDHA phosphorylation in TKO cells as compared to WT cells (Fig. 3G). By contrast, the S161A mutation reduced the phosphorylation level of LDHA also in WT cells close to that observed in TKO cells, while the S319A mutation was less effective. Thus, by combining both *in vitro* and cellular data, it can be concluded that S161 is the major physiologically relevant PIM phosphorylation site on LDHA.

PIM-induced phosphorylation of LDHA suppresses its ubiquitination

While searching for the mechanism to explain the lower nuclear expression levels of LDHA in TKO cells as compared to WT cells, we noticed that LDHA was abnormally highly ubiquitinated in TKO clones. This was consistently observed in PC3-derived cells transiently over-expressing HA-tagged ubiquitin when either endogenous LDHA (Fig. 4A) or co-over-expressed FLAG-tagged LDHA protein (Fig. 4B) was immunoprecipitated and stained with HA, LDHA or FLAG antibodies. The results from subcellular fractionation experiments with TKO cells based on PC3 or MCF7 (Fig. 4C) indicated that the ubiquitinated LDHA was predominantly localized in the nuclear fraction. The nuclear ubiquitination was suppressed by transient over-expression of His-tagged PIM1 (Fig. 4D), confirming the protective role of PIM kinases there. Furthermore, mutation of the PIM-targeted serine 161 of LDHA into alanine was sufficient to induce nuclear LDHA ubiquitination in PC3 WT cells, while the corresponding mutation of serine 319 had no major effects (Fig. 4E). These data suggest that S161 is the key site for PIM-dependent protection of LDHA from nuclear ubiquitination. In addition, subcellular fractionation experiments confirmed that the ubiquitination triggered by the S161A mutation in WT cells was enriched in the nuclear fraction, similar to what was seen with WT LDHA in TKO clones (Fig. 4F).

Next, we immunoprecipitated FLAG-tagged LDHA from PC3 WT and TKO cells and blotted the samples with antibodies against the K48-specific polyubiquitin chains, which are known to be associated with proteasomal degradation [41]. While K48 ubiquitin was also observed in WT cells, its conjugation to LDHA was strongly enhanced in TKO cells (Fig. 4G) as well as in WT cells expressing the S161A mutant of FLAG-tagged LDHA (Fig. 4H), suggesting that phosphorylation of LDHA at serine 161 suppresses its K48-linked polyubiquitination.

To determine, whether a lack of PIM-dependent phosphorylation affected LDHA protein conformation and thereby increased its susceptibility to ubiquitination, we performed protein crosslinking assays with glutaraldehyde. However, we did not observe any significant differences in the amounts of endogenously expressed LDHA monomers, dimers or tetramers between PC3 WT and TKO cells (Fig. 4I), or between ectopically expressed flag-tagged WT LDHA and the S161A mutant (Fig. 4J). Thus, the observed effects on ubiquitination cannot be explained by differences in LDHA protein folding and oligomerization.

14-3-3 proteins are also essential for the suppression of LDHA ubiquitination

As 14-3-3 proteins had recently been reported to suppress LDHA ubiquitination [35], this prompted us to investigate interactions between LDHA and 14-3-3 proteins in WT and TKO clones. Performing proximity ligation assays with PC3 cell samples together with LDHA and pan-14-3-3 antibodies, we demonstrated that endogenously expressed LDHA and 14-3-3 proteins physically interact with each other in WT cells, but not in PIM TKO clones (Fig. 5A). Also, in co-immunoprecipitation experiments with PC3 or MCF7 cell samples, much less LDHA was pulled down together with 14-3-3 proteins in TKO clones as compared to WT cells (Fig. 5B). These data suggest that PIM-dependent phosphorylation of LDHA is required to maintain interactions between LDHA and 14-3-3 proteins. More specifically, we observed that transiently over-expressed FLAG-tagged WT LDHA bound strongly with HA-tagged 14-3-3ε in WT PC3 cells, but not in TKO cells, while the S161A mutation in LDHA decreased the interaction also in WT cells (Fig. 5C). Furthermore, we observed that transient over-expression of 14-3-3ε partially suppressed LDHA ubiquitination in PC3 TKO cells (Fig. 5D), resulting in slightly increased nuclear expression of LDHA (Fig. 5E). These effects may be explained by our observations, according to which there was some residual binding between LDHA and endogenously or ectopically expressed 14-3-3 proteins also in the absence of LDHA phosphorylation (Fig. 5B,C). Yet, the striking differences between phosphorylated and non-phosphorylated samples indicate that PIM-induced phosphorylation of LDHA at S161 is vital for the interaction between LDHA and 14-3-3ε proteins and thereby for the ability of 14-3-3 proteins to protect nuclear LDHA from ubiquitin-mediated degradation.

Discussion

Despite several reports on the presence of LDHA in the nucleus [23,25,28,42–44], it has conventionally been depicted as a cytosolic enzyme. Notably, immunohistochemistry stainings have revealed both cytoplasmic and nuclear LDHA expression in lung cancer cells [25,28]. In addition, transmission electron microscopy experiments have confirmed the existence of LDHA in the nucleus of Hela cells [44]. Here, we have observed that LDHA is expressed in both cytosolic and nuclear fractions of PC3 prostate and MCF7 breast cancer cells. However, the majority of LDHA proteins and their activities are located in cytosolic fractions, which

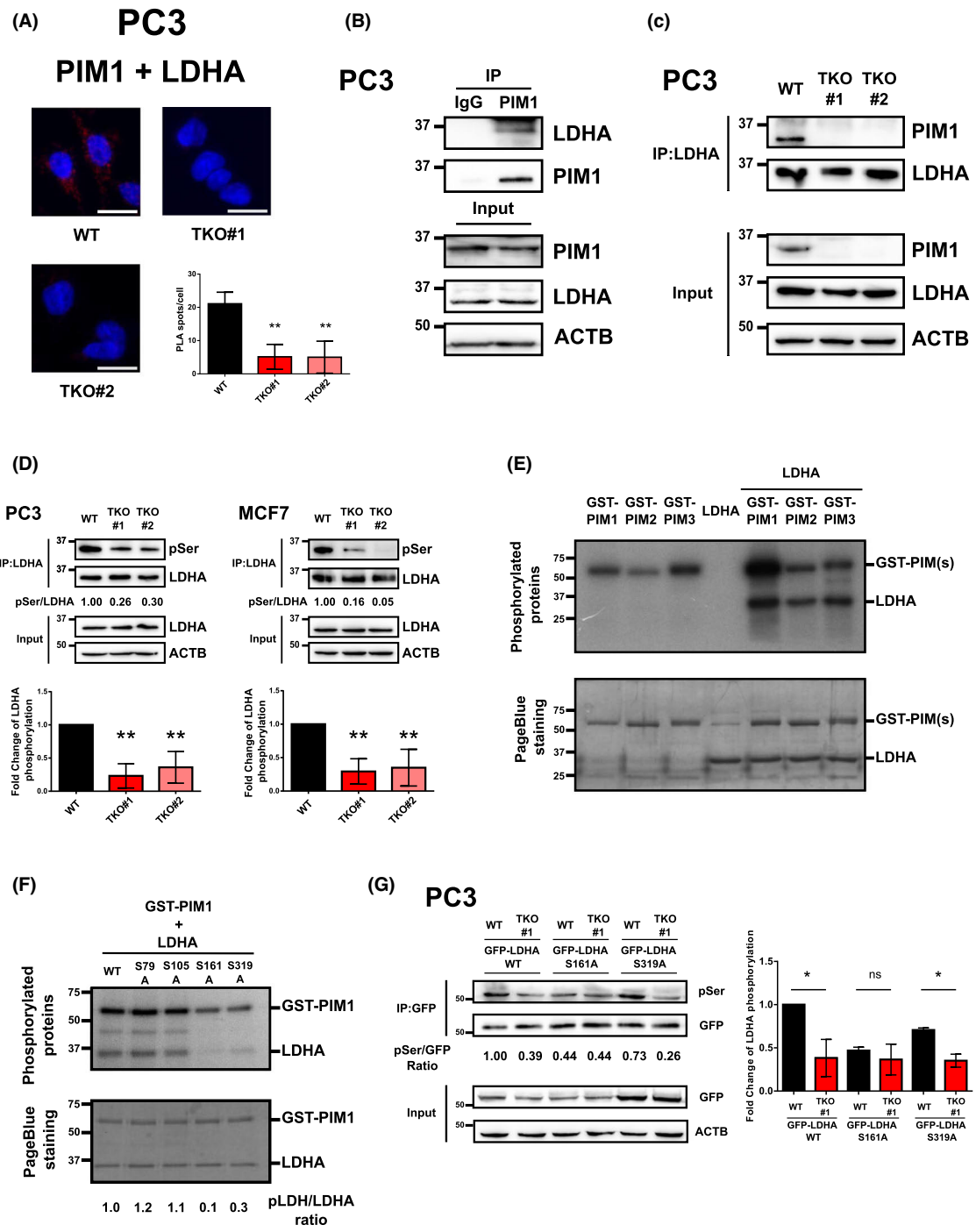

is in agreement with previous observations, e.g. from PC12 cells [43]. So far, there are at least two independent reports on the phosphorylation of LDHA at both serine and tyrosine residues [42,43]. While the functional consequences of tyrosine phosphorylation of LDHA have been actively explored [33,34], studies on

Fig. 3. PIM kinases interact with LDHA inside cells and phosphorylate it at Ser161. (A) Proximity ligation assays (PLA) were performed to demonstrate physical interactions between endogenously expressed PIM1 and LDHA proteins in WT, but not PIM-deficient (TKO#1 and TKO#2) PC3 cells. Shown are representative images and quantification from PLA assays with anti-PIM1 and anti-LDHA antibodies (Scale bar = 5 μm). For immunoprecipitation analyses, PC3 WT and TKO cell lysates were immunoprecipitated and the blotted samples were stained with indicated antibodies. Ten per cent of each cell lysate had been set aside and stained with indicated antibodies to control for the input amounts of proteins. (B) Co-IP of endogenous LDHA protein with IgG or PIM1 antibodies in WT cells. (C) Co-IP of endogenous PIM1 with LDHA antibodies in WT or TKO cells. (D) Relative serine phosphorylation levels of LDHA in TKO cells as compared to WT cells. Shown are representative images as well as bar charts (average values ± SD, $n = 3$). (E) Radioactive *in vitro* kinase assays were performed by incubating GST-PIMs and/or LDHA in the presence of ^{32}P-ATP. Phosphorylated proteins were visualized by autoradiography (upper panel) and protein loading by Page Blue staining (lower panel). Shown is a representative image out of two repeated experiments. (F) Radioactive *in vitro* kinase assays were performed by incubating GST-PIM1 with different LDHA mutants (S79A, S105A, S161A and S319A). (G) PC3 WT and TKO cells were transiently transfected with plasmids expressing GFP-LDHA (WT, S161A or S319). After 24 h, cell lysates were immunoprecipitated with GFP antibodies and blotted samples were stained with indicated antibodies. Shown are representative images as well as bar charts with relative serine phosphorylation levels of LDHA in TKO cells as compared to WT cells (average values ± SD, $n = 3$). Student's *t*-test was used to determine the statistical significance. Significant differences ($P < 0.05$ and $P < 0.01$) were marked with * and **, respectively; ns refers to no significance. Error bars represent standard deviations.

serine phosphorylation are lagging behind. In this report, we have focused on PIM-dependent serine phosphorylation of LDHA and identified serine 161 as the major physiologically relevant PIM target site. In high-throughput phosphoproteomic analyses, this site has been found to be phosphorylated under *in vivo* conditions, but the regulatory kinases and the functional consequences have remained unknown [45]. However, here we revealed two important roles for this phosphorylation, as according to our data it supports interactions between LDHA and 14-3-3ε and thereby protects nuclear LDHA from undergoing K48-mediated ubiquitination and subsequent degradation.

Lactate dehydrogenase A ubiquitination has been observed in AGS gastric cancer cells [32], PLC liver cancer cells exposed to MG132 treatment [35], L6 muscle and COS7 kidney cells exposed to oxidative stress as well as skeletal muscles of rats taken to spaceflights [46]. Here, we show that K48-mediated ubiquitination of LDHA occurs predominantly in the nuclear fractions of both PC3 and MCF7 knock-out cells lacking expression and activity of PIM kinases. It has been reported that shRNA knockdown of 14-3-3ζ in HEK293T cells results in robust LDHA ubiquitination, while binding between 14-3-3 proteins and LDHA protects it from ubiquitination [35]. Even more interestingly to us, binding between LDHA and 14-3-3ζ was shown to depend on the phosphorylation status of LDHA, but the critical LDHA phosphorylation site (s) and corresponding upstream kinase(s) remained unknown. Here, we show that the interaction between LDHA and 14-3-3ε proteins is strictly regulated by PIM-dependent phosphorylation of S161 on LDHA. Although over-expressed 14-3-3ε partially suppresses LDHA ubiquitination, it cannot fully restore nuclear LDHA expression in PIM-deficient cells, most likely due to its remarkably reduced capacity to bind to unphosphorylated LDHA. While our study was ongoing, a multi-subunit complex of E3 ligases was reported to be involved in the ubiquitination of LDHA [47]. Given the existence of examples on 14-3-3 proteins suppressing ubiquitination by shielding binding of E3 ubiquitin ligases to their substrates [48], it would be of interest to determine whether the E3 ligase complex is involved in the nuclear LDHA ubiquitination observed in PIM-deficient cells. Ultimately, all these data suggest that the expression and activities of both PIM kinases and 14-3-3ε proteins are involved in the regulation of nuclear LDHA expression, while further studies are required to examine the possibilities of the involvement of other 14-3-3 isoforms.

In line with the ubiquitination pattern, knocking out all three PIM family members in PC3 and MCF7 cells resulted in decreased nuclear LDHA expression, but no appreciable changes in cytosolic LDHA expression. Even though only a minority of cellular LDHA proteins reside in the nucleus, several important roles for nuclear LDHA have been proposed. For example, it serves as a transcription factor to support histone H2B expression in S-phase [49,50]. In addition, the α-HB metabolite generated by nuclear LDHA promotes the upregulation of H3K79 trimethylation as well as the expression of antioxidant and Wnt target genes [23]. Recently, it has also been found that lactate serves as a substrate for histone lysine lactylation [51], and that elevated histone lactylation levels are associated with poor survival of cancer patients [52]. While increased amounts of exogenous glucose or lactate eventually lead to increased histone lactylation levels [51], mice with enforced nuclear LDHA expression display larger tumour volumes than mice with enforced cytoplasmic LDHA expression, suggesting a tumour-promotive role for nuclear LDHA [23]. Conversely, inhibition of PIM kinases decreases nuclear LDHA expression and also

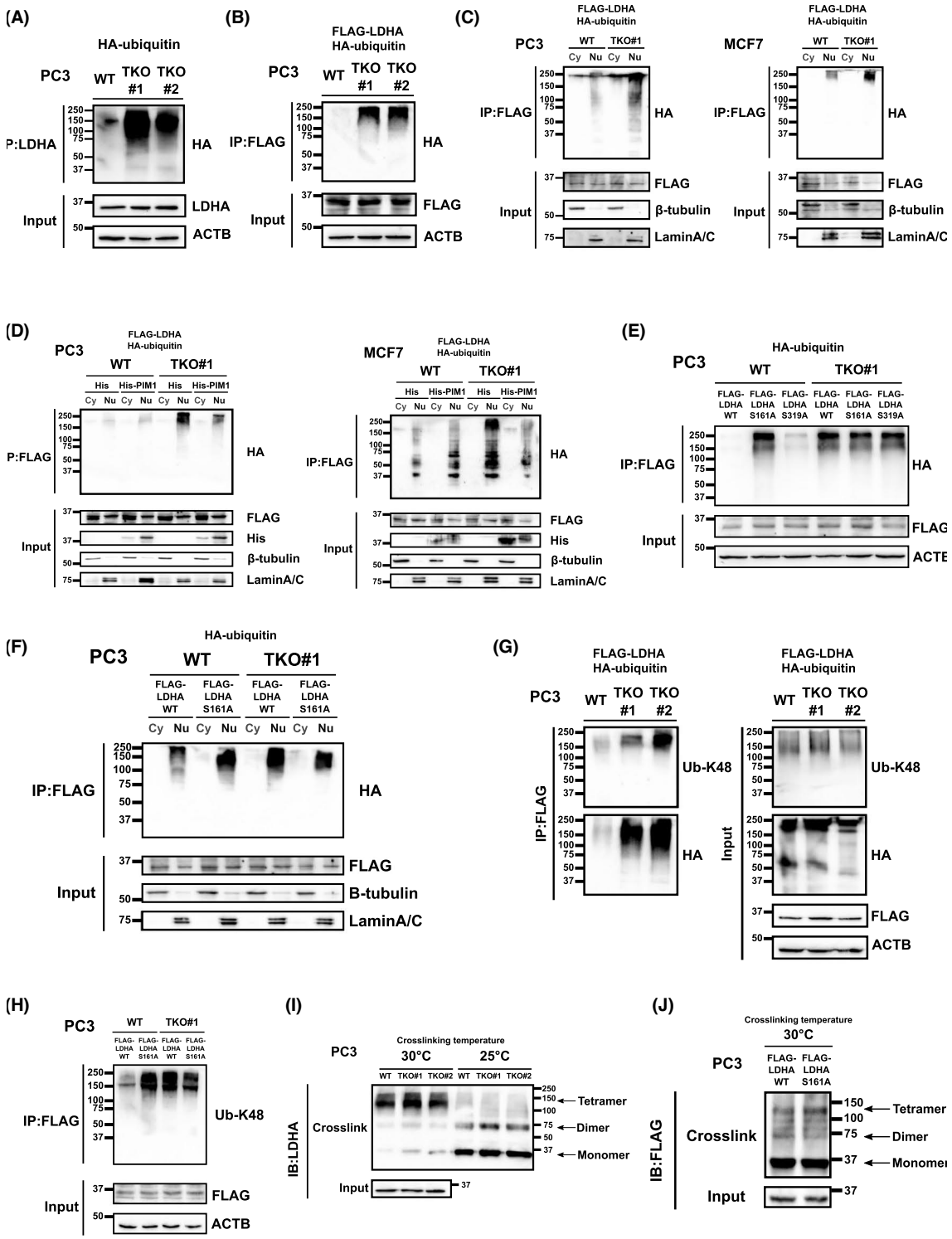

Fig. 4. PIM-induced phosphorylation of LDHA protects it from ubiquitination. PC3 or MCF7 WT and TKO cells were transiently transfected with indicated plasmids expressing HA ubiquitin, WT or mutant FLAG-tagged LDHA, His-tag and/or His-tagged PIM1. After 24 h, cell lysates were immunoprecipitated (IP) and blotted samples were stained with indicated antibodies. Ten per cent of each cell lysate had been set aside and stained with indicated antibodies to control for the input amounts of proteins. Shown are co-IPs of HA ubiquitin with (A) endogenously expressed LDHA, (B) ectopically expressed FLAG-LDHA (n = 3), (C) FLAG-LDHA from cytosolic (Cy) and nuclear (Nu) fractions (n = 3), (D) FLAG-LDHA from His- or His-PIM1-expressing fractionated cells, (E) FLAG- LDHA (WT, S161A or S319A) (n = 2) and (F) FLAG-LDHA (WT, S161A) from fractionated cells (n = 2). Presence of K48-specific polyubiquitin chains was similarly analysed from co-IPs with (G) FLAG-LDHA (n = 3) (H) or FLAG-LDHA (WT or S161A) (n = 2). The oligomerization status of LDHA was analysed by crosslinking assays with glutaraldehyde from (I) WT and TKO cells or (J) from WT cells expressing FLAG-tagged LDHA (WT or S161A).

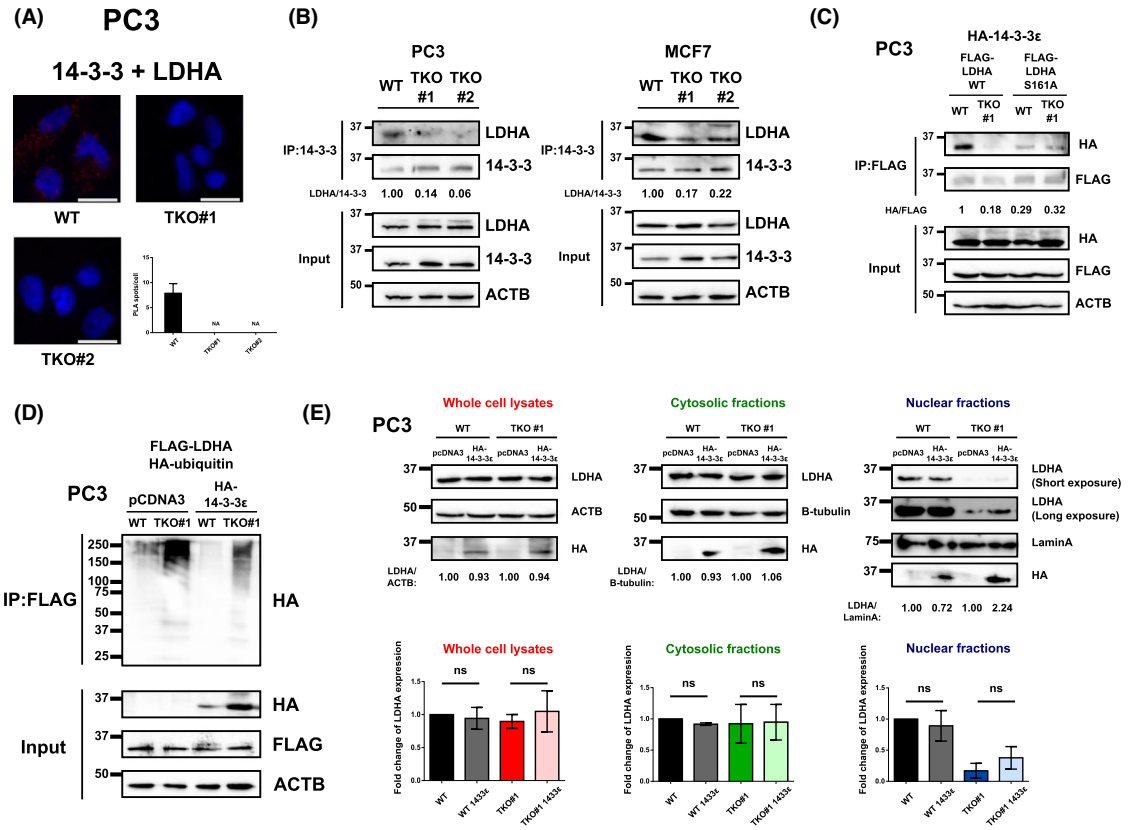

Fig. 5. PIM-induced phosphorylation of LDHA is essential for its interaction with 14-3-3ε. (A) Proximity ligation assays (PLA) were performed to demonstrate the physical interactions between endogenously expressed LDHA and 14-3-3 proteins in WT, but not PIM-deficient (TKO#1 and TKO#2) PC3 cells. Shown are representative images and quantification from PLA assays with anti-LDHA and anti-pan-14-3-3 antibodies (Scale bar = 5 μm). For additional interaction studies, PC3 WT and TKO cells were used as such or transiently transfected with indicated plasmids expressing WT or mutant FLAG-tagged LDHA, HA tag, HA-tagged 14-3-3ε and/or HA ubiquitin. After 24 h, cell lysates were immunoprecipitated (IP) and blotted samples stained with indicated antibodies. Ten per cent of each cell lysate had been set aside and stained with indicated antibodies to control for the input amounts of proteins. (B) Co-IP of endogenous LDHA with endogenous 14-3-3 proteins (n = 3). (C) Co-IP of HA-14-3-3 ε with FLAG-LDHA (WT or S161A). (D) Co-IP of HA ubiquitin with FLAG-LDHA (n = 3). (E) LDHA expression in whole-cell lysates or cytosolic and nuclear fractions of WT and TKO#1 cells. Shown are representative images of western blots as well as bar charts with relative LDHA expression of each fraction as compared to mock-transfected cells (average values ± SD, n = 3). Student's t-test was used to determine the statistical significance. Significant differences ($P < 0.05$ and $P < 0.01$) were marked with * and **, respectively; ns refers to no significance. Error bars represent standard deviations.

decreases tumour size in tumour-bearing mice [2,53]. Thus, in future studies, it would be of interest to dissect the impact of PIM inhibition on LDHA nuclear activities, such as histone methylation and histone lactylation, as such studies may help to establish a rationale for targeting nuclear LDHA as a novel therapeutic option for patients.

Materials and methods

Cell culture reagents and DNA constructs

MCF7 breast cancer and PC3 prostate cancer cells were obtained from American Type Culture Collection (Manassas, VA, USA), and were cultured in Dulbecco's modified Eagle's medium (DMEM) and RPMI-1640 medium (Sigma-Aldrich, St. Louis, MI, USA) respectively. Both media were supplemented with L-glutamine, 10% fetal bovine serum and antibiotics. MEM Non-Essential Amino Acids (Gibco, #11140050; Thermo Fisher Scientific, Waltham, MA, USA) and Sodium Pyruvate (Gibco, #11360070; Thermo Fisher Scientific) were further added to RPMI-1640-based medium for PC3 cells to facilitate cell growth. FuGENE® HD Transfection Reagent (Promega, Madison, WI, USA) was used for plasmid transfections according to the manufacturer's protocol. The use of CRISPR/Cas9-based genome editing to prepare knock-out derivatives of MCF7 and PC3 cells lacking all three members in the PIM family has previously been described [13]. Eukaryotic and bacterial vectors pcDNA™3.1/V5-His-C and pGEX-6P-1 for expression of wild-type (WT) human PIM kinases have been described previously [10]. Expression vectors pcDNA3-HA-14-3-3ε (Addgene Europe, Teddington, UK, #13272) and HA ubiquitin (Addgene Europe, #18712) were kind gifts from Cecilia Sahlgren (Åbo Akademi University, Finland) and Jukka Westermarck (University of Turku, Finland) respectively. Human LDHA was cloned into pGEX-6P-1 (GE Healthcare Life Sciences, Little Chalfont, UK), pFLAG-CMV2 (#E7033, Sigma-Aldrich) and pEGFP-C2 vectors (Clontech Laboratories Inc., Takara Bio USA, San Jose, CA, USA). Site-directed mutagenesis of LDHA was performed using Ultra Pfu DNA Polymerase (Stratagene, San Diego, CA, USA) according to the manufacturer's protocol. The primers used are described in Table S1.

Expression of GST-tagged or His-tagged fusion proteins in *Escherichia coli*

pGEX-6P-1 plasmids (expressing GST-PIMs and GST-LDHAs) were transformed into BL21 *E. coli* strain for protein production. Overnight bacterial cultures were grown at 30 °C until OD_{600} of 0.6. Isopropyl-β-D-galactosidase (250 μM; Sigma-Aldrich) was added to induce protein expression, and the cells were cultured for another 4 h (GST-PIMs) or 24 h (GST-LDHAs). For some of the experiments as indicated, the GST tag was removed using the Pierce™ HRV 3C Protease Solution Kit (Thermo Scientific 88947) according to the manufacturer's protocol. The following purification steps of GST-tagged proteins have been described previously [12].

Western blotting

Cells were lysed for 10 min in ice-cold 50 mM Tris–HCl, pH 8.0, buffer containing 150 mM NaCl, 2 mM EDTA, 1% NP-40, 5 mM NaF, 1 mM Na_3VO_4, 1 mM PMSF, 2 $\mu g \cdot mL^{-1}$ leupeptin, aprotinin, pepstatin A, 5 mM NEM, 5 mM chloroacetamide and Mini EDTA-free protease inhibitor tablet (Roche, Basel, Switzerland). Cell lysates were sonicated for 1 min and supernatants were collected after 5 min of centrifugation at 21 000 × ***g***. Protein concentrations were determined using the Bio-Rad Protein Assay Dye Reagent or Pierce™ BCA Protein Assay Kit according to manufacturers' protocols. Protein aliquots (20–90 μg) were separated by 10% SDS/PAGE and transferred onto a PVDF membrane (Millipore, Burlington, MA, USA). The membranes were incubated overnight at +4 °C with primary antibodies (Table S2). Secondary antibody staining (1 : 5000) was performed for 1 h at RT with HRP-linked goat anti-mouse IgG #7076 or goat anti-rabbit IgG #7074 antibodies (Cell Signalling Technology, Beverly, MA, USA).

For immunoprecipitation experiments with ubiquitin, SDS concentration in the lysis buffer was adjusted to 1% prior to sonication. After sonication, the lysates were diluted to 0.1% SDS before loading onto the agarose beads. For immunoprecipitation of endogenous proteins, antibodies were incubated with protein G agarose (Thermo Scientific #20398) overnight at +4 °C, washed twice with lysis buffer and incubated with protein lysates. For immunoprecipitation of Flag-tagged proteins, 0.2–1 mg aliquots of protein lysates were incubated with 10 μL of anti-Flag® M2 affinity agarose gel (#A2220, Sigma-Aldrich). After 1 h incubation with rotation at +4 °C, the agarose gel was washed three times with the lysis buffer. Samples were prepared for western blotting by adding 2× Laemmli sample buffer directly to the agarose gel and by heating the samples for 10 min at +95 °C prior to gel loading. Chemiluminescence was detected by Bio-Rad Clarity or Clarity Max ECL western blotting substrates. Results were visualized with the ChemiDoc™ MP Imaging System and analysed with IMAGE LAB software Version 5.2.1 (Bio-Rad Laboratories, Inc., Hercules, CA, USA).

cDNA synthesis and quantitative RT-PCR

Cells were lysed directly with TRIzol™ Reagent (Thermo Fisher) and RNA samples were extracted according to the manufacturer's protocol. Prior to cDNA synthesis, samples

were treated with RNase-free DNase 1 (Thermo Scientific EN0521) to ensure the complete absence of DNA. cDNA was synthesized from 1 ug RNA using RevertAid First Strand cDNA Synthesis Kit (Thermo Scientific K1622) according to the manufacturer's protocol. Quantitative RT-PCR was carried out in Mic qPCR Cycler (Bio Molecular Systems) with GoTaq® qPCR Master Mix (Promega) according to the manufacturer's protocol. The primers were synthesized by Integrated DNA Technologies (Table S3). The fold change of gene expression was normalized with ACTB and calculated using the $2^{-\Delta\Delta CT}$ method [54].

Nuclear/Cytoplasmic fractionation

Nearly confluent cells (~ 80% confluence) were collected from 10 cm plates by scraping them into 1 mL aliquots of PBS. After 10 s centrifugation at 21 000 × ***g***, supernatants were discarded and the pellets were lysed for 15 min in 500 μL of lysis buffer: 10 mM Tris–HCl, pH 7.5, 10 mM NaCl, 3 mM $MgCl_2$, 0.5% Nonidet P-40, 5 mM NaF, 1 mM PMSF, 2 $\mu g \cdot mL^{-1}$ leupeptin, aprotinin and pepstatin A, 5 mM NEM, 5 mM chloroacetamide and mini-EDTA-free protease inhibitor tablet. After centrifugation at 500 × ***g*** for 5 min at +4 °C, the supernatants contained the cytoplasmic compartments, while the nuclei were in the pellets. The pellets were washed three times with 500 μL lysis buffer and centrifuged each time at 500 × ***g*** for 5 min at +4 °C, after which they were suspended in 200 μL of lysis buffer and sonicated for 30 s. After additional centrifugation at 500 × ***g*** for 1 min, the supernatants were collected which contained nuclear fractions. The cytoplasm-containing solutions were centrifuged at 12 000 × ***g*** for 15 min at +4 °C, after which the supernatant was collected. Lamin A/C or Lamin A and beta-tubulin were used as nuclear and cytosolic markers, respectively, to evaluate fractionation efficiency.

In vitro kinase assays and mass spectrometry of phosphorylated substrates

The procedure for performing radioactive *in vitro* kinase assays has previously been described [55]. Briefly, 0.5–2.0 μg of PIM kinases and their substrates were used in each reaction. Samples were separated by SDS/PAGE and stained with Page Blue™ protein staining solution (#24620, Thermo Fisher Scientific). Band intensities were quantitated by the IMAGE LAB software Version 5.2.1 (Bio-Rad). For mass spectrometry analyses of phosphorylated substrates, additional *in vitro* kinase assays were performed similarly but with the use of non-radioactive ATP. Protein bands were visualized by ProQ® Diamond Phosphoprotein Gel Stain (Thermo Fisher Scientific) after SDS/PAGE. In-gel digestion of proteins with trypsin, liquid chromatography–electrospray ionization–tandem mass spectrometry (LC-ESI-MS/MS) with phosphopeptide enrichment and data analysis have been previously described [56,57].

Enzymatic assays

Lactate dehydrogenase enzyme activities were measured as previously described [23] but with slight modifications. Cells were lysed in nuclear/cytoplasmic fractionation buffer and separated into whole cell lysate, cytosolic fraction and nuclear fraction. Protein concentrations for each fraction were determined using the Pierce™ BCA Protein Assay Kit according to manufacturers' protocols. Aliquots of protein from whole-cell lysates (2 μg), cytosolic fractions (2 μg) and nuclear fractions (60 μg) were added into the reaction mixture buffer that consisted of 50 mM Tris–HCl, pH 7.4, 20 μM NADH, and 3.3 mM pyruvate (or 3.3 mM sodium 2-ketobutyrate) in a total volume of 200 μL. LDHA activities were measured by the decrease in fluorescence (Ex. 350 nm, Em. 470 nm) corresponding to the conversion of NADH to NAD^+ at 25 °C, and normalized to the amount of LDHA protein.

Proximity ligation assay (PLA)

Cell samples seeded on coverslips were fixed for 10 min with 4% paraformaldehyde, washed twice with PBS, once with 0.1% Triton X-100 in PBS for 10 min and twice with PBS. Thereafter, the assays were continued using the Duolink® *In Situ* Detection Reagent kit (DUO9207, Sigma-Aldrich) according to manufacturer's instructions. Samples were imaged by the Nikon fluorescent microscope with NIS-Elements AR software (Nikon, Tokyo, Japan) and analysed by IMAGEJ/FIJI (Wayne Rasband, National Institutes of Health, Bethesda, MD, USA).

Protein crosslinking assay

Cells were lysed in a buffer containing 40 mM HEPES pH 7.5, 150 mM NaCl, 0.1% NP-40, 1 mM PMSF, 2 $\mu g \cdot mL^{-1}$ leupeptin, aprotinin and pepstatin A and mini-EDTA-free protease inhibitor tablet. After 30 min of centrifugation at 16 000 × ***g***, supernatants were collected and protein concentrations were determined using the Pierce™ BCA Protein Assay Kit. For crosslinking reactions, 100 μg aliquots of protein were incubated with glutaraldehyde (final concentration 0.0625%; Sigma-Aldrich) for 10 min at 25 °C or 30 °C, followed by the addition of glycine (final concentration 50 mM) for 10 min to terminate the reactions. Samples were then subjected to SDS/PAGE analysis.

Statistical analysis and figure preparation

Bar charts were produced using GRAPHPAD PRISM 6.0 (GraphPad Software, San Diego, CA, USA) and the results were analysed using Student's *t*-test. Significant differences ($P < 0.05$ and $P < 0.01$) were marked with * and ** respectively. Error bars represent standard deviations. Inkscape was used for figure preparation.

Acknowledgements

This study was financially supported by the Academy of Finland (grant 287040) and the Turku University Foundation to PJK, the Drug Research Doctoral Programme of the University of Turku, the Cancer Society of Finland, the Maud Kuistila Foundation and the Ida Montin Foundation to KLM, and the Center of Excellence in Cellular Mechanostasis at Åbo Akademi University to AM. The funding bodies had no influence on the design or execution of the studies or the preparation of the manuscript. We thank C. Sahlgren and J. Westermarck for providing expression vectors, A. Mohan in AM group for technical advice, W. Eccleshall in PJK group for critical comments and the Biocenter Finland core facilities of Turku Bioscience for assistance in microscopy (Cell Imaging and Cytometry Core with J. Sandholm).

Conflict of interest

The authors declare no conflict of interest.

Author contributions

The study was designed and written by KLM and PJK. Experiments were performed by KLM. AM provided expertise and reagents for ubiquitination assays. All authors have read and approved the manuscript.

Peer review

The peer review history for this article is available at https://publons.com/publon/10.1111/febs.16653.

Data availability statement

The data that support the findings of this study are available from the corresponding author (paivi.koskinen@utu.fi) upon reasonable request.

References

1 Brault L, Gasser C, Bracher F, Huber K, Knapp S, Schwaller J. PIM serine/threonine kinases in the pathogenesis and therapy of hematologic malignancies and solid cancers. *Haematologica*. 2010;**95**:1004–15.
2 Brasó-Maristany F, Filosto S, Catchpole S, Marlow R, Quist J, Francesch-Domenech E, et al. PIM1 kinase regulates cell death, tumor growth and chemotherapy response in triple-negative breast cancer. *Nat Med*. 2016;**22**:1303–13.
3 Eerola SK, Kohvakka A, Tammela TLJ, Koskinen PJ, Latonen L, Visakorpi T. Expression and ERG regulation of PIM kinases in prostate cancer. *Cancer Med*. 2021;**10**:3427–36.
4 Nawijn MC, Alendar A, Berns A. For better or for worse: the role of Pim oncogenes in tumorigenesis. *Nat Rev Cancer*. 2011;**11**:23–34.
5 Warfel NA, Kraft AS. PIM kinase (and Akt) biology and signaling in tumors. *Pharmacol Ther*. 2015;**151**:41–9.
6 Santio NM, Koskinen PJ. PIM kinases: From survival factors to regulators of cell motility. *Int J Biochem Cell Biol*. 2017;**93**:74–85.
7 Qian KC, Wang L, Hickey ER, Studts J, Barringer K, Peng C, et al. Structural basis of constitutive activity and a unique nucleotide binding mode of human Pim-1 kinase. *J Biol Chem*. 2005;**280**:6130–7.
8 Aho TLT, Sandholm J, Peltola KJ, Mankonen HP, Lilly M, Koskinen PJ. Pim-1 kinase promotes inactivation of the pro-apoptotic Bad protein by phosphorylating it on the Ser112 gatekeeper site. *FEBS Lett*. 2004;**571**:43–9.
9 Eerola SK, Santio NM, Rinne S, Kouvonen P, Corthals GL, Scaravilli M, et al. Phosphorylation of NFATC1 at PIM1 target sites is essential for its ability to promote prostate cancer cell migration and invasion. *Cell Commun Signal*. 2019;**17**:148.
10 Santio NM, Landor SK-J, Vahtera L, Ylä-Pelto J, Paloniemi E, Imanishi SY, et al. Phosphorylation of Notch1 by Pim kinases promotes oncogenic signaling in breast and prostate cancer cells. *Oncotarget*. 2016;**7**:43220–38.
11 Landor SKJ, Santio NM, Eccleshall WB, Paramonov VM, Gagliani EK, Hall D, et al. PIM-induced phosphorylation of Notch3 promotes breast cancer tumorigenicity in a CSL-independent fashion. *J Biol Chem*. 2021;**296**:100593.
12 Santio NM, Vainio V, Hoikkala T, Mung KL, Lång M, Vahakoski R, et al. PIM1 accelerates prostate cancer cell motility by phosphorylating actin capping proteins. *Cell Commun Signal*. 2020;**18**:121.
13 Mung KL, Eccleshall WB, Santio NM, Rivero-Müller A, Koskinen PJ. PIM kinases inhibit AMPK activation and promote tumorigenicity by phosphorylating LKB1. *Cell Commun Signal*. 2021;**19**(1):68.
14 Beharry Z, Mahajan S, Zemskova M, Lin Y-W, Tholanikunnel BG, Xia Z, et al. The Pim protein kinases regulate energy metabolism and cell growth. *Proc Natl Acad Sci USA*. 2011;**108**:528–33.
15 Song JH, An N, Chatterjee S, Kistner-Griffin E, Mahajan S, Mehrotra S, et al. Deletion of Pim kinases elevates the cellular levels of reactive oxygen species and sensitizes to K-Ras-induced cell killing. *Oncogene*. 2015;**34**:3728–36.
16 Din S, Konstandin MH, Johnson B, Emathinger J, Völkers M, Toko H, et al. Metabolic dysfunction

consistent with premature aging results from deletion of Pim kinases. *Circ Res*. 2014;**115**:376–87.
17 Hoover D, Friedmann M, Reeves R, Magnuson NS. Recombinant human Pim-1 protein exhibits serine/threonine kinase activity. *J Biol Chem*. 1991;**266**:14018–23.
18 Yu Z, Zhao X, Huang L, Zhang T, Yang F, Xie L, et al. Proviral insertion in murine lymphomas 2 (PIM2) oncogene phosphorylates pyruvate kinase M2 (PKM2) and promotes glycolysis in cancer cells. *J Biol Chem*. 2013;**288**:35406–16.
19 Yang T, Ren C, Qiao P, Han X, Wang L, Lv S, et al. PIM2-mediated phosphorylation of hexokinase 2 is critical for tumor growth and paclitaxel resistance in breast cancer. *Oncogene*. 2018;**37**:5997–6009.
20 Casillas AL, Chauhan SS, Toth RK, Sainz AG, Clements AN, Jensen CC, et al. Direct phosphorylation and stabilization of HIF-1α by PIM1 kinase drives angiogenesis in solid tumors. *Oncogene*. 2021;**40**:5142–52.
21 Leverson JD, Koskinen PJ, Orrico FC, Rainio EM, Jalkanen KJ, Dash AB, et al. Pim-1 kinase and p100 cooperate to enhance c-Myb activity. *Mol Cell*. 1998;**2**:417–25.
22 Mishra D, Banerjee D. Lactate dehydrogenases as metabolic links between tumor and stroma in the tumor microenvironment. *Cancer*. 2019;**11**:750.
23 Liu Y, Guo J-Z, Liu Y, Wang K, Ding W, Wang H, et al. Nuclear lactate dehydrogenase A senses ROS to produce α-hydroxybutyrate for HPV-induced cervical tumor growth. *Nat Commun*. 2018;**9**:4429.
24 Stambaugh R, Post D. Substrate and product inhibition of rabbit muscle lactic dehydrogenase heart (H4) and muscle (M4) isozymes. *J Biol Chem*. 1966;**241**:1462–7.
25 Koukourakis MI, Giatromanolaki A, Sivridis E, Bougioukas G, Didilis V, Gatter KC, et al. Lactate dehydrogenase-5 (LDH-5) overexpression in non-small-cell lung cancer tissues is linked to tumour hypoxia, angiogenic factor production and poor prognosis. *Br J Cancer*. 2003;**89**:877–85.
26 Rong Y, Wu W, Ni X, Kuang T, Jin D, Wang D, et al. Lactate dehydrogenase A is overexpressed in pancreatic cancer and promotes the growth of pancreatic cancer cells. *Tumour Biol*. 2013;**34**:1523–30.
27 Koukourakis MI, Giatromanolaki A, Panteliadou M, Pouliliou SE, Chondrou PS, Mavropoulou S, et al. Lactate dehydrogenase 5 isoenzyme overexpression defines resistance of prostate cancer to radiotherapy. *Br J Cancer*. 2014;**110**:2217–23.
28 Koukourakis MI, Giatromanolaki A, Sivridis E. Lactate dehydrogenase Isoenzymes 1 and 5: differential expression by neoplastic and stromal cells in non-small cell lung cancer and other epithelial malignant tumors. *Tumor Biol*. 2003;**24**:199–202.
29 Dennison JB, Molina JR, Mitra S, González-Angulo AM, Balko JM, Kuba MG, et al. Lactate dehydrogenase B: a metabolic marker of response to neoadjuvant chemotherapy in breast cancer. *Clin Cancer Res*. 2013;**19**:3703–13.
30 McCleland ML, Adler AS, Shang Y, Hunsaker T, Truong T, Peterson D, et al. An integrated genomic screen identifies LDHB as an essential gene for triple-negative breast cancer. *Cancer Res*. 2012;**72**:5812–23.
31 Zhao D, Zou S-W, Liu Y, Zhou X, Mo Y, Wang P, et al. Lysine-5 acetylation negatively regulates lactate dehydrogenase A and is decreased in pancreatic cancer. *Cancer Cell*. 2013;**23**:464–76.
32 Li X, Zhang C, Zhao T, Su Z, Li M, Hu J, et al. Lysine-222 succinylation reduces lysosomal degradation of lactate dehydrogenase a and is increased in gastric cancer. *J Exp Clin Cancer Res*. 2020;**39**:172.
33 Fan J, Hitosugi T, Chung T-W, Xie J, Ge Q, Gu T-L, et al. Tyrosine phosphorylation of lactate dehydrogenase A is important for NADH/NAD+ redox homeostasis in cancer cells. *Mol Cell Biol*. 2011;**31**:4938–50.
34 Jin L, Chun J, Pan C, Alesi G, Li D, Magliocca K, et al. Phosphorylation-mediated activation of LDHA promotes cancer cell invasion and tumour metastasis. *Oncogene*. 2017;**36**:3797–806.
35 Zhong X, Tian S, Zhang X, Diao X, Dong F, Yang J, et al. CUE domain-containing protein 2 promotes the Warburg effect and tumorigenesis. *EMBO Rep*. 2017;**18**:809–25.
36 Muslin AJ, Tanner JW, Allen PM, Shaw AS. Interaction of 14-3-3 with signaling proteins is mediated by the recognition of phosphoserine. *Cell*. 1996;**84**:889–97.
37 Fu H, Subramanian RR, Masters SC. 14-3-3 proteins: structure, function, and regulation. *Annu Rev Pharmacol Toxicol*. 2000;**40**:617–47.
38 Pennington KL, Chan TY, Torres MP, Andersen JL. The dynamic and stress-adaptive signaling hub of 14-3-3: emerging mechanisms of regulation and context-dependent protein–protein interactions. *Oncogene*. 2018;**37**:5587–604.
39 Macdonald A, Campbell DG, Toth R, McLauchlan H, Hastie CJ, Arthur JSC. Pim kinases phosphorylate multiple sites on Bad and promote 14-3-3 binding and dissociation from Bcl-XL. *BMC Cell Biol*. 2006;**7**:1.
40 Peng C, Knebel A, Morrice NA, Li X, Barringer K, Li J, et al. Pim kinase substrate identification and specificity. *J Biochem (Tokyo)*. 2007;**141**:353–62.
41 Komander D, Rape M. The ubiquitin code. *Annu Rev Biochem*. 2012;**81**:203–29.
42 Cooper JA, Reiss NA, Schwartz RJ, Schwartz RJ, Schwartz RJ, Hunter T. Three glycolytic enzymes are phosphorylated at tyrosine in cells transformed by Rous sarcoma virus. *Nature*. 1983;**302**:1–223.

43 Zhong XH, Howard BD. Phosphotyrosine-containing lactate dehydrogenase is restricted to the nuclei of PC12 pheochromocytoma cells. *Mol Cell Biol*. 1990;**10**:770–6.
44 Chen Y-J, Mahieu NG, Huang X, Singh M, Crawford PA, Johnson SL, et al. Lactate metabolism is associated with mammalian mitochondria. *Nat Chem Biol*. 2016;**12**:937–43.
45 Hornbeck PV, Zhang B, Murray B, Kornhauser JM, Latham V, Skrzypek E. PhosphoSitePlus, 2014: mutations, PTMs and recalibrations. *Nucleic Acids Res*. 2015;**43**:D512–20.
46 Onishi Y, Hirasaka K, Ishihara I, Oarada M, Goto J, Ogawa T, et al. Identification of mono-ubiquitinated LDH-A in skeletal muscle cells exposed to oxidative stress. *Biochem Biophys Res Commun*. 2005;**336**:799–806.
47 Maitland MER, Kuljanin M, Wang X, Lajoie GA, Schild-Poulter C. Proteomic analysis of ubiquitination substrates reveals a CTLH E3 ligase complex-dependent regulation of glycolysis. *FASEB J*. 2021;**35**:e21825.
48 Dar A, Wu D, Lee N, Shibata E, Dutta A. 14-3-3 proteins play a role in the cell cycle by shielding Cdt2 from ubiquitin-mediated degradation. *Mol Cell Biol*. 2014;**34**:4049–61.
49 Dai R-P, Yu F-X, Goh S-R, Chng H-W, Tan Y-L, Fu J-L, et al. Histone 2B (H2B) expression is confined to a proper NAD+/NADH redox status*. *J Biol Chem*. 2008;**283**:26894–901.
50 He H, Lee M-C, Zheng L-L, Zheng L, Luo Y. Integration of the metabolic/redox state, histone gene switching, DNA replication and S-phase progression by moonlighting metabolic enzymes. *Biosci Rep*. 2013;**33**: e00018.
51 Zhang D, Tang Z, Huang H, Zhou G, Cui C, Weng Y, et al. Metabolic regulation of gene expression by histone lactylation. *Nature*. 2019;**574**:575–80.
52 Yu J, Chai P, Xie M, Ge S, Ruan J, Fan X, et al. Histone lactylation drives oncogenesis by facilitating m6A reader protein YTHDF2 expression in ocular melanoma. *Genome Biol*. 2021;**22**:85.
53 Santio NM, Eerola SK, Paatero I, Yli-Kauhaluoma J, Anizon F, Moreau P, et al. Pim kinases promote migration and metastatic growth of prostate cancer xenografts. *PLoS ONE*. 2015;**10**:e0130340.
54 Livak KJ, Schmittgen TD. Analysis of relative gene expression data using real-time quantitative PCR and the $2-\Delta\Delta CT$ method. *Methods*. 2001;**25**:402–8.
55 Kiriazis A, Vahakoski RL, Santio NM, Arnaudova R, Eerola SK, Rainio EM, et al. Tricyclic benzo[cd] azulenes selectively inhibit activities of Pim kinases and restrict growth of Epstein-Barr virus-transformed cells. *PLoS ONE*. 2013;**8**:e55409.
56 Kauko O, Laajala TD, Jumppanen M, Hintsanen P, Suni V, Haapaniemi P, et al. Label-free quantitative phosphoproteomics with novel pairwise abundance normalization reveals synergistic RAS and CIP2A signaling. *Sci Rep*. 2015;**5**:13099.
57 Imanishi SY, Kochin V, Eriksson JE. Optimization of phosphopeptide elution conditions in immobilized Fe (III) affinity chromatography. *Proteomics*. 2007;**7**:174–6.

Supporting information

Additional supporting information may be found online in the Supporting Information section at the end of the article.

Table S1. List of primers for LDHA plasmid mutagenesis.
Table S2. List of antibodies used in the experiments.
Table S3. List of primers for PCR.

Table S1. Primers for mutagenesis

Target	Primer Type	Sequence
LDHAS79A	Forward	GAACACCAAAGATTGTCGCTGGCAAAGACTATAATGTAAC
LDHAS79A	Backward	GTTACATTATAGTCTTTGCCAGCGACAATCTTTGGTGTTC
LDHAS105A	Forward	GTCAGCAAGAGGGAGAAGCCCGCCTTAATTTGGTCCAG
LDHAS105A	Backward	CTGGACCAAATTAAGGCGGGCTTCTCCCTCTTGCTGAC
LDHAS161A	Forward	CCGTGTTATCGGAGCCGGTTGCAATCTGGATTC
LDHAS161A	Backward	GAATCCAGATTGCAACCGGCTCCGATAACACGG
LDHAS319A	Forward	GAGGCCCGTTTGAAGAAGGCTGCAGATACACTTTGGGGG
LDHAS319A	Backward	CCCCCAAAGTGTATCTGCAGCCTTCTTCAAACGGGCCTC

Table S2. Antibodies

Protein or tag	Company	Product Code	Dilution
PIM1	Santa Cruz	12H8	1:500
PIM2	Cell Signaling Technology	#4730	1:1000
PIM3	Cell Signaling Technology	#4165	1:1000
PIM1 (PLA assay)	Merck	MABC553	1:500
pan 14-4-3	Santa Cruz	sc-1657	1:2000
Beta-actin	Cell Signaling Technology	#3700	1:5000
HA-tag	Santa Cruz	sc-805	1:5000
His-tag	Cell Signaling Technology	#12698	1:1000
FLAG-tag	Sigma	F1804	1:1000
LDHA	Cell Signaling Technology	#3582	1:1000
β-Tubulin	Cell Signaling Technology	#86298	1:5000
Lamin A/C	Cell Signaling Technology	#4777	1:5000
Lamin A	Sigma	L2193	1:5000
Ubiquitin K-48	Sigma	ZRB2150	1:1000
Mouse IgG control	Santa Cruz	sc-2025	NA

Table S3. Primers for PCR

Target	Primer Type	Sequence
LDHA	Forward	ACC CAG ATT TAG GGA CTG ATA AAG
LDHA	Backward	CCA ATA GCC CAG GAT GTG TAG
ACTB	Forward	GGA AAT CGT GCG TGA CAT TAA G
ACTB	Backward	AGC TCG TAG CTC TTC TCC A

TURUN
YLIOPISTO
UNIVERSITY
OF TURKU

Painosalama, Turku, Finland 2023

ISBN 978-951-29-9194-5 (PRINT)
ISBN 978-951-29-9195-2 (PDF)
ISSN 0355-9483 (Print)
ISSN 2343-3213 (Online)